Liquid loaded microneedles for the intradermal delivery of botulinum toxin for Primary Focal Hyperhidrosis

Barbara Maria Torrisi

A thesis submitted to Cardiff University in accordance with the requirements for the degree of Doctor of Philosophy. Cardiff School of Pharmacy and Pharmaceutical Sciences, July 201

To my parents….

Acknowledgements

I would like to express my utmost appreciation to my supervisors Dr Sion Coulman and Dr James Birchall for their supportive guidance, advice and enthusiasm throughout the course of this research project. Special thanks go to Dr Sion Coulman for critically reviewing my Thesis. Without his precious help this Thesis would not have been written.

I extend my gratitude to Cardiff University Welsh School of Pharmacy and Pharmaceutical Sciences for funding this research project and giving me the opportunity to present this work at national and international conferences.

I would also like to acknowledge Prof Mark Prausnitz and Dr Vladimir Zarnitsyn of Georgia Institute of Technology in Atlanta (USA) for providing the microneedle devices employed in this study.

I must also thank Dr Andrew Jones for helping me with the use of the spectrophotometer at the beginning of the study and Dr Andrea Brancale for his time spent restoring my laptop.

Many thanks go also to my colleagues, in particular to Bal, Chris, Ezra, Harsha, Keng, Leanne, Marc, Rosie, Tina and Xin for their support as well for their sincere friendship. Their presence has made me feel less lonely and homesick. Particular thanks go to Harsha for her valuable advice as well as our inspiring scientific debates and venting of frustration, which helped me during the project.

Many thanks go to my beloved friend Marisa for encouraging me throughout the entire course of this work and to Sue and Jeff for making me feel at home. Other friends I would like to acknowledge are: Rosario, Carmen, Lorenzo, Lydia, Michele, Diego, Giancarlo, James, Edwin, Rhyd, Tris, Sri, Andy, Magda, Alessandra and Emanuele.

Finally, I want to give special thanks to my family, in particular to my mum and dad for their immeasurable love, trust, encouragement and support they provided me through every single day of my life. Without them this work would not have been possible.

Abstract

Primary focal hyperhidrosis (PFHH) is a medical condition characterised by over-activity of the eccrine sweat glands, primarily occurring on palmar, plantar and axillary regions. PFHH can have a significant adverse impact on a patient's quality of life. Multiple intradermal injections of a commercial formulation of botulinum toxin A (BTX A) (Botox®) is the most effective non-surgical treatment currently licensed in the UK for cases of severe PFHH. Although effective, intradermal BTX A injections are associated with considerable pain and discomfort for the patient and are time-consuming for the administering clinician. This study aims to evaluate the potential of using pocketed microneedle devices for minimally invasive intradermal delivery of BTX A, as a liquid formulation, into human skin.

Pocketed microneedles, metallic 700 μm-long needles containing a cavity within the needle shaft, were selected as an appropriate and relatively untested intradermal delivery device. Pocketed microneedle devices (PMDs) were liquid loaded by immersion into a 'Botox® like' formulation that mimicked the composition of the commercial Botox® formulation, with the exception of BTX A, which was replaced by the model macromolecular protein β-galactosidase (~465 kDa). A water-soluble dye was also included to enable visualisation. Microneedles were assessed for loading uniformity by light microscopy and the formulation residency time was evaluated by monitoring evaporation using a digital camera. The microneedle loading capacity was determined using an established quantitative assay for β-galactosidase. Studies using excised human breast skin, maintained in organ culture, examined delivery of the model β-galactosidase from liquid loaded PMDs and the time-dependent diffusion of the protein within the dermal tissue. A more clinically representative model of BTX A, formaldehyde inactivated BTX A, i.e., botulinum toxoid, was used to determine the deposition pattern of the therapeutic within the skin. Following skin delivery the toxoid was detected by immnohistochemical staining and fluorescence imaging, following its conjugation to an appropriate fluorophore.

Immersion of the PMD into a 'Botox® like' formulation resulted in successful uptake and retention of the model protein solution. Quantitative studies indicated that nanogram quantities (~100 ng/microneedle array) of the β-galactosidase model can be loaded and retained on individual microneedles, in a liquid state. These results suggest that the loading capacity of the microneedle device is appropriate for therapeutic botulinum toxin formulations, although loading uniformity will need to be addressed. Histological analysis revealed effective delivery of the model β-galactosidase from a PMD to the epidermal and the dermal layers of the skin. Rapid and extensive diffusion of the protein within the deeper dermis was also demonstrated. Further, immunohistochemical and fluorescence studies indicated effective PMD loading and successful delivery of botulinum toxoid to the dermis of human skin. These data suggest that it should be possible for BTX A to access its therapeutic target (the eccrine sweat glands) following delivery via PMDs.

This study has demonstrated for the first time that pocketed microneedles represent a viable, minimally invasive alternative, for the intradermal delivery of botulinum toxin A (Botox®). Future pre-clinical and clinical studies are now required to test and optimize a microneedle-based delivery system that is most suited to clinical practice.

Contents

Glossary

µg	microgram-s
µl	microlitre-s
µm	micrometre-s
2-ME	2-mercaptoethanol
AchE	acetylcholinesterase
Ach	acetylcholine
AP	alkaline phosphatase
APS	ammonium persulfate
AUC	area under the curve
BCA	bicinchoninic acid
BCIG	bromo-chloro-indolyl-galactopyranoside
BTXs	botulinum toxins
BSA	bovine serum albumin
BT	botulinum toxoid
BTX	botulinum toxin
C	control
cm	centimetres
CMC	carboxymethylcellulose
CNS	central nervous system
d	day-s
D	protein under denaturing conditions
Da	Daltons
DAB	3-3’-diaminebenzidine
De	dermis
DLQI	Dermatology Life Quality Index
DMEM	Dulbecco’s modified Eagle medium
DMF	N,N-dimethylformamide
DMSO	dimethylsulphoxide
DNA	deoxyribonucleic acid
DTT	dithiothreitol
ELISA	enzyme-linked immunosorbent assay

Ep	epidermis
ETS	endoscopic transthoracic sympathectomy
FBS	foetal bovine serum
FDA	Food and Drug Administration
g	gram-s
H&E	haematoxylin and eosin
HA protein	haemagglutinin protein
HEPES	(4-(2-hydroxyethyl)-1-piperazineethanesulfonic acid)
HIV	human immunodeficiency virus
HPLC	high performance liquid chromatography
HRP	horseradish peroxidase
HSA	human serum albumin
Ig	immunoglobulin
IHC	immunohistochemistry
ID	intradermal
IM	intramuscular
kDa	kilodalton-s
LOD	limit of detection
m.w.	molecular weight
MA	maleic anhydride
MD	microneedle device
mg	milligram-s
min	minute-s
ml	millilitre-s
mm	millimitre-s
n.a.	not applicable
n	number of replicates
N	protein under native conditions
NADP+	nicotinamide adenine dinucleotide phosphate
neg.	negative
ng	nanogram-s
NHS	National Health Service
nl	nanolitre-s
NPMD	non pocketed microneedle device

NTNH protein	non toxin non haemagglutinin protein
OCT	optical coherence tomography
OCT	optimal cutting temperature
ONP	o-nitrophenol
ONPG	o-nitrophenyl-β-D-galactoside
p	probability value
P	partition coefficient
PBS	phosphate-buffered saline
PCR	polymerase chain reaction
PE/Cy7	phycoerythrin and cyanine
PFHH	primary Focal Hyperhidrosis
pg	picogram-s
PLA	poly-L-lactide acid
PLGA	polylactic-co-glycolic acid
PMD	pocketed microneedle device
PMVE	poly methylvinylether
pos.	positive
R^2	squared correlation coefficient
RSD	relative standard deviation
s	seconds
Sc	stratum corneum
SD	standard deviation
SDS PAGE	sodium dodecyl sulphate polyacrylamide gel electrophoresis
SDS	sodium dodecil sulphate
SEM	scanning electron microscopy
SNAP-25	synaptosome-associated protein
SNARE	soluble n-ethylmaleimide-sensitive-factor attachment receptor
SPB	sodium phosphate buffer
SS	salbutamol sulphate
TBS buffer	Tris-buffered saline buffer
TDDS	transdermal delivery systems
TEMED	N, N, N-tetramethylendiamine
TCA	trichloroacetic acid
TWI	tap water iontophoresis

U	unit-s
UV	ultraviolet
UK	United Kingdom
v/v	volume/volume
w/v	weight/volume
w/w	weight/weight
β-gal	β-galactosidase
θ	contact angle
λabs max	maximal absorption wavelength
λem	emission wavelength
λex	excitation wavelength

List of Figures

List of Tables

Chapter 1

General Introduction

1.1 Overview

Botulinum toxin A (BTX A) is an extremely potent neurotoxin that has increasing applications in both the cosmetic and the medical industry. As a therapeutic, BTX A is directly administered to its site of action to treat hypersecretory or muscular defects. Multiple injections of BTX A (Botox®-5ng per vial) is the most effective licensed treatment for primary focal hyperhidrosis (PFHH) in the UK (Glaser et al. 2007c). Local intradermal administration targets the site of action, the eccrine sweat glands in the dermis, and reduces the risk of systemic uptake (Moreau 2003; Naumann et al. 1998b). However, the treatment relies upon numerous painful injections by skilled clinicians. This Thesis investigates the use of microneedle array devices (MDs) as an alternative minimally invasive approach to deliver BTX A to human skin for the treatment of PFHH.

In order to evaluate the cutaneous delivery capability of a MD, it is crucial to understand the structural features of human skin. This introductory Chapter provides some background information of the anatomy of the skin with particular focus upon the structure of the dermis and the eccrine sweat glands here located. This is followed by more detailed information regarding the use of BTX A in the treatment of this PFHH, the therapeutic options currently available for this condition and their limitations. Alternative methods employed to date for minimally invasive BTX A administration are also outlined. In addition, general information regarding the different BTX A drugs currently available in the market, as well as their therapeutic and cosmetic applications, are provided. Subsequently, an overview of the microneedle concept and the principal microneedle applications is given. The Chapter terminates with a brief summary of the key points previously illustrated and an explanation of how they combine to provide a rationale for using microneedles as an alternative delivery method for BTX A administration.

1.2 Physiology of the skin

The skin is the largest organ of the body constituting approximately 15% of the entire body weight in humans (Kanitakis 2002). It can be defined as a barrier which separates and protects the internal body structures from external insults such as chemicals, pathogen microorganisms, radiation, physical injuries and varying

temperatures (Elias 2005). Skin plays also a key role in preventing water loss from the organism, stimulating immune responses, maintaining homeostasis of body temperature and perceiving various sensations such as pain, heat or pressure (Baroni et al. 2012).

The skin is essentially constituted of two distinct but mutually interacting layers (Figure 1.1); i) the epidermis, a stratified epithelium, which communicates with the external environment and ii) the dermis, a connective tissue, underlying the epidermis, which constitutes the major part of the skin. The junction between dermis and epidermis, termed dermo-epidermal junction, provides mechanical support to the skin and controls migration of cells and molecules between the two layers. The adipose tissue, residing at the bottom of the dermis, provides mechanical protection of the underlying organs (Barry 1983b).

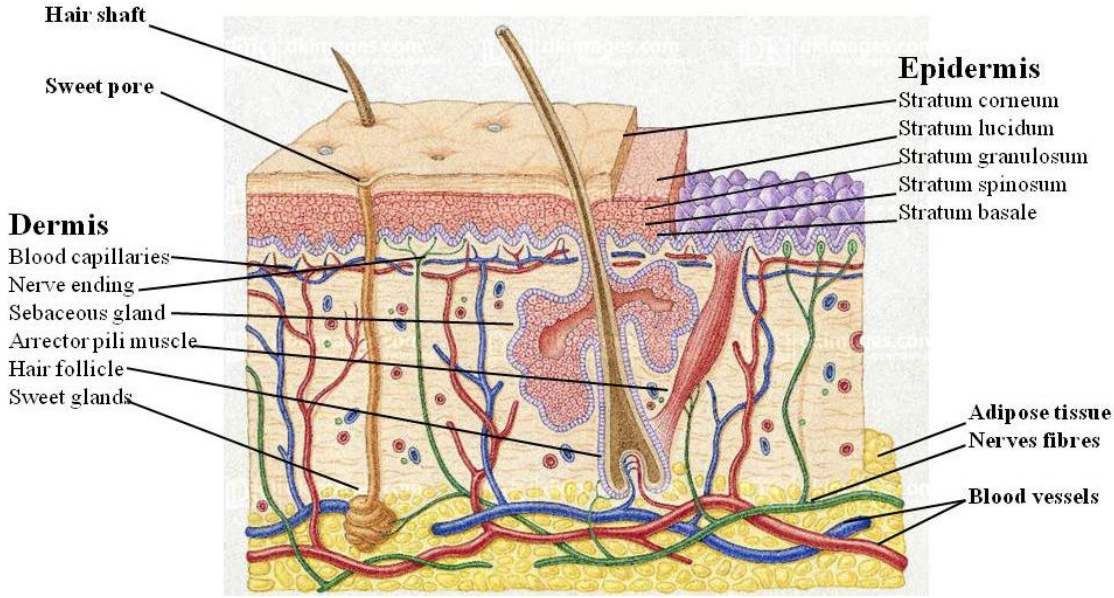

Figure 1.1 An illustration of the structural features of human skin. Figure adapted from http://www.dkimages.com/discover/home/Health-and-Beauty/Human-Body/Skin-Hair-and-Nails/Skin-Hair-and-Nails-43.html (undated).

1.2.1 Epidermis

The epidermis is a multilayered epithelium whose thickness varies according to anatomic sites, from 0.8-1 mm on the palms and the soles to 60 µm on the eyelids (Barry 1983b). It is constituted for the major part by cells called keratinocytes, so

termed due to the presence of the protein keratin, the main structural protein of the skin. Other cell populations are Langerhans cells, known to stimulate immune responses, Merkel cells, receptor cells associated with the sense of touch and shape discrimination and melanocytes, cells producing the cutaneous pigment melanin (Haake 2001). The epidermis can be divided in two main layers: the stratum corneum and the viable epidermis. The first one represents the outermost layer of the epidermis and consists of a 15 μm-thick, flattened, non-nucleated (dead) cell layer (Barry 1983b). This layer acts as a lipophilic barrier limiting access to the underlying epidermis to low molecular weight (< 500 Da) and relatively lipophilic compounds (Benson 2008). The lipophilic nature of this layer prevents loss of epidermal water and thus maintains hydration of the skin. Due to the extremely high molecular weight and hydrophilic nature of proteins such as BTX A, delivery of this medicament into the skin currently relies on the use of hypodermic needles, which actively perforate the stratum corneum barrier.

The viable epidermis, representing the larger portion of the entire epidermis, resides underneath the stratum corneum. It is so termed due to the presence of proliferative cells, which are responsible for conservation and regeneration of the epidermal structure (Baroni et al. 2012). These cells undergo progressive morphological changes while migrating from the viable epidermis, where they are nucleated and metabolically active, to the stratum corneum where they became keratinised corneocytes that are shed from the body surface in the desquamation process. Migration of keratinocytes from the stratum basale to the stratum corneum usually occurs in 21 days (Roberts 1998). Once reached the stratum corneum, the corneocytes usually reside for subsequent 13-14 days before shedding in the desquamation process (Barry 1983b).

1.2.1.1 Structure of the viable epidermis

The viable epidermis is composed of four distinct sub layers, which differ in thickness, cells morphology and function. The characteristic of each sub layer, from the innermost stratum germinativum to the outermost stratum lucidum are described in detail overleaf:-

The stratum basale

The stratum basale is constituted by one of two layers of columnar or cuboidal keratinocytes approximately 6 μm wide (Kanitakis 2002). Two major classes of keratinocytes can be found at this level. The first one is represented by stem cells which actively divide to compensate the loss of dead cells from the skin surface during the desquamation process (Fuchs 1990). The second cellular population is represented by keratinocytes which function to anchor the basal membrane to the underlying dermis (Simpson et al. 2011). Secure connection between keratinocytes in the basal layer and extracellular components of the underlying basale membrane (at the dermo-epidermal junction) is ensured by the presence of protein filaments called hemidesmosomes. Human disorders associated with production of these proteins and/or loss of specific cytoskeletal keratin filaments, to which the hemidesmosomes are attached, results in blistering and epidermal fragility (Simpson et al. 2011).
The basement membrane plays also an important role in controlling the migration of substances from the dermis to the epidermal layer. Water, electrolytes and small molecules overcome the membrane to provide supply of nutrients to the overlying epidermis from the blood vessels (Barry 1983b).

The stratum spinosum

The stratum spinosum (5-15 layers) is located between the stratum basale and the overlying stratum germinativum (Kanitakis 2002). The prickle appearance of this layer is due to the presence of large keratin filaments produced in the cytoplasm of the keratinocytes and extending out from the cellular surface. Protein complexes called desmosomes interact with these filaments producing intercellular bridges between adjacent cells (Fuchs 1990). These intercellular connections provide structural and mechanical support to the skin. Presence of granules enriched with lipids, termed lamellar bodies, can be detected in the cytoplasm of the outer cells layers of the stratum spinosum, especially in proximity of the overlying stratum granulosum (Jensen and Proksch 2009).

The stratum granulosum

The cells of the stratum granulosum (1-3 layers) appear flattened, oriented parallel to the skin surface and contain numerous granules of keratohyalin, polygonal granules constituted by assembly of profilaggrin and keratin (Kanitakis 2002). The cells of the

outer most layers of the stratum granulosum contain also numerous lamellar bodies involved in the desquamation process and the formation of the lipid intercellular matrix of the stratum corneum (Sondell et al. 1995).

The stratum lucidum

The stratum lucidum is a thin translucent layer, located at the interface between the underlying stratum granulosum and the overlying stratum corneum. This layer is found only in specific anatomic sites such as the palm of the hand and the sole of the foot (Barry 1983b).

1.2.1.2 The stratum corneum

The stratum corneum is composed by highly flattened, hexagonal, keratinized corneocytes, which represent the last differentiation stage of viable keratinocytes. Corneocytes are devoid of nuclei and cytoplasmatic organelles (Roberts 1998). These cells are embedded in an extracellular matrix constituted by lipids, produced and released by keratinocytes during their differentiation process. Although the stratum corneum is generally described as a 15-µm thick layer (Barry 1983b), its thickness varies tremendously depending of the anatomic site. For example, the thickness of the stratum corneum of palmar or plantar skin is approximately ten times higher than the rest of the body (Roberts 1998).

The corneocytes are mainly composed of a thick matrix of cytoskeletal keratin filaments interconnected by disulfide bonds and a cellular envelop consisting of a complex of cross-linked proteins such as loricrin, cystatin α and involucrin (Kanitakis 2002; Roberts 1998). It is believed the proteins of the cellular envelop interact covalently with specific lipids of the extracellular matrix, maintaining the structural integrity of the stratum corneum (Jensen and Proksch 2009) and thus its barrier function. Nevertheless, cohesiveness of the stratum corneum is also and more importantly ensured by the presence of modified desmosomes called corneodesmosomes. These are proteinaceous filaments that covalently cross link components of the cell envelop, providing strong connections between adjacent corneocytes (Ishida-Yamamoto et al. 2011).

Different lipids such as ceramides, cholesterol, free fatty acids and fatty acids esterified with cholesterol constitute the extracellular matrix. Ceramides and

cholesterol are the most represented components representing respectively the 40% (w/v) and the 27 % (w/v) of the entire lipids population (Baroni et al. 2012). The lipidic composition of the extracellular matrix provides an extraordinary barrier to chemical penetration.

Cutaneous permeation of a substance from the outside environment mainly occurs through the intercellular lipid matrix. Absorption via skin appendages (sweat glands and pilosebaceous glands) can be considered negligible for the majority of materials due to their limited distribution in the skin (Rizwan et al. 2009). In anatomic sites such as the palms and the soles which are devoid of hair follicles but rich of sweat glands, cutaneous penetration may be expected to occur mainly through the sweat ducts due to the high thickness of the stratum corneum. However, cutaneous absorption of various materials like allergens or histamine is very restricted here, thus indicating that the intra-appendageal route is not significant (Barry 1983a).

Due to the lipophilic composition of the stratum corneum, successful penetration of a substance through the intact barrier depends on its capability to partition into the lipid matrix and therefore on its lipophilicity. The grade of lipophilicity of a substance is associated to the partition coefficient value (log P) (Amorosa 1998a), defined as the ratio of concentrations of the substance in two immiscible solvents (usually represented by octanol and water). Therefore higher log P values define more lipophilic compounds.

However, despite the lipophilic nature of the stratum corneum, aqueous regions can be found in the underlying viable epidermis. In particular the presence of the so called aqueous boundary region, a hydrophilic barrier located between the stratum basale and the stratum granulosum, may oppose significant resistance to permeation of highly lipophilic compounds (Roberts et al. 1978; Roberts 1998). As a consequence of the mixed composition of the skin, substances capable to dissolve in both oil and water (log P 1 and 3) would diffuse through the cutaneous layers at relatively high rate (Benson 2008).

1.2.2 The dermis

The dermis is the major component of the skin having a thickness of about 1- 3 mm (Jensen and Proksch 2009). Its main functions reside in: i) providing flexibility and mechanical resistance to the skin ii) interacting with the overlying epidermis to

develop and maintain the integrity of the dermo-epidermal junction, iii) protecting epidermal appendages (eccrine and apocrine sweat glands and pilosebaceous units), blood vessels, nerves and lymphatic fibres (Haake 2001).

The dermis is a connective tissue consisting of approximately 80% fibrous proteins i) collagen (75%), ii) elastin (4%) and iii) reticulin (0.5%) and for the remaining 20% an amorphous matrix of non-fibrous filaments constituted by glycoproteins, proteoglycans and glycosaminoglycans (Barry 1983b). These filamentous proteins compose the 'ground substance' in which all components of the dermis are embedded. Cellular components of the dermis include fibroblasts, dendritic cells and macrophages. Fibrous and non-fibrous components as well as cell populations in the dermis will be described in more details in the following Sections.

Two main portions can be distinguished in the dermis: an upper papillary region and a lower reticular region (Haake 2001) (Figure 1.2). The papillary region, located at the interface with the overlying epidermis, contains loose bundles of thin collagen and elastic fibres running perpendicularly to the skin surface and immersed in large inter-fibrillar spaces (Kanitakis 2002). This layer is characterised by greater metabolic and proliferative cellular activities compared to the reticular region. It is at this level that the major part of proteoglycans are produced and released into the extracellular space. The underlying reticular region is characterised by thicker collagen and elastic bundles, which tend to align horizontally to the skin surface (Kanitakis 2002; Montagna 1974).

The papillary region is so termed as it contains finger-like projections (dermal papillae), rich in blood vessels, nerves fibres and lymphatic vessels, which alternate with epidermal ridges. These inter-digitations increase the surface area and thus the rate of exchange of materials between the dermis and epidermis (Sorrell and Caplan 2004). Blood vessels provide nutrients and oxygen to the epidermis and also regulate body temperature and pressure. Nerve fibres modulate cutaneous sensations (i.e touch, pain and pressure), whereas lymphatic vessels remove plasma proteins from the extravascular space.

At the interface with the reticular region resides a vascular complex, the rete subpapillare, that is sustained by an additional plexus, the rete cutaneum, located in the deep dermis (Figure 1.3) (Sorrell and Caplan 2004). This complex vasculature is responsible for conveying blood to the dermis itself, the cutaneous appendages and the subcutaneous fat.

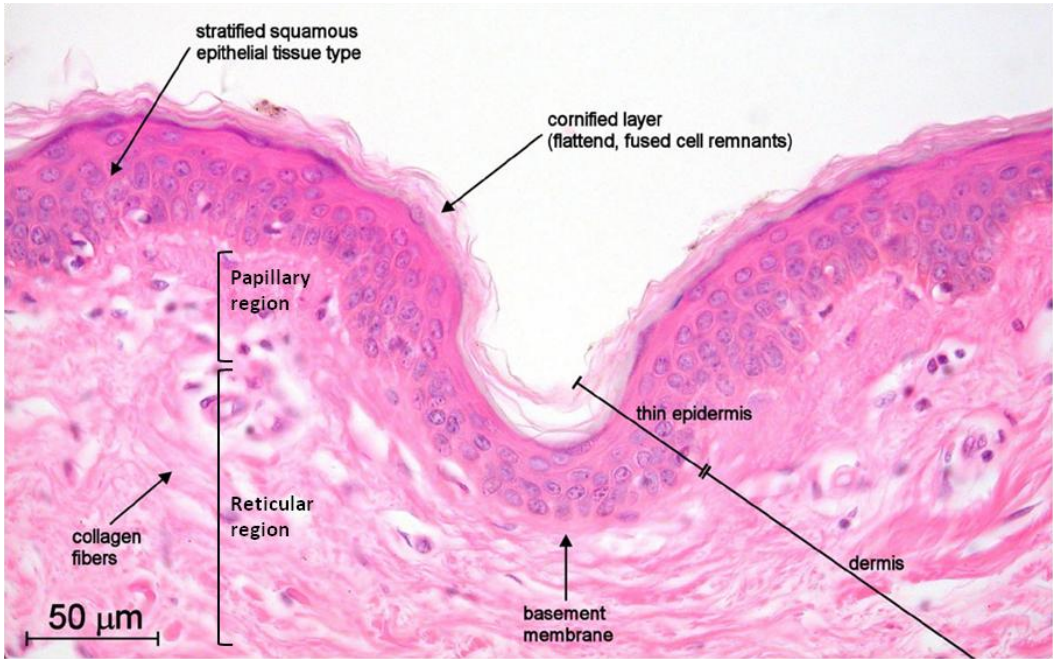

Figure 1.2: Light micrograph of skin. The main components of the Figure are outlined. Figure adapted from http://www.microscopy-uk.org.uk/mag/imgaug02/HistPaper01_Fig2.jpg (undated)

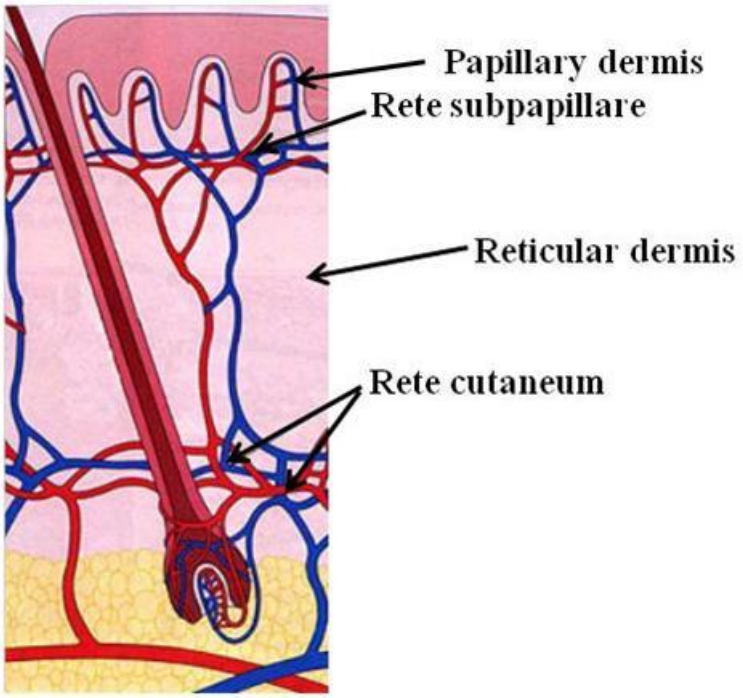

Figure 1.3: A schematic representation of the vasculature in human skin. Figure adapted from http://cai.md.chula.ac.th/lesson/lesson4410/data/image_s17.jpg (undated).

1.2.2.1 Fibrous components of the dermis

Collagen

Collagens are the main fibrous component of skin, bone, ligament and cartilage. Although more than 20 genetically distinctive collagens have been reported, collagens I, III and V are the most represented in the dermis with the first one counting for the 80-90% of the entire collagen weight (Haake 2001). Collagen VI is also a fundamental component of the dermal connective tissue and it is mainly located within the papillary dermis, the matrix surrounding blood vessels, the nerves, the epidermal appendages and the dermo-epidermal junction (Kielty and Shuttleworth 1997).

The protein collagen consists of a 300 nm long triple helical complex constituted by three polypeptide α chains, each chain containing approximately 1000 residues (Kadler 1996). Collagen is produced by fibroblasts in the form of a soluble precursor termed tropocollagen, which undergoes enzymatic hydroxylation and glycosylation before being released as an insoluble product into the extracellular space. Outside the cells, tropocollagens molecules are enzymatically cleaved by collagen

metalloproteinases. Several molecules align and interact covalently with each other to aggregate into banded collagen fibrils, which can be detected by light microscopy. These are attached to proteoglycan molecules, which are thought to stabilise the collagen structure (Montagna 1974).

Elastin

Elastic fibres extend from the dermo-epidermal junction to the bottom of the dermis and are also associated to blood vessels and hair follicles. Their main function resides in providing elasticity to the skin due to their capability of stretching and deforming under a specific mechanical stress and reverting to the original shape once the stress is relieved.

Two main components can be identified in the elastic fibres: one inner amorphous portion composed by the insoluble protein elastin and an outer portion consisting of different non elastic protein microfibrils (Barry 1983b). The microfibrilis are constituted by a variety of glycoproteins, with fibrillin, a 350 kDa molecule, being the most characterised (Sakai et al. 1986). Elastin is produced by the dermal cells in the form of the soluble precursor tropoelastin. Similarly to collagen, tropoelastin molecules undergo enzymatic modifications before aggregating into insoluble elastin complexes (Montagna 1974).

Reticulin

Reticulin fibres present in minute amount in the dermis are composed by an assembly of collagen I and III fibres and fibronectin (Kanitakis 2002).

1.2.2.2 Non-fibrous component of the dermis: the 'ground substance'

The 'ground substance' is a 'gel-like' milieu where the different constituents of the dermis (connective fibres, cells, cutaneous vasculature, nerve fibres and skin appendages) are embedded. It also contains water, proteins, sugars and electrolytes derived from the blood vessels as well as metabolic products of the dermal cells such as proteoglycans and glycoproteins (Montagna 1974). The 'gel-like' composition of this matrix facilitates migration of cells through this cutaneous layer. Proteoglycans are large (100-2500 kDa), hydrophilic compounds formerly constituted by

glycosaminoglycans attached to a core protein (Kanitakis 2002). The protein is specific for each proteoglycan and determines which compound will be incorporated in the complex. Glycosaminoglycans consist of 100 up to 5000 monosacharide residues organised into repeating disaccharide units. Each unit is usually constituted by a molecule of glucuronate or galactose linked to hexosamine. Negative charges are distributed along the entire length of the units in the form of either carboxyl or ester sulphate groups (Montagna 1974). Various glycosaminoglycan types have been identified in the 'ground substance', such as hyaluronate, chondroitin 4 or 6 sulfate, dermatan sulphate and heparin sulphate, with the first two types being the most abundant. Although glycosoaminoglycans exist in the dermis as proteoglycans, the hyaluronate is generally not linked to any protein and it is therefore mostly present in the form of glycosaminoglycan alone. Different species of proteoglycans (such as biglycan, versican, decorin) have been detected in the skin and their distribution varies between the two layers of the dermis (papillary and reticular layers) (Haake 2001). Decorin for example is largely expressed in the papillary layer, whereas versican is produced at higher level in the underlying reticular layer (Sorrell and Caplan 2004). The extremely large size of the proteoglycans complexes and thus the high number of hydrophilic chains control the water content of the dermis and affect the compressibility of the skin. Due to the presence of these molecules, the dermis is the most hydrophilic compartment of the skin, being composed of 70% water in comparison to 10-25% of the epidermis (Amorosa 1998b). Proteoglycans also interact with cytokines and growth factors and are therefore implicated in stimulating inflammatory responses, tissue repair and cell proliferation (Oh et al. 2011).

1.2.2.3 Cellular populations in the dermis

Fibroblasts, the most abundant cells in connective tissue, are responsible for the synthesis of the main components of the dermis (i.e., collagen, elastin fibres and the 'ground substance'). Structurally fibroblasts are characterised by a large nucleus, well-developed endoplasmic reticulum and Golgi apparatus and numerous cytoplasmic filaments. In particular, the Golgi apparatus is believed to represent the site of production of polysaccharides in the dermis and to also mediate collagen secretion from the cytosol to the extracellular space (Montagna 1974).

Although the majority of fibroblasts are localised within the papillary dermis and around the cutaneous vessels, dermal cells can also be found within the reticular layer in the spaces between the collagen bundles (Haake 2001). Fibroblasts are also known to be involved in tissue repair, wound healing and inflammatory process (Haake 2001). Other cells populations are dendritic cells, macrophages and mast cells. Dendritic cells and macrophages are immunocompetent cells of the skin and constitute, together with the Langherans cells in the epidermis, the cutaneous immune system (Roberts 1998). As such, their main function resides in detecting allergens in the skin and presenting these agents to T-lymphocytes in the cutaneous lymph nodes (German 2005; Merad et al. 2002). Mast cells secrete specific mediators that play a key role in stimulating allergic reactions, phagocytosis and others functions in the skin (Haake 2001).

1.2.3 The sweat glands

Human skin contains approximately 3-4 million sweat glands (Saga 2002) located in the deep region of the dermis at the border with the subcutaneous fat (Figure 1.1). They can be divided into apocrine, so called as they produce a secretion by pinching-off the apical part of the glandular cells, and eccrine glands, where secretion is produced as a liquid with no disintegration of the glandular cells (Sato et al. 1989).

Eccrine sweat glands

The human body contains 1.6 to 4 million eccrine sweat glands evenly distributed over the body surface except for specific anatomic sites such as the genital areas, lips, and external ear canal. The density of the glands differ according to individuals and anatomic sites with an average density estimated at approximately 200 glands per cm^2 (Wilke et al. 2007). Sites of greatest distribution are the palms, soles, axillae and forehead. Sato *et al.* (1989) reports a surface area density of i) 64 sweat glands/cm^2 on the back, ii) 108 sweat glands/cm^2 on the forearm, iii) 181 sweat glands/cm^2 on the forehand and iv) 600-700 sweat glands/cm^2 on palms and soles. Moreover, eccrine sweat glands in the palmar and plantar skin have larger dimensions than the rest of the body. In all areas however these glands cannot be seen with the naked eye as they have a dimension ranging between 0.05 and 0.1 mm (Hurley 2001).

The eccrine sweat glands consist of a simple tubular epithelium constituted by a ductal and a secretory component (Hurley 2001). While the secretory component is a tubule located in the deep dermis, the ductal portion consists of a coiled segment, which extends into the dermis as a straight dermal duct before crossing the epidermis for its entire length (Figure 1.4). The ductal portion, 2-5 mm long, consists of two cell layers called basal (outer) and laminal (inner) layers. The secretory component has approximately the same length as the ductal portion and it is constituted by myoepithelial cells surrounding secretory cells (Saga 2002). Myoepithelial cells provide mechanical strength to the tubule wall and induce sweat expulsion from the secretory cells through contraction. Myoepithelial cells are restricted to the secretory portion of the glands as the coiled duct, the straight dermal duct and the intraepidermal duct are devoid of these cells (Ellis 1965).

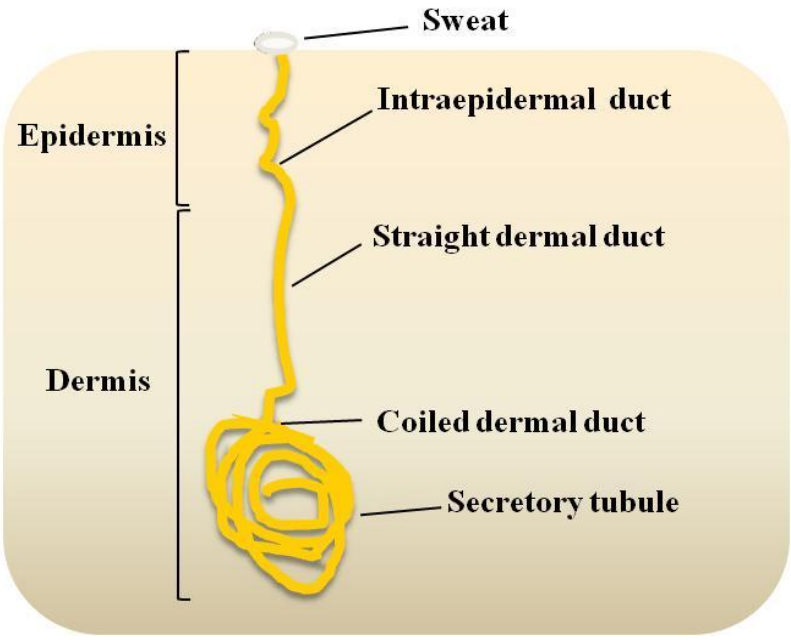

Figure 1.4: A schematic representation of the distinct portions of the eccrine sweat gland. The coiled portion in the deep region of the dermis consists of a secretory tubule and a coiled dermal duct. The long straight portion of the duct extends from the dermis into the epidermis. The sweat is released on the surface of the skin.

Eccrine sweat glands produce an odourless secretion, which is mainly composed of water and electrolytes. This secretion is delivered to the surface of the epidermis by

the intradermal duct, which connects the coiled gland with the intraepidermal portion and terminates with an open pore on the surface of the skin (Figure 1.4).

Sweat reduces body temperature by dissipating the heat by evaporation. Therefore, eccrine sweat glands play a key role in thermoregulation. Body temperature is extremely well controlled in mammals. Thermosensitive neurones, located in specific areas of the hypothalamus in the central nervous system (CNS), detect changes in core temperature and initiate appropriate responses to maintain the body temperature constant (~37 °C) (Wilke et al. 2007). These neurones are also stimulated by hormones, physical activity and emotions (e.g. fear or anxiety). Afferent impulses originated by peripheral thermo-receptors located in the skin and in the spinal cord further stimulate these neurones thus contributing to sweat production (Holzle 2002). Acetylcholine (Ach) is the main neurotransmitter involved in sweat gland activation. Cholinergic fibres surrounding the secretory tubule of the glands release the neurotransmitter into the synaptic space. Once released, Ach activates muscarinic receptors located in both secretory and myoephitelyal cells inducing sweat release (Kurzen et al. 2004).

Sweat secretion is believed to be triggered by an electrochemical gradient due to the numerous ion channels and ion transporters that have been detected in the secretory portion of the glands (Wilke et al. 2007). However, the exact mechanism by which this gradient is formed is still not completely understood. Excessive sweat production gives rise to hypersecretory disorders such as PFHH. This condition will be discussed in more detail in Section 1.3.

Apocrine sweat glands

The apocrine glands are less numerous than the eccrine sweat glands and are located predominantly in the axillae, the groin and in the pubic area (Sato et al. 1989). Although similar in structure to the eccrine sweat glands, apocrine glands contain coiled portions which are approximately ten times larger than the eccrine sweat glands and intradermal ducts which empty into a hair follicle (Hurley 2001). Contrarily to the eccrine sweat glands, they produce a viscous sweat that is rich in fats, and proteins and is characterised by a specific odour (Saga 2002).

Although the specific function of these glands is still poorly understood, it is believed that they act as scent glands to stimulate sexual attraction in mammals. These glands are not thought to be involved in PFHH (Grunfeld et al. 2009).

1.3 Primary Focal Hyperhidrosis (PFHH)

Primary Focal Hyperhidrosis (PFHH) is a chronic disorder characterized by an over-activity of the eccrine sweat glands, which results in excessive and uncontrollable sweating (Farrugia and Nicholls 2005). Although the exact pathogenesis of this condition is not clearly understood, evidence of a genetic link has been reported (Ro et al. 2002). PFHH has an onset during childhood or adolescence and occurs mainly on specific anatomic sites such as the axillae, palms, soles and craniofacial region, either alone or in combination (Hamm and Neumann 2009).

This chronic disorder has been estimated to affect approximately 1% of population in UK (Atkins and Butler 2002; http://www.nhs.uk 2011a) and 3-4% of population in USA (Grunfeld et al. 2009) and it has a noticeable impact on a patient's quality of life in terms of personal interactions, daily activities and work productivity (Hamm et al. 2006; Weber et al. 2005). A study assessing the quality of life of patients affected by PFHH revealed a Dermatology Life Quality Index (DLQI) score higher than other skin conditions such as acne vulgaris, psoriasis and vitiligo (Swartling et al. 2001).

Histological studies, comparing the morphology of the eccrine sweat glands in patients affected by PFHH with normal individuals, highlighted that neither the number, the dimension nor the structure of the glands appear to be modified (Bovell et al. 2001). This suggests that PFHH is more likely related to excessive neuronal stimulation more than structural abnormalities of the sweat glands.

1.3.1 Therapy options in PFHH

Different treatment options have been employed for PFHH. These therapies have been summarised as follows:-

Topical agents: Over the counter antiperspirants such as aluminium chloride salts are commonly used as first line therapy for the treatment of moderate cases of PFHH. They are usually used at a concentration of 15% (in aqueous solution thickened with methylcellulose) to treat hyperhidrotic armpits or at increased concentrations (i.e., 25-35%) for hyperhidrotic palms and soles (Hamm and Naumann 2009). These compounds are known to block mechanically the duct of eccrine sweat glands thus preventing sweat release (Hoorens and Ongenae 2012). This treatment has the

disadvantage of requiring daily applications, which often results in skin irritation and painful sensation. Moreover it is usually poorly effective for treating anatomic sites, other than the axillary region, such as the palms and the soles (Hamm and Naumann 2009)

The use of a topical anticholinergic such as 0.5-2% topical glycopyrrolate has also been reported (Kim et al. 2008; Sanchez et al. 2010). Although effective and generally well tolerated, the treatment relies on repeated applications due to the short lasting effect (i.e., euhidrosis was only reported for 2 days) (Kim et al. 2008).

Iontophoresis: Tap water iontophoresis (TWI) is an FDA approved treatment for palmo-plantar hyperhidrosis (Glaser et al. 2007c; Hoorens and Ongenae 2012). The treatment is generally performed by placing feet or hands into basins filled with tap water through which electric current (usually 15-20 mA) is applied for approximately 15-30 minutes with the aid of electrode devices (Reinauer et al. 1993). Although the mechanism by which TWI inhibits sweat production is not entirely known, it is believed that the electric current plugs the ducts of the eccrine glands with ions, thus obstructing sweating secretion (Karakoc et al. 2002). As a non-invasive technique, it is generally the treatment of option for patients for whom the topical agents have not produced an acceptable therapeutic effect. Even if effective, it has the disadvantages of requiring long and repeated treatments. A range of 6 to 10 treatments are usually required to produce a significant sweating reduction, with the need to repeat the procedure every 1 to 4 weeks to maintain the therapeutic effect (Hamm and Naumann 2009). Additionally, TWI is usually associated with side effects such as erythema, pain sensation, skin burning and vesicular formation (Karakoc et al. 2002). Moreover, although TWI has been reported to be effective for palmo-plantar PFHH (Dahl and Glent-Madsen 1989; Glaser et al. 2007c; Shrivastava and Singh 1977), practical considerations limit its use for other forms of PFHH.

Anticholinergics such as glycopyrrolate or hexopyrronium bromide administered through iontophoresis have shown to prolong the anhidrotic effect compared to TWI (Abell and Morgan 1974; Dolianitis et al. 2004) However, systemic side effects related to the anticholinergic activity of these drugs (i.e. blurred vision, urinary retention, constipation, dry mouth and others) have been reported (Abell and Morgan 1974).

Oral drugs: Anticholinergic drugs (i.e.,glycopyrronium and propantheline bromide) administered orally have been shown to significantly reduce the secretion of sweat. However, the emergence of systemic side effects has limited their use in clinical practice (Bajaj and Langtry 2007). These drugs are not licensed in the UK for the treatment of PFHH and none has been clinically assessed for this indication (Glaser et al. 2007c).

Other oral agents such as benzodiazepines, anxiolytics and β-blockers have been used for patients with PFHH triggered by stress and anxiety (Praharaj and Arora 2006). However, the first two types of medications can be considered advantageous only if administered for short periods, due to their sedative effect and the potential to induce dependency (Atkins and Butler 2002).

Botulinum toxin A (BTX A) by intradermal injection: BTX-A (serotype A of *Botulium* toxin) has been officially licensed in the UK since 2004 for the treatment of axillary PFHH, becoming a valid alternative treatment for patients for whom topical treatments have failed (Price J. 2008a). This alternative treatment is discussed in greater details later in this Chapter (Section 1.5). Delivery of BTX A by iontophoresis and phonophoresis will also be discussed (Section 1.5.3).

Surgical treatments:

1. **Sweat gland excision**. Surgical removal of the eccrine sweat glands from the armpit regions of patients affected by axillary PFHH has represented the most effective method to achieve a euhidrotic state. However, this treatment has largely been abandoned due to the high incidence of complications reported (i.e. impairment of arm movement, infections, extensive scars and haematomas) (Hoorens and Ongenae 2012).
2. **Endoscopic Transthoracic Sympathectomy (ETS)**. Although highly effective, ETS represents the most invasive surgical treatment for PFHH. This procedure involves surgical interruption of the cholinergic message from the ganglia to the cholinergic nerve endings, thus resulting in block of glandular secretion (Atkinson et al. 2011). ETS has most commonly been employed for the treatment of palmar and plantar PFHH as its use for axillary and facial hyperhidrosis has been reported as less effective (Hamm and

Naumann 2009, Smidfelt and Drott 2011). Common drawbacks associated with this procedure are the occurrence of surgical complications as well as the appearance of compensatory sweating in areas not previously affected by PFHH (usually the back, the abdomen and the legs), some months after the treatment (Lin et al. 2001a). Therefore, this treatment it is usually reserved for those individuals who have not responded to all the other therapeutic options (Hamm and Naumann 2009).

1.4 Botulinum toxin: structure and function

Botulinum toxin (BTX) was first identified in the 19th century (Van Ermengem 1897), as the product of the bacterium *Clostridium botulinum* and the causative agent of 'botulism' (Erbguth 2009). This is a clinical condition characterized by reduction of motor capacity that can progress to respiratory paralysis and death (Pinder 2007).

Different strains of *Clostridium botulinum* produce different serotypes of BTX, classified with the letter A through G (Dolly and Aoki 2006). All toxin serotypes have the same mechanism of action. They prevent the release of acetylcholine (Ach) by the cholinergic fibres into the pre-synaptic space, thus inducing muscular paralysis and blockade of glandular secretion. The duration of the effect is transitory. Recovery of the neurotransmission is eventually re-established through nerve regeneration and secretion of new Ach within about 3 months (De Paiva et al. 1999).

The toxin consists of a single-chain polypeptide of molecular mass 150 kDa which is inactive or partially active until cleaved by specific proteases either produced by the bacteria or the intoxicated organism (Dressler and Bigalke 2009). Once cleaved, the activated BTX consists of two chains: one light chain of 50 kDa and one heavy chain of 100 kDa. Both chains are connected by a disulphide bond, and non-covalent interactions. The integrity of the disulphide bridge is essential for the activity of the toxin making this compound extremely fragile to high temperatures (e.g. temperatures higher than 90°C denaturate the toxin in few minutes (Jay 2005)).

The 100 kDa-heavy chain mediates binding of the toxin to the surface of pre-synaptic nerves and subsequent internalisation of the toxin by endocytosis (Arnon 2001) (Figure 1.5). The 50 kDa-light chain contains a zinc-dependent protease that recognises specific membrane proteins called **s**oluble **n**-ethylmaleimide-**s**ensitive-factor **a**ttachment **re**ceptor (SNARE) proteins (Arnon 2001). These proteins

aggregate in a fusion complex, which is responsible for exocytosis of the neurotransmitter Ach from the nerve endings to the synaptic space. In particular, BTX A cleaves specifically the 25 kDa synaptosome-associated protein (SNAP-25), while other BTX serotypes recognise different proteins of the complex (Figure 1.5). This results in inhibition of Ach release from the nerve endings with subsequent block of muscle contraction and glandular secretion.

When released by bacteria the toxin is non-covalently associated with accessory proteins to form a macromolecular complex, the botulinum complex, with a molecular weight of up to 900 kDa. These accessory proteins are non toxic protein components consisting of haemagglutinins (HA) and non toxic non haemagglutinin (NTNH) proteins (Simpson 2004).

The presence of these proteins seems to play a key role in the process of oral intoxication due to their capability to protect the toxin from the extreme conditions in the gut (i.e., low pH and presence of proteolytic enzymes) (Simpson 2004). These proteins dissociate at physiological pH. This implies that the toxin should be released from the complex once it has entered the systemic circulation. Thus, accessory proteins assist migration of the toxin to the ultimate targets of the neuronal cells.

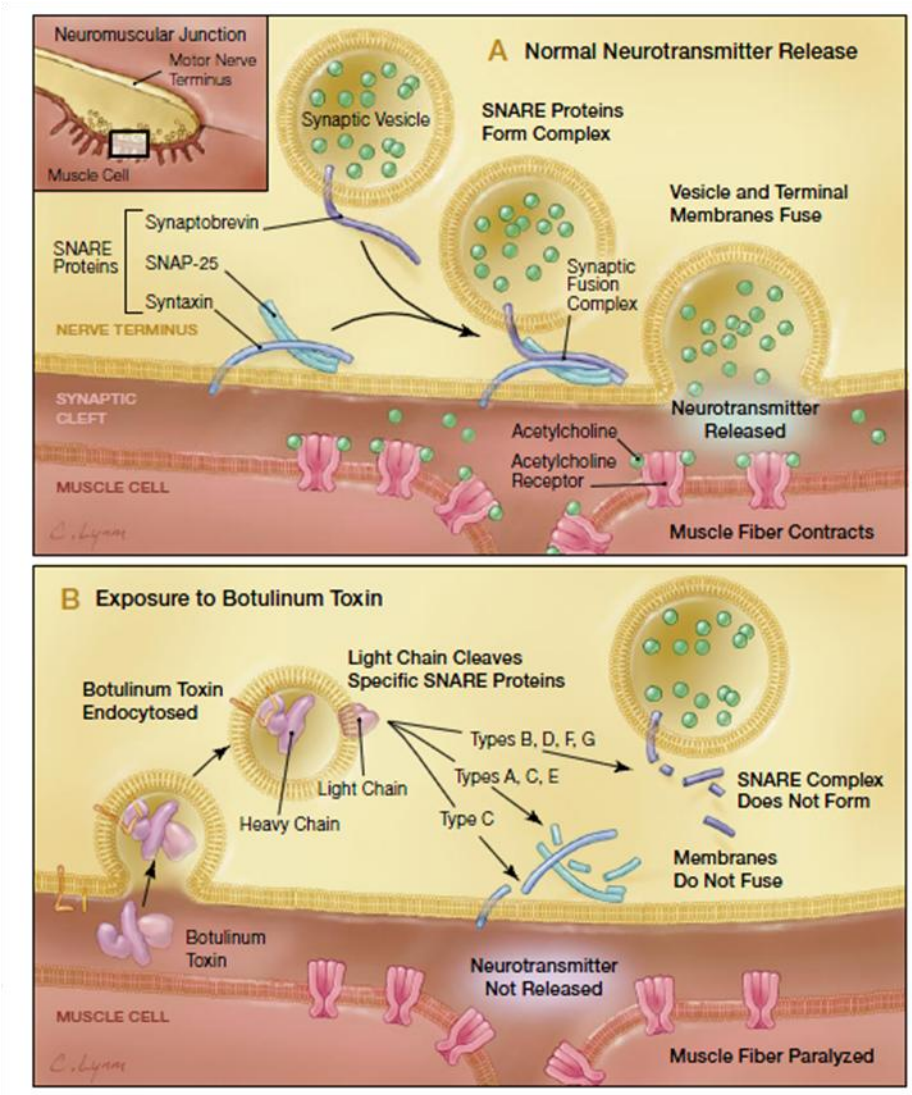

Figure 1.5: The mechanism of action of botulinum toxins (BTXs) (A) The fusion complex SNAREs (consisting of the proteins Synaptobrevin, SNAP-25 and Syntaxin) mediate exocytosis of the neurotrasmitter Ach to the synaptic cleft. Once released, Ach binds receptors specifically located on muscle/glandular cells. **(B)** BTX is internalised into the nerves by endocytosis following interaction of the heavy chain of the toxin with specific membrane receptors. The light chain of BTX cleaves specific SNARE proteins preventing formation of the synaptic fusion complex and thus blocking Ach release. In particular, BTX A, C and E cleave SNAP-25, BTX B, D, F and G cleave Synaptobrevin and BTX C cleaves Syntaxin. This results in block of muscle contraction and glandular secretion (only muscle fibre is illustrated in the Figure). Figure adapted from (Arnon 2001).

The discovery that BTX was able to reduce muscle activity by blocking the release of Ach was made in 1949 (Price J. 2008a). Since that time, many studies have been performed in order to evaluate the structure and mechanism of action of BTX and to exploit its properties for therapeutic purposes. Among the different BTX serotypes isolated, only types A and B are clinically used. Type A (BTX-A) is the most extensively employed, being the serotype with the longer duration of action (ranging from 3 to 6 months) (Dolly and Aoki 2006).

Many different BTX products are currently available in the market for the treatment of neurological disorders involving involuntary muscle contraction and excessive glandular secretions. The different BTX drugs, as well as their therapeutic applications, are discussed in greater detail in the following Section.

1.4.1 Commercially available botulinum toxin formulations

Five BTX drugs are currently available in the market (Price J. 2008b), four of these contain BTX A (Xeomin®, Dysport®, Botox® and Vistabel®), and only one BTX B (Neurobloc®) (Table 1.1). The latter is commercialised as Myobloc® in USA and Canada and it is generally used for those patients who have developed an immune response against the serotype A (Truong and Jost 2006).

Table 1.1: **Different BTX products currently available in the market and their licensed therapeutic applications.**

Product and licensed date	Serotype	Manufactured by	Licensed indications	Available in UK?	Molecular weight (kDa)
Botox® (1989)	A	Allergan Inc (Irvine California, USA)	Blepharospasm, Hemifacial spasm Cervical dystonia Upper limb spasticity Chronic migrane **Hyperhidrosis**	Yes	900
Vistabel® (2006)	A	Allergan Inc	Glabellar lines	Yes	900
Dysport® (1990)	A	Ipsen Ltd (Berkshire, UK)	Blepharospasm Hemifacial spasm Cervical dystonia	Yes	~ 500
Xeomin® (2005)	A	Merz Pharmaceuticals (GmbH, Frankfurt, German)	Blepharospasm Cervical dystonia Focal spasticity	Yes*	150
NeuroBloc®/**Myobloc**® (2001)	B	Eisai Co., Ltd. (Tokyo, Japan) in Europe, Solstice Neuroscience Inc in USA and Canada	Cervical dystonia	Yes	600

*Only for the treatment of glabellar lines (Dressler 2012)

Other BTX A drugs include Hengli® (Lanzhou Institute of Biological Products, Lanzhou, Gansu Province, China), distributed in some Asian and South American countries with the commercial name of CBTX A or Prosigne® and Neuronox® (Medy Tox, Ochang, South Korea) sold in Korea and in some other Asian countries (Dressler and Bigalke 2009).

Indications for BTX products currently licensed in Europe, including conditions such as cervical dystonia, strabismus and PFHH, are outlined in Table 1.1. PFHH will be discussed in greater detail in the following Section (1.5). Off label use is extremely extensive and comprises: i) neurological disorders (such as various forms of focal dystonias (Truong 2012), tremors and focal spasticity (Das 2009; Truong and Jost 2006)), ii) urological and gastrointestinal defects (such as overactive bladder (Denys et al. 2012) and anal fissure with associated constipation (Keshtgar et al. 2009)), iii) skin related conditions (i.e., dyshidrotic hand eczema, inverse psoriasis, pachyonichia congenital (for a review see (Feily et al. 2011)), iv) various hypersecretory defects (i.e., Frey syndrome (De Bree et al. 2009) and hot flushes in menopausal patients (Yagima Odo et al. 2011)) and v) numerous conditions of pain (i.e., musculoskeletal pain (Benecke et al. 2011) and headache (Silberstein 2009)).

Beside the therapeutic use, BTX A represents the most common aesthetic procedure employed in the world, with millions of treatments performed every year in the USA (www.surgery.org). For cosmetic uses, the toxin is intramuscularly injected to facial muscles to reduce the appearance of wrinkles located on the forehand (glabellar lines), on the periocular region (‘crow’s feet’) or around the lips (Ghalamkarpour et al. 2010; Sposito 2002).

1.4.1.1 Characteristics of different botulinum toxin products

Clinically approved BTX products contain various protein complexes, consisting of the 150 kDa BTX associated to non toxic accessory proteins (as mentioned above). This results in different molecular weight BTX dugs. For example, Botox® (manufactured by Allergan) is produced in the form of a 900-kDa complex, whereas Dysport® (manufactured by Ipsen) comprises only a small proportion of the 900-kDa complex and it is mainly constituted by various molecular weight BTX A complexes (ranging between 500 and 700 kDa). Conversely, Xeomin® (manufactured by Merz) contains only BTX A in the form of the naked toxin (150 kDa) (Aoki et al. 2006).

Although complexing proteins increase the size of the neurotoxin, studies comparing diffusion of different BTX drugs within target tissues have not highlighted any significant differences in the extent of toxin diffusion between Xeomin® and Botox® when delivered either to skin (Dressler 2009) or muscles (Carli et al. 2009; Hexsel et al. 2008). This seems to be associated with a rapid dissociation of the BTX complex at physiological pH (Eisele and Taylor 2008), so that diffusion would depend exclusively on the size of the naked toxin (150 kDa), which is the same for both BTX drugs. Nevertheless, a recent study indicated that dissociation of the BTX complex occurs within the therapeutic preparation itself (Eisele et al. 2011) and therefore BTX would be delivered within the tissue already in its naked form.

All the BTX drugs differ in terms of excipients and dose of neurotoxin (Price J. 2008a) as outlined in Table 1.2. Excipients used include sucrose or lactose as a means to maintain conformation of the toxin, human serum albumin (HSA) to prevent it from aggregating on to the wall of vial or other surfaces and specific buffer systems (Carruthers and Carruthers 2008; Panicker and Muthane 2003). The reduced pH (5.6) of Myobloc®/Neurobloc® in comparison to the other BTX drugs (pH= 7.4) has been associated with a more intense pain at the injection site (Dressler et al. 2002; Yamauchi and Lowe 2004). All BTX preparations, except for MyoBloc®/NeuroBloc®, consist of a powder to be reconstituted with 0.9% w/v $NaCl/H_2O$ (saline solution) and stored at refrigerated conditions (below 8°C). All BTX drugs have a shelf life ranging between 24-36 months when stored at 4-8°C (i.e. Dysport® shelf life is equal to 24 months, whereas Botox® and Myobloc®/Neurobloc® is 36 months), with the exception for Xeomin®, which is stable for at least 48 months at room temperature (Dressler 2012).

Significant differences between BTX drugs are related to their biological activity, expressed as a mouse unit (MU) (or simply in units (U)), defined as the dose of toxin that is able to kill 50% of a mouse population following intraperitoneal injection with a BTX drug (Dressler and Bigalke 2009). As the assay methods used to determine the activity vary among the different BTX drugs manufactures, the activity labelling of the drugs cannot be compared directly. The potency of Botox® has been reported to be identical to Xeomin® (i.e, 1 MU of Xeomin® is clinically equivalent to 1 MU of Botox®) (Dressler et al. 2008), whereas the potency of Dysport® has been estimated to be approximately 1/3 (Ranoux et al. 2002) or 1/4 of Botox® (Moreau

2003). As a consequence of the numerous differences between the product formulations, the BTX drugs are not interchangeable.

Table 1.2: Characteristics of different BTX products currently available in the market.

Brand name	Generic name	Units per vial	Dose (ng) per vial	Form	pH	Dose of excipients per vial
Botox®	Onabotulinum toxinA	100	5	Vacuum dried	7.4	HSA 500 µg, NaCl 900 µg, buffer system.
Vistabel®		50	2.5			
Dysport®	Abobotulinum toxinA	500	12.5	Lyophilised	7.4	HSA 125 µg, lactose 2500 µg, buffer system.
Xeomin®	Incobotulinum toxinA	100	0.6	Vacuum dried	7.4	HSA 1 mg, sucrose 4.7 mg, buffer system.
NeuroBloc®/MyoBloc®	Rimabotulinum toxinB	2500, 5000 or 10000 (5000/ml)	25, 50 or 100	Solution	5.6	HSA 0.5 mg/ml, NaCl 0.1M, disodium succinate 0.01M, H_2O, HCl.

1.5 BTX products for the treatment of PFHH

As previously mentioned (Section 1.3), Botox® represents the sole BTX A preparation currently licensed in the UK for the treatment of axillary PFHH. Botox® approval was based on a large double-bind, placebo-controlled trial that clearly indicated the beneficial effect of BTX A, through inhibition of excessive sweat secretion and improvement in quality of life, in patients affected by axillary PFHH (Naumann and Hamm 2002; Naumann et al. 2001). The treatment was successful in 82%-94% of the patients treated and lasted for several months.

Nevertheless, a large variety of published studies have documented the suitability of Botox® as a means to reduce sweat secretion in hyperhidrotic sites other than the axillary region, such as palms (Gregoriou et al. 2010; Naver et al. 1999, 2000; Shelley et al. 1998), soles (Campanati et al. 2003), trunk (Hexsel et al. 2009; Kim et al. 2009a) and cranio-facial region (Geddoa et al. 2008; Hexsel et al. 2008; Komericki and Ardjomand 2012; Trindade de Almeida et al. 2007). The efficacy of BTX A at these sites, assessed both subjectively and quantitatively, has been reported to be as high as axillary PFHH (around 80-90%).

Although Botox® remains the most widely studied preparation for PFHH, reports have indicated that this condition can be successfully treated by using other BTX drugs i.e. Xeomin® (Dressler 2009), Dysport® (Moreau 2003) and Neurobloc®/Miobloc® (Dressler et al. 2002; Yamauchi and Lowe 2004). Therapeutic effects, comparable to Botox®, have been reported by adopting specific dose ratios, due to the difference in the potency between different BTX drugs (Section 1.4.1). For example, in a study conducted by Moreau *et al.* (2003) a conversion factor of 1:4 was used for Botox® and Dysport® in the treatment of palmar PFHH. Conversely, in the studies reported by Dressler *et. al.* (2002) and Yamauchi and Lowe (2004) a ratio 1:20 was adopted for Botox® and Neurobloc®/Miobloc® for the treatment of axillary and cranial PFHH respectively. Conversely, due to the equivalency between Botox® and Xeomin® a conversion ratio of 1:1 was used to treat cranial, axillary and palmar PFHH (Dressler 2009).

1.5.1 Dose and injection grid of Botox® for PFHH

BTX administration for PFHH involves a grid of intradermal injections into the affected site(s). The number of injections depends on the size of the area to be treated, on the anatomic differences among individuals and on the severity of the hypersecretory disorder (Glaser et al. 2007b). These injections require high precision and necessitate administration by trained personnel in hospitals and specialist centres.

For the treatment of axillary PFHH, Allergan (http://www.allergan.com/index.htm 2011) recommends to dissolve the entire vial of Botox® (100 U of toxin = 5 ng) in 4 ml of 0.9% preservative-free sterile saline solution. Each armpit is subsequently treated with 50 U (2.5 ng) of toxin injected intradermally by using a 30 gauge needle, in 0.1-0.2 ml aliquots, uniformly distributed in 10-15 sites, spaced 1-2 cm apart. The monograph suggests to insert the hypodermic needle to a 2 mm depth and to orientate it at a 45° angle to the skin surface with the bevel faced up in order to prevent leakage of the formulation and maintain the needle within the dermis (http://www.allergan.com/index.htm 2011). However, in clinical practice the range of dilutions, the injected volumes and the number of injections are varied according to the severity of the sweating and the personal preferences of the physician (Glaser et al. 2007b). Dilution volumes ranging between 1.5-5 ml, distributed in aliquots of 0.05-0.1 ml, have most frequently been reported (Campanati et al. 2003; De Almeida et al. 2011; Glaser et al. 2007b; Gulec 2012; Talarico-Filho et al. 2007). Conversely, injection volumes larger than 0.1 ml have been less commonly been employed due to their higher potential to diffuse to unwanted areas (such as the muscles) or to extrude from the injection site (Glaser et al. 2007b).

Although the Botox® monograph recommends the use of preservative-free saline to reconstitute the drug, studies have indicated that preserved saline can be used to reduce injection pain (Alam et al. 2002). Moreover, Gulec *et al.* (2012) reported reduction of pain when reconstituting the preparation Botox® with preservative-free saline previously mixed to the anaesthetic lidocaine.

Similar procedures and techniques are usually employed to treat palms and soles, although the latter usually requires larger doses. Botox® doses ranging between 25-220 U (corresponding to a mass of toxin of 1.25-11 ng) have been administered per hand (fingers included) by a number of 5-50 injections for palmar PFHH (Figure 1.6

B) (Glaser et al. 2007c; Holmes and Mann 1998; Lowe et al. 2002; Naver et al. 1999). Plantar PFHH has been treated by administering a range of 50-180 U (i.e., 2.5-9 ng) of toxin per sole distributed in 15-50 sites (Figure 1.6 A) (Campanati et al. 2003; Vadoud-Seyedi 2004). Studies regarding the treatment of PFHH in the craniofacial region have indicated BTX A doses ranging between 20-100 U (0.1-5 ng) can be administered to a specific area of the face (i.e. the forehead or the nose) by a series of 20-30 injection (Geddoa et al. 2008; Glaser et al. 2007a; Tan and Solish 2002). Due to the temporary ability of BTX to block sweat production, the treatment has to be repeated every 4-6 months (Hamm and Naumann 2009).

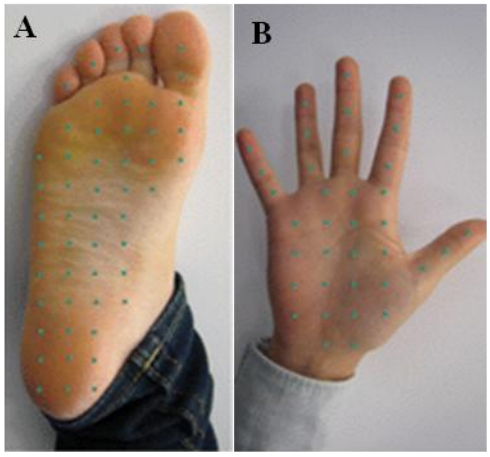

Figure 1.6: Injection grids for plantar (A) and palmar (B) PFHH. The areas to be treated are highlighted with a marker pen (blue dots in the images). These markings can be imaged as a grid of injection sites. Figures adapted from (Doft et al. 2012).

1.5.2 Side effects related to the administration of BTX A using conventional hypodermic needles

Due to the large number of injections required to effectively treat hyperhidrotic areas, administration of BTX is associated with intense pain and discomfort for the patient (Gulec 2012; Naumann et al. 1998b; Naver et al. 2000; Sanli et al. 2004). Studies have reported that pain is not only perceived during the injection procedure (as a consequence of needle penetration and liquid extrusion into the skin) but that it also persists up to 1-2 days in the treated areas (Saadia et al. 2001). Therefore, adequate anaesthesia is required to eliminate or alleviate pain when administering

BTX A, especially to sensitive areas such as the palms and soles. Nerve block is generally employed as local anaesthesia for hands and feet (Grunfeld et al. 2009) because it enables more precise injections and better comfort for the patients. This is usually performed by injecting 2-4 ml of lidocaine or mepivacaine 1-2% to block the ulnar and median nerves (wrist block) of the hand and the posterior tibial and sural nerves of the feet (Hamm and Naumann 2009). Conversely, topical lidocaine 4% is generally sufficient to induce adequate anaesthesia in other anatomic sites (i.e. facial and axillary region) characterised by a reduced skin thickness (Glaser et al. 2007a, b).

Potential risks associated with nerve blocking anaesthesia include vascular puncture and permanent nerve damage, especially for prolonged and repeated treatments (Campanati et al. 2004; Grunfeld et al. 2009; Hayton et al. 2003). Furthermore, the discomfort caused to the patient has to be taken into account. The duration of the anaesthesia lasts over 1 hour after the treatment and if feet or hands have been treated at the same time, the patient will require assistance for several hours after the procedure.

Vibration anaesthesia, administered with handled massagers or other similar devices, and cryoanesthesia, employing ice or cold packs of liquid nitrogen to numb the area before injections, do not generally provide sufficient analgesia, especially for plantar PFHH due to the thicker stratum corneum on the soles (Glaser et al. 2007b; Grunfeld et al. 2009; Yamashita et al. 2008). The use of MED-JET® MBX (Medical International Technologies, Montreal, QC, Canada), a needle free device that utilises air pressure to inject a drug formulation, has also been reported to deliver lidocaine 2% to hyperhidrotic palms and feet (Benohanian 2007). However, this device has the disadvantage of requiring a large number of injections (i.e. an average of 50 injections in the palm and 30 in the sole) to induce an appropriate analgesic effect. The use of a similar device (commercialised as Dermojet®) has also been reported for intradermal delivery of BTX A (Botox®) and will be discussed in greater detail in Section 1.5.3.

Muscle weakness

The most common side effect associated with BTX A treatment is a temporary weakness of muscles adjacent to the injection. Muscles weakness usually occurs contemporaneously to the reduction of sweat (generally 1 week after the treatment)

and lasts for 4-8 weeks. This has most frequently been reported for palmar (Naver et al. 2000; Saadia et al. 2001; Sevim et al. 2002) and forehead PFHH (Kinkelin et al. 2000; Tan and Solish 2002) usually resulting in weakened pinch between the thumb and index fingers and partial disability in frowning or wrinkling the muscles of the forehead. Conversely, only one study in the published literature has reported the emergence of weakness of the muscles in the soles of the feet (Sevim et al. 2002).

Muscle weakness seems to be correlated to the number of injections, volume and dose used and to the difficulty in controlling the injection depth when performing the intradermal injection using the Mantoux technique (Glaser et al. 2007b). Published studies reporting the use of hypodermic needles with a reduced exposed length (i.e. ~2-3 mm) have indicated reduction or absence of muscular weakness in treated palms (De Almeida et al. 2001; Zaiac et al. 2000). In particular, De Almeida *et al*. (2001) reported the use of a device adapted from a cartridge rubber used in dental syringe, to reduce the length of a 30 gauge hypodermic needle from 7 to 3 mm. Although a better control of injection depth was achieved, the BTX A treatment still required nerve block anaesthesia in the palms to reduce the pain at the injection sites.

Soreness and dry skin

Another side effect related to BTX administration is soreness at the injection sites. This has occurred in BTX treated palms and it has required application of moisturizers to reduce the discomfort (Naver et al. 2000).

Systemic effects

Systemic adverse effects related to the anticholinergic activity of BTX (blurred vision, dry mouth, constipation, urinary retention) have not frequently been reported and are more likely related to the use of BTX B (Neurobloc®/Miobloc®) (Dressler et al. 2002).

Bleeding and loss of drug formulation

Other events, typically associated with intradermal administration by conventional needles and syringes, are bleeding at the injection site (Hexsel et al. 2008; Trindade de Almeida et al. 2007) and extrusion of some formulation (Glaser et al. 2007b). Presence of blood during BTX administration represents a professional hazard as it exposes personnel to needle stick injuries and thus to potential infections such as

HIV and hepatitis. Additionally, loss of drug formulation during administration determines waste of expensive material and reduction of dose accuracy.

1.5.3 Use of less invasive methods for intradermal delivery of BTX A

Due to the considerable pain and discomfort associated with BTX treatment and the need to repeat the procedure every 4-6 months, efforts have been made to reduce the invasiveness of the treatment, but success has been variable (Collins and Nasir 2010; Glogau 2007; Vadoud-Seyedi 2004).

A limited number of published studies have reported intradermal delivery of BTX A by iontophoresis for the treatment of palmar PFHH (Andrade et al. 2011; Kavanagh 2006). Davarian (2008) indicated that palms treated by BTX A administered by iontophoresis showed significant sweat reduction 1 week after the treatment and that dryness persisted for up to 12 weeks. On the contrary, iontophoresis of hands with normal saline showed reduction of therapeutic effect 3 weeks after the treatment. The treatment was associated with a good safety profile, as typical BTX A-related side effects such as hand muscle weakness were not reported.

The exact mechanism through which iontophoresis mediates cutaneous delivery of a non ionic, large compound such as BTX A, is not completely understood. It has been postulated that penetration of BTX A across the skin following application of an electric field may be determined by a combination of multiple factors such as: i) induction of a flux of liquid solvent containing the uncharged drug through pre-existing pores in the stratum corneum (electro-osmosis), ii) formation of new pores in the skin (electroporation) or iii) increase in size of pre-existing pores (such as hair follicles and sweat gland ducts) (Davarian et al. 2008). In particular, iontophoresis is believed to force BTX A down the sweat ducts and thus to facilitate direct interaction of the medicament with the sweat glands (Kavanagh 2006).

BTX A has also been delivered to palmar skin by phonophoresis, a technique which uses ultrasounds to enhance delivery of topically applied drugs (Byl 1995). There is only one study in literature reporting the use of this method for the delivery of BTX A for palmar PFHH (Andrade et al. 2011). Within this study, phonophoresis and electrophoresis were compared and used as a pre-treatment prior to topical application of Botox®, mixed with an emollient cream (carbopol cream 1%), on

hyperhidrotic palms. Improvements in sweating were reported for both techniques but only after 10 days of a 10 daily treatment session. The therapeutic effect was maintained over 16 weeks of follow up (after the end of the 10 days-treatment) without any occurrence of adverse effects.

In a study conducted by Chow and Wilder-Smith (2009), simple unassisted (without using iontophoresis or phonophoresis) transdermal penetration of BTX A was investigated in patients affected by palmar PFHH. For this purpose palms were exposed to a thermal lamp before topical application of a BTX A formulation (Botox®). The lamp was used as a means to increase opening of the pores through the heat and thus facilitate internalization of BTX A. The study failed to show significant sweat reduction, thereby demonstrating that BTX A cannot penetrate passively into the skin.

Other studies have reported the use of a needle-free, jet injector device (Dermojet®) to deliver a BTX A formulation for PFHH. The Dermojet® is a medical device consisting of an air driven injector which fires a liquid jet into the skin at high speed (http://www.robbinsinstruments.com/equipment/dermojet/modelg.html). The liquid perforates the stratum corneum barrier and penetrates to the internal layers of the skin. The Dermojet® has been commonly used for intradermal injection of local anaesthetics (Carpenter C. L. et al. 1965) as well as corticosteroids and bleomycin for the treatment of warts and keloids (Saray and Gulec 2005). This device has been used to deliver BTX A to hyperhidrotic palms, axillae (Naumann et al. 1998a) and soles (Vadoud-Seyedi 2004; Vadoud-Seyedi et al. 2000). However, in the study reported by Neumann (1998a) intradermal administration of BTX A by using Dermojet® was considerably less effective in reducing sweat production in comparison to conventional hypodermic needles. Moreover, the use of Dermojet® is not recommended for PFHH due to the high risk of damage to nerves and blood vessels in the palms (Vadoud-Seyedi 2004). Better results, in term of patient safety, were reported for BTX A administration into the soles of the feet due to the deeper location of blood vessels and nerves, in comparison to the hands (Vadoud-Seyedi 2004). Moreover, the treatment was reported to be effective for 80% of the patients and sweating cessation lasted for up to 6 months.

Topical application of BTX A formulations following combination with transport peptides and mixture with emollient creams has also been evaluated for PFHH as well as cosmetic applications (Brandt 2011; Collins and Nasir 2010). In a study

reported by Glogau (2007) axillary PFHH was treated with the BTX A cream RT001 (*Botulinum* Toxin Type A Topical Gel, Revance Therapeutic, Inc.). RT001 contains 200 U of BTX A (Botox®) non-covalently bound to a peptidyl transport system which enables cutaneous permeation of the toxin via a pinocytosis process (Collins and Nasir 2010). The study indicated a significant sweat reduction in BTX A treated axillae (200 U/per site) in comparison to the placebo-control axillae, four weeks after BTX A application (significant reduction of ~ 65% compared to the placebo-treated reduction of ~25%). In addition, RT001 application was not associated with systemic side effects, although local cutaneous reactions such as eczema and erythema were reported. Data regarding the duration of the effect were not reported in the study.

The variety of investigations seeking alternative BTX A delivery methods testifies that there is a clear need for a safer and less invasive administration method for this medicament. For this reason MDs are proposed as a minimally invasive device to facilitate cutaneous administration of BTX A.

1.6 Microneedle array devices (MDs)

A MD is somewhere between a hypodermic needle and a trans-dermal patch (Figure 1.7). The device consists of from 1 up to many hundreds of microneedles, generally ranging from 100 to 1000 μm in length and projecting from a solid planar support. A MD is designed to perforate the stratum corneum barrier to provide direct access for medicaments to the underlying epidermis or dermis.

By bypassing the stratum corneum, microneedles have significantly enhanced the cutaneous delivery of molecules, which could not normally be administered across the skin. Examples include i) small hydrophilic compounds (Gill and Prausnitz 2007a; Henry et al. 1998; Park et al. 2006), ii) peptides (Burton et al. 2011; Cormier et al. 2004; Wu et al. 2010), iii) proteins (Kim et al. 2009b; Matriano et al. 2002; Saurer et al. 2010), iv) oligonucleotides (Lin et al. 2001b), v) plasmid DNA (Birchall et al. 2005; Chen et al. 2010), and v) nano and microparticles (Coulman et al. 2009; Gill and Prausnitz 2007b; McAllister et al. 2003)

Microneedles are designed to successfully perforate the stratum corneum barrier without reaching the nerves fibres and blood vessels located in the more internal layers of the skin (Figure 1.8). MD insertion has been reported as minimally painful, effortless and blood free (Birchall 2006; Haq et al. 2009; Kaushik et al. 2001).

Therefore, MDs allow a safe and minimally invasive administration of medicaments and offer the potential of a self administration.

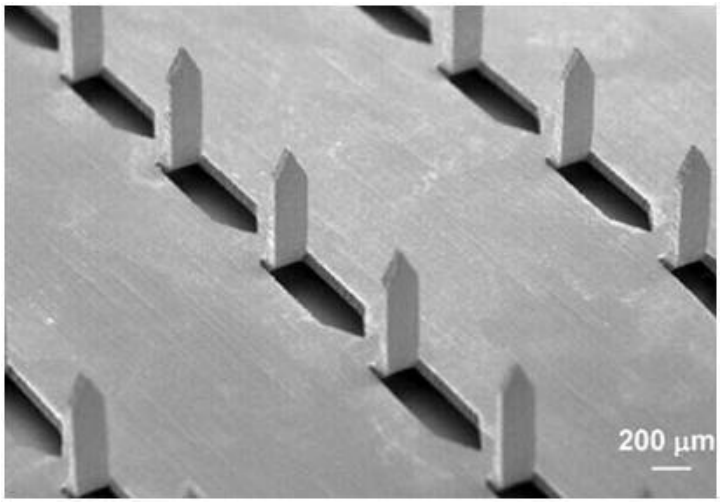

Figure 1.7: Appearance of a microneedle array device. Figure adapted from (Gill and Prausnitz 2007b)

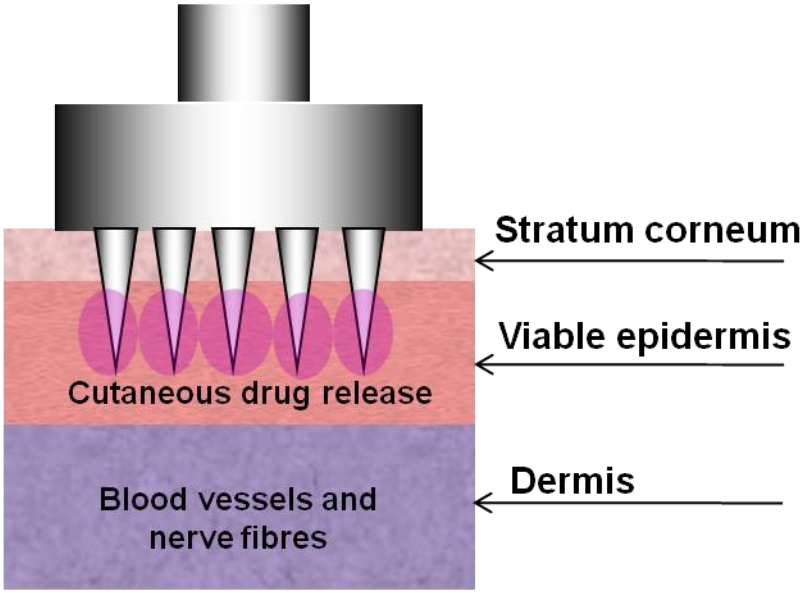

Figure 1.8: Schematic representation of the mechanism of action of a microneedle array device. The device perforates the stratum corneum providing direct access of drugs to the underlying viable epidermis, without reaching blood vessels and nerve fibres located in the dermis.

Although the first MD was proposed in the 1970s (Gerstel 1976), its practical application was only demonstrated in the 1990s as a consequence of advances in the microelectronic industry. The first MD, realized in 1998 by Dr Mark Prausnitz *et al.* at the Georgia Institute of Technology, consisted of an array of micron sized silicon

needles over a solid support (Henry et al. 1998). This study reported the first demonstration of drug delivery in human skin by using a microneedle array device.
Various materials, shapes and designs have been employed in the fabrication of microneedles. While initial microneedles were manufactured by using silicon as a material, (Arora et al. 2008), metals (steel, titanium and nickel-iron), glass and polymers have lately been employed (Birchall 2006).

1.6.1 Mechanism of action of different MD designs

Different designs of MDs have been produced, each one tailored to the specific application required (Figures 1.9 and 1.10). They can be summarised as follows:-

1. **Solid microneedles**. Usually constituted by silicon or metal, solid microneedles can either be pressed or scraped onto the skin and then withdrawn. Subsequently, a drug formulation can be topically applied to the MD treated skin. The drug will then diffuse through the microchannels to the underlying epidermis or dermis (McAllister et al. 2003; Wu et al. 2010).

2. **Solid coated microneedles**. The drug is encapsulated in a formulation that has been dry coated onto solid microneedles (Chen et al. 2009; Gill and Prausnitz 2007b; Widera et al. 2006). Following insertion of the array into the skin, the coated layer dissolves rapidly (within minutes) in the epidermis or dermis and the array is subsequently withdrawn.

3. **Dissolving microneedles**. Dissolving microneedles have been manufactured by using biodegradable or water-soluble polymers. Drug molecules have been incorporated within these microneedles for rapid or sustained release within the skin following microneedle application. Materials employed in the fabrication of this kind of microneedles include poly-L-lactide (PLA), polylactic-co-glycolic acid (PLGA) and copolymers of methylvinylether and maleic anhydride (PMVE/MA) for controlled drug release (ranging from hours to months) (Donnelly et al. 2011; Park et al. 2006) or sugars (i.e., carboxymethylcellulose (CMC), trehalose, maltose and sucrose) for rapid (within minutes) drug release (Lee et al. 2008; Martin et al. 2012).

4. **Hollow microneedles**. Hollow microneedles contain individual bores through which a drug solution can be infused in a manner similar to hypodermic injections. Infusion occurs through application of a specific pressure that is normally generated by a syringe, to which one single microneedle or an array or multiple microneedles can be attached (Alarcon et al. 2007; Van Damme et al. 2009). Syringe pumps (Gupta et al. 2009) and application springs (Burton et al. 2011) have also been reported to control the flow of the liquid through the needle bores. Hollow microneedles have also been employed as a microconduits through which a formulation can diffuse from a drug reservoir (Hafeli et al. 2009).

5. **Pocketed microneedles.** Pocketed microneedles are solid microneedles containing a central cavity within the needle shaft. They have been generally used to facilitate delivery of model drugs in a dry state in a similar manner to non pocketed solid microneedles (Gill and Prausnitz 2007b; Gill and Prausnitz 2008). The use of this specific microneedle design has not extensively been reported within the microneedle research community. As such, this represents a relatively novel approach to transdermal drug delivery. Characteristics of pocketed microneedles will be discussed in greater detail in the following Chapter.

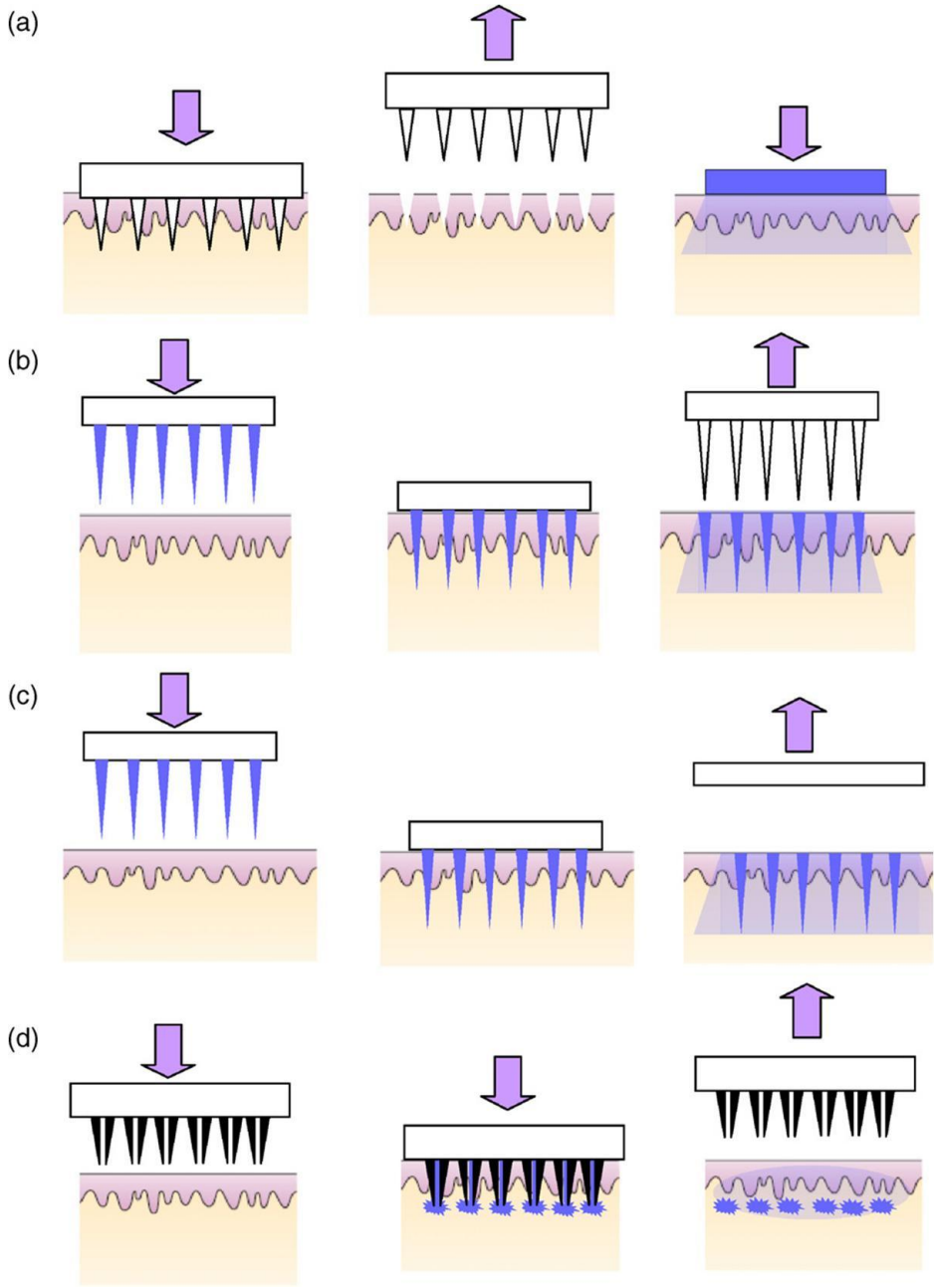

Figure 1.9: Schematic representation of mechanism of action of different designs of microneedles: a) solid microneedles for increasing the permeability of a drug formulation by creating micro-holes across the skin, b) coated microneedles for rapid dissolution on the skin of the coated drug c) polymeric microneedles incorporating a drug for rapid or controlled release into the skin, d) hollow microneedles to puncture the skin followed by active infusion or diffusion of the formulation through the needle bores. Figure adapted from (Arora et al. 2008).

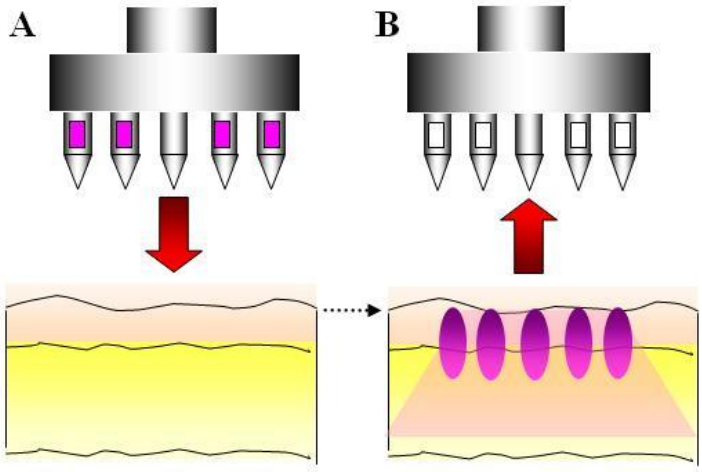

Figure 1.10: Schematic representation of a pocketed microneedle device. The formulation, retained within the needle cavities, is released following insertion of the microneedles into the skin.

1.6.2 Microneedle parameters

The design of a MD is affected by a variety of parameters. First of all, microneedles must possess sufficient strength to permit insertion into the skin without breaking. Solid microneedles fabricated out of metals are usually robust enough to penetrate the skin without failing (Park et al. 2005). Conversely, when polymers are used, specific fabrication materials must be selected in order to ensure appropriate microneedle strength.

Other parameters such as sharpness of tip, length, shape and width of the needles all affect the force required to apply the microneedles into skin and that required to prevent their fracture. In particular, microneedles with sharpened tips require a lower force to pierce the skin, whereas microneedles with higher wall thickness, greater wall angle and lower length can withstand higher force before failure (Davis et al. 2004; Park et al. 2005).

The most commonly reported geometries of a micro-delivery system can be summarised as follows (Arora et al. 2008):

- Length: range between 150-1000 µm
- Base width: range between 50-250 µm
- Tip diameter: range between 1-25 µm

1.6.3 Current microneedle applications

The capability of a MD to facilitate cutaneous delivery of drugs has been extensively studied *in vitro*, in animals and in humans. Therapeutic compounds have been administered for local action in the skin or for systemic effect following adsorption of the compounds into the bloodstream. Examples of medicaments administered by microneedle devices are discussed in the following Sections.

1.6.3.1 Cutaneous delivery of low molecular weight drugs

Low molecular weight drugs such as naltrexone, an opioid receptor antagonist used for the treatment of alcoholism and opioid addiction, and the anaesthetic lidocaine have been delivered across the skin via microneedles. Therapeutic doses of naltrexone were delivered from a transdermal patch following permeabilization of the skin through insertion of solid microneedles (Wermeling et al. 2008). Lidocaine was delivered into pigs following application of a lidocaine coated MD. Lidocaine levels assessed in excised skin biopsies were considered appropriate to induce sustained local anaesthesia (Zhang et al. 2011). In a more recent study, the anaesthetic was delivered into humans by hollow microneedles and compared to conventional intradermal administration by hypodermic needles (Gupta et al. 2012). The study revealed comparable local anaesthesia between the two delivery systems. However, microneedle treatment was perceived as significantly less painful and it was strongly preferred by all individuals in the study. Other small hydrophilic compounds have been administered by microneedles, as recently been reviewed by Kim *et al.* (2012).

1.6.3.2 Cutaneous delivery of biopharmaceutics

Microneedles have also been extensively studied as a means to deliver biopharmaceutic drugs across the skin. These are peptides, proteins and DNA that normally cannot be administered orally (because of poor oral bioavailability) or transdermally (because of the high molecular weight) and that are thus almost entirely delivered by hypodermic injections. Insulin represents the most widely investigated drug among biopharmaceutics. Significant reduction of blood-glucose levels has been reported in human subjects and animal models following insertion of

solid MDs, as a pre-treatment prior to topical application of an insulin formulation (Martanto et al. 2004; Wu et al. 2010) or by hollow microneedle application for insulin infusion (McAllister et al. 2003; Nordquist et al. 2007).

A large variety of other biopharmaceutics have been delivered by microneedles to animal models. Drugs such as low molecular weight heparin (Ito et al. 2008), desmopressin (Fukushima et al. 2011) and human growth hormone (Burton et al. 2011; Lee et al. 2011) have been delivered by dissolving or hollow microneedles. Desmopressin (Cormier et al. 2004) and parathyroid hormone (Ameri et al. 2009) have also been administered by dry coated microneedles, while water soluble polymeric microneedles in combination with iontophoresis have been employed to facilitate delivery of insulin and BSA (Garland et al. 2012)

Clinical trials are also underway. Hollow microneedles have been used to administer insulin to type 1 diabetes subjects (Gupta et al. 2009, 2011a) and parathyroid coated microneedles are now advancing into a phase III clinical trial for the treatment of osteoporosis (Daddona 2011).

1.6.3.3 Cutaneous delivery of vaccines

Microneedles have been extensively investigated as a means to deliver vaccines into the skin. The skin offers numerous immunological advantages over conventional subcutaneous administration, due to the presence of immunocompetent cells in the epidermis (Langherans cells) and dermis (dermal dendritic cells). However, cutaneous administration of vaccines has been limited due to the poor reliability of the conventional (Mantoux) intradermal injection method. Unlike the Mantoux technique, where hypodermic needles have to be inserted at an angle almost parallel to the skin surface, microneedles can be applied perpendicularly in the skin due to their reduced length, thus enabling more accurate control of the deposition depth (Mikszta et al. 2006). Coated microneedles have been largely investigated for vaccine administration. In particular *in vivo* animal studies have indicated that influenza vaccines that are delivered from dry coated MDs provide comparable or superior immune responses to those administered by intramuscular injections (Chen et al. 2009; Koutsonanos 2011; Pearton et al. 2010; Quan et al. 2010; Zhu et al. 2009). Additional vaccines delivered to animal models from coated MDs include: hepatitis C DNA vaccine (Gill et al. 2010), hepatitis B surface antigen (Andrianov et

al. 2009), human papilloma (Corbett et al. 2010), herpes simplex virus (Chen et al. 2010) and others.

Hollow microneedles have also been used for intradermal delivery of vaccines such as anthrax (in the form of a recombinant *Bacillus* anthracis antigen) in animal models (Mikszta et al. 2006) and influenza vaccines in both animals and humans (Alarcon et al. 2007; Van Damme et al. 2009).

Clinical trials have been carried out in healthy adults (Beran et al. 2009) and elderly people (Holland et al. 2008) using Soluvia™. This is a microinjection device, consisting of a 1.5 mm long, small gauge, hypodermic needle attached to a syringe prefilled with influenza vaccine (http://www.bd.com 2012). Although the needle contained in Soluvia™ is arguably too long to be defined as a microneedle, its use is worth mentioning as it represents the first therapeutic device, based on the microneedle concept, which has received marketing authorization. Soluvia™ is currently commercialised worldwide as IDflu®, Intanza® and Fluzone Intradermal® for intradermal vaccination (http://en.sanofi.com 2009).

1.6.3.4 Microneedle products currently approved in the market

In addition to the aforementioned Soluvia™, other microneedle products are currently available in the market, the majority of which have been used for cosmetic purposes. Dermaroller®, consisting of metal, 0.2-2.5 mm long-microneedles projecting from a cylindrical roller, was firstly sold in Germany in 1999 and it is currently commercialised around the world (http://www.dermaroller.com/ 2011). The device is designed for home use to improve skin texture (smaller microneedles) or to be used in clinics (longer needles) to reduce the appearance of scars. An additional commercialised product is represented by LiteClear® used to treat acne in China and skin cosmetic imperfections in the rest of the world (http://www.nanomed-skincare.com 2010; Kim 2012).

Finally, Micronjet® has received FDA clearance in February 2010 (http://www.nanopass.com). This device consists of four hollow, less that 500 μm long, silicon microneedles protruding from a plastic device, which can be mounted onto any conventional syringe (Van Damme et al. 2009).

1.6.5 Pain after application of a MD

The ability of microneedles to pierce the stratum corneum in a painless or minimally painful way is determined in part by the length of the needles. Studies have reported that the insertion of an array containing 400 microneedles, 150 µm long, was perceived as painless in comparison to a 26 gauge hypodermic needle (Kaushik et al. 2001). In a more recent study the effect of various microneedle parameters (i.e., microneedle length, base width, wall thickness, tip radius and number of microneedles per array) on the intensity of pain perceived was investigated and compared to conventional hypodermic needles (Gill et al. 2008).

According to this study, pain was determined mainly by the microneedle length i.e., a 3-time increase in microneedle length (i.e., 500-1500 µm) resulted in a 7-fold increase in perceived pain. The number of microneedles per array also influenced pain sensation but in a less significant way i.e., a 10 fold increase in the number of microneedles (from 5 to 50) produced a 2.5 fold increase in the pain, while other geometrical parameters did not affect pain considerably. Overall the studied microneedles were significantly less painful than hypodermic needles. Similarly, insertion of microneedles shorter than 400 µm has been referred to as painless in other studies (Haq et al. 2009; Mikszta et al. 2002).

Moreover, pain caused by liquid delivery during insertion has been investigated for hollow microneedles. A study published by Gupta *et al.* (2011b) indicated that insertion of an hollow microneedle to a skin depth of 1mm and infusion of up to 600 µl of saline was perceived as minimally painful by human subjects and was overall preferred over hypodermic needles. Similar results were confirmed by other studies reporting intradermal administration of lidocaine and insulin from a hollow microneedle up to 900 µm long (Gupta et al. 2012; Gupta et al. 2011a).

1.6.6 Safety of MD application

Microneedles have been associated with mild side effects such as localised transient erythema and skin irritation in humans and animal models (Gupta et al. 2009, 2011a; Martanto et al. 2004; Matriano et al. 2002; Nordquist et al. 2007; Wang et al. 2006). These reactions are usually transient and resolve completely within few hours. Bleeding has generally not been associated with the use of microneedles up to 1 mm long (Alarcon et al. 2007; Dean et al. 2005; Gill et al. 2008; Martanto et al. 2004;

McAllister et al. 2003). Conversely, the occurrence of small blood droplets at the microneedle insertion sites has been reported for longer needles (i.e., 1000-1500 μm) (Gill et al. 2008, Laurent et al. 2007b). Oedema has occurred when using hollow microneedles (Burton et al. 2011). However, it is believed that this represents a visual indication of the "bleb" of fluid injected, also observed following an intradermal injection, rather than an inflammatory reaction.

1.7 Rationale of the project

This research project has been stimulated by the large number of clinical studies reporting intense pain upon treatment of PFHH with intradermal botulinum toxin injections. In addition to the discomfort related to the numerous and repeated injections required, significant side effects have often been reported. Among these, muscle weakness is undoubtedly the most problematic, especially when it occurs at anatomic sites such as the hands and the soles of the feet. Delivery of the toxin to unwanted sites is mainly determined by the difficulty of performing intradermal injections using conventional hypodermic needles. This also results in waste of a very expensive therapeutic formulation, as well as reduction of dose accuracy and possibly drug efficiency. In addition, the high number of intradermal injections required at each treatment site increases the risk of needle-stick injuries and thus the potential transmission of blood-borne infections to both patients and healthcare providers. Numerous clinical studies report microneedle application as painless or associated with minimum discomfort. Driven by these considerations the use of microneedles is proposed in this research project as an alternative to hypodermic needles. It is hoped that, by using a MD for BTX A intradermal delivery, not only will the invasiveness of BTX A administration be mitigated but also the efficacy and the safety of the treatment will be enhanced and the occurrence of side effects reduced.

1.8 Thesis aim and objectives

The aim of this project is to investigate the potential of microneedles to deliver potent macromolecules such as BTX A to the dermis of human skin. The study has been organised to achieve the following objectives:-

- To characterise pocketed MDs manufactured for liquid loaded delivery.
- To evaluate the capability of pocketed MDs to uniformly accommodate a formulation mimicking the composition of the commercial preparation Botox® and to compare results with established solid MDs.
- To evaluate the loading capability of pocketed MDs and to compare results with established solid MDs.
- To assess the deposition and distribution of high molecular weight molecules delivered to the skin by liquid loaded PMDs and to compare results with established solid MDs.
- To deliver a commercial BTX A preparation (Vistabel®) and a formaldehyde inactivated botulinum toxin A (i.e., botulinum toxoid A) into *ex vivo* human skin following application of liquid loaded pocketed MDs.

Chapter 2

Characterisation and loading of solid microneedle devices (MDs) with BTX A model formulations

2.1 Introduction

The main purpose of the present research project is to assess the feasibility of a pocketed MD to deliver commercially available BTX A preparations (Botox®) to the dermis of human skin. The experiments reported in this Chapter will investigate the capability of pocketed MDs to uniformly accommodate a formulation mimicking the composition of the commercial preparation Botox®. Established dry coated non-pocketed MDs will be used as a direct comparator for liquid loaded pocketed MDs.

2.1.1 Dry coated MDs

A number of published studies have described solid MDs that have been coated with a dried form of a candidate drug, which rapidly (within minutes) dissolves off the microneedles when inserted into the skin. Studies have established that small hydrophilic compounds (Gill and Prausnitz 2007b; Xie et al. 2005), but also DNA (Chen et al. 2009; Chen et al. 2010), peptides, proteins (Ameri et al. 2009; Ameri et al. 2010; Cormier et al. 2004; Widera et al. 2006; Xie et al. 2005), and microparticles (Gill and Prausnitz 2007a) can be dry coated onto solid MDs and successfully delivered to human and animal skin. Further studies have demonstrated the capability of MDs, coated with influenza antigens, to induce an immune response comparable or greater than intradermal/intramuscular administration (Chen et al. 2012; Kim et al. 2010; Kim et al. 2009b; Pearton et al. 2010; Weldon et al. 2011). Human clinical trials are also ongoing; parathyroid hormone coated MDs (Macroflux®, Zosano Pharma) (Daddona 2011) for the treatment of osteoporosis have successfully completed phase II clinical trials and are advancing into a Phase III clinical study.

MDs can be drug coated by immersion into a coating formulation contained within a specifically designed dip coating apparatus (Gill and Prausnitz 2007a). Microneedles are usually immersed several times with specific time intervals (usually from 10 to 30 seconds) between each immersion to allow drying of the coating film. Due to the reduced dimensions of the MDs, restricting access of the liquid to the shaft of the needles without contaminating the base of the array is particularly challenging to achieve. Automated dip coating devices have been specifically manufactured for this purpose. The use of a coating device employing a roller drum rotating into a drug formulation reservoir has been reported (Ameri et al. 2010; Trautman 2008).

Following contact of the drum with the formulation, a layer of liquid of controlled thickness (~100 μm) is deposited on the drum's surface. Such coating methodology has been employed to succesfully coat hormones (desmopressin and the parathyroid hormone) (Cormier et al. 2004; Daddona 2011) and proteins (ovalbumin) (Widera et al. 2006) onto microneedles. Furthermore, Weldon *et al.* (2011) reported the use of an automated dip coating device, adapted from Gill and Prausnitz (2007a), consisting of a chamber with a coating solution and a microneedle holder attached to a linear stage connected to a computer. Microneedles with a length of 700 μm were moved in the x and y dimensions with an accuracy of 0.4 μm (2011) and were successfully coated with influenza vaccines. Other studies reported reasonable spatial control of the coating process on equal microneedle designs (i.e. coatings placed selectively on 25%, 50%, 75% and 100% of the length of 700 μm long microneedles). The same coating apparatus was employed but movement of the microneedle holder was performed manually (the details of the coating apparatus employed by Gill and Prausnitz will be described in Section 2.3.2.1.1 and discussed in Section 2.4.2).

Dry coating methodologies that do not involve a dip coating procedure have also been investigated as a means to successfully coat proteins and DNA vaccines on silicon MDs. Studies have reported the use of a gas jet drying approach to coat a densely packed (up to 20,000 microneedles/cm^2) microneedle patch (called Nanopatch^{TM}), with a single microneedle length ranging between 30-100 μm (Chen et al. 2011; Chen et al. 2009). A gas jet of coating formulation (6-8 m/s) was applied to the microneedles at specific incident angles (20°-70°) to allow selective deposition of the coating either on the entire length of the microneedles or selectively on their apical part. This was achieved by specifically rotating the incident angle, i.e. by blowing the coating formulation with an angle of 20°, coatings were placed over the entire microneedle length and also on the surface of the patch, whereas increasing the angle to 70° allowed selective deposition of the coating on the microneedle tip. Microneedles were rotated while coatings were applied to allow uniform coating.

Mechanically controlled dip coating technologies have been used to achieve coating reproducibility and uniformity but composition of the coating formulation plays an equally important role. Specific excipients, such as viscosity enhancers and surfactants are usually needed to improve coating efficiency (Ameri et al. 2010; Chen et al. 2011; Widera et al. 2006; Zhang et al. 2011). A study published by Gill and Prausnitz (2007b), assessing coating uniformity by using differently formulated

solutions, compared a variety of viscosity enhancers ((i.e., carboxymethylcellulose (CMC), sucrose, hyaluronic acid, xanthan gum, sodium alginate, polyvinylpyrolidone) and surfactants (Lutrol®/Pluronic® F68 and Tween® 20). According to this study, coating formulations containing a viscosity enhancer produced a thicker microneedle coating. This was because more viscous formulations allowed retention of increased volumes of liquid on the microneedles upon each immersion. While thicker, the coating appeared localised along the centre of the microneedle shaft. Uniform coverage of the entire microneedle length was prevented by the high surface tension of the viscous solution. Conversely, when a surfactant was added to the formulation a more uniform coating was observed over the entire microneedle body as a direct result of the reduced surface tension and increased wettability of the microneedle surface. Therefore, combining a viscosity enhancer with a surfactant enabled a simultaneously thicker and more homogeneous coating. The best coating uniformity was observed when the viscosity enhancer CMC and the surfactant Lutrol® F68 were used at concentrations of 1% w/v and 0.5% w/v in deionised water, using sulforhodamine as the model compound. Similarly, the use of other viscosity enhancers such as xanthan gum, sodium alginate and poly(vinylpyrrolidone) resulted in enhanced coating efficiency. The combination of a viscosity enhancer and a surfactant was shown to be a versatile approach as macromolecules (such as BSA and insulin) and 10-20 μm particles could be loaded as uniform coatings on the studied microneedles (Gill and Prausnitz 2007a, b).

Optimization of excipient concentrations in a coating formulation is required in order to facilitate spatial control of MD coating. Ameri *et al.* (2010) reported that a 0.2% w/w concentration of the surfactant Tween® 20 was optimal as it enabled selective deposition of coatings on the tip of the microneedles (~100 μm). On the contrary, higher surfactant concentrations determined spreading of the formulation over the entire microneedles body and even on the base of the array as a result of the reduced surface tension and thus increased wettability of the microneedle surface. Conversely, lower concentrations or absence of surfactant resulted in contraction of the coating formulation (due the high surface tension of the coating formulation) and thus non-uniform coverage of the microneedle tip.

When dry coated MDs are prepared, lyo/cryoprotectants may also be required to maintain the stability of therapeutic proteins such as vaccines (Kim et al. 2010; Koutsonanos 2011; Pearton et al. 2010; Weldon et al. 2011). Coating solid

microneedles with a drug solution involves a phase change of the solution to a dry coated layer. Drying of vaccine formulations has been associated with reduction of antigen stability due to denaturation and aggregation of antigen molecules (Amorij et al. 2007). Use of stabilizers such as trehalose and inulin for vaccines during the formulation of a dry powder has been previously reported (Amorij et al. 2007; Maa et al. 2004). A study assessing the capability of different stabilizers (such as trehalose, inulin, sucrose, glucose and dextrans) to prevent loss of antigen activity of influenza vaccines coated onto microneedles has been published (Kim et al. 2010). This study revealed that trehalose was the most effective among the stabilizers tested, as its addition to a coating formulation containing CMC 1% w/v and Lutrol® F68 0.5% w/v was essential to maintain antigen activity. This was due to the capability of the sugar to prevent increase in the antigens particle size, which is known to lead to particles aggregation and degradation during the drying phase (Amorij et al. 2008). Similarly Weldon *et al*. (2011) reported that the trimeric structure of an influenza virus prepared in a coating solution containing CMC 1% w/v and Lutrol® F68 0.5% w/v was destroyed during microneedle coating. The addition of trehalose 15% w/v to the coating formulation preserved the structure and the immunological property of the coated vaccine.

2.1.2 Liquid loaded pocketed MDs

Pocketed MDs, a variant of solid MDs, contain one or multiple voids in their needle shaft that are designed to accommodate a drug in solution following a simplistic one step immersion process into a liquid loading formulation. The approach relies on capillary action to load a drug in a liquid form. Following application of the MD to the skin, the therapeutic can be rapidly released into the tissue (Gill and Prausnitz 2007b).

Pocketed MDs have been used for the delivery of small hydrophilic molecules (e.g., fluorescein and sulforhodamine) and 10-20 μm microparticles (Gill and Prausnitz 2007a, b, 2008) to human skin. Studies have indicated that the formulation can be loaded in the pockets either as a liquid or dry phase depending on the specific coating excipients employed. According to these studies, coating formulations containing glycerol 80% v/v as the sole excipient enabled retention of model drugs (such as fluorescein and sulforhodamine) in the pockets in a liquid state for approximately 24

hours. Conversely, the use of other viscosity enhancers, such as sucrose 25% w/v, was associated with the production of solid drug layers in the pockets as a result of an increased solid content in the coating formulations.

The same studies showed that controlled deposition of a drug solution on a pocketed microneedle could be achieved by combining specific excipients in the coating formulations. Dipping the microneedles into a coating formulation containing a viscosity enhancer (e.g., glycerol 80% v/v or sucrose 25% w/v) as the sole excipient resulted in selective loading of the liquid in the pockets with no coating the shaft of the needle. This was because the high surface tension of the formulation prevented the surface (shaft) of the needles being wetted by the liquid formulation. Conversely, the addition of a surfactant (e.g. Tween® 20 0.2% w/v) resulted in the simultaneous filling of the pocket and coating the shaft of the microneedle, as a consequence of the reduced surface tension of the formulation.

The suitability of pocketed microneedles to accommodate multiple drug formulations has also been demonstrated (Gill and Prausnitz 2007b). By using a more complex multi step immersion process, three different model solutions, containing glycerol as viscosity enhancer, were selectively loaded into each of the three pockets contained in a pocketed microneedle. This indicated that pocketed microneedles may be employed for those therapeutic scenarios, which require delivery of different drug formulations from the same microneedle.

Liquid loaded pocketed MDs represent a valid alternative for drugs unsuited to the dry coating process and the associated aspects of formulation. This method of delivery may be more suited to the delivery of BTX A. The rationale is that liquid loaded pocketed microneedles may offer potential advantages compared to the dry coating approach such as: i) greater cutaneous diffusion of the medicament as a liquid compared to a dry state, thus facilitating downward and lateral diffusion of BTX A to its therapeutic target (the sweat glands) that are located in the deep dermis, ii) more uniform and rapid release of the medicament; drug release would in fact not rely on dissolution of a dry layer from the needles and it would be expected to occur instantaneously following insertion of the needles in the skin, iii) facilitated release of formulations containing high molecular weight drugs such as BTX A (formulated in Botox® within a complex of up to 900 kDa), which may be difficult to coat on the microneedle surface or which would be more likely to wipe off onto the surface of the skin upon microneedle insertion (Gill and Prausnitz 2007a, b); iv) possible use of

MDs for the delivery of existing BTX A commercial formulations, therefore simplification of the eventual use of the MDs in clinical trials.

A restriction of using MDs is the limited amount of solution that can be loaded into the needles due to their micron-sized dimensions. As previously mentioned (Section 1.4.1), different BTX A pharmaceutical preparations are currently commercially available (Botox®, Vistabel®, Dysport® and Xeomin®). A vial of Botox®, the only BTX A preparation licensed for the treatment of axillary PFHH, contains i) 5 ng of BTX A (100 U), ii) 0.5 g of human serum albumin (HSA) and iii) 0.9 mg of sodium chloride (NaCl). The vial is currently reconstituted using a volume of 0.9% w/v saline solution usually ranging between 1.5 and 5 ml, according to the preference of the clinician (Section 1.5.1). The resulting solution is delivered by multiple intradermal injections, each one generally with a volume of 0.05-0.1 ml. Therefore, in order to enable loading of effective doses of BTX A on pocketed MDs, the medicament will have to be reconstituted with smaller volumes, possibly in the microlitre range. Therefore, the limit of solubility of HSA and NaCl will be investigated in this Chapter in order to establish whether volumes contained in the microlitre range can be employed to dissolve a Botox® preparation.

2.1.3 Use of the enzymatic protein β-galactosidase as a model representative of BTX A

Commercially available pharmaceutical formulations of BTX A contain BTX A within protein complexes of different molecular weights, ranging between 150 kDa (Xeomin®) up to 900 kDa (Botox®). BTX A is currently difficult to detect, expensive and laboratory use of the pure toxin is associated with a number of safety concerns. The enzymatic protein β-galactosidase (β-gal) consists of a tetramer with a molecular weight of ~465 kDa, with each subunit possessing a molecular weight of 116.3 kDa (Fowler 1977). This molecule was therefore selected as a detectable model protein with a molecular weight that is comparable to BTX A.

2.1.4 Aim and objectives of the Chapter

This Chapter will investigate the capability of pocketed MDs to uniformly accommodate a formulation mimicking the composition of the commercial

preparation Botox®. Solid MDs, loaded by using established dry coating methodologies, will be used as a comparator for liquid loaded pocketed MDs.

The experimental objectives of this Chapter are to:-

1) Characterise pocketed and non-pocketed MDs by bright field and scanning electron microscopy (SEM).
2) Assess the uniformity of coatings on non-pocketed MDs by using an established dry coating methodology and fluorescent detectable molecules.
3) Evaluate the solubility of the excipients present into the commercial preparation Botox® when employing volumes in the microlitre range.
4) Load a representative model formulation of the commercial Botox® preparation ('Botox® like' formulation) onto pocketed MDs.
5) Compare the microneedle loading efficiency of liquid loading to the more established dry coating methodology.
6) Evaluate the residency time of a 'Botox® like' formulation in the pockets of MDs.
7) Assess the effect of viscosity enhancers on the retention time of a solution in the pockets of MDs.

2.2 Materials

2.2.1 Reagents

All reagents were used as received and were purchased from Sigma-Aldrich Ltd (Poole, UK), unless otherwise stated.

Deionised water was obtained from an Elga reservoir (High Wycombe, UK). Sodium chloride was purchased from Fischer Scientific (Loughborough, UK).

2.3 Methods

2.3.1 MD fabrication and characterisation

Solid metal MDs, with and without an integrated pocket, were used. They were named, respectively, pocketed microneedles devices (PMDs) and non pocketed microneedle devices (NPMDs). NPMDs were cut from stainless steel sheets using an infrared laser (Trinity Brand Industries, SS 304; McMaster-Carr, Atlanta, GA, USA) as described elsewhere (Gill and Prausnitz 2007a). Integrated pockets within the microneedle shafts were created as outlined by the methodology described by Gill and Prausnitz (2008). Following manufacture, PMDs and NPMDs were electropolished, washed and dried as described elsewhere (Gill and Prausnitz 2007a). MDs were attached on aluminium stubs and characterised by scanning electron microscopy (SEM) (FEI XL30, Eindhoven, The Netherlands). Images of MDs were also captured by using a bright field light microscope (Zeiss Stemi 2000-C Stereomicroscope, Carl Zeiss, Welwyn Garden City, UK) associated to a digital camera (Olympus C 3040-ADL, Watford, UK). An external light source (Schott KL-1500, Schott AG, Stafford, UK) was also employed to better visualize the samples.

For light microscopy analysis, the base of each MD was held between the two edges of a metallic tweezer. A small strip of adhesive tape was wrapped around those two edges in order to maintain the device in position. The mounted MD was then placed on the stage of the light microscope.

2.3.2 Dry coating NPMDs

Dry coating was performed for NPMDs as reported elsewhere (Gill and Prausnitz 2007a) with the aid of a dip coating reservoir device whose details are outlined in the following Section.

2.3.2.1 Dry coating NPMDs using a micro scale dip coating reservoir device

The dip coating reservoir device (Figure 2.1) consists of a coating solution reservoir produced between two aligned poly(methylmethacrylate) plates, referred to as 'bottom plate' and 'upper plate'. The first one includes a central feeding channel, connected to an inlet port from which the coating solution (around 20-30 µl) can be dispensed. The upper plate possesses five microholes positioned at the same interval as the microneedles of the MD to be coated. When the coating formulation is injected to the central feeding channel, it reaches the microholes, each one acting as a single micro reservoir. A MD can be then coated by being dipped and withdrawn, for a variable number of times, in the reservoirs.

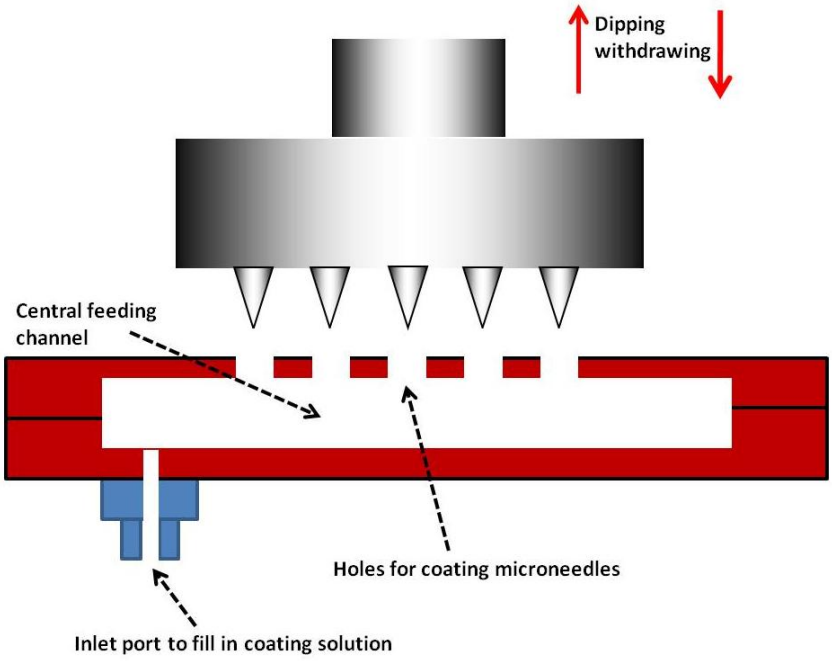

Figure 2.1: Schematic representation of a micro scale dip coating device. Microneedles are aligned with the microholes present in the upper plate of the dip coating reservoir device.

2.3.2.1.1 Dry coating of NPMDs with fluorescent molecules

Preliminary experiments were conducted by loading detectable molecules onto microneedles in order to assess the coating uniformity. The coating methodology reported by Gill and Prausnitz (2007b) and the dip coating reservoir device, described previously (Section 2.3.2.1), were employed. Sulforhodamine (λex: 583 nm, λem: 603 nm, m.w. = 606 Daltons) and latex sulphate modified fluorescent nanoparticles (λex: 575 nm, λem: 610 nm, particles diameter size: 100 nm) were chosen as representative models of small hydrophilic drugs and high molecular weight controlled release/nanoparticulate delivery systems respectively.

Sulforhodamine

An aqueous coating formulation containing sulforhodamine 0.05% w/v, CMC 1% w/v and Lutrol® F68 0.5% w/v was dispensed (approximately 20 µl) into the micro scale dip coating reservoir. Ten stainless steel NPMDs, divided into two groups (n=5), were used in this experiment. Each group was immersed either 5 or 15 times into the coating formulation. Intervals of 15 seconds were employed between each microneedle immersion in order to allow drying of the coating. The dip coating reservoir was refilled with approximately 10 µl of fluorescent solution after ten NPMD immersions. Once coated, NPMDs were allowed to dry for 24 hours at room temperature, protected from light. They were subsequently analysed using a light/fluorescence microscope (Light/Fluorescent Olympus BX50, Olympus, Watford, UK) and representative images were digitally captured (Olympus DP 10, digital camera, Watford, UK).

Fluorescent nanoparticles

A coating suspension containing 100 nm fluorescent red nanoparticles was used in this experiment. NPMDs were immersed 5 (n=3) or 15 (n=3) times into the suspension, as described for sulforhodamine coating formulation. Once coated, NPMDs were allowed to dry over night at room temperature, protected from light. Coated NPMDs were subsequently analysed by light and fluorescent microscopy.

2.3.3 Evaluation of the solubility of the excipients contained in the commercial preparation Botox®

As previously mentioned (Section 2.1.2), loading a PMD with effective doses of BTX A would require dissolution of the commercial preparation Botox® by using volumes in the microlitre range. As the excipients NaCl and HSA are contained in the vial in mg amounts (0.9 mg and 0.5 mg respectively) (Section 1.4.1.1), using such constrained volumes may result in incomplete dissolution of the preparation. Conversely, the quantity of BTX A contained in the vial is extremely low (5 ng) and therefore the toxin is not expected to interfere with dissolution of the preparation.

For this reason the experiment reported in this Section will investigate the solubility of the excipients contained in a vial of Botox® when using a volume less than or equal to 100 µl.

The following solutions were freshly prepared:

- NaCl 90 mg/10 ml in 0.9% saline solution=0.9 mg/100 µl
- HSA 5 mg/ml in 0.9% saline solution=0.5 mg/100 µl

Saline solution (0.9%) was used as it is the diluent recommended by Allergan (Botox® manufacture) to reconstitute BTX A commercial preparations (Section 1.5.1). In addition, solutions containing a decreasing volume of 0.9% saline solution were prepared (as outlined by Table 2.1) in order to assess the limit of solubility of each of the excipients. The volumes of 0.9% saline solution used to assess the solubility of HSA and NaCl ranged, respectively, between 1 and 0.1 ml and 10 to 1 ml (Table 2.1).

Table 2.1: Formulations used to determine the limit of solubility of single excipients contained in a vial of Botox®.

HSA (mg)	0.9% saline solution (ml)	NaCl (mg)	0.9% saline solution (ml)
5	1	90	10
	0.9		9
	0.8		8
	0.7		7
	0.6		6
	0.5		5
	0.4		4
	0.3		3
	0.2		2
	0.1		1

The solubility of the excipients when contemporaneously present was also assessed. Five mg of HSA were transferred into a microcentrifuge tube and added to 100 µl of NaCl (0.9 mg/100 µl) and 900 µl of saline solution 0.9% w/v. Therefore, the resulting solution contained 0.9 mg of NaCl and 0.5 mg of HSA per 100 µl. Moreover, 9 solutions containing a decreasing volume of saline solution 0.9% (from 800 to 100 µl) were prepared (Table 2.2), in order to detect the limits of solubility. All of the prepared solutions were inspected with the naked eye against a black and a non-glare white panel to assess the presence of undissolved particulate traces. Moderate manual agitation was performed to facilitate solubilisation.

Table 2.2: Formulations used to assess the limit of solubility of HSA and NaCl in saline solution. Masses are representative of a vial of the commercial Botox® formulation.

Solution	HSA (mg)	NaCl (90 mg/10 ml) µl	0.9% Saline solution (µl)	Approximate total volume (µl)
1	5	100	800	900
2	5	100	700	800
3	5	100	600	700
4	5	100	500	600
5	5	100	400	500
6	5	100	300	400
7	5	100	200	300
8	5	100	100	200
9	5	100	/	100

2.3.4 Liquid loading PMDs and NPMDs

PMDs and NPMDs were manually loaded by a single immersion into a reservoir containing a small volume (~20 µl) of a β-gal loading formulation. Excess formulation that was accidentally collected on the base of the MD during the microneedle immersion process was carefully removed using a lintless tissue paper.

2.3.4.1 Liquid loading PMDs with a 'Botox® like' formulation

To predict the residency time of a liquid BTX A formulation, a 'Botox® like' formulation (final volume of 150 µl) was freshly prepared using 0.9% saline solution as a diluent buffer. The formulation contained the following components:-

1. ~5 ng of β-gal
2. 0.9 mg of NaCl
3. 0.5 mg of HSA
4. 20% v/v of blue colour indicator (a brilliant blue and carmoisine solution)

The formulation provided a mimic of the commercial BTX A formulation, Botox®, with the exception of the toxin, which was replaced by the model protein β-gal and the inclusion of a dye to enable visualisation. Both PMDs (n=3) and NPMDs (n=3) were loaded with the 'Botox® like' formulation and visualized under light microscope (Zeiss Stemi 2000-C Stereomicroscope). The evaporation process from PMDs was monitored using a digital camera (Olympus C3040-ADL). An external light source (Schott KL-1500) was also used to enable better visualisation of the microneedles.

2.3.4.2 Liquid loading MDs with a high concentration of the model BTX A (β-gal)

A loading solution of the model BTX A (β-gal 1.3 µg/µl) was freshly prepared in a bovine serum albumin (BSA)/bicine buffer (bicine buffer 50 mM pH 7.5 + BSA 100 µg/ml). Similar to that previously described (Section 2.3.4.1), a blue colour indicator was included to permit visualisation of the formulation in the pockets. PMDs (n=3) were loaded by a single immersion into a liquid formulation (as described in Section 2.3.4). PMDs were observed under the light microscope and the evaporation process captured with a digital camera.

An increased concentration of β-gal, compared to Section 2.3.4.1, was selected for this experiment as equal/similar concentrations will be employed to perform quantitative analysis of PMD loading capacity and cutaneous delivery studies, described respectively in Chapter 3 and 4. A higher concentration of β-gal was required to allow detection of the protein using the methodologies described in those Chapters. The aim of this experiment is therefore to evaluate the residency time of the protein solution in the pockets of the PMD to determine the time that would be available, following loading, to insert the loaded PMD into the skin and enable delivery of the protein in a liquid state.

2.3.4.3 Enhancing the retention of liquid loaded drug formulations in microneedle pockets

A viscosity enhancer was added to loading solutions in order to reduce the evaporation rate and thus increase the residence time of the film within the microneedle pockets.

Aqueous loading solutions were prepared with increasing amounts of glycerine

- Formulation 1: blue (food) colour indicator 100% v/v.
- Formulation 2: ~20% w/v glycerine plus ~80% v/v of blue food colour indicator.
- Formulation 3: ~50% w/v glycerine plus ~50% v/v of blue food colour indicator.
- Formulation 4: ~80% w/v glycerine plus 20% v/v of blue food colour indicator.

PMDs were loaded with formulation 1 (n=5), 2 (n=3), 3 (n=3) and 4 (n=3) at room temperature. The duration of an intact film within the pocket of each microneedle was recorded by regular observation under a light microscope (Zeiss Stemi 2000C Stereomicroscope) with the aid of an external fibre optic light source (Schott KL-1500). Observations were conducted consistently for the first 2 minutes and subsequently at 30 minutes, 1 hour, 24 hours 48 hours, 120 hours (5 days), 288 hours (12 days), 408 hours (17 days), 624 hours (26 days) and 768 hours (32 days). The

number of pockets retaining the formulation at each observation time was reported as a percentage relative to the total number of pockets examined.

2.4 Results and Discussion

2.4.1 MD characterization

PMDs and NPMDs, fabricated by laser etching stainless steel into the desired pattern and geometry, were characterised by SEM and light microscopy. Figures 2.2 (A) and (B) show a representative NPMD and PMD, imaged by the light microscope. Figures 2.2 (C) and 2.2 (D) depict two representative adjacent non-pocketed and pocketed microneedles, imaged by SEM. PMDs possessed individual needle dimensions of ~700 x 340 x 65 µm (y, x and z plane respectively). Only 4 out of 5 needles contained an internal pocket, each measuring ~365 x 140 x 65 µm (y, x and z plane). Each needle of a NPMD measured ~700 x 170 x 70 µm (y, x and z plane) and the tip to tip distance between two adjacent microneedles measured ~ 1.5 mm for both PMDs and NPMDs. The characterised MDs were manufactured and provided by Professor Marc Prausnitz *et al*. based at the Georgia Institute of Technology, Georgia, Atlanta, USA.

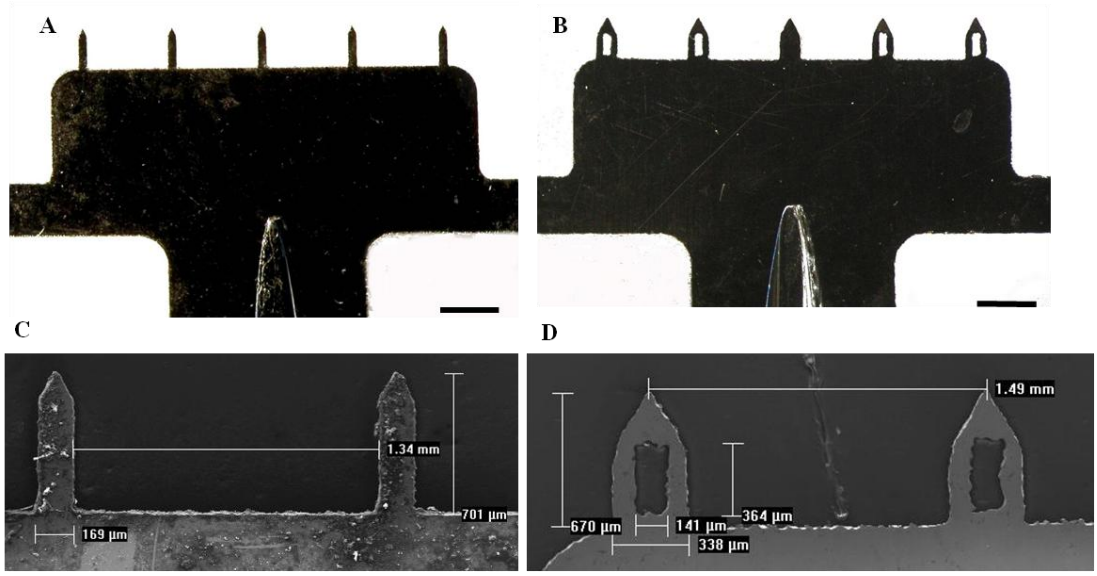

Figure 2.2 (A-D): Characterisation of NPMDs and PMDs. Brightfield micrographs of an in-plane row of five non-pocketed microneedles (NPMD) (A) and pocketed microneedles (PMD) (B). Scale bar = 1 mm. Scanning electron micrographs of two adjacent non pocketed (C) and pocketed microneedles (D).

As depicted by SEM images (Figure 2.2 D), an irregularity can be observed on the edges of both the pockets and the needles of the studied PMDs. These devices represented the first PMD generation and PMDs with more regular pockets/needles edges have now been produced as a result of manufacturing optimization (Gill and Prausnitz 2008).

The presence of irregularities in the pockets may provide an advantage when loading the PMDs. When a liquid interacts with a solid surface, the wettability of this surface is described by the contact angle (θ) (Forch R. 2009), proposed by Young and defined as the angle at which the liquid/vapour meets the solid. The contact angle is influenced by the liquid-solid surface tension and can (in principle) assume any value between 180° and 0° depending on the degree of wettability of the solid surface by the liquid. Greater wettability, defined by a smaller contact angle and a lower surface tension, is normally observed for smooth and regular surfaces. Conversely, rough or heterogenous surfaces are generally associated with multiple and increased contact angles, a phenomen called contact-angle hysteresis (Blake 1997). This phenomen determines a reduction of the mobility of the so-termed wet line, defined as the boundary interface between liquid, solid and vapour. The mobility of a liquid is

therefore reduced for an irregular surface and thus drug formulations loaded on the studied PMDs may be better retained.

2.4.2 Dry coating NPMDs with fluorescent molecules

Using an established dip coating procedure (Gill and Prausnitz 2007a), fluorescent molecules were dry coated onto NPMDs. Increseasing the number of immersions of NPMDs into a loading formulation resulted in more uniform and intense coatings. Figures 2.3 (A) and 2.3 (B) depict the appearance of NPMDs after 5 and 15 immersions into a sulforhodamine 0.05% w/v coating formulation containing CMC 1% w/v and Lutrol® F68 0.5% w/v as excipients.

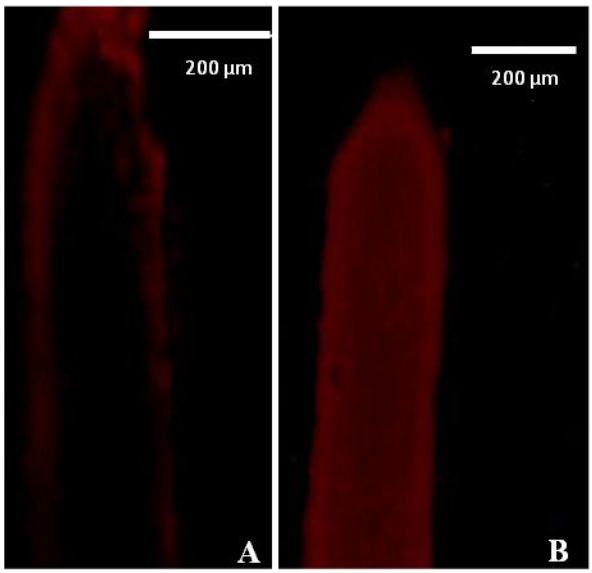

Figure 2.3 (A, B): Dry coating of NPMDs with sulforhodamine. Fluorescent micrographs of single microneedles dry coated with sulforhodamine after 5 (A) (n=5) and 15 (B) (n=5) immersions in sulforhodamine aqueous solution 0.05% w/v containing CMC 1% w/v and Lutrol® F 68 0.5% w/v as excipients.

Similarly, an increased number of immersions of NPMDs into a 100 nm nanoparticle suspension resulted in a thicker coating and thus increased levels of fluorescence (Figure 2.4 A-D). The results indicated that relatively uniform and thick coatings could be achieved even when using an excipient free solution. This could be due to an inherent high level of viscosity of the nanoparticle suspension and/or a possible electrostatic interaction between the nanoparticles and the metallic surface.

The use of excipient free coating formulations may be particularly desirable for MD loading because some excipients may be incompatible with certain drugs. In addition, if excipients are avoided, the drug loading capacity of the coating formulation may be optimised and thus greater MD loading may be achieved. Moreover, MDs could be used for existing drug formulations such as BTX A commercial preparations, without the need to reformulate. This will be discussed further in Section 2.4.4.

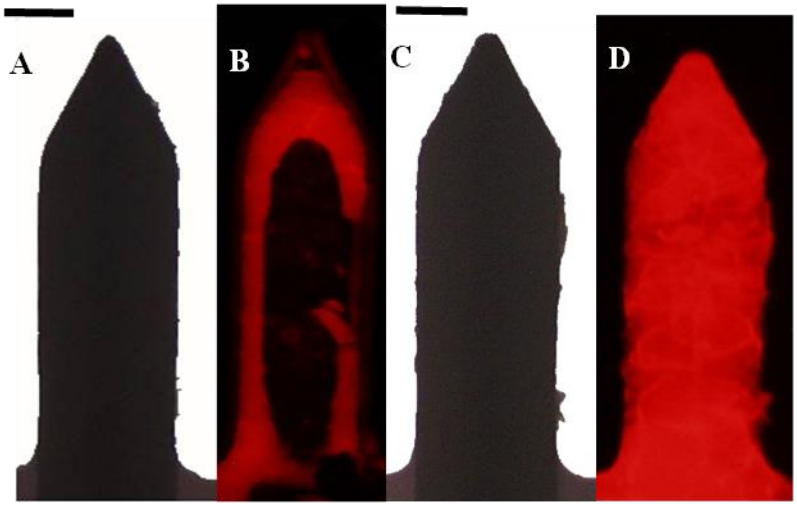

Figure 2.4 (A-D): Dry coating of NPMDs with fluorescent nanoparticles. Fluorescent and brightfield micrographs of single microneedles dry coated with 100 nm polystyrene nanoparticles after 5 (A, B) (n=3) and 15 (C, D) immersions (n=3) in a fluorescent nanoparticle coating suspension. Scale bar = 100 μm.

However, coating sulforhodamine/nanoparticles selectively on the shaft of the microneedles was almost impossible to achieve. Undesired contact between the coating formulation/suspension and the base of the microneedles was reported for all the NPMDs used. Additionally, single coated microneedles contained in the same NPMD showed different fluorescent intensities. This indicated that the needles were not coated in a reproducible manner (Figures 2.5 A and B).

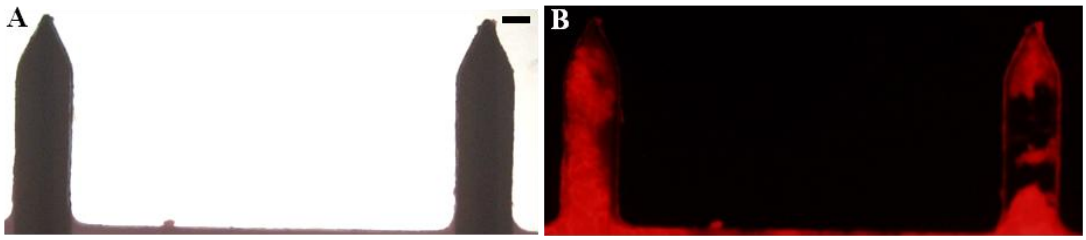

Figure 2.5 (A, B): The coating variability of fluorescent nanoparticles on MDs. Fluorescent and brightfield micrographs of two adjacent microneedles in a row of five microneedles (in the same NPMD), dry coated with 100 nm polystyrene nanoparticles after 15 immersions (n=3) in a fluorescent nanoparticle coating suspension. Scale bar = 100 μm.

Since the coating was performed manually, control of the process was extremely difficult to achieve. The insertion of microneedles into the microholes of the dip coating reservoir device (Section 2.3.2.1) resulted in overflow of a proportion of the coating solution and therefore contamination of the base of the array. In addition, when the solution was injected into the reservoir device, a hetereogenous distribution of the solution between the microholes was often observed. As a consequence, some needles collected more solution than others, thus resulting in poor uniformity of the coating. Moreover, due to the extremely reduced size of the device, maintaining the microneedles in a perfectly aligned position while being inserted into the holes was difficult to perform using manual methods. Gill and Prausnitz (2007a) reported the use of micropositioners, one holding the dip coating reservoir device and one the MD, to align the microneedles with microholes of the reservoir device. The MDs micropositioner was moved manually to allow immersion of the microneedles into the coating formulation. Initial coating attempts were performed using such micropositioners. However, due to the difficulty in maintaining the array in a stable position on the MDs micropositioner, their use was abandoned. The process was subsequently perfomed by placing the coating reservoir on a flat surface and inserting the microneedles into the reservoir by hand.

An automation of the process is certainly nedeed to increase the uniformity of the coating. Several published studies indicate efficient spatial control of microneedle coatings when using engineered coating procedures. As previosuly mentioned (Section 2.1.1), Weldon *et al.* (2011) adopted the coating apparatus described by Gill and Prausnitz (2007a) (and employed in the experiments detailed in this Thesis) to

coat stainless steel microneedles (each microneedle having a length of 750 µm and a width of 200 µm) with recombinant influenza vaccines. The coating was performed using an automated process. The MDs micropositioner was attached to a linear stage which enabled insertion of the MDs into the microholes of the dip coating device with an accuracy of 0.4 µm. The process was captured by a video camera connected to a computer. Furthermore Ameri *et al*. (2010) described the use of a robust dip coating apparatus, engineered to place minute volumes of parathyroid hormone (m.w.= ~4 kDa) formulation on the tip (~100 µm) of titanium microneedle arrays (Macroflux®) (Daddona 2011). The Macroflux® patch system consists of a 2 cm^2 array containing 1300 microneedles affixed to an adhesive patch. Each needle has a length of 190 µm and a tip featuring a small arrow-head with a length and a width of respectively 100 µm and 115 µm. The coating apparatus described by Ameri *et al*. (as mentioned in Section 2.1.1) employed a roller drum which collected a film of coating formulation with a controlled thickess (~100 µm). It achieved this by rotating (at 50 rpm) into a coating formulation reservoir (containing ~2 ml of formulation). Microneedles, moving in the same direction as the rotating drum, were coated by multiple immersions (passes) through the film of coating formulation collected on the surface of the drum (Trautman 2008). Specific excipients such as viscosity enhancers (sucrose ~16% w/w) and surfactants (Tween® 20 0.2% w/w) were also employed in these studies. The described technology was shown to be feasibile for coating large proteins such ovalbumin (~44 kDa) (Widera et al. 2006) and the peptide desmopressin (~1.1 kDa) (Cormier et al. 2004) on similarly designed microneedles.

It may be hypothetised that a coating technology such as this would reduce the variability of the results obtained in the study. The coating apparatus employed in our experiments relies on the alignment of microholes on the upper plate of the micro scale coating device (Section 2.3.2.1) with the microneedles to be coated. This was technically challenging and resulted in poor reproducibility of the coatings (as discussed above). In the coating technology described by Ameri *et al.* (2010) the needles are immersed into a continous film of coating formulation placed on the surface of the rotating drummer. The absence of microreservoirs and the controlled immersion process, may permit more uniform collection of the coating formulation by the microneedles. Comparable volumes of formulation are placed on each needle at each immersion and therefore higher coating reproducibility is obtained.

Moreover, due to the automation of the process, the depth at which the microneedles are immersed can be controlled and therefore contamination of the base of the array is avoided. The microneedles used in our study have a length of 700 µm (Section 2.4.1). Therefore, if the Macroflux® coating procedure was to be employed to coat these microneedles, the drug formulation could be selectively coated onto a small portion (e.g.100 µm of the shaft) of the entire microneedle length. The drawback would be a significant reduction of the dose loaded per array. However this could be overcome by either adapting the coating apparatus to increase the thickness of the film of formulation collected on the surface of the drum (and thus on the microneedles surface) or by modifying the MD design to increase the number of microneedles per array.

Nevertheless, other approaches could be used to obtain more uniform coatings with the micro reservoir approach e.g. using the coating procedure described by Gill and Praunitz (2007a). Alternatively, MD design could be tailored in order to reduce contamination of the base of the array. For example the length of the needles could be increased so that only a portion of the microneedle is immersed in the reservoir. This would prevent contact between the coating solution and the surface of the needle during the coating procedure. Additionally, a cover layer, such as a removable microfilm, could be applied on the base of the array to prevent contact of the base plate with the solution during microneedle immersion. The microfilm could subsequently be removed after microneedle coating.

2.4.3 Evaluation of the solubility of the excipients contained in the commercial Botox® formulation

As previously mentioned (Section 2.1.2 and 1.5.1), a vial of Botox® is reconstituted in the clinical setting usually by using volumes between 1.5 and 5 ml. Such relatively large volumes are required as administration of the medicament currently relies on the use of conventional needles and syringes. If PMDs were to be used as an alternative delivery tool, considerably smaller volumes (e.g. in the microlitre range) would have to be used to reconstitute the drug due to the reduced size of the microneedles. A greater concentration of the reconstituted Botox® formulation would therefore be required to facilitate loading of PMDs with efficient doses of BTX A.

Experiments were conducted in order to assess the solubility of the excipients contained in a vial of Botox® (HSA 0.5 mg and NaCl 0.9 mg) when using volumes contained in the low microlitre range. Saline solution 0.9% was chosen as a diluent as it represents the diluent recommended by Allergan to dissolve a vial of BTX A and therefore this was also used in these experiments to evaluate solubility.

The results indicated (Table 2.3) that 5 mg of HSA can be dissolved in a volume of diluent ranging between 0.3 and 1 ml, as the solutions obtained appeared perfectly clear and free of any visible particulate traces. This indicated that 0.5 mg could be dissolved in volumes as low as 30 µl. Conversely, when volumes below 0.3 ml were used (0.2 and 0.1 ml), the presence of particulates were detected in the solution, even after manual shaking was performed. The result suggested a limit of solubility of HSA in saline solution equal to 0.5 mg/30 µl (~16 µg/µl). The data are in agreement with the product information sheet provided by HSA manufacturer (Sigma Aldrich) indicating a solubility of the protein in water of 50 mg/ml (50 µg/µl) (http://www.sigmaaldrich.com 1996).

Additionally, diluent volumes spanning from 1 to 10 ml successfully dissolved 9 mg of NaCl, without requiring manual shaking. This therefore indicated that 0.9 mg of NaCl could be dissolved in volumes as low as 10 µl. This is in agreement with the solubility specification outlined for NaCl by the British Pharmacopeia (i.e., NaCl is freely soluble in water) (http://www.pharmacopoeia.co.uk 2012).

Table 2.3: Assessment of the limit of solubility of single excipients contained in a vial of Botox®.

HSA mass (mg)	0.9% saline solution (ml)	Solubility	Manual shaking required	NaCl mass (mg)	0.9% saline solution (ml)	Solubility	Manual shaking required
5	1	✓	Yes	90	10	✓	No
	0.9	✓	Yes		9	✓	No
	0.8	✓	Yes		8	✓	Yes
	0.7	✓	Yes		7	✓	Yes
	0.6	✓	Yes		6	✓	Yes
	0.5	✓	Yes		5	✓	Yes
	0.4	✓	Yes		4	✓	Yes
	0.3	✓	Yes		3	✓	Yes
	0.2	x	Yes		2	✓	Yes
	0.1	x	Yes		1	✓	Yes

The solubility of the excipients when contemporaneously present was also assessed to better mimic the commercial Botox® formulation (Table 2.4). A solution free of any visible particulates was obtained when 5 mg of HSA were dissolved in 0.1 ml of NaCl (0.9 mg/0.1ml) plus 0.9 ml of saline solution 0.9%. This indicated that both of the excipients were dissolved in 100 µl of diluent.

Moreover, the data indicated that 5 mg of HSA can be dissolved by using total volumes of solutions (consisting of 0.1 ml of NaCl 0.9mg/0.1 ml plus 0.8 ml to 0 ml of saline solution 0.9%) ranging between 0.9 and 0.3 ml. Volumes below 0.3 ml were not sufficient, as particulates could be visualised in the solution even after vigorous manual shaking was applied.

As a conclusion, the data show that both excipients contained in a vial of Botox® can be dissolved with volumes in the microlitre range, as low as 30 µl. The solubility of BTX A was not assessed in this experiment due to the extremely low dose of toxin (5 ng) contained in the vial and the safety concerns related to the handling of larger quantities of BTX A. However, nanogram quantities of the protein are not expected to interfere with the reconstitution of the pharmaceutical preparation, even when dealing with volumes in the microlitre range. Therefore, the results indicate that significantly smaller volumes compared to the ones currently used in the clinical setting (1.5-5 ml) could be used to reconstitute an entire vial of Botox®.

However, handling volumes in the range of microlitres is technically challenging. For example, if a volume of diluent as low as 30 µl was to be used, the solution obtained would be difficult to withdraw from the vial. This would lead to waste of the costly therapeutic material and inaccuracy of the dose loaded (and thus delivered). Therefore, increased volumes may have to be used in order to facilitate better handling of the solution. As a consequence, PMD loading of a more diluted BTX A formulations may require improvement in the PMD loading capacity. This may be achieved by modifying the PMD design (for example increasing the number of needles per array). The experiments reported in the following Chapter aim to determine the PMDs loading capacity. This will help to estimate the volume of Botox® formulation which could be accommodated by a PMD and therefore to understand whether optimization of the PMD design is required.

Table 2.4: Evaluation of the limit of solubility of HSA and NaCl in saline solution. Masses are representative of a vial of the commercial Botox® formulation.

Solution	HSA (mg)	NaCl (90mg/10ml) ml	Saline solution 0.9% (ml)	Approximate total volume (ml)	Solubility
1	5	0.1	0.8	0.9	✓
2	5	0.1	0.7	0.8	✓
3	5	0.1	0.6	0.7	✓
4	5	0.1	0.5	0.6	✓
5	5	0.1	0.4	0.5	✓
6	5	0.1	0.3	0.4	✓
7	5	0.1	0.2	0.3	✓
8	5	0.1	0.1	0.2	x
9	5	0.1	/	0.1	x

2.4.4 Liquid loading PMDs with a 'Botox® like' formulation

PMDs and NPMDs were liquid loaded by immersing the needles into a 'Botox® like' formulation. Figure 2.6 (A-C) depicts a representative PMD (A, B) and NPMD (C) after one immersion into a 'Botox® like' formulation. The pockets of the PMD were uniformly filled for a short duration after immersion. Videos captured by a digital camera indicated complete evaporation of the liquid component of the formulation from the pockets within approximately 90 seconds. Immediately after loading, the formulation was visualised on the needles of a NPMD by the naked eye and by light microscopy. The same was observed for liquid coated on the shaft of the pocketed microneedles and on the central non pocketed microneedle of the PMD (the presence of a central non pocketed microneedle in the studied PMDs was shown in Section 2.4.1). Subsequent analysis of the NPMD under the light microscope revealed a film (Figure 2.6 C) on the surface of the needles. Similarly, analysis of the PMD after evaporation of the loaded solution resulted in a film coated on the shaft of the needles and also the interior surfaces of the pockets (Figure 2.6 B).

The results indicate that a Botox® formulation can be loaded and retained, in a liquid state, by the pockets of a PMD. Importantly, observations suggest that the formulation can be maintained in its liquid state for a sufficient time to allow PMD application to the skin. Moreover, following evaporation of the solvent, the needles of both the PMDs and NPMDs appeared to be uniformly coated after only one immersion. This suggests that a Botox® formulation could be loaded onto the MDs as either a liquid formulation or a dry coat by a simplistic one step immersion process. The inherent viscosity of the protein based formulation, most likely due to the high

concentration of HSA, promoted retention of the formulation in the pockets of microneedles without requirement to reformulate. Avoiding reformulation would significantly reduce regulatory hurdles and would simplify clinical use of the MD as a means to deliver a BTX A formulation.

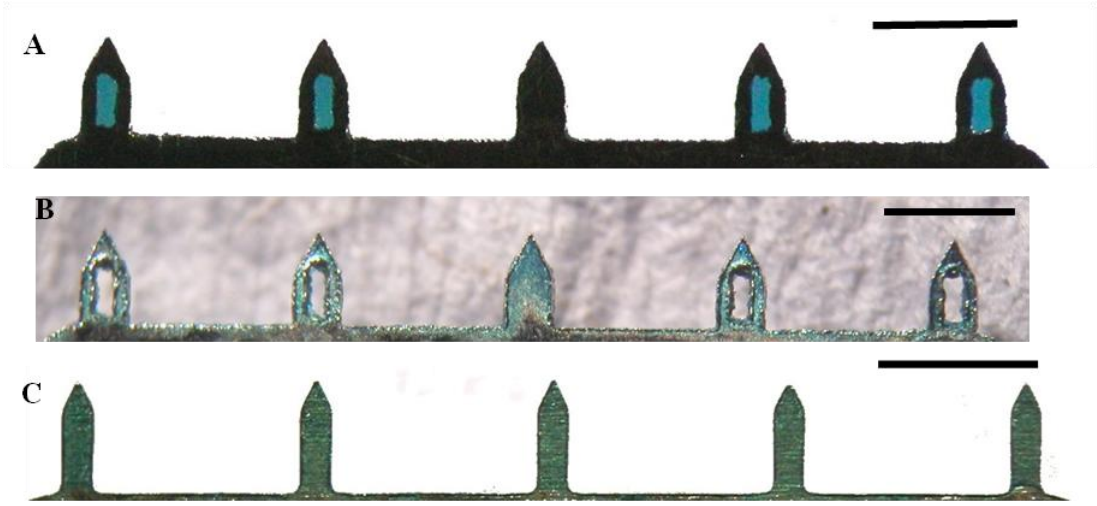

Figure 2.6 (A-C): Loading of a 'Botox® like' formulation in PMDs and NPMDs. Representative brightfield micrographs of a PMD (A, B) and a NPMD (C) after immersion into a 'Botox® like' formulation. For visualizing purpose, a blue dye was added to the loading formulation. The excess of solution accidentally collected on the base of the MDs during immersion into the loading formulation was carefully removed by using lintless tissue paper. Scale bar = 1 mm.

PMDs offer the advantage of visualisation of the loaded solution. The presence of a coloured solution can be detected in the pockets with the naked eye. This would be particularly useful in a clinical context, as it would allow the clinician and/or patient to i) ensure that successful and uniform loading has occurred before application into the skin and ii) visualise whether the drug formulation has been delivered into the skin after insertion of the loaded PMD.

2.4.4.1 Liquid loading MDs with a high concentration of the model β-galactosidase

Loading experiments were performed on PMDs using a higher concentration of the model BTX A (β-gal 1.3 μg/μl in BSA/bicine buffer) than the concentration

employed in a 'Botox® like' formulation (β-gal 5 ng/150 µl in saline solution). The increased concentration was selected to provide a BTX A model concentration that could be employed to perform quantitative analysis of PMD loading capacity (Chapter 3) and enable visualisation of cutaneous delivery (Chapter 4). Increased concentrations are required to enable loading of PMDs with doses of the BTX A model, which can be detected using established experimental methodologies. Therefore, the aim of this experiment was to evaluate the residency time of a high concentration BTX A model solution in the pockets of a PMD to determine the time that would be available to insert a loaded PMD into the skin whilst maintaining the model protein in a liquid state.

The results indicated that loading PMDs with a higher concentration of the model BTX A does not affect the uniform loading of the pockets. The formulation was retained in the pockets for approximately 90 seconds, after which the solvent evaporated. Therefore, the data indicated that loading PMDs with a concentrated solution allows retention of the liquid in the pockets for a sufficient time to permit application of the loaded PMDs into the skin and delivery the protein in a liquid state.

2.4.5 Enhancing the retention of liquid loaded drug formulations in microneedle pockets

The evaporation process of a solution is highly affected by its level of viscosity (Chen 1983). Evaporation of a liquid occurs when molecules in a liquid state collide, transferring energy to each other and thus becoming gaseous. The rate of the evaporation depends on the level of interaction between the molecules in the solution. Liquids that do not evaporate at a given temperature are composed of molecules that do not tend to rapidly transfer energy to each other and thus do not generate enough heat to be converted into vapour. In this case, the evaporation process will be less visible as it will occur at a considerably lower rate.

Increasing concentrations of the viscosity enhancer glycerine were assessed as a means to enhance retention of aqueous solutions in MD pockets. Figure 2.7 indicates that the longevity of the liquid filled pockets can be dramatically increased by the addition of glycerine. Loading formulations containing glycerine 80% w/v were retained in the microneedle pockets for up to one month. Conversely, loading

solutions without glycerine visibly evaporated from the pockets within seconds. Addition of viscosity enhancers may therefore prove useful when volatile liquid formulations have to be loaded, in order to increase the residency time prior to application to the skin.

These results confirmed the importance of viscosity for the sustained loading of the microneedle pockets (Section 2.4.4). Viscosity enhancers could therefore be added to a BTX A drug in order to reduce the evaporation rate of the formulation. This would ensure a more stable retaining of the drug into the pockets in a liquid state and may turn useful in clinical scenario as it would provide the clinician with an extended application time. However, addition of such excipients would determine the need for reformulation of existing commercial BTX A formulations and thus a considerable increase in the number of regulatory hurdles that would have to be overcome. Studies will be required in order to assess the effect of glycerine on the efficacy of BTX A. Such viscous formulations may affect the conformation of the toxin and/or reduce its migration to therapeutic targets once delivered within the skin.

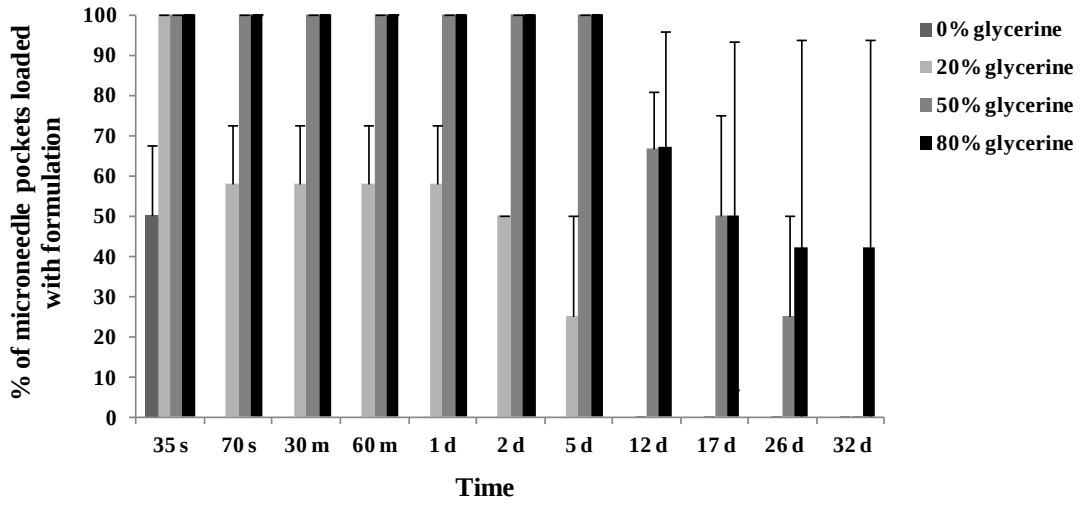

Figure 2.7: Effect of viscosity enhancers on PMD loading. The percentage of microneedle pockets retaining a glycerine based formulation is shown as a function of time. s = seconds, m = minutes, d = day/s.

2.5 Conclusion

Small hydrophilic molecules and nanoparticles can be coated onto NPMDs, in a dry state, by using established coating methodologies. Increasing the number of immersions in the coating formulation results in better coating efficiency. However, automation of the process and/or specific MD design tailoring is needed in order to improve coating uniformity.

Solubility studies indicate that the contents of a Botox® vial (HSA 0.5 mg and NaCl 0.9 mg) can be dissolved in volumes that are small enough to enable effective MD loading of the toxin. PMDs and NPMDs can be uniformly loaded after one single immersion into a 'Botox® like' formulation. The inherent viscosity of the formulation promotes retention of the solution in the pockets of a PMD for a sufficient time that would allow subsequent application of the loaded device into the skin. After complete evaporation has occurred, a dry layer can be detected on the shaft of NPMDs and PMDs. This suggests that a Botox® formulation could be loaded onto the MDs and retained either as a liquid formulation or a dry coat.

The results suggest that the studied MDs are suitable for successfully loading existing BTX A formulations. BTX A loaded MDs are therefore a potential means of delivering the therapeutic toxin into the skin.

Chapter 3

Evaluating the loading capacity of pocketed microneedle devices (PMDs)

3.1 Introduction

Due to the constrained dimensions of microneedle devices (MDs), the mass of drug that can be loaded on each microneedle is limited. For this reason, dry coated MDs have been studied as a means to deliver potent biopharmaceutics such as vaccines (Kendall 2006; Kim et al. 2011; Quan et al. 2010) and hormones (Ameri et al. 2009; Cormier et al. 2004) with effective doses in the range of micrograms (Crommelin et al. 2003; Kenney et al. 2004). Due to the high potency of BTX A, therapeutic doses of the toxin reside in the low nanogram range (Section 1.4.1.1). Therefore, BTX A is a good candidate for MD loading. The experiments reported in Chapter 2 (Section 2.4.4) indicated that a model of the commercial preparation Botox® (called 'Botox® like' formulation), can be uniformly coated onto PMDs. The experiments described within this Chapter aim to investigate the suitability of PMDs as a means to retain therapeutically effective doses of BTX A in a liquid form. The term effective refers to the therapeutic doses employed in the treatment of palmar PFHH (Section 1.5.1). The loading capacity of liquid loaded PMDs will be compared to the more established NPMDs.

The different strategies that have been employed to coat medicaments onto solid MDs (with or without pockets) were previously discussed (Sections 2.1.1 and 2.1.2), with a particular focus on the coating strategies for high molecular weight therapeutics such as proteins and vaccines. These therapeutics are more closely aligned to BTX A than small drug molecules. This introductory Section will provide an overview of the doses of medicaments that have been coated on solid MDs (with or without pockets) and the different factors that are known to affect the MD coating capacity.

3.1.1 The coating capacity of dry coated solid MDs

Numerous studies have reported MD dry coating with a range of molecules including low and high molecular weight model drugs and therapeutics (Daddona 2011; Gill and Prausnitz 2007a, b). As previously stated (Section 2.1.1), MDs are generally coated by multiple immersions into a coating formulation, with specific time

intervals between each immersion to permit drying of the loaded drug. Specific excipients such as viscosity enhancers and surfactants are typically added to the coating formulations in order increase the coating efficiency.

Within the published studies, MD coating capacity has been reported to be significantly affected by parameters such as i) number of immersions (dips) of the microneedles into a coating formulation: increasing the number of immersions into a coating formulation results in thicker coatings and thus increased dose of medicament per microneedle (Ameri et al. 2010; Gill and Prausnitz 2007b; Zhang et al. 2011; Zhu et al. 2009); ii) microneedle design: arrays containing an higher number of microneedles can be coated with more material and therefore with greater doses of drug (Ameri et al. 2009; Ameri et al. 2010; Cormier et al. 2004; Daddona 2011; Gill and Prausnitz 2007b; Zhang et al. 2011); iii) concentration of the medicament in the coating formulation: more concentrated formulations enable greater loading of medicaments per microneedle per immersion (Ameri et al. 2010; Cormier et al. 2004; Gill and Prausnitz 2007b; Zhu et al. 2009); iv) viscosity of the coating formulation: formulations containing viscosity enhancers (e.g., CMC or sucrose) and/or high concentrations of high molecular weight compounds, such as peptide and proteins, are usually associated with a higher level of viscosity compared to water (Ameri et al. 2010). More viscous formulations allow retention of increased volumes of liquid at each microneedle immersion. This promotes thicker coatings and thus greater dose loading (e.g., use of CMC within coating formulations has been associated with dose coating more than one order of magnitude higher than CMC-free coating formulations (Kim et al. 2010)). A summary of medicaments that have been coated on differently designed MDs, the doses at which they have been coated and the different parameters mentioned above, are summarised in Table 3.1.

Table 3.1: A summary of drugs coated on differently designed MDs and factors affecting MD coating capacity. MD coating capacity varies according to multiple parameters such as: number of immersions (dips) into the coating formulation, number of needles per array (N), composition of the coating formulation (concentration of the drug to be coated and/or concentration of the viscosity enhancer).

Drug coated (molecular weight)	Mass coated (µg)/ MD (or needle/pocket as indicated)	Material and number of microneedles per MD (n)	Individual microneedle dimensions (µm)	Coating formulation composition	Number of immersions	Reference
Inactivated influenza virus (A/PR/8/34)	Up to 0.94	Stainless steel n=5	700 (length) 160 (width) 50 (thickness)	Inactivated virus1mg/trehalose 15% w/v*	6	(Kim et al. 2010)
Inactivated influenza virus (A/PR/8/34)	~ 0.5-3.5	Stainless steel n=5	500 (length) 200 (width) 50 (thickness)	Inactivated virus 5 mg/ml*	3-9	(Zhu et al. 2009)
	9.8	Stainless steel n=5	500 (length) 200 (width) 50 (thickness)	Inactivated virus10mg/m*	9	
BSA (~66 kDa)	10	Stainless steel n=5	500 (length) 200 (width) 50 (thickness)	BSA 0.15% w/v*	1	(Zhu et al. 2009)
Virus like particles (H1N1 A/PR8/34)	0.35	Stainless steel n=5	700 (length) 170 (width) 55 (thickness)	Inactivated virus 5mg/ml, trehalose 15% w/v*	9	(Quan et al. 2010)
Riboflavin (~380 Da)	0.002-2.6 (per needle)	Stainless steel n=5	700 (length) 160 (width) 50 (thickness)	Riboflavin 0.01-4% w/v*	6	(Gill and Prausnitz 2007b)

Riboflavin	0.2-6.4 (per needle)	Stainless steel n=5	700 (length) 160 (width) 50 (thickness)	Riboflavin 3% w/v*	1-24	(Gill and Prausnitz 2007b)
Riboflavin	The mass of drug per MD was increased of ~ ten fold (data not shown)	Stainless steel n=50	700 (length) 160 (width) 50 (thickness)	Riboflavin 3% w/v*	6	(Gill and Prausnitz 2007b)
Riboflavin	0.01-0.06 (per pocket)	Stainless steel n=5 (pocketed microneedles)	700 (length) 160 (width) 50 (thickness). Pocket dimensions: 400 (length) 50 (width)	Riboflavin 1-3% w/v, sucrose 25% w/v	6	(Gill and Prausnitz 2007b)
Riboflavin	0.6-1.8 (per needle)	Stainless steel n=5	700 (length) 160 (width) 50 (thickness)	Riboflavin 1-3% w/v*	6	(Gill and Prausnitz 2007b)
Riboflavin	0.01- 1.79 (per needle)	Stainless steel n=5	700 (length) 170 (width) 50 (thickness)	Riboflavin 0.01-3% w/v*	1	(Gill and Prausnitz 2008)
	0.02-2.8 (per needle: pocket + shaft)	Stainless steel n=5 (pocketed microneedles)	Pocket dimensions: 400 (length) 50 (width)	Riboflavin 0.01-3% w/v*	1	
Lidocaine (~290 Da)	~ 90	Liquid crystalline polymer n~316	~500 (length) (other dimensions not specified)	Lidocaine 30% w/w, dextrane 30% w/w	1	(Zhang et al. 2011)
	~225	Liquid crystalline polymer n~316	~500 (length) (other dimensions not specified).	Lidocaine 30% w/w, dextrane 30% w/w	2	

Desmopressin hormone (1.1 kDa)	23	Titanium (Macroflux®) n~640	200 (length) 170 (width) 35 (thickness)	Desmopressin 24% w/w**	Not specified	(Cormier et al. 2004)
	80	Titanium (Macroflux®) n~640	200 (length) 170 (width) 35(thickness)	Desmopressin 40% w/w**		
Parathyroid hormone (~4.1 kDa)	40	Tianium (Macroflux®) n=1300	190 (length) 115 (width) 25 (thickness)	Parathyroid hormone 12% w/w***	5	(Ameri et al. 2010)
	40	Tianium (Macroflux®) n=1300	190 (length) 115 (width) 25 (thickness)	Parathyroid hormone 17% w/w***	3	
Ovalbumin (~44 kDa)	0.5	Titanium (Macroflux®) n=up to 1314	Up to 600 (length) 100 (width) 35 (thickness)	Ovalbumin 2% w/w, sucrose 30% w/w**	1	(Widera et al. 2006)
	25	Titanium (Macroflux®) n=up to 1314	Up to 600 (length) 100 (width) 35 (thickness)	Ovalbumin 20% w/w, sucrose 48% w/w**	12	
Ovalbumin	43.3	Nanopatch™ n>20.000/cm^2	65 (length) ~40 (width) Thickness not specified	25nCi ^{14}Ovalbumin methyl-cellulose 1.5% w/w	Not applicable	(Crichton et al. 2010)

*plus CMC 1% w/v and Lutrol® F68 0.5% ; ** and Tween® 20 0.2 w/w; ***plus sucrose 16.6% w/w and Tween® 20 0.2% w/w.

Published studies reporting MD coating with vaccines, and in particular influenza vaccines, have indicated vaccine coatings with doses ranging between 0.3 to 10 µg per MD (Kim et al. 2010; Koutsonanos DG 2009; Koutsonanos 2011; Quan et al. 2010; Zhu et al. 2009). MDs employed within these studies contain a reduced number (5) of relatively long (700 µm) stainless microneedles per array. MD coating with influenza vaccines does not require further optimization of the coating capacity as those vaccines are typically of low microgram doses. Conversely, maximization of MD coating capacity has been reported for medicaments that require larger doses. Typically, this is achieved by using more densely packed MDs. For example up to 40 µg of parathyroid hormone and 80 µg of desmopressin have been coated on titanium MDs (Macroflux®) by coating the tip (~100 µm) of the microneedles, which number between 280 and 1314 microneedles per array (Ameri et al. 2010; Cormier et al. 2004; Daddona 2011). An additional published study indicates that up to 225 µg of the anaesthetic lidocaine can be coated on MDs containing approximately 316 microneedles (Zhang et al. 2011).

As previously mentioned (Section 2.1.1), vaccines have also been coated on short densely packed (~20000 microneedles/cm^2) silicon MDs (Nanopatch™) by using a gas jet coating procedure (Chen et al. 2009; Chen et al. 2010). Recent studies reported that such MDs were successfully coated with the commercial trivalent influenza vaccine Fluvax® 2008 (Chen et al. 2012; Fernando et al. 2010). Details regarding the mass of vaccines coated on the MDs are not provided. However, previous studies performed using ovalbumin as a model antigen indicated that a mass of 43.3 +/-1.73 (standard deviation) µg of protein was coated onto the Nanopatch™ (Crichton et al. 2010). Quantitative analysis of the doses of Fluvax® 2008 delivered to the skin of animal models revealed that Nanopatch™ technology enables doses sparing of up to 30 folds compared to intramuscular injections.

In summary, the capability of solid MDs to accommodate high molecular weight therapeutics such as vaccines, proteins and hormones has been widely assessed. Doses in the range of micrograms have been reported for all the medicaments tested. This suggests that MDs offer the potential to retain effective doses of BTX A (Botox®). However, some research groups have reported poor reproducibility of the MD coating dose (Cormier et al. 2004; Gill and Prausnitz 2007b; Zhang et al. 2011).

This has been generally associated with the use of manual and/or poorly optimised coating methodologies, which have resulted in reduced spatial control of the coating deposition. Coating uniformity on microneedles has to be guaranteed in order to ensure dose reproducibility. This is critical for therapeutic drug delivery and is particularly important for potent and potentially toxic therapeutics such as BTX A (Botox®). For this reason, the experiments reported in this Chapter will investigate the reproducibility of BTX A (Botox®) doses loaded on the studied PMDs and NPMDs.

3.1.2 Liquid loaded capacity of pocketed MDs

As previously reported (Section 2.1.2), a variant of solid microneedles is a microneedle containing single or multiple pockets that may be able to accommodate low volume liquid formulations. The concept of this device differs from dry coated MDs in that it is hoped that the pockets of this microneedle design can retain the drug in a liquid form. Quantitative analysis of the loading capacity of such MDs has been studied by Gill and Prausnitz (2007b; 2008) using the model compound riboflavin. Within these studies the drug model was loaded on the microneedles as a dry coat by using specific excipients. To the best of our knowledge no additional studies regarding pocketed MDs have been published. The studies were conducted on stainless steel microneedle rows containing 5 microneedles (700 x 200 x 50 µm; y, x and z plane), each having a rectangular pocket (400 x 50 x 50 µm; y, x and z plane). Similarly designed pocketed MDs, with slightly larger needles and pockets, are used in the current research study (as shown in Section 2.4.1). Gill and Prausnitz (2007b) compared the dose of riboflavin loaded selectively into the pocket of a pocketed microneedle to the amount of riboflavin coated on the surface of a non-pocketed microneedle (700 x 200 x 50 µm, y, x and z plane). The studies indicate that filling drug selectively into the pocket of a pocketed microneedle reduced the mass of drug loaded per microneedle compared to the non pocketed microneedle (i.e., 0.066 +/- 0.013 µg of riboflavin was loaded into the pocket of a pocketed microneedle, which was immersed 6 times into a 3% w/v riboflavin coating

formulation, whereas 1.8 µg was coated on the entire surface of a non pocketed microneedle).

Furthermore, the loading capacity of pocketed MDs with both shaft coatings and filled pockets was compared to the coating capacity of non pocketed MDs (Gill and Praunitz 2008). These results indicate that the dose of riboflavin loaded on the entire pocketed microneedle (pocket + shaft of the needle) was slightly greater compared to non pocketed microneedles (i.e., 2.8 µg of riboflavin was loaded on a pocketed microneedle following only one immersion into a riboflavin 3% w/v coating solution, while 1.79 µg was coated on a non pocketed microneedle). However, the difference in the loading capacity of the two needle designs was not statistically significant. This indicates that the presence of the pockets on microneedles does not increase the total dose of drug loaded. Therefore, although pocketed microneedles may enable medicaments such as BTX A (Botox®) to be delivered in a liquid form, they do not increase drug loading capacity of microneedles.

3.1.3 Specific aims and objectives of the Chapter

Experiments reported within this Chapter will aim to quantify the drug loading capacity of PMDs following a single immersion in to a liquid drug reservoir and will compare results to established NPMDs.

The experimental objectives of the Chapter are to:-

1) Determine the dose of a well-characterised low drug (salbutamol sulphate, SS, m.w.= 233 Da) that can be loaded on to PMDs. An established high performance liquid chromatography (HPLC) assay method will be employed in order to enable robust quantitative analysis.
2) Determine the mass of a model high molecular weight protein (β-gal) that can be loaded, as a liquid formulation, on to PMDs. Calibrated spectroscopy methods will be established in order to enable robust quantitative analysis.
3) Determine the reproducibility of PMD liquid loading for low and high molecular weight molecules.

4) Determine if a therapeutic dose of BTX A (i.e., 0.1-0.25 ng per each administration site) can be loaded, as a liquid, on a PMD using a Botox® mimic formulation.

3.2 Materials

3.2.1 Reagents

All reagents were used as received and were purchased from Sigma-Aldrich Ltd (Poole, UK), unless otherwise stated.

Deionised water was obtained from an Elga reservoir (High Wycombe, UK). Micronised salbutamol sulphate (SS) (mean diameter of 50%; particle population ≤ 3.07 µm) was purchased from Micron Technologies Ltd (Dartford, UK). Methanol 99.9%, sodium chloride, Tris Base (Tris(hydroxymethyl)aminomethane), Triton X-100, trichloroacetic acid 99.8+%, citric acid monohydrate 99.9+%, acetic acid glacial, nuclease free water, Tris HCl (Tris(hydroxymethyl)aminomethane hydrochloride), glycerol 100% and formaldehyde solution 37% was purchased by Fisher Scientific (Loughborough, UK). Sodium dodecyl sulphate (SDS), TEMED (N, N, N-tetramethylendiamine) and bromophenol blue were purchased from Bio-Rad Laboratories (Hemel Hempstead, UK). Full range rainbow recombinant protein molecular weight marker was purchased from GE Healthcare (UK)**.**

3.3. Methods

3.3.1 Calculation of the theoretical loading volume of a PMD

The theoretical volume of a formulation which can be accommodated by a pocket of a single microneedle was calculated by multiplying the three pocket dimensions (length (mm), width (mm) and depth (mm)) obtained following visualization of the PMD by SEM (Section 2.4.1). The value calculated is the volume expressed as mm^3. Knowing that 1 µl is equivalent to 1 mm^3, the theoretical volume was converted to µl. As each PMD contain 4 pockets, the calculated value was multiplied by four in order to obtain the total theoretical volume accommodated by a PMD.

3.3.2 Quantitative analysis of MD loading capacity

Quantitative analysis of MD loading was performed using an established (Ameri et al. 2009; Ameri et al. 2010; Cormier et al. 2004; Gill and Prausnitz 2007b; 2008; Zhang et al. 2011) two step process consisting of i) collection of the drug loaded on the MD by rinsing the array into a determined volume of appropriate buffer and ii) quantification of the drug released from the microneedles by calibrated spectroscopy or HPLC analysis.

3.3.2.1 Quantifying salbutamol sulphate (SS) loading on MDs using HPLC

SS loading capacity of MDs was assessed by a HPLC methodology, established in our laboratories (Bains 2010), as detailed below.

Preparation of the internal standard

An internal standard solution was freshly prepared by dissolving 8 mg of bamethane in 400 ml of methanol before being made up to 1000 ml with deionised water to achieve a final bamethane concentration of 8 µg/ml. Six SS standard solutions (n= 3 for each standard solution) with a concentration ranging from 1 to 80 µg/ml, were freshly prepared from a stock solution of 10 mg/ml, by using the internal standard solution as a diluent. HPLC data (consisting of the area under the curve (AUC) ratios between the known concentration of SS and the bamethane internal standard) were used to generate a calibration curve (included in Section 3.4.2.2).

Preparation of the mobile phase

A buffer solution consisting of 1-heptane sulphonic acid (0.83 mg/ml) was freshly prepared in deionised water. One drop of glacial acetic acid was added to the buffer solution to adjust the pH to 3.2. Subsequently, methanol was added to the solution to achieve a final concentration ratio of methanol 40% v/v-buffer 60% v/v. A 0.2 µm Whatman® nylon membrane filter (Whatman International Ltd., Maidstone, UK) was then used to filter the mobile phase prepared.

Preparation of samples

The loading formulation was prepared by dissolving 100 mg of SS into 1 ml of deionised water. PMDs (n=10) and NPMDs (n=10) were then drug loaded by manually immersing the microneedle shafts once into SS solution as previously described (Section 2.3.4). Once loaded, each MD (NPMDs and PMDs) was immediately transferred into individual polypropylene microcentrifuge tubes, containing 500 µl of internal standard. After 1 hour, a 400 µl aliquot (sample solution) was withdrawn from each tube. Samples were then analysed by HPLC and Chem Quest® 4.1 software (Thermo Electron Corporation, Altrincham, UK). The characteristics of the HPLC equipment and the chromatographic conditions are outlined in Table 3.2.

The calibration curve (Section 3.4.2.2) was used to determine SS concentration for each sample solution. The mass of SS loaded on each MD was then calculated by multiplying the measured concentration by the volume used for removal of the SS coating from the MDs. This value was used to calculate the volume of formulation that was loaded on each MD. A two tailed Mann Whitney U test was performed to compare two different groups (PMDs versus NPMDs), with significant differences indicated by p values <0.05.

Table 3.2: HPLC analysis of SS

HPLC equipment	Pump:	P200
	Autosampler:	AS 3000
	Detector:	UV 2000
	Chromquest software	
Chromatographic Column	Genesis C18, 15 cm x 4.6 mm, 120 Å 4 um (Grace Vydac, Bannocburn, Illinois, USA).	
Assay conditions	Flow rate of mobile phase:	1 ml/min
	UV wavelength:	278 nm
	Injection volume:	100 µl
	Retention time SS:	6 minutes
	Retention time bamethane:	10 minutes

3.3.2.2 Quantifying MD loading with a model BTX A formulation using spectrophotometric techniques

The enzyme β-gal, used as a model for BTX A (as previously indicated in Section 2.1.3), was quantified using an established assay method that involves spectrophotometric measurements of the formation of the yellow chromophore o-nitrophenol (ONP) (λabs max: 420 nm). This compound is the product of the hydrolytic reaction between the enzyme and the colourless substrate o-nitrophenyl-β-D-galactoside (ONPG) (Figure 3.1.) (Griffith and Wolf 2002).The reaction product has a peak of absorbance at 420 nm and therefore wavelengths ranging between 410 and 430 nm are used to obtain the greatest sensitivity (www.promega.com 2006).

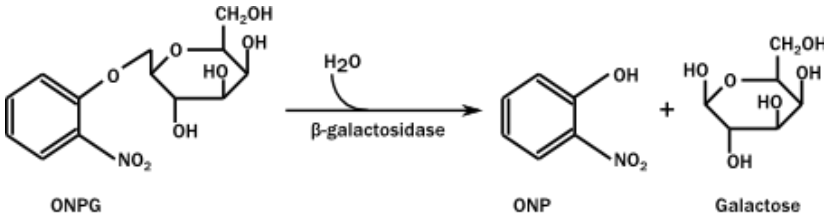

Figure 3.1: Schematic representation of the reaction between the enzyme β-gal and the substrate ONPG. Adapted from http://2011.igem.org/File:ONPG.png 2011.

The spectrophotometric methodology used was performed according to protocols reported by Sigma Aldrich (www.sigmaaldrich.com 1994, 1999) with the modifications outlined in details below. The reagents used to perform the analysis are outlined in Table 3.3.

Table 3.3: Components of the ONPG assay solution

ONPG-assay solution	
Reagents	**Concentration**
A) Sodium phosphate solution*[1], monobasic, anhydrous, solution	100 mM
B) Sodium phosphate buffer (SPB) pH 7.3 at 37°C*[2], solution	100 mM
C) ONPG solution (to be prepared in reagent B)*[3]	68 mM
D) Magnesium chloride ($MgCl_2$) solution in deionised water	30 mM
E) 2-Mercaptoethanol solution (2-ME) in deionised water	3.36 M

**[1] To be prepared in deionised water using sodium phosphate, monobasic, anhydrous powder.*

**[2] To be prepared in deionised water using sodium phosphate, dibasic, anhydrous powder. Adjust to pH 7.3 at 37 °C with reagent A.*

**[3] Solution to be gently warmed until the reagent is completely dissolved*

Spectrophotometric assay method for BTX A model determination

The BTX A model, β-gal (β-gal from *Escherichia Coli*, Grade VI lyophilized powder, 1000 U) was reconstituted in 1 ml of Sodium phosphate buffer (SPB) 100 mM, pH 7.3 at 37°C, to a concentration of 2.6 µg/µl. The solution was then aliquoted and stored at -20°C. An aliquot of the solution was defrosted on the day of the experiment and diluted to a concentration of β-gal 1.3 µg/µl in SPB. MDs were loaded either with the aid of the micro scale dip coating device (Section 2.3.2.1) or as described in Section 2.3.4 (the methodology employed for each experiment will be specified in the following Section).

Once loaded with the BTX A model, the protein was removed for quantification by soaking the device in 300 µl of SPB for 1hour. Subsequently, an aliquot (100 µl) was withdrawn from each sample solution and added to specific assay reagents to produce the test solutions. The assay reagents and the order in which they were added are outlined in Table 3.4. After 40 minutes, the reaction was arrested by increasing the pH to 11 using sodium carbonate (1 M). This assay was repeated for matched blank solutions and also a range of standards (0.4-6.6 ng/µl) with a number of standard solutions ≥5. To quantify the colour change, an aliquot (200 µl) was

withdrawn from each assay solution and transferred in triplicate into a 96 well polypropylene flat-bottomed optically clear plate. Absorbance values were measured at λ = 410 nm using a Fluostar fluorometer (BMG Lab technologies, Ortenberg, Germany). The results were expressed as a mean of the three readings obtained +/- standard deviation.

Standard solutions were used to generate a calibration curve, which was used to determine BTX A model concentration of each sample solution. The mass of the BTX A model in the solution was thus calculated by multiplying the measured concentration by the volume of SPB used for protein removing from the MDs. The mass of protein that was retained by each microneedle was then calculated. Knowing the concentration of the BTX A model in the formulation (1.3 µg/µl), the mass value obtained was used to predict the volume of formulation loaded on each MD.

Each test solution was constituted by a sample solution and the corresponding matched blank solution. The total volume of each test solution prepared was 5 ml. Test solutions of BTX A model standards (standard solutions and matched blank solutions) were also prepared according to the sequence outlined by the Table below.

Table 3.4: Sequence of addition of the reagents for the preparation of test solutions.

	Reagent	Volume added (µl)	Addition of the reagent to the test solution?	Addition of the reagent to the blank solution (negative control)?
Step 1	Sodium phosphate buffer (100 mM) pH 7.3 at 37 °C (SPB)	2600	Yes	Yes
Step 2	Magnesium cloride ($MgCl_2$) 30 mM	100	Yes	Yes
Step 3	β-gal solution	100	Yes	No
Step 4	2-Mercaptoethanol (2-ME) 3.36 M	100	Yes	Yes
	Mix and equilibrate to 37 ºC			
Step 5	ONPG (substrate) 68 mM	100	Yes	Yes
	Mix and incubate for 40 minutes at 37ºC			
Step 6	Sodium Carbonate ($NaCO_3$) 1 M	2000	Yes	Yes
Step 7	β-gal solution	100	No	Yes

Assessing the feasibility of the spectrophotometric assay

Initial experiments were performed in order to assess the suitability of the spectrophotometric assay, previously described, to successfully detect the mass of the BTX A model liquid that will be loaded on to a MD.

A standard curve was constructed by using a BTX A model concentration ranging between 0.4-6.6 ng/µl (the calibration curve is included in Section 3.4.2.1)

Comparison of PMDs and NPMDs loading capacity

The spectrophotometric methodology described above was used to compare the mass of the BTX A model loaded onto PMDs and NPMDs after a single immersion into the BTX A model solution (1.3 µg/µl). In this experiment PMDs (n=8) were manually loaded by a single immersion into a reservoir containing a small volume (~20 µl) of the BTX A model formulation as previously described (Section 2.3.4). NPMDs (n=8) were drug loaded with the aid of a micro scale dip coating reservoir device described in Section 2.3.2.1 After the immersion, excess formulation

accidentally collected on the base of each PMD and NPMD was carefully removed using lintless tissue paper.

The experiment described above was repeated in order to compare the loading capacity of PMDs (n=10) and NPMDs (n=10) when loaded without the aid of a microscale dip coating reservoir. Loading was performed as reported above for PMDs and described in Section 2.3.4. A two tailed Mann Whitney U test was performed to compare two different groups (PMDs versus NPMDs), with significant differences indicated by p values < 0.05.

3.3.3 Assessing the feasibility of a PMD to load a therapeutic dose of BTX A, as a liquid, using a 'Botox® blank' formulation.

The commercial formulation Botox® contains a dose of BTX A (5 ng), which is considerably difficult to detect by using standard laboratory techniques. As previously mentioned (Section 2.1.2), other constituents of Botox® are the excipients HSA and NaCl. Within a single vial of Botox® there is 0.5 mg of HSA. HSA was chosen as a surrogate measure of BTX A due to its greater mass in the formulation and therefore the ability to detect it. MDs were loaded with a dose of HSA that was representative of the dose in the clinical formulation and this could be detected by standard laboratory methodologies. MDs were liquid loaded with a 'Botox® blank' formulation containing the same constituents of Botox® (HSA 0.5 mg and NaCl 0.9 mg) but devoid of BTX A. After loading, MDs were immersed for 1 hour at room temperature into an appropriate diluent. The protein released in the diluent was subsequently characterised by SDS-PAGE (sodium dodecyl sulphate polyacrylamide gel electrophoresis) and visualised by silver staining methodologies.

3.3.3.1 Assessing the feasibility of SDS-PAGE and silver staining methodology for characterization of the HSA contained in the commercial preparation Botox®

Initial experiments were performed in order to assess the feasibility of electrophoretic and silver staining techniques to detect the mass of HSA (0.5 mg) contained in Botox®.

The commercial BTX A preparation Vistabel® (containing the same excipients as Botox®) was employed as a substitute of Botox®. Standard solutions of the protein bovine serum albumin (BSA, 66 kDa) were used as a positive control.

SDS-PAGE methodology

Preparation of 10% polyacrlyamide resolving gel

A 10% polyacrylamide resolving gel was prepared by mixing the following ragents at the volumes indicated:

i) 2.5 ml of 40% acrylamide/bisacrylamide
ii) 1.25 ml of 3 M Tris buffer pH 8.8
iii) 0.1 ml of 10% sodium dodecyl sulphate (SDS)
iv) 6.1 ml of deionised water
v) 0.0075 ml of TEMED (N, N, N-Tetramethylendiamine)
vi) 0.075 ml of ammonium persulfate (APS) 10% w/v in deionised water

Preparation of 4% polyacrlylamide stacking gel

A 4% polyacrylamide resolving gel was prepared by mixing the following reagents at the volumes indicated:

i) 0.5 ml of 40% acrylamide/bisacrylamide
ii) 0.65 ml of 1 M Tris HCl buffer pH 6.8
iii) 0.05 ml of 10% sodium dodecyl sulphate (SDS)
iv) 3.8 ml of deionised water
v) 0.005 ml of TEMED (N, N, N-Tetramethylendiamine)
vi) 0.0375 ml of APS 10% w/v in deionised water

Preparation of Vistabel® sample formulation and BSA solution.

A vial of Vistabel® containing HSA 0.5 mg was reconstitued in 200 µl of 0.9% saline solution to a HSA concentration of 2.5 µg/µl. An aliquot (40 µl) of Vistabel® was diluted to a HSA concentration of ~1.8 µg/µl in loading buffer ((DTT (DL-dithiothreitol) ~0.18 M, Tris-HCl pH 6.8 (at 25°C) ~14.2 mM, SDS ~0.53% w/v, bromophenol blue ~5.3 x 10^{-04} % w/v, and glycerol ~1.9% v/v))

A stock solution of bovine serum albumin (BSA) 1 µg/µl was freshly prepared in 0.9% saline solution. An aliquot (20 µl) of this stock solution was furthermore diluted to a concentration of ~0.3 µg/µl in loading buffer (as above). This was used as a positive control (pos. control)

The sample and control solutions obtained were heated to 96°C for 5 minutes (Tube Boiler, Grant, Fisher, UK). Subsequently, aliquots (15 µl) of each solution were loaded in triplicate into the polyacrylamide gel previously prepared. Therefore, the gel contained ~4.5 µg of BSA (per well) and ~27 µg of HSA (per well). A molecular marker (Full-Range Rainbow Molecular Weight Marker, GE Healthcare, UK) was also loaded in duplicate (5 µl per well).

The gel was subsequently dipped in 1X running buffer (per litre distilled water, 3.03g Tris base, 14.4 g glycine, 1.0 g SDS) and run for 70 minutes at 110 Volts in a Biorad Mini-PROTEAN Tetra Cell (10-well, 1.0 mm thickness, 4-gel system + Mini Trans-Blot Module) powered by a GE Healthcare EPS-601 power supply. Subsequently, the gel was transferred into a weighing boat (Fisher Scientific, UK) containing approximately 5 ml of deionised water and washed for 5 minutes at room temperature on a rocking platform (Gyro rocker, Stuart, Fisher Scientific, UK). The gel was then transferred into a new weighing boat containing approximately 5 ml of TCA (trichloroacetic acid 20% w/v in deionised water) and washed overnight at room temperature on a rocking platform. Subsequently the gel was processed as described below for silver staining methodology.

Silver staining methodology

Visualisation of the protein bands following SDS-PAGE was performed by a silver staining methodology as outlined by Dunn (2002). The following incubation steps were performed at room temperature on an orbital platform.

Step 1: Sensitization

The gel was washed twice (2 x 20 minutes) in deionised water before being soaked in glutaraldehyde 10% v/v for 30 minutes followed by 3 x 20 minutes washes in deionised water.

Step 2: Staining

The gel was incubated for 30 minutes with a freshly prepared silver diamine staining solution consisting of 21 ml of sodium hydroxide 0.36% w/v, 74 ml of deionised water, 1.4 ml of ammonium hydroxide and 4 ml of silver nitrate 20% w/v. The latter was added dropwise with constant stirring. Subsequently, the gel was washed three times in deionised water, 5 minutes each time.

Step 3: Development and Stopping

Visualisation of protein bands was obtained by soaking the gel in a developing solution consisting of citric acid 0.005% w/v and formaldehyde 0.019% v/v in deionised water. This treatment was performed for approximately 1 minute before being terminated by immersing the gel in stopping solution (ethanol 40% v/v, acetic acid 10% v/v in deionised water).

Step 4 Imaging

The gel was subsequently washed twiced (2 x 15 minutes) in deionised water before being imaged by ChemiDoc XRS + System (Bio-Rad Laboratories, Hemel Hempstead, UK).

3.3.3.2 Comparison of PMDs and NPMDs loading of BTX A from a 'Botox® blank' formulation

A 'Botox® blank' formulation containing only the excipients of the commercial preparation, 0.5 mg of HSA and 0.9 mg of NaCl, was freshly prepared in 150 µl of 0.9% saline solution. Saline solution is the diluent recommended by Allergan to reconsitute a vial of Botox® (Section 1.5.1) and therefore the blank formulation provides a close representation of the clinical formulation, the only omission being 5

ng of BTX A, This 'Botox® blank' formulation differs from the so termed 'Botox® like' formulation described in Section 2.3.4.1 in that it does not contain β-gal as a model for BTX A.

PMDs (n=6) and NPMDs (n=6) were liquid loaded by a a single immersion into the 'Botox® blank' formulation as previously described (Section 2.3.4). The loaded protein was released by soaking each MD in 0.9% saline solution (200 µl) for 1 hour at room temperature. An aliquot (40 µl) was withdrawn from each solution where a single MD was immersed and diluted to a concentration of approximately 70% v/v in loading buffer ((DTT (DL-dithiothreitol) ~0.18 M, Tris-HCl pH 6.8 (at 25°C) ~14.2 mM, SDS ~0.53% w/v, bromophenol blue ~5.3 x 10^{-04} % w/v, and glycerol ~1.9% v/v)).

Additionally, a stock standard solution (HSA 1 µg/µl) was freshly prepared in 0.9% saline solution 0.9% w/v. From this stock solution, six diluted HSA solutions were prepared in loading buffer (as above) to a final HSA concentration of approximately 0.9-180 ng/µl.

The sample and the standard solutions were subsequently heated at 96 °C for 5 minutes (Tube Boiler, Grant, Fisher Scientific, UK) as previously described (Section 3.3.3.1). Aliquots (15 µl) of HSA standard solutions were transferred into each of 2 polyacrylamide gels (gel 1 and gel 2), prepared according to the methodology earlier described (Section 3.3.3.1). Aliquots (15 µl) of the sample solutions obtained either from PMDs or NPMDs were loaded respectively into gel 1 (PMDs) and gel 2 (NPMDs). Each gel contained a decreasing mass of HSA standard, ranging between approximately 13 and 2700 ng. SDS-PAGE and silver staining methodology were therefore performed as previously described (Section 3.3.3.1).

The concentration of HSA in the sample solutions was determined by visually comparing the intensity of these bands to the intensity of HSA bands generated by HSA standards. The mass of HSA loaded on the MDs was subsequently estimated (semi-quantitative) by multiplying the sample concentrations by the volume of diluent used to remove HSA from the microneedles (200 µl). The volume of formulation loaded on each MD was then calculated and the mass of BTX A potentially loaded on a MD was subsequently extrapolated.

3.4 Results and Discussion

3.4.1 Calculation of the theoretical loading volume of a PMD

The PMDs dimensions characterised by SEM (Section 2.4.1) and reported in the schematic diagram below (Figure 3.2), were used to calculate the volume that could theoretically be loaded into each pocket of a PMD.

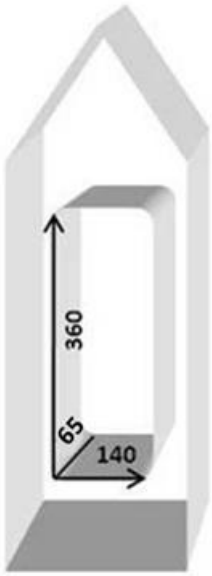

Figure 3.2: Schematic diagram of a pocketed microneedle. The length, the width and the depth (μm) of a single microneedle pocket are shown in the Figure.

According to the pocket dimensions, the theoretical volume occupied by each pocket was:

0.360 mm x 0.140 mm x 0.065 mm= ~0.003 mm^3= ~0.003 μl= ~3nl/pocket.

Each array contains 4 pocketed microneedles and therefore 12 nl could be theoretically loaded into the 4 pockets after immersion of the PMD into a solution. The difference between the theoretical volume and the experimental volumes obtained by the quantitative analysis of PMD loading capacity, described in the subsequent section, will be discussed in Section 3.4.2.3.

3.4.2 Quantitative analysis of MD loading capacity

Determination of PMD loading capacity for both low molecular weight compounds (salbutamol sulphate, SS) and high molecular weight molecule (the BTX A model, β-gal) was performed respectively by HPLC and calibrated spectroscopy. Established NPMDs were used as direct comparison with PMDs.

3.4.2.1 Quantifying MD loading with a model BTX A formulation using spectrophotometric techniques

A calibration curve was generated from spectrophotometric data (Figure 3.3). The R^2 of the curve was 0.99 and therefore the linear equation was considered valid for calculating the concentration of the BTX A model (β-gal) released by loaded MDs. The calculated concentration was then used to obtain the mass of BTX A model that was loaded on each PMD.

The data confirmed the feasibility of the assay as a means to quantify the dose of the BTX A model loaded onto PMDs. The results indicated (Figure 3.4) that after a single immersion into a BTX A model formulation (1.3 μg/μl), an average of 351.53 +/- 245.80 ng of the BTX A model was loaded on the PMD (n=5). This is equivalent to a loaded volume of 270 nl per PMD. The associated standard deviation value indicated above (+/- 245.80) revealed high variability of the loading capacity between the studied PMDs.

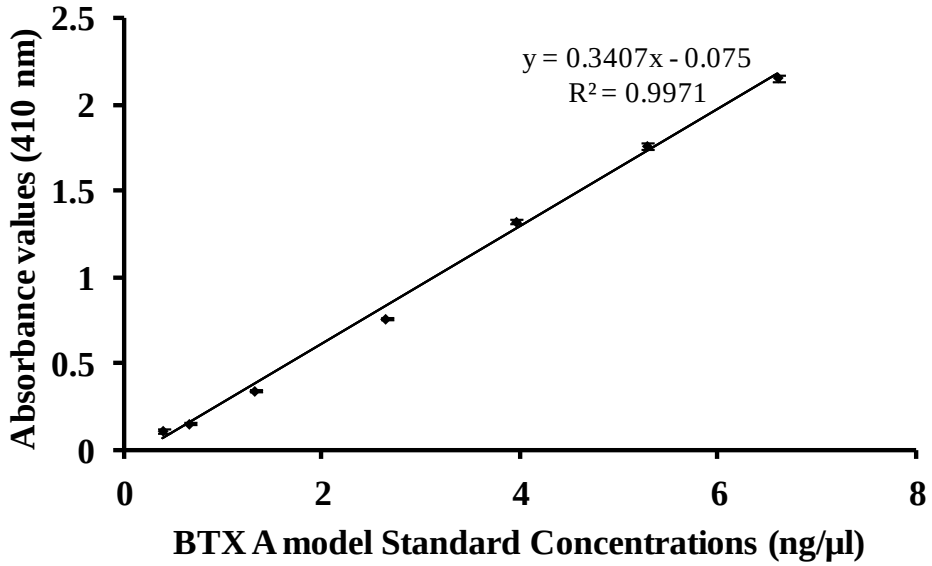

Figure 3.3: Calibration curve for the quantification of the BTX A model (β-gal). Data are presented as mean (standard-blank) of three absorbance readings (n=3) obtained from each standard solution and its matched blank solution +/- SD.

The protein concentration of the model β-gal in the BTX A model formulation employed in this experiment (and furthermore adopted in the subsequent spectrophotometric analysis) was considerably higher than the concentration of BTX A, which would be used in a clinical setting. As previously mentioned (Section 1.5.1), the entire vial of Botox®, containing 5 ng of BTX A, is usually reconstituted in volumes ranging between 1.5-5 ml to a concentration of approximately 1-3 pg/µl. This concentration is approximately one million times smaller than the one employed in our experiments. However, the greater concentration was required to enable loading of PMDs with protein quantities that were above the limits of detection of the methodologies employed in our experiments.

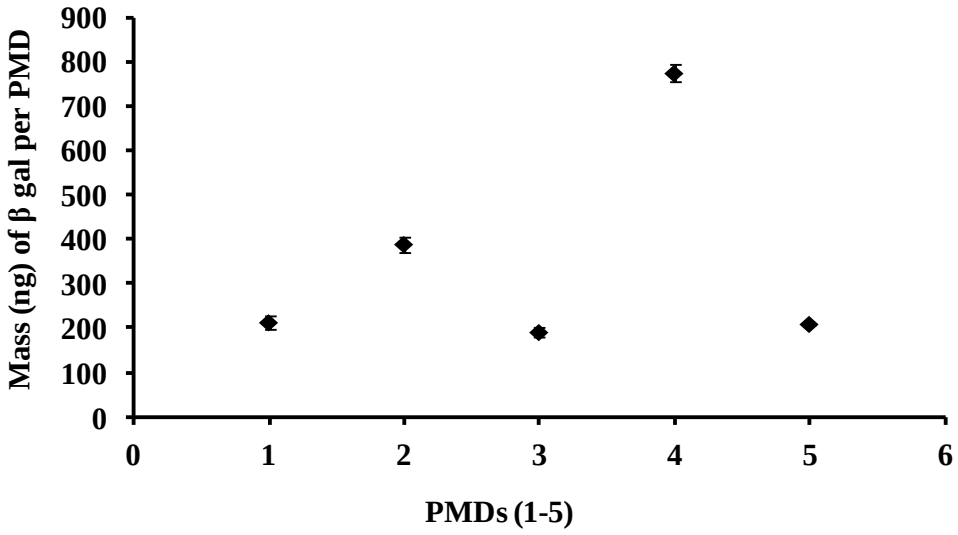

Figure 3.4: Assessing the feasibility of the spectrophotometric assay to determine the mass of the BTX A model (β-gal) liquid loaded on PMDs (n=5). Data are presented as a mean +/-SD of three readings obtained from each sample and its matched blank solution.

The experiment was repeated in order to compare the loading capacity of MDs when loaded with (NPMDs (n=8)) and without (PMDs (n=7)) the aid of the microscale dip coating reservoir device, which was described in Section 2.3.2.1. This was performed in order to assess whether the use of the dip coating reservoir device increased the reproducibility of MD loading. The data (Figure 3.5) indicates that an average of 84.74 ng (+/- 44.59) and 134.09 ng (+/- 74.29) of protein could be loaded into a PMD (n=7) and a NPMD (n=8), respectively after a single immersion into the BTX A model formulation (1.3 μg/μl). This suggested that a volume of approximately 65 nl and 103 nl could be therefore loaded onto a PMD and a NPMD respectively. Similarly to preliminary experiments, the data were associated with high standard deviation values, indicating a lack of reproducibility for MD loading capacity. These results also demonstrated that the use of the dip coating reservoir device did not result in improved loading reproducibility. Statistical analysis indicated that there was no significant difference between the loading capacity of the two microneedle designs, PMDs and NPMDs (p=0.19).

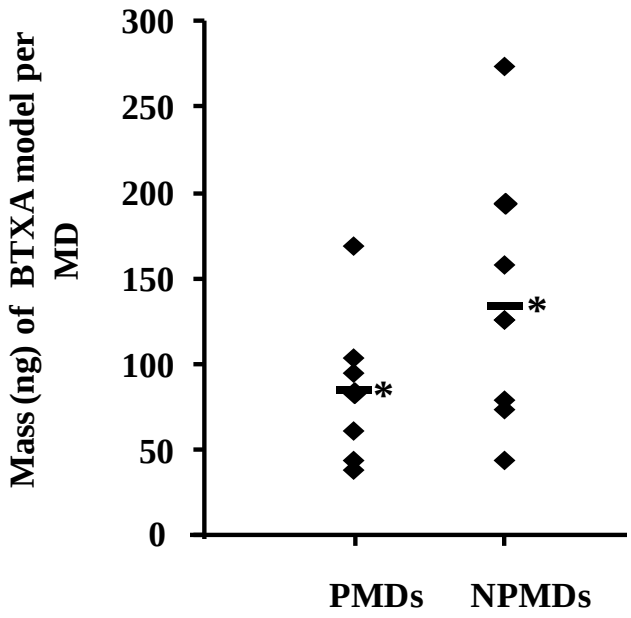

Figure 3.5: Comparison of the amount (ng) of the BTX A model (β-gal) loaded onto a PMD (n=7) and a NPMD (n=8) when using two different drug loading procedures. NPMDs were loaded with the aid of a micro scale dip coating device (Section 2.3.2.1), PMDs were manually loaded by a single immersion into a reservoir containing a small volume (~20 µl) of a BTX A model formulation (Section 2.3.4) *= average. N value for PMDs was reduced to 7 as one of the data points was considered to be an outlier (the value was almost 10 fold higher than the highest value detected for PMDs).

The loading capacity of PMDs (n=10) and NPMDs (n=10), using the technique described in Section 2.3.4, was assessed. The results indicated (Figure 3.6) that a mean average of 66.5 ng (+/- 52.27) and 75.8 ng (+/- 89.05) of the BTX A model was loaded on the PMD and a NPMD respectively. Therefore, a volume of approximately 50-60 nl of the BTX A model was loaded onto both the NPMD and PMD. However, standard deviations values were again high and the difference in the loading capacity between the two microneedle designs (PMDs and NPMDs) was not statistically significant (p=0.79).

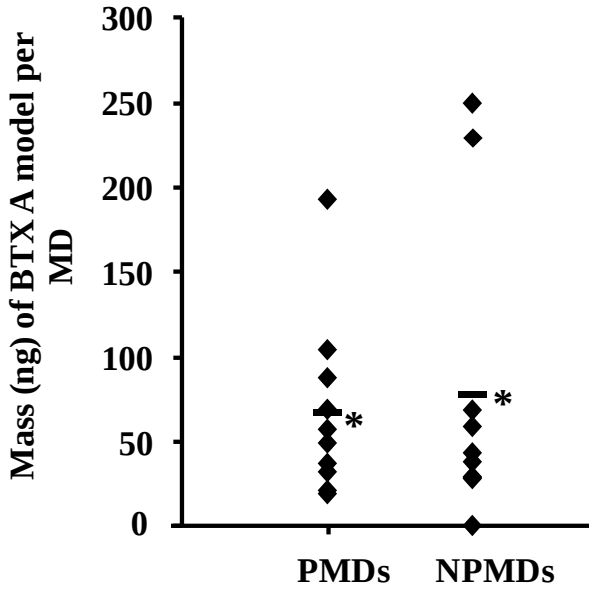

Figure 3.6: Comparison of the amount (ng) of the BTX A model (β-gal) loaded onto a PMD (n=10) and a NPMD (n=10) when using the same drug loading procedure. PMDs/NPMDs were manually loaded by a single immersion into a reservoir containing a small volume (~20 µl) of a BTX A model formulation (Section 2.3.4) *= average.

3.4.2.2 Quantifying salbutamol sulphate (SS) loading on MDs using HPLC

To determine whether the poor reproducibility of the MD loading was a specific problem for the macromolecular analyte β-gal or a limitation of the device/loading process, MDs were also loaded with a well characterised small drug molecule, salbutamol sulphate (SS).

A calibration curve was generated from HPLC data (Figure 3.7). The mass of SS loaded per each MD was then calculated. The data (Figure 3.8) indicates that an average of 13.57 µg (+/- 8.84) and 7.50 µg (+/- 5.20) of SS were loaded on to a PMD and NPMD respectively, after a single immersion into a SS loading solution (0.1 g/ml). This equates to a volume of approximately 136 nl (PMD) and 75 nl (NPMD) of SS solution. This data supports the results previously obtained for the BTX A model, indicating that the MD loading methodology used is associated with an

inherent level of variability. Equally, the difference in the loading capacity of the two microneedle designs was not statistically significant (p=0.08).

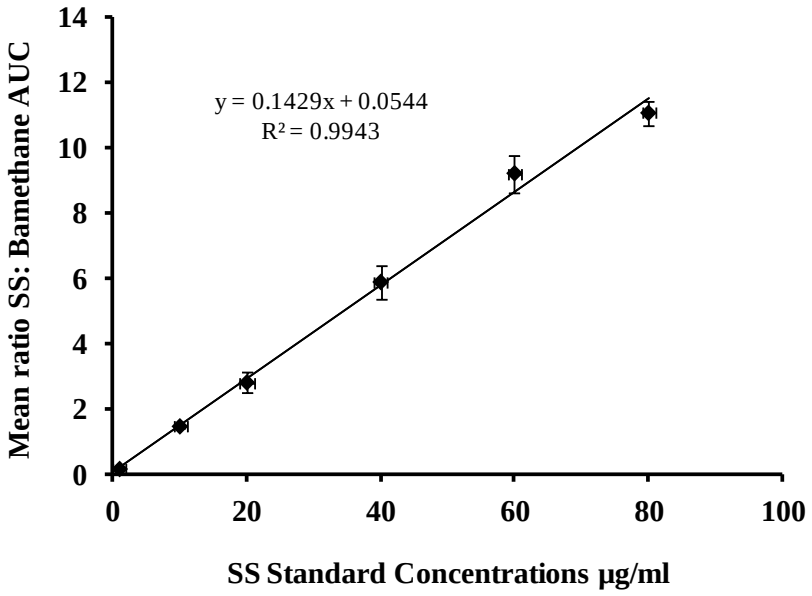

Figure 3.7: Calibration curve for the quantification of SS. Data are presented as mean (standard-blank) ± SD; n = 3.

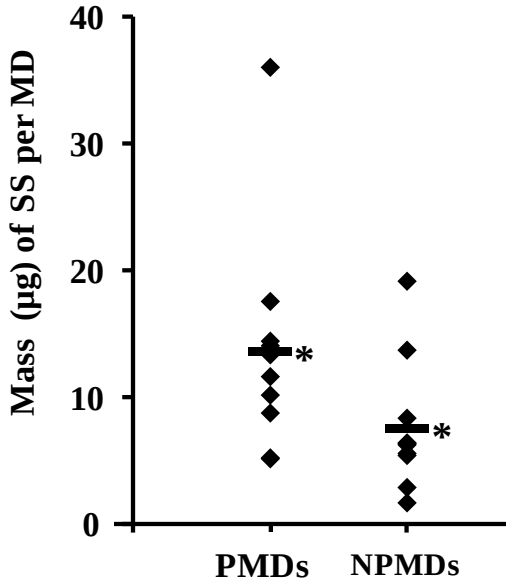

Figure 3.8: Quantification of the mass (µg) of SS per PMD (n=10) and NPMD (n=10). PMDs/NPMDs were manually loaded by a single immersion into a reservoir containing a small volume (~20 µl) of a BTX A model formulation (Section 2.3.4). *= average.

3.4.2.3 Safety, efficacy and reproducibility of the doses of BTX A that can potentially be loaded on MDs

The experiments previously reported (Sections 3.4.2.1 and 3.4.2.2) highlighted the high level of variability of the MD loading capacity. This was observed for both high and low molecular weight compounds (β-gal and SS) quantified by two different robust methodologies, calibrated spectroscopy and HPLC. This indicates that the variability of the results obtained is not specifically related to the physicochemical characteristics of the analyte to be loaded and/or to the methodology employed to quantify it, but most likely to the loading process. The experiments described in Chapter 2 also identified the loading process as a potential source of variability. This is a manual procedure requiring immersion of the micron-sized microneedle shaft into a liquid formulation. The small scale of the microneedle devices and the low volumes used to load the MDs implies that during this process microneedles are typically immersed to slightly different depths. Therefore, for some needles liquid may be loaded on to the base of the array and others only the microneedle shaft.

Excess formulation that was collected on the base of the MD during the microneedle immersion process was carefully removed using lintless tissue paper. However, uniform removal of the formulation from the arrays was considerably difficult to achieve.

Calculation of PMD theoretical loading capacity (Section 3.4.1) indicated that a single pocket of a pocketed microneedle could accommodate a volume of approximately 3 nl and thus 12 nl could be accomodated by a PMD (containing four pocketed microneedles), a volume which is considerably smaller than all the volumes calculated in our experiments (50-270 nl per PMD). Such discrepancy between theoretical and experimental volumes furthermore suggested that at each PMD immersion a considerable volume of liquid was retained on the shaft of the needle (as indicated by the experiment described in Section 2.4.4) and potentially on the base of the array. Also the central non pocketed microneedle contained in each PMD (Section 2.4.1) would also retain a certain volume of formulation (as indicated by the experiment reported in Section 2.4.4), thus contributing to the total PMD loading capacity.

Few published studies have reported variability of MD loading. This was mainly associated with the use of non automated and or not optimised coating procedures. This results in poor spatial control of deposition of the coating formulation over the length of the microneedles and deposition of the formulation on the base of the array. In a study published by Zhang *et al.* (2011), assessing the use of lidocaine coated MDs as a means to deliver the anaesthetic to animal models, drug loading was associated with relative standard deviation (RSD) values higher than 10%. For example a mass equal to 90.5+/-14.5 µg of drug was loaded onto one array of approximately 360 needles following one immersion into a coating formulation containing lidocaine 30% w/w and dextran 30% w/w as a excipient (as indicated in Table 3.1). The coating apparatus employed in the study was not specified. However, it can be assumed that coating was performed manually as the authors stated that automation of the process would have been introduced in future work in order to reduce variability.

Gill and Prausnitz (2008) quantified the dose of the model drug riboflavin coated on pocketed and non pocketed stainless steel microneedles by using the dip coating

reservoir device previously described (Section 2.3.2.1). The authors reported average relative standard deviation values equal to 19% of the results obtained. For example, a dose of riboflavin equal to 0.066+/-0.013 µg was loaded into each pocket (400 µm long x 50 µm wide) of a pocketed microneedle, following immersions into an aqueous formulation containing riboflavin 3% w/v and sucrose 25% w/v as excipient (Table 3.1).

The acceptance criteria for the production of pharmaceutical dosage forms such as capsules and tablets is set at RSD ≤ 5% (http://www.fda.gov 2003). Our data has a RSD value of > 50%. This clearly indicates that reproducible doses of drug could not be loaded on the studied MDs using the loading methodologies currently employed. Therefore, an automation of the loading process and/or an optimization of the microneedles design are certainly needed in order to reduce the level of variability (different strategies to increase MD loading uniformity were discussed in Section 2.4.2). Dosing uniformity and accuracy is critical for therapeutic drug delivery and is particularly important for potent and potentially toxic therapeutics such as BTX A. However, therapeutic doses of BTX A are safe due to its large therapeutic window. The lethal dose of the toxin is estimated at 1ng/kg of body weight (Gill 1982). An entire vial of Botox® contains 5 ng of drug. Therefore, administration of lethal doses of toxin is extremely unlikely (impossible) and to date no episodes of fatalities related to treatment have been reported.

When comparing microneedles to other delivery systems such as Transdermal Delivery Systems (TDDS) and topical patches, one of the major safety concerns related to the use of these devices is the excess of drug which is retained after their application into the skin (http://www.fda.gov 2011). TDDS and topical patches contain a larger amount of drug than the dose intended to be administered. This is to ensure an efficient diffusion gradient of the drug through the skin and thus to facilitate delivery of effective doses to the patient. Current TDDS and topical patches can retain up to 95% of the dose originally loaded after their application onto the skin (http://www.fda.gov 2011). This represents a potential safety issue for patients and other individuals in their vicinity. Accidental death of children exposed to the discarded TDDS has been reported (http://www.ismp-canada.org 2005). Also there is evidence of side effects for patients who fail to remove the TDDS after the required

duration of use (http://www.fda.gov 2011; Roberge 2000). Our results suggest that a volume of excess loading formulation may also be retained on the base of the PMDs and NPMDs. To translate this into a clinical context, if we were to use a Botox® loaded PMD to treat palmar PFHH, we may expect that this excess of formulation may still remain on the PMD after its application to the skin and may therefore be present on the discarded PMD. Some formulation may also be deposited on the surface of the skin. The presence of this excess formulation is not expected to be a safety concern as the dose of toxin in such constrained volumes would be lower than the therapeutic doses. Particular care should be taken if PMDs were discarded in places accessed by children, due to their reduced total body weight. However, if trained personnel in monitored environments such as hospitals or clinics used these devices, this risk would be reduced. Residual unused drug formulation on the base of a PMD may pose an economic issue though for an expensive drug such as Botox®. Poor reproducibility of PMD loading would result in variable dose delivery and therapeutic effects. However the dose range of BTX A currently used in the clinical setting is relatively large, as dose is adjusted based on the response of the patient (Naver et al. 1999). As previously mentioned (Section 1.5.1) Botox® manufacturing company (Allergan Pharmaceuticals Irvine, CA, USA) recommends to reconstitute the drug (BTX A-5ng) in 4 ml of 0.9% saline solution i.e., to a concentration of 1.25 ng/ml. However in the clinical practice setting different dilutions are used, depending on the mass of toxin to be administered and the clinician's preference.

For the treatment of palmar PFHH dilutions ranging between 1.5-5 ml have most frequently been reported (Glaser et al. 2007b). BTX A doses of 1.25-11 ng per palm (corresponding to a number of BTX A (Botox®) Units ranging between 25-220 U), administered by up to 50 intradermal injections, spaced 1-1.5 cm apart, have resulted in satisfactory sweat reduction (Glaser et al. 2007b; Holmes and Mann 1998; Naver et al. 1999). Injection volumes ranging between 0.05 and 0.1 ml have generally been employed and BTX A is usually delivered at doses of 0.1-0.25 ng at each administration site (Glaser et al. 2007a). In particular, a study published by Moreau *et al.* (2003), reported a clinically effective dose of approximately 3.5 ng of BTX A for each treated palm. In this study, the entire vial, containing 5 ng of drug was reconstituted with 4 ml of 0.9% saline solution to achieve a concentration of 0.125

ng per 0.1 ml. Aliquots (0.1 ml) of the Botox® formulation were then injected into 28+/-1 sites (mean +/- standard deviation) located on each palm. Therefore, if the PMD were to directly replace intradermal injections it would need to be applied to approximately 28 sites on the palm of the hand and fingers, spaced at approximately 1-1.5 cm intervals. It would need to deliver approximately 0.1 ml volume of BTX A and therefore a dose of 0.125 ng per treatment site. Our studies have demonstrated that both the PMD and NPMD have the capacity to deliver this dose of drug.

However, the limitation of the device is the volume of solution that can be loaded on to the needles and therefore, in order to load and thus deliver a therapeutically relevant dose using a MD, the medicament would have to be reconstituted using lower volumes than in current clinical practice, i.e. the formulation would need to be re-constituted with a volume in the microlitre range (e.g. 50-200 µl).

Experiments were previously conducted in order to determine whether the contents of the Botox® vial could be dissolved in volumes that are low enough to enable MD mediated delivery of the toxin (Section 2.4.3). These studies confirmed that HSA (0.5 mg) and NaCl (0.9 mg) can be dissolved in 0.9% saline solution using volumes less than 50 µl. These low volumes would facilitate MD mediated delivery in the clinical setting. For example, if we assume that 50 µl of 0.9% saline solution was added to a Botox® vial to obtain a 0.1ng/µl solution, it would be needed to deliver only approximately 35 µl of this solution to each palm (3.5 ng) to achieve a clinical response. If we assume that PMDs were a direct replacement for the intradermal injection and a person would be treated with 28 PMD applications, then only 1.25 µl of the Botox® formulation (0.125 ng) would have to be loaded onto each PMD. Our results (Section 3.3.2.1) indicate that volumes of a BTX A model (β-gal) formulation ranging between 50 and 270 nl can be accommodated by a PMD, containing only 5 microneedles, following one immersion into the formulation. Therefore, although we recognise loading is currently variable, a PMD should have the capacity to hold a volume of approximately 100 nl, a value 12 times smaller than the required volume (1.25 µl). Guided by this analysis, PMDs containing 60 needles, i.e. 10 x 6 out-of-plane microneedles distributed in an area of ~2 cm^2, could therefore be used to deliver a therapeutically relevant dose of medicament.

Even if PMDs were to only deliver a total volume of Botox® equal to 80% (28 µl) of the intended volume (35 µl) per palm, a therapeutic effect would still be likely as this volume would deliver 0.1 ng of BTX A per administration site, a dose which is within the therapeutic range. This indicates that a variability of up to 20% of the dose may be accepted by regulators as it would be comparable with current clinical administration of Botox®, which has a large therapeutic window.

Loading methodologies currently used in our experiments are therefore currently not suitable for BTX A loading in the clinical setting as consistent effective doses of the medicament would not be guaranteed. However, variable therapeutic effects have been noted in patients treated by intradermal administration of Botox® using the traditional syringe and needle (Naver et al. 1999; Saadia et al. 2001). These intradermal injections of Botox® are currently performed using the Mantoux technique. This is a technique, which relies on the insertion of a needle almost parallel to the skin to selectively penetrate the dermal layer without (in theory) reaching the underlying tissues. Performing this technique requires training and practice and it is frequently poorly reliable and inefficient (Laurent et al. 2007b). Accidental delivery of the formulation to unwanted sites such as muscles, usually determines appearance of side effects such as muscle weakness (Swartling et al. 2001) and also reduces the accuracy of the dose. Consistency of the dose delivered cannot be guaranteed due to additional factors such as variability of the syringe filling volumes, the presence of air bubbles during the purging process, retaining of volume of formulation in the syringe after injection (Laurent et al. 2007b) and back pressure causing expulsion of some formulation over skin surface while injected.

In conclusion, therapeutic doses of BTX A could potentially be loaded onto specifically tailored MDs (i.e. PMDs containing a greater number of microneedles) in a safe manner. However, in agreement with Gill and Prausnitz (2008) (Section 3.1.2), when comparing dose loading of PMDs and NPMDs, there is not a significant difference in the loading capacity of the two microneedle designs. Therefore, although pocketed microneedles may enable BTX A to be delivered in a liquid form, they would not increase the drug loading capacity of microneedles. However, reproducible MD loading of BTX A could not be guaranteed by using the loading procedures employed in our experiments. Therefore, reduction of such variation is

certainly needed in order to ensure uniform therapeutic effects. According to our analysis, to load PMDs with effective doses of BTX A would require reconstitution of the Botox® vial in a volume of 50 µl. As previously mentioned (Section 2.4.3), this would represent a technical challenge. The reconstituted formulation would be difficult to withdraw from the vial and this would lead to a waste of the costly medicament. Use of larger volumes (i.e. 500-1000 µl) would certainly facilitate easier handling of the formulation but would require PMDs with a greater number of microneedles (i.e. 600-1200 microneedles). Alternative microneedle devices with increased loading capacity such as hollow microneedles may potentially be more suitable for BTX A loading.

3.4.3 Assessing the feasibility of a PMD to load a therapeutic dose of BTX A as a liquid using a 'blank Botox®' formulation.

Previous experiments were performed by using a BTX A model formulation containing the enzymatic protein β-gal as representation of BTX A. However the composition of this formulation differed from the commercial Botox® preparation. Firstly, in order to enable detection, the concentration of the BTX A model was greater (1.3 µg/µl) than in Botox® (~1-3.3 pg/µl). Secondly**,** the solution was not formulated with any of the excipients which are present in the Botox® preparation (HSA 0.5 mg and NaCl 0.9 mg). It is thus reasonable to assume that the physicochemical properties of the two formulations would be different.

Experiments were therefore performed to obtain an indication of the loading capacity of PMDs and NPMDs when loaded with a formulation that contained the same excipients (HSA and NaCl) as present in Botox®. The commercial preparation was therefore employed in these studies. Due to the small mass of BTX A in the formulation, HSA was used as an indicator of loading efficiency to enable detection by the methodologies employed.

3.4.3.1 Assessing the feasibility of SDS-PAGE and silver staining methodology for characterization of the protein HSA contained in the commercial preparation Vistabel®

Preliminary experiments were performed to assess the feasibility of SDS-PAGE and silver staining methodology to characterise the HSA contained in the commercial BTX A preparation Vistabel®. This is a commercial preparation, manufactured by Allergan, which is identical to Botox®, except that it contains half the mass of BTX A, is therefore less expensive, and is licensed for cosmetic application only (Section 1.4.1). Vistabel® was therefore selected in this experiment as less expensive substitute for Botox®.

Figure 3.9 illustrates the appearance of a polyacrylamide gel loaded (in triplicate) with Vistabel® and BSA (positive control) solutions and processed by SDS PAGE and silver staining methodology. A prominent band with a molecular weight ranging between 52 and 76 kDa was resolved for both solutions loaded. As the molecular weight of HSA and BSA is 66 kDa, the band detected indicated the presence of serum albumin in both samples.

The dense HSA bands obtained indicate that the amount of protein loaded in the gel was too high for the sensitivity of the staining methodology (limit of detection 2-5 ng of protein/well) (http://www.qiagen.com 2011).This sensitive technique was selected to enable detection of quantities of proteins loaded on MDs, as described in the following Section.

Additional protein bands (Figure 3.9) were detected below 52 kDa for both Vistabel® and BSA solution. These bands may be related to impurities in the solutions loaded. Interestingly, no bands between 66 (HSA) and 225 kDa were detected for Vistabel® formulation, probably due to the higher purity of the commercial formulation compared to the BSA solution. The detection of bands with a molecular weight <66 kDa (HSA), suggests possible fragmentation of the protein and/or presence of impurities with a molecular weight smaller than 66 kDa in both formulations (Vistabel® and BSA). The results indicated that the selected methodologies were suitable to detect the HSA contained in BTX A commercial preparations (i.e. Vistabel®) and were therefore adopted for subsequent experiments.

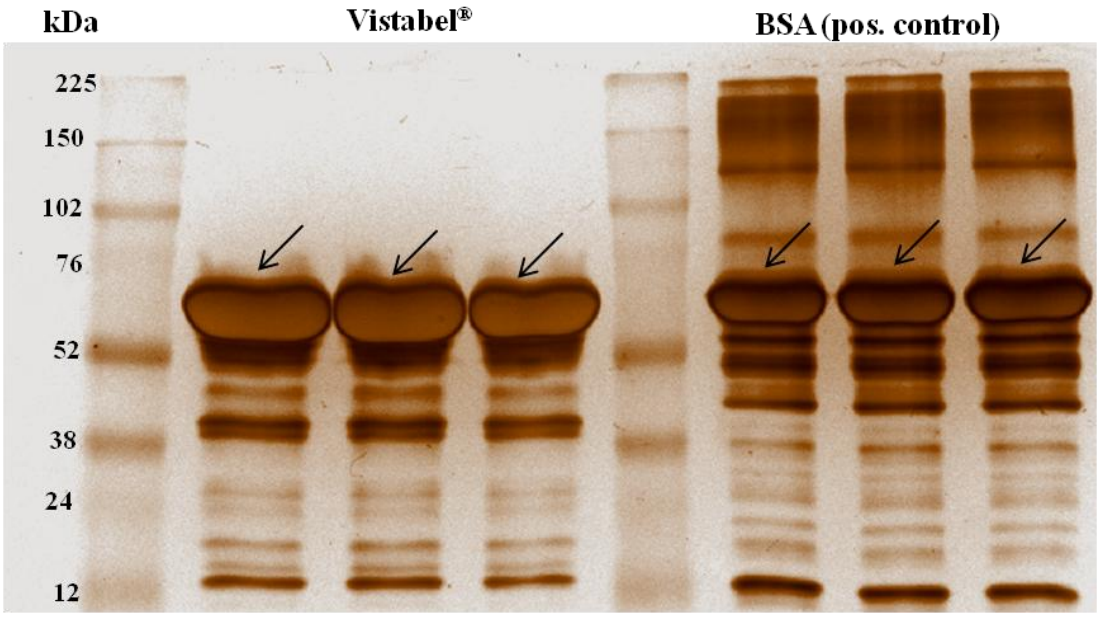

Figure 3.9: Assessing the feasibility of silver staining methodology to detect HSA, contained in Vistabel®. The Figure depicts the appearance of a polyacrylamide gel with each well loaded (in triplicate) with ~27 µg of HSA (Vistabel®) and ~4.5 µg of BSA (positive control). The arrows point to the serum albumin bands (66 kDa). The molecular marker (5 µl) was loaded in the first and the fifth lane (by left). The marker bands with their relative molecular weights are indicated.

3.4.3.2 Comparison of PMDs and NPMDs loading of BTX A from a 'Botox® blank' formulation

HSA loaded on MDs was characterised by SDS-PAGE and silver staining methodologies (Figure 3.10 A, B). Comparison of samples with the standard profile indicated that an approximate dose of HSA ranging between 180 and 2000 ng was loaded on a MD following immersion into a Botox® blank formulation (HSA ~3.3 µg/µl). This suggests that a formulation volume between ~55 and 605 nl could be accommodated onto a MD (i.e ~11 to 120 nl per needle). If this experiment had been performed with the commercial preparation, the concentration of BTX A would have been 5 ng/150 µl (~33 pg/µl). Therefore, a single MD containing 25-300 microneedles would have accommodated 3 µl of Botox® formulation and thus approximately 0.1 ng of BTX A, a dose which is within the therapeutic range (0.1-

0.25 ng of BTX A per injection site). However, HSA could not be detected in some NPMDs samples (Figure 3.10 B): in NPMDs line 3 and 6 the amount HSA was below the limit of detection, in NPMD line 5 HSA failed to be detected due to improper loading of the sample formulation in the gel). Therefore, the results obtained suggest variability of MD loading.

As suggested by the previous analysis (Section 3.4.2.3), a MD containing 60 microneedles could load therapeutic doses of BTX A. In that case it was assumed that the entire vial of Botox® was dissolved in 50 µl of diluent. However, this experiment required greater volume and therefore was performed using an increased dilution (150 µl). It is reasonable to assume that if a smaller volume (i.e., 50-100 µl) was used to prepare the Botox® blank formulation, detectable doses of HSA may have been loaded on all the studied MDs and thus effective dose loading could have been achieved for all the MDs. However, due to the high level of variation and the semi-quantitative nature of the analysis, accurate predictions cannot be made.

Previous experiments indicated that a Botox® like formulation was successfully loaded on both PMDs and NPMDs (Section 2.4.4). This was confirmed by the present study, as the HSA loaded was detected for the majority of the MDs analysed. Therefore, physicochemical properties of the Botox® formulation are suitable for successful MD loading. The 'Botox® blank' formulation employed in the present experiment differed from the so termed 'Botox® like' formulation described in Section 2.3.4.1. The latter contained 5 ng of the BTX A model β-gal to mimic the dose of BTX A (5 ng) contained in the commercial preparation Botox®. In the experiment reported in this Section, the BTX A model was not added to the formulation employed as this low mass of protein would not have enabled loading of MDs with detectable quantities of protein.

In conclusion, the result suggested that PMDs and NPMDs with an increased number of microneedles have the capacity to accommodate therapeutic doses of BTX A after only one immersion in a Botox® formulation. However, as previous quantitative loading analysis indicated (Sections 3.4.2.1 and 3.4.2.2), dose reproducibility cannot be guaranteed by using the existing drug loading methodologies.

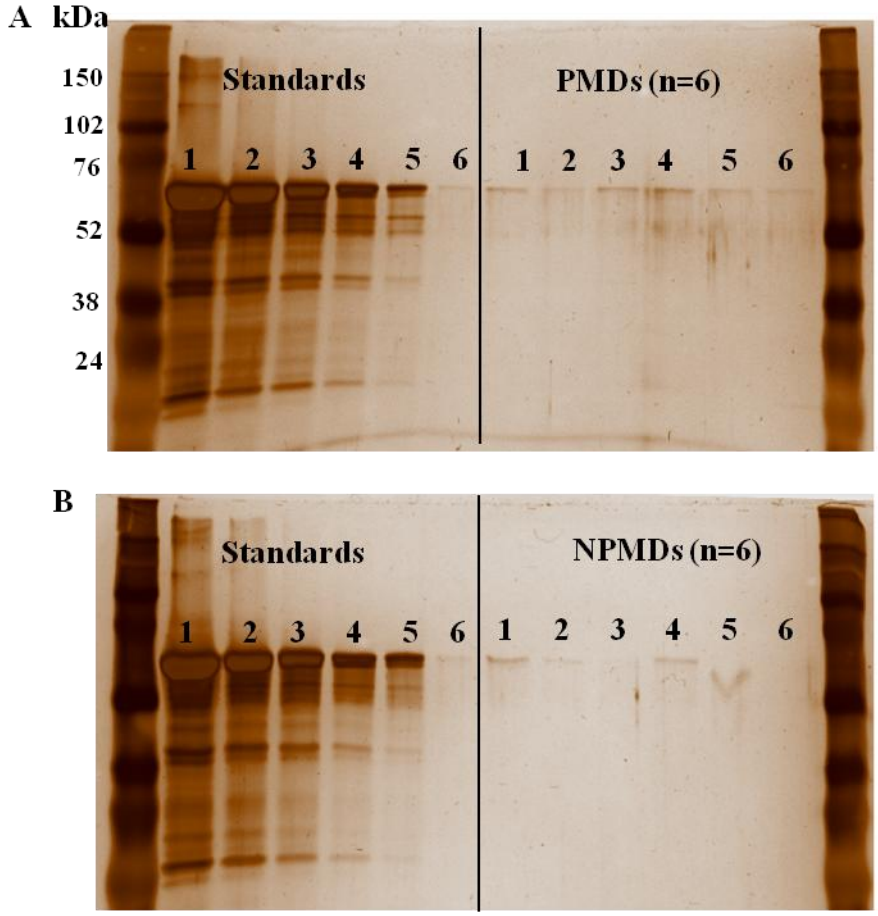

Figure 3.10 (A, B): Characterization of HSA loaded on PMDs and NPMDs. The images depict the appearance of two polyacrylamide gels processed by SDS-PAGE and silver staining methodology. The gels were loaded with HSA standard solutions and samples solutions generated by PMDs and NPMDs loaded with a 'Botox® blank' formulation (HSA ~3.3 µg/µl, NaCl 6 µg/µl). Successful characterization of HSA is indicated by the presence of a band at 66 kDa. The approximate concentration (ng/µl) of the HSA standards loaded on the first 6 lanes (indicated by numbers 1-6) of both of the two gels are the following: 180 (1), 80 (2), 40 (3), 20 (4), 10 (5), 0.9 (6). The approximate mass of HSA in the sample solutions generated from PMDs and NPMDs loading was estimated by multiplying the concentrations of HSA standard 5 and 6 by the volume of diluents (200 µl) used to rinse the MDs after HSA loading. The molecular marker (5 µl) was loaded on the first and last lane (by left) on each gel. The marker bands with their relative molecular weights are indicated. The line in (A) and (B) was drawn to facilitate differentiation between the standards (lanes 1-6, by left) and the samples (lanes 1-6, by right).

3.5 Conclusion

PMDs employed in the current research project do not have the capacity to load effective doses of BTX A due to the reduced number of microneedles contained in each device. However, PMDs containing 25-300 microneedles would allow loading of therapeutic doses of the existing commercial preparation Botox®, re-constituted with volumes of 50-150 µl.

Microneedle loading of low molecular weight (salbutamol sulphate) and macromolecular compounds (β-gal and HSA) was associated with a significant level of variability. Therefore, PMD loading of reproducible and efficient doses of Botox® would not be guaranteed by using the existing loading methodologies. However, given the large therapeutic window of BTX A, therapeutic dose loading may potentially be achieved by employing robustly engineered loading methodologies and/or specifically tailored MD designs.

Due to absence of statistical difference in the loading capacity of the two microneedle designs studied, PMDs would not increase the dose of BTX A compared to NPMDs. Nevertheless, PMDs may offer the potential to deliver BTX A in a liquid form as well as enable dose monitoring.

Chapter 4

Characterising cutaneous delivery of a BTX A model from liquid loaded pocketed microneedle devices (PMDs)

4.1. Introduction

The experiments reported in this Chapter will assess the feasibility of liquid loaded PMDs to deliver the enzymatic protein, β-gal (~465 kDa), into the dermis of human skin. As previously mentioned (Section 2.1.3), this protein was selected as a high molecular weight compound that is representative of the BTX A forms that are contained in commercially available preparations (molecular weight ranging between 150 and ~900 kDa).

For the treatment of skin disorders such as PFHH, targeted delivery to a specific depth of the skin is important in order to ensure optimal interaction between the toxin and its therapeutic target (the eccrine sweat glands). As previously mentioned (Section 1.2.3), the eccrine sweat glands are located in the deep dermis and are distributed in the skin with a density which varies tremendously according to the anatomic site e.g. 64 sweat glands/cm^2 on the back versus 600-700 glands/cm^2 on the palm on the hands (Sato et al. 1989). The use of PMDs is proposed in the current research study to promote minimally invasive delivery of BTX A formulation to the epidermis and the superficial layer of the dermis. Therefore, in order to ensure successful interaction with the sweat glands, BTX A would then have to diffuse to the deep dermis. For this reason the use of liquid loaded PMDs is proposed as an alternative to the dry coated approach, as it is hoped that the delivery of BTX A in a liquid state would assist lateral and downwards diffusion of the protein to the lower dermal region.

4.1.1 Cutaneous delivery of macromolecules using MDs

The capability of a MD to facilitate cutaneous delivery of high molecular weight molecules such as peptides, proteins and vaccines has been extensively reported. Numerous studies have been conducted in *in vivo* and *in vitro* systems in both humans and animal models for the cutaneous delivery of macromolecules using hollow (Alarcon et al. 2007; Burton et al. 2011; Gupta et al. 2009; Hafeli et al. 2009; Harvey et al. 2011; Laurent et al. 2007b; McAllister et al. 2003; Mikszta et al. 2006; Van Damme et al. 2009; Wang et al. 2006) and solid microneedles fabricated with a variety of materials including metal (Cormier et al. 2004; Kim et al. 2009b; Quan et al. 2010) glass (McAllister et al. 2003; Wang et al. 2006) silicon (Chen et al. 2012;

McAllister et al. 2003; Wu et al. 2010) and biodegradable polymers (McAllister et al. 2003; Park et al. 2005, 2006). Water soluble MDs, made out of sugars, have also been reported to enhance *in vitro* transdermal permeation of proteins such as BSA (~66 kDa) and recombinant protective antigen (83 kDa) in split-thickness human cadaver skin (Wendorf et al. 2011). Soluble microneedles have also been used to pierce the skin as a pre-treatment before application of a macromolecule drug formulation ("poke with patch approach" (Prausnitz 2004)). Using this approach, Li *et al.* (2009) showed *in vitro* delivery of the human IgG (150 kDa) across the epidermal and dermal layer of rat skin following application of 500 µm-long maltose microneedles.

4.1.2 Intradermal delivery capability of PMDs

The delivery capability of pocketed microneedles has been assessed in studies conducted by Gill and Prausnitz (2007b, 2008) by using the small hydrophilic molecule sulforhodamine (~600 Da). This was coated either in a dry (Gill and Prausnitz 2008) or a liquid form (Gill and Prausnitz 2007b) on 700 µm long-pocketed microneedles and delivered up to a depth of ~600 µm in porcine cadaver skin. Although this study did not show delivery of high molecular weight molecules to the skin, it indicates that a pocketed microneedle can successfully penetrate the skin and deliver material to the dermis. No additional studies regarding the use of pocketed microneedles have been published to date.

4.1.3 Intradermal delivery of macromolecules using dry coated NPMDs

There are a variety of studies in literature reporting delivery of proteins and vaccines to the epidermal/dermal layer of skin (Chen et al. 2012; Pearton et al. 2010; Saurer et al. 2010). Widera *et al.* (2006) investigated the suitability of ovalbumin (~44 kDa) coated titanium MDs (Macroflux®) to elicit immune response in hairless guinea pigs (HGP). Within this study the site of deposition of ovalbumin delivered by MDs within the different layers of the skin was assessed *in vitro* using three different microneedle lengths: 225, 400 or 600 µm. The HGP was used as an animal model as it has a more comparable skin anatomy (i.e. skin thickness) to humans, compared to

other animal models such as mice and rats (Sueki et al. 2000). The authors indicate successful delivery of ovalbumin to the epidermal/dermal region of the skin for all MD designs employed. Cutaneous delivery of ovalbumin was furthermore confirmed by *in vivo* immunisation studies indicating that a comparable or greater immune response was registered in animals treated with MDs and IM administration. A previous study (Pearton et al. 2010) has been performed by using solid MDs with the same design as the NPMDs employed in the current research project. NPMDs with a microneedle length of 700 μm were dry coated with influenza virus like particles and manually inserted into *ex vivo* excised human skin. Histological analysis indicated deposition of the particles within the epidermis and superficial layers of the dermis. Similarly, Saurer *et al.* (2010) showed intradermal delivery of the enzymatic protein bovine pancreatic ribonuclease A (~13 kDa) to porcine cadaver skin using NPMDs.

4.1.4 Detection of the BTX A model β-gal in the skin

The organic substrate X gal (also abbreviated BCIG for bromo-chloro-indolyl-galactopyranoside) is hydrolysed by the enzyme β-gal to form a blue coloured insoluble compound. The X-gal staining methodology optimised by Coulman (2006) will be adopted in the experiments reported in this Chapter in order to allow visible detection of the enzyme β-gal, delivered to the skin by using PMDs.

4.1.5 Specific aims and objectives of the Chapter

The aim of this Chapter is to assess the deposition and distribution of a high molecular weight protein when delivered into the skin using a liquid loaded PMD. The cutaneous delivery capabilities of liquid loaded PMDs will be compared to more established NPMDs.

The experimental objectives are to:-

1) Determine the concentration of β-gal that produces a blue pigmentation that can be visibly detected in solution.
2) Evaluate the capability of established dry coated NPMDs to successfully deliver β-gal to both the epidermal and dermal layers of human skin.

3) Assess the effective release of a β-gal solution from the pockets of a PMD following insertion of the microneedles into human skin.
4) Evaluate the capability of a liquid loaded PMD to successfully deliver β-gal to both the epidermal and dermal layer of human skin.
5) Evaluate the effect of a mechanical vibration on the deposition and distribution of a β-gal solution from the pockets of a PMD.
6) Evaluate the time-dependent diffusion of β-gal in the dermis.

4.2 Materials

4.2.1 Reagents

All reagents were used as received and purchased from Sigma Aldrich Ltd (Poole UK), unless otherwise stated.

Deionised water was obtained from an Elga reservoir (High Wycombe, UK). Foetal Bovine Serum (FBS), penicillin, streptomycin, Dulbecco's modified Eagle medium (DMEM) 25 mM HEPES were purchased from Invitrogen Corporation, (Paisley, UK). Optimal Cutting Temperature (OCT) embedding media was purchased from RA Lamb Limited, (Eastbourne UK). X-gal powder and Tris buffer (Tris (hydroxymethyl) methylamine) were purchased from Fisher Scientific (Loughborough, UK). Potassium ferrocyanide trihydrate, A.C.S. reagent grade was purchased from ICN Biomedicals Inc. (Aurora, Ohio). Harris' Haematoxylin and Gurrs' Eosin were purchased from Lab 3 (Bristol, UK).

4.3 Methods

4.3.1 Evaluating the limit of visible detection of the BTX A model β-gal in solution

As previously mentioned (Section 4.1.4), the enzyme β-gal can be visualised in the skin as a result of the reaction with the substrate X-gal. The experiment described in this Section will assess the concentration of β-gal, which produces a blue pigmentation in solution that can be visibly detected.

β-gal (from *Escherichia coli*, Grade VI lyophilized powder, 1000 U equal to 2638 µg) was reconstituted in 1 ml of BSA/bicine buffer (bicine buffer 50 mM pH 7.5 containing BSA 100 µg/ml) to a concentration of 2.6 µg/µl. The solution was aliquoted and stored at -20°C. On the day of the experiment, one aliquot was defrosted and the solution obtained was used to prepare standard solutions (outlined in Table 4.1) with a β-gal concentration ranging between 0.0001 µg/µl and 0.6 µg/µl in a final volume of 200 µl of BSA/bicine buffer.

Table 4.1: β-gal standard concentrations used to assess the limit of visible detection of β-gal in solution.

Solution	β-gal concentration µg/µl
1	0.6
2	0.1
3	0.06
4	0.01
5	0.006
6	0.001
7	0.0006
8	0.0001

The X-gal staining solution (Coulman 2006) was freshly prepared using the reagents listed in Table 4.2. Additionally, two negative control solutions consisting of i) BSA/bicine buffer (200 µl) (negative control solution 1) and ii) X-gal staining solution (500 µl) (negative control solution 2) were also prepared.

Five hundred µl of X-gal staining solution were mixed with 200 µl of each β-gal standard solution outlined in Table 4.1 and to negative control solution 1. The solutions obtained and negative control solution 2 were incubated at 37°C/5% CO_2 and inspected for a colour change after 1 hour and 24 hours.

Table 4.2 Components of X-gal staining solution.

X-gal staining solution		
Reagent	**Concentration**	**% v/v**
X-gal*	40 mg/ml	5
Potassium ferricyanide	0.6 M	0.84
Potassium ferrocyanide	0.6 M	0.84
Magnesium chloride	1 M	0.2
Tris-HCl, pH 8.5	Tris 200 mM HCl 1M	50
Deionised water	/	To 100%
Incubation conditions	/	37 °C

**X-gal powder is made up to a 40 mg/ml with N-N-dimethylformamide.*

4.3.2 Human skin studies

The experiments reported in this Chapter were conducted by using skin tissues obtained from human subjects in order to generate data that more closely resemble the *in vivo* human conditions. The skin tissues were obtained from patients undergoing breast reduction or mastectomy procedures at the Royal Gwent Hospital, Newport, Wales, following informed patient consent and full ethical approval. Once excised from the patients, the tissue samples were immediately transferred into a suitable nutrient media (usually consisting of DMEM 25 Mm HEPES, 5% foetal bovine serum and 1% penicillin-streptomycin) and transported to the laboratory at controlled temperature (4°C), as outlined by Pearton *at al*. (2010). The skin was then used on arrival (‘fresh’ skin) or stored at -20°C (‘frozen’ skin). When ‘frozen’ skin was used for experiments, it was defrosted on the day of the experiment, at room temperature for approximately 90 minutes, in order to allow it to thermally equilibrate with the environment. In all cases subcutaneous fat was removed from the skin tissue by blunt dissection. The tissue was pinned, epidermis face up, into a dissection board in order to ease MD insertion.

4.3.3 Cutaneous delivery of the BTX A model β-gal from dry coated NPMDs

The coating formulations employed in the experiment described in this Section were prepared in BSA/bicine buffer and consisted of:

1) Coating formulation A: β-gal 0.65 µg/µl, CMC 1% w/v and Lutrol® F68 0.5% w/v.
2) Coating formulation B (excipient free coating formulation): β-gal 0.65 µg/µl.
3) Coating formulation C (negative control): CMC 1% w/v and Lutrol F68 0.5% w/v.

These formulations were freshly prepared from an aliquot of β-gal enzyme (2.6 µg/µl) in BSA/bicine buffer, defrosted on the day of the experiment as described previosuly (Section 4.3.1).

NPMD coating

NPMDs were coated by multiple immersions (i.e. 15) into the appropriate coating formulation by using the micro scale dip coating reservoir device as described in Section 2.3.2.1 The device was first loaded with coating formulation C and the first three NPMDs were coated. Afterwards, coating formulation A and then coating formulation B were loaded in order to coat the remaining six NPMDs (n=3 per each coating formulation). After each coating, the microholes of the dip coating device were rinsed under tap water for ~1 minute and then immersed into a basin filled with tap water (~3 litres) for 30 minutes. Afterwards, the coating device was allowed to dry at 30°C. Once coated, all the MDs were stored at - 20°C for 24 hours in order to allow them to dry. Such storage temperature (i.e. -20°C) was employed as this represents the temperature recommended by the manufacture for β-gal storage.

Insertion of NPMDs into human skin

The experiment was performed on a skin sample aged 56 year old, which was defrosted on the day of experiment (‘frozen’ skin sample). Each NPMD, previously coated with either formulation A, B or C, was inserted into the skin and left in place for 5 minutes before withdrawal. NPMDs were applied to skin sites that were spaced approximately 1 cm from each other. To facilitate handling of the NPMDs during

application into the skin, a metallic twezeer was used to hold the NPMD (i.e. the base of the NPMD was held between the two edges of the metallic tweezers). Once inserted into the skin, a moderate pressure was applied to the array for ~5 seconds in order to facilitate penetration of the microneedles into the tissue. The base of the array was then released from the tweezer and the NPMD was left *in situ* for 5 minutes (as mentioned above). The same methodology was employed for the experiments described in the following sections unless otherwise specified. Following removal of NPMDs from the skin, the treated regions were excised to form tissue samples measuring ~1 cm^2 that were subsequently treated as described below.

In order to assess the β-gal activity in viable human skin tissue, the same experiment was repeated on a skin sample obtained from a 60 year old donor and was processed within ~2 hours of surgical removal ('fresh' skin sample).

4.3.3.1 Culturing and X-gal staining of skin samples

The samples obtained were cultured as described elsewhere (Birchall et. al 2005) and this experimental set-up is illustrated in Figure 4.1. Briefly, the skin samples were positioned on lens tissue paper placed on a sterile steel mesh, contained in a six well culture plate. Each well containing the skin samples (generally 3 samples per well) was filled with 8 ml of freshly prepared nutrient media consisting of 5% v/v foetal bovine serum (FBS) and 95% v/v of DMEM 25 mM HEPES. The lens tissue on the mesh was soaked with the media by a wicking effect. Skin was incubated at the air-liquid interface for 1½ hours at 37°C/ 5% CO_2.

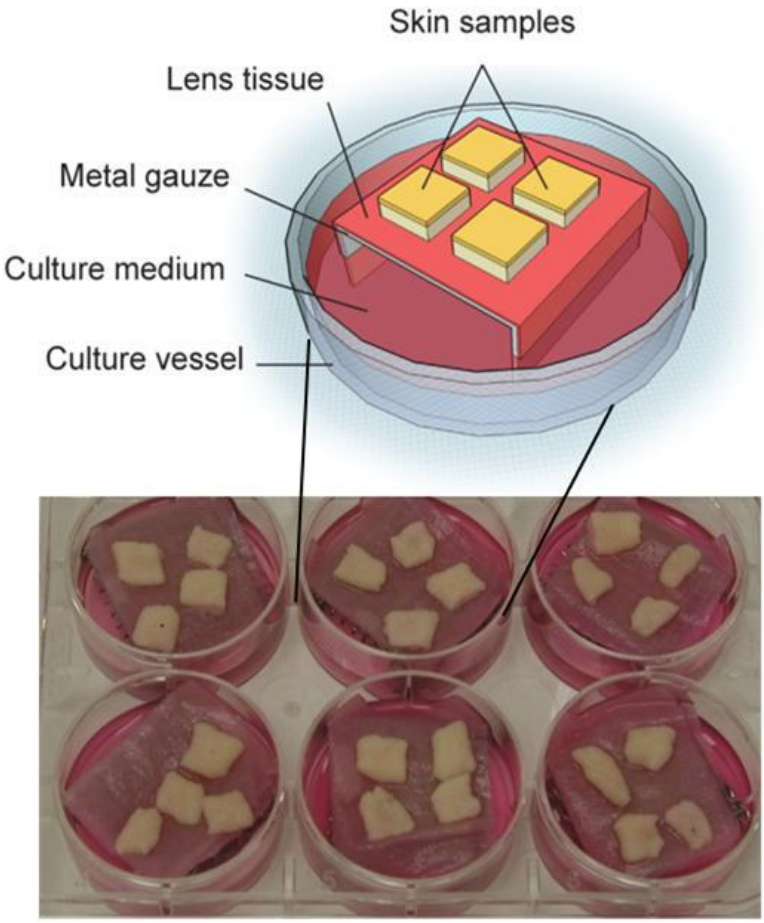

Figure 4.1: Schematic diagram and image of skin samples incubated at the air-liquid interface in organ culture. Figure adapted from (Ng et al. 2009)

After incubation, each sample was washed with 2 ml of Phosphate buffer solution (PBS)/$MgCl_2$ 4 mM for 15 minutes and subsequently fixed for 2 hours in 2 ml of glutharaldeyde 2% v/v in PBS/MgCl 4mM on ice. Each sample was then rinsed in 2 ml of PBS/$MgCl_2$ 4 mM for 15 minutes before being trasferred into 2 ml of X-gal staining solution and incubated at 37°C/5%CO_2 for 24 hours to detect the presence of the β-gal enzyme. Following incubation, the samples were rinsed twice in PBS (2 x 15 minutes), and subsequently stored over night in fresh PBS at 4°C before being analysed both *en face* and histologically.

4.3.3.2 *En face* analysis of skin samples

The skin samples were positioned between two Superfrost Plus® microscope slides and subsequently imaged by using a light microscope (Zeiss Stemi 2000-C Stereomicroscope, Carl Zeiss, Welwyn Garden City, UK) attached to a digital camera (Olympus C 3040-ADL, Watford, UK). An external electronic light source (Schott KL-1500, Schott AG, Stafford, UK) was also used to better visualise the skin samples.

4.3.3.3 Histological analysis of skin samples

The skin samples were embedded in moulds containing OCT, which was frozen quickly in a hexane bath on dry ice before being stored at -80 °C. The samples were subsequently processed into 10-12 μm cryosections (CM3050S cryostat, Leica Microsystems, Milton Keynes, UK), which were collected onto Superfrost Plus® microscope slides. The skin sections were inspected by light microscopy (Olympus®, BX50 light/fluorescent microscope, Watford, UK) under various magnifications. Representative sections were digitally imaged (Olympus DP-10 digital camera, Watford, UK) and a microscope graticule was employed to calculate the image scale. Selected slides were stained with Harris' Haematoxylin and Gurrs' Eosin (H&E staining) according to the methodology described below.

4.3.3.4 H&E staining methodology

Selected slides were fixed in acetone for 10 minutes and subsequently allowed to dry at room temperature. Slides were then rinsed in tap water (5 immersions, 2 seconds

each one) before being immersed in Harris' Haematoxylin for 5 minutes. Subsequently, they were rinsed in tap water as above and then immersed in acid alcohol (ethanol 70%-chloric acid (HCl) 1M 1%) for 2 seconds. The slides were rinsed once more time in tap water before being immersed in Gurrs' Eosin for 2 seconds. They were subsequently rinsed under running tap water for ~1 minute and then transferred in tap water for 10 minutes. Afterwards, the slides were allowed to dry at room temperature.

4.3.4 Cutaneous delivery of the BTX A model β-gal from liquid loaded PMDs

4.3.4.1 Loading and de-loading visualisation of a BTX A model formulation from PMDs

The following experiment was performed to i) assess the capability of a liquid loaded PMD to deliver the BTX A model β-gal to human skin; ii) investigate whether complete release of the formulation from the pockets occurred following insertion of the microneedles in the skin.

The experiment was carried out on a skin sample obtained from a 60 year old donor. The tissue was defrosted on the day of the experiment ('frozen' skin sample).

Loading formulations

The following loading formulations were freshly prepared from a β-gal stock solution (2.6 µg/µl in BSA/bicine buffer):

- Formulation A: β-gal 1.3 µg/µl in BSA/bicine buffer
- Formulation B: β-gal 1.3 µg/µl, 20% v/v orange food dye (consisting of water, quinoline yellow and allura red) + 30% v/v of BSA/bicine buffer. This formulation was used for visualisation purposes.

PMD loading and application into human skin

The PMDs were loaded by manual immersion into the appropriate formulations (A or B) as previously described (Section 2.3.4). Following loading of PMDs with

formulation B, the pockets were visually inspected (to the naked eye). Loaded PMDs were inserted into the skin as follows:

- Four PMDs loaded with formulation A were manually inserted into the skin and maintained *in situ* for 5 seconds before being withdrawn.
- Three PMDs loaded with formulation A were manually inserted into the skin and maintained *in situ* for one minute before being withdrawn.
- Three PMDs loaded with formulation B were manually inserted into the skin and maintained *in situ* one minute before being withdrawn. After removal, the PMDs were inspected to the naked eye in order to assess whether successful release of the formulation from the pockets had occurred.

PMDs that were removed after 5 seconds were held in place manually before being removed. PMDs that were inserted in the skin for 1 minute were held in place for 5 seconds. The base of each array was then released from the edges of the metallic tweezer (as previously described for dry coated NPMDs in Section 4.3.3) and the PMD was left in place for the remaining time. Following PMD removal, the skin was dissected in ~1 cm^2 samples which were subsequently processed as detailed previously (Sections 4.3.3.1-3).

4.3.4.2 Application of a mechanical vibration to enhance the cutaneous delivery capabilities of liquid loaded PMDs

The experiment was performed to assess the effect of a mechanical vibration on the delivery and distribution of the BTX A model β-gal into human skin from liquid loaded PMDs. The brush of a commercially available electric toothbrush (Oral B Vitality 3709, Braun, Germany) was removed from the device and a cavity was created to accommodate a MD.

The experiment was carried out on a skin sample aged 75 years old, which was defrosted on the day of the experiment (‘frozen’ skin). PMDs (n=3) and NPMDs (n=3) were loaded by manually immersion into a β-gal loading solution (0.65 μg/μl in BSA/bicine buffer) as previously described (Section 2.3.4).

Once loaded, each MD was inserted into each skin sample as follows:

- Three PMDs attached to an electric toothbrush were inserted into skin sample and manually held *in situ* for 5 seconds.
- Three NPMDs not attached to the electric toothbrush were inserted into the skin sample and manually held *in situ* for 5 seconds.

After MD removal, skin samples of ~1 cm^2 were excised from the tissue and treated as previously described (Sections 4.3.3.1-3).
In order to compare the delivery capabilities of liquid loaded PMDs/NPMDs when applied to the skin with and without mechanical vibration, the experiment was repeated on skin tissue obtained from a 57 year old donor ('frozen' skin) according to the following scheme:

- Three PMDs and three NPMDs attached to an electric toothbrush were inserted into the skin sample and manually held *in situ* for 5 seconds.
- Three PMDs and three NPMDs not attached to the electric toothbrush were inserted into the skin sample and manually held *in situ* for 5 seconds.

4.3.5 Diffusion of the BTX A model β-gal within the dermal layer of human skin

The experiments described in this section were performed with the aim to assess the extent of diffusion of a β-gal formulation topically applied to the dermis of a skin tissue as a function of time and concentration. The experiments were performed separately (on three different days) on three 'frozen' skin tissues obtained from three different donors. The size of the skin samples employed in the experiments described in the previous Sections (4.3.3 and 4.3.4) was ~1 cm^2. Conversely, skin samples with an increased size (i.e. ranging between ~1.5-3.5 cm^2, see below for details) were required in the following experiments to visualise the total area of β-gal diffusion. For this reason, only 2 replications (n=2) could be used for each treatment, due to the constrained dimensions of the skin tissue available. Details of the experiments described below are also outlined in Table 4.4.

Experiment 1: evaluating the diffusion of β-gal as a function of the time (30 minutes versus 240 minutes)

The experiment was performed on skin sample obtained from a 43 year old donor (skin tissue 1). Four skin samples, two measuring ~1.5 cm^2 and two measuring ~2 cm^2 were dissected from the tissue.

The four skin samples were placed, epidermis side down, in an organ culture set up as previously described (Section 4.3.3.1). Each sample was placed within one well of a six well culture plate. Subsequently, ten µl of β-gal solution (0.65 µg/µl in BSA/bicine buffer) was topically applied to the central portion of the dermis of each sample. The first two samples (measuring ~1 cm^2) were then cultured at 37°C/5% CO_2 for 30 minutes, whereas the other two (measuring ~2.5 cm^2) were cultured for 240 minutes.

Experiment 2: evaluating the diffusion of β-gal as a function of the concentration of β-gal

The experiment was performed on a skin sample excised from an 86 year old donor (skin tissue 2). Eight skin samples, four measuring ~1.5 cm^2 and four ~2.5 cm^2, were dissected from the tissue. The eight skin samples obtained were placed, epidermis side down, in an organ culture set up as described above. Subsequently, 10 µl of β-gal solution (0.65 µg/µl in BSA/bicine buffer) was topically applied to the central portion of the dermis of each skin sample. Additionally, 10 µl of a more diluted β-gal solution (0.065 µg/µl in BSA/bicine buffer) was applied to the remaining four skin samples as reported for the more concentrated β-gal formulation. Skin samples measuring ~1.5 cm^2 (n=4) were cultured at 37°C/5% CO_2 for 30 minutes, whereas skin samples measuring ~2 cm^2 (n=4) were cultured for 240 minutes.

Experiment 3: evaluating diffusion of β-gal over an extended time

The experiment was performed on skin sample excised from a 52 year old donor (skin tissue 3). Eight skin samples measuring ~1.5 cm^2 (n=2), ~2 cm^2 (n=2) and ~3.5 cm^2 (n=4) were dissected from the skin tissue and transferred into an organ culture set up as above. Subsequently, 10 µl of β-gal solution (0.65 µg/µl in BSA/bicine buffer) was topically applied on the central portion of the dermis of each sample. The skin samples were cultured, as described above, at four increasing incubation times (as outlined in Table 4.4) according to their size.

Culturing and X-gal staining of skin samples

After incubation in organ culture, the samples were treated as described earlier (Section 4.3.3.1). Due to the increased size of the samples treated in this study (compared to the previous experiments), the volume of the solutions employed to perform each step described in Section 4.3.3.1 was at least four times bigger than the size of the skin sample treated (e.g. for a skin sample measuring ~3.5 cm^2 fixation was performed in 15 ml of glutaraldehyde 2% v/v/ PBS/MgCl). The samples were subsequently analysed *en face* (Section 4.3.3.2) and imaged by using a digital camera (an Olympus DP 10 Digital or a Canon digital Ixus 82 IS). The diffusion area (cm^2) was calculated using ImageJ software (available at http://rsb.info.nih.gov/ij; developed by Wayne Rasband, National Institute of Health, MD, USA). Data were presented as average +/- standard deviation (SD).

Table 4.4 Layout of the diffusion experiments: diffusion of the BTX A model β-gal in the dermal region of human skin. The experiments were performed on skin tissues obtained from three different skin donors (skin tissues 1-3). Ten µl aliquots of β-gal solution (either 0.65 µg/µl or 6.5 µg/µl) were topically applied to the dermis of the skin samples. The samples were cultured at 37°C/5% CO_2 for an increased time (depending on their size) in order to assess the extent of diffusion as a function of time and β-gal concentration. n.a.= not applicable.

Skin tissue	Number of samples (n)	Concentration of β-gal (µg/µl)	Samples cultured for 30 minutes	Samples cultured for 240 minutes	Samples cultured for 480 minutes	Samples cultured for 1200 minutes
1	4	0.65	2	2	n.a.	n.a.
2	4	0.65	2	2	n.a.	n.a.
	4	0.065	2	2	n.a.	n.a.
3	8	0.65	2	2	2	2

4.4 Results and Discussion

4.4.1 Evaluating the limit of visible detection of the BTXA model β-gal in solution

The experiment was performed with the aim to assess the concentration of the BTX A model (β-gal) which produced a blue visible pigmentation to be adopted for subsequent skin experiments. Figure 4.2 (A-C) depicts the appearance of a range of β-gal standard solutions after 1 (A) and 24 (B) hours of incubation with the substrate X-gal at 37°C/ 5% CO_2. The results indicated that the reaction is time dependent as a more intense blue colouration was observed for equally concentrated solutions after 24 hours (B) compared to 1 hour (A). In addition, the most suitable concentration values ranged between solution 5 (β-gal 0.006 µg/µl) and solution 1 (β-gal 0.6 µg/µl) as they provided the most intense colouration. Therefore, in order to enable loading of the MDs with a sufficient amount of protein that would allow delivery and detection of β-gal in the skin, concentrations equal or higher to standard solution number 1 were selected for subsequent experiments. As previously reported (Section 3.4.2.1), β-gal concentrations comparable to the concentration of BTX A used in a

clinical setting (i.e. ~1-3 pg/µl) could not be employed, as they would not have been detected by the methodology employed in our experiments. This implies that the dose of β-gal delivered into the skin was considerably higher that the dose of BTX A delivered in a clinical setting. This will be discussed later in this Chapter (Section 4.4.4).

No blue colouration was observed for negative control solution 1 (diluting buffer) and negative control solution 2 (diluting buffer plus X-gal staining solution). This confirmed the specificity of the reaction of the enzymatic assay.

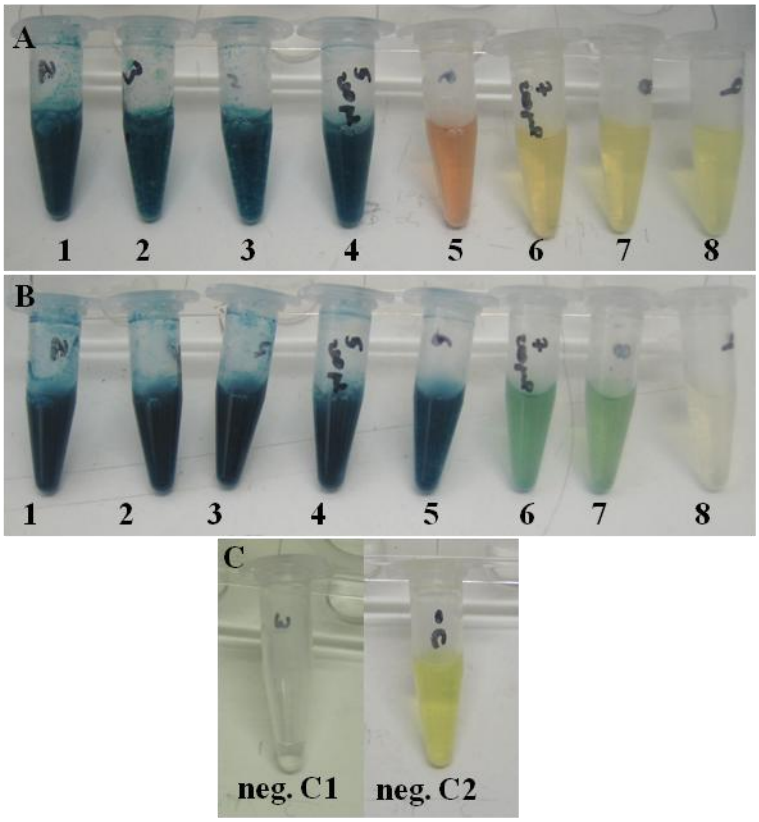

Figure 4.2 (A-C): Limit of visible detection of the BTX A model (β-gal) in solution. Standard concentrations ranging between 0.0001 (standard solution 8) and 0.6 µg/µl (standard solutions 1). The solutions were inspected for a colour change after 1 hour (A) and 24 hours (B) of incubation at 37°C/ 5%CO_2 with X-gal staining solution. The presence of blue colouration indicates successful interaction between the enxyme β-gal and its substrate X-gal; (C) The absence of blue pigmentation of negative control solution 1 (neg. C1) (diluting buffer) and negative control solution 2 (neg. C2) (diluting buffer plus X-gal staining solution) denotes the specificity of the enzymatic assay.

4.4.2 Cutaneous delivery of the BTX A model β-gal from dry coated NPMDs

Published studies regarding dry coated MDs report the use of specific excipients to enhance the uniformity of the coated layer on microneedles (Gill and Prausnitz 2007b). As previously mentioned (Section 2.1.1), excipients commonly used for this purpose are viscosity enhancers and surfactants, used to improve the coating outcome by increasing the thickness and the uniformity of the coated microfilm. The experiments described in this Section were performed in order to evaluate the

delivery capability of the BTX A model (β-gal) from NPMDs that were dry coated with an established coating technique (Gill and Prausnitz 2007a). For this purpose, NPMDs were coated using a micro scale dip coating reservoir device, previously described (Section 2.3.2.1), and a β-gal coating formulation containing CMC (viscosity enhancer) and Lutrol® F68 (surfactant) as excipients. An excipient-free β-gal formulation was also employed in order to assess whether the presence of excipients was fundamental to NPMD coating and thus delivery of the protein into the skin.

Successful delivery of β-gal, indicated by the occurrence of blue stained areas at the sites of microneedle penetration, was revealed by *en face* analysis (Figures 4.3 A and 4.4 A, B). A microneedle array is also shown in Figure 4.3 A for comparison. Histological analysis confirmed delivery of β-gal within the epidermal and dermal layer of the skin (Figures 4.3 B, C and 4.4 C).

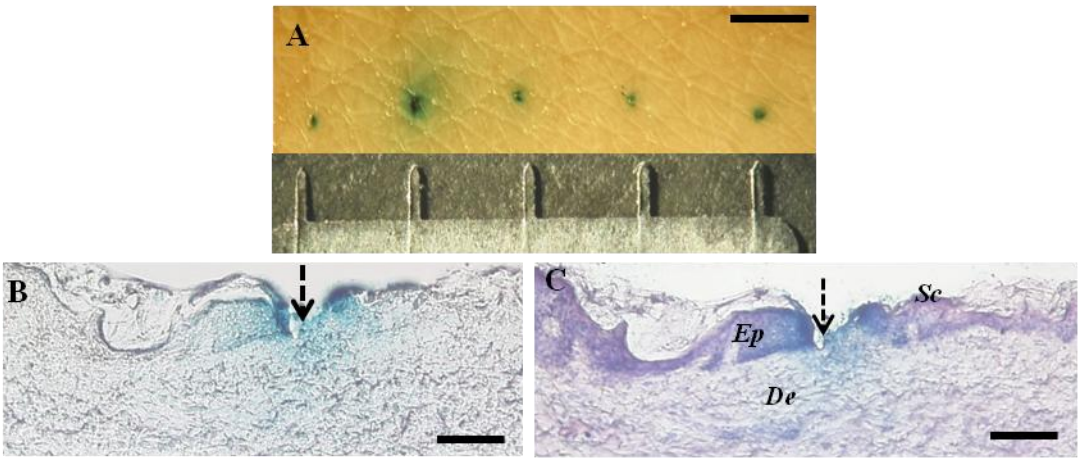

Figure 4.3 (A-C): Cutaneous delivery of the BTX A model (β-gal) from a dry coated NPMD formulation without specific coating excipients: (A) E*n face* images of β-gal stained microchannels and the NPMD, providing a visual reference. Unstained (B) and H&E counterstained (C) histological section of β-gal stained microchannels (indicated by the arrows). NPMDs were coated by a β-gal (0.65 µg/µl) excipients free-coating formulation.
The successful delivery of β-gal is shown by the presence of a blue pigmentation surrounding the microneedle insertion sites (A). The cryosection (B, C) exhibits delivery of β-gal to the epidermis and upper dermis and diffusion of the protein to the more internal layers of the dermis. (A) Scale bar = 1 mm, (B, C) Scale bar = 100 µm; *Sc* = stratum corneum, *Ep* = epidermis, *De* = dermis.

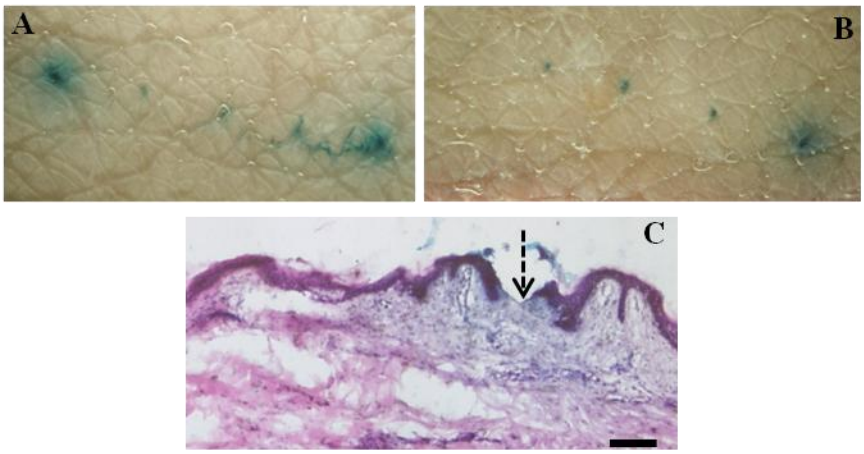

Figure 4.4 (A-C): Cutaneous delivery of a BTX A model (β-gal) from a dry coated NPMD. Use of a formulation containing specific coating excipients. *En face* images (A, B) and H&E counterstained histological section (C) of human skin treated with β-gal coated NPMDs. NPMDs were dry coated by using a formulation containing β-gal (0.65 µg/µl) and CMC and Lutrol® F68 as excipients. (C) The arrow points to the blue stained microchannel generated by NPMD application. (C) Scale bar = 100 µm.

Microchannels created in skin following application of dry coated NPMDs appeared as approximately 150 µm depth interruptions of the stratum corneum and epidermis. The discrepancy between the penetration depth and the length of the microneedles (700 µm) was most likely related to the innate elasticity of the skin which resulted in a folding of the tissue around the microneedle tip. This has been commonly reported in literature for microneedle arrays inserted manually or using hand-held applicators (Burton et al. 2011; Coulman et al. 2011; Hansen 2009; Pearton et al. 2010). Automated applicators i.e., electrically driven devices (Verbaan et al. 2008) and rotator drilling methods (Wang et al. 2006) have been reported as a means to increase microneedle penetration efficiency. It is expected that similarly manufactured applicators may improve piercing performance of the MDs employed in our study.

The data indicated that the BTX A model was released into the skin when using an excipient-free coating formulation (Figure 4.3 A-C). This was not surprising as previous experiments (Section 2.4.2) indicated that high molecular weight molecules could be successfully coated on NPMDs without excipients. In control experiments, where skin was treated with NPMDs dry coated with β-gal free formulation, blue staining was not reported (Figure 4.5), thus confirming the specificity of the β-gal assay in the skin tissue.

Figure 4.5: *En face* image of human skin treated with a NPMD dry coated with BSA/bicine buffer and CMC and Lutrol® F 68 as excipients (negative control).

In Figures 4.4 A and B, it is apparent that the extent of blue staining was not uniform, thus indicating a certain variability in β-gal delivery. This was most likely related to the poor reproducibility of the coating procedure. As previously discussed (Sections 2.4.2 and 3.4.2.3), uniform microneedle coating could not be guaranteed in our experiments by using the established coating methodologies. This implies that at each immersion, each microneedle was coated with a slightly different dose of β-gal and that a portion of the coating was also placed in the space between adjacent microneedles (i.e. the base of the array). This resulted in i) occurrence of blue stained areas of variable intensity at the microneedles insertion sites, ii) absence of some positively stained microchannels (i.e. only 4 out of 5 blue microchannels were detected as depicted by Figure 4.4 B, thus suggesting that only 4 microneedles of a NPMD were coated); iii) appearance of blue stained areas between microneedles due to the dissolution of the coating retained on the space between adjacent microneedles.

Another possible cause for the variability may reside in the non-uniform insertion of the microneedles into the skin and/or incomplete dissolution of the coating from the microneedles. As previously described (Section 4.3.3), NPMDs were manually inserted into the skin by applying a light pressure for 5 seconds, after which they were left in the tissue for 5 minutes. Insertion times ranging between 1 and 15 minutes have been commonly reported for dry coated MDs with the aim to allow dissolution of the coating by the interstitial fluids in the skin (Chen et al. 2011; Gill and Prausnitz 2007b; Widera et al. 2006). Even when NPMDs were inserted into the skin and held in place, not all microneedles remained in position for the entire

duration of the application (i.e. 5 minutes), due to the elasticity of the skin. As a consequence, a portion of the coating may have not been released in the tissue from some microneedle, thus resulting in variability of the intensity of the stained areas.

Application of a force (i.e. a downward pressure) on the NPMDs may have maintained the microneedles *in situ* in a more uniform way. However, this could not be performed due to the in-plane design of the NPMD (i.e. NPMDs consist of one-dimensional arrays containing a row of five microneedles orientated parallel to the base of the array) and the narrow surface of the base of the array. If out-of-plane microneedles arrays (i.e. two-dimensional arrays consisting of microneedles orientated at 90° out of the base plate of the device) had been used, application of a downward force on the base of the device could have been performed. This may have provided a more consistent insertion of the microneedles into the skin and thus a more uniform release of the coating. However, the purpose of this study is the use of PMDs for delivery of BTX A in a liquid form, which is thus expected to be released in the skin quicker (within seconds) than a dry coat. With this in mind, we did not pursue the studies related to the dry coated NPMDs further than the experiments reported in this Section.

Delivery of β-gal from dry coated NPMDs was also carried out on freshly excised skin (‘fresh’ skin). This was performed to assess the effect of proteases (i.e. aminopeptidases and carboxipeptidases), physiologically present in the skin (Hotchkiss 1998), on the activity of the delivered protein.

Given that, in order to assess metabolic activities the viability of the tissue has to be ensured (Steinsträsser and Merkle 1995), the skin employed in this experiment was processed within a short time (~2 hours) of surgical removal and maintained in a defined organ culture media (Birchall et. al 2005). Successful enzymatic activity indicated by the emergence of blue stained areas at microneedle insertion sites was reported as for ‘frozen’ skin (data not shown). This indicated that β-gal model maintained its integrity in viable skin, thus suggesting that therapeutic proteins such as BTX A should retain their activity once delivered into the skin by MDs.

4.4.3 Cutaneous delivery of the BTX A model β-gal from liquid loaded PMDs

4.4.3.1 Loading and de-loading visualisation of a BTX A model formulation from PMDs

In attempt to assess whether uniform unloading of a BTX A model (β-gal) formulation occurred from a PMD following insertion of the microneedles into the skin, PMDs were loaded with a formulation containing a dye. Following one immersion of the pocketed microneedles in the formulation, the pockets appeared uniformly loaded thus confirming the data of previously reported experiments (Section 2.4.4). Visual inspection of the pocketed microneedles after insertion and subsequent removal from the skin revealed the unexpected persistency of formulation in some pockets. Despite this, successful delivery of β-gal was reported for all skin sample treated, as revealed by the appearance of positively blue stained microchannels (Figures 4.6 A, B and 4.7 A, B). Histological analysis demonstrated the capability of the PMDs to deliver β-gal to both the epidermal and dermal layer of the skin (Figure 4.7 B). Varying the PMDs residence time into the skin i.e., 5 seconds (Figure 4.6 A, B) against 1 minute (Figure 4.7 A, B), did not result in any significant difference in the extent of delivery of the macromolecule. This therefore indicated that the formulation was released almost instantaneously to the skin following application of the liquid loaded PMD.

Contrary to that described for dry coated NPMDs (Section 4.4.2), PMDs were liquid loaded by manual immersion into a small volume (~20 µl) of formulation contained in a reservoir (Section 2.3.4). Therefore, the micro scale dip coating device previously described (Section 2.3.2.1) was not used for PMD loading. The subsequent results highlighted a certain variability in the diffusion of the protein, as indicated by differences in the blue staining areas surrounding the microneedle insertion sites (Figures 4.6 A and B). Variability was also observed previously for NPMDs dry coated by using established coating methodologies and therefore the results confirmed that both the employed coating methodologies do not facilitate uniform and reproducible loading/coating on either PMDs or NPMDs. This may represent an issue if PMDs were to be used clinically to deliver BTX A, as uniformity of the delivered dose must be guaranteed. The strategies which could

potentially increase uniformity and reproducibility of MD loading have been discussed previously (Section 2.4.2)

The extent of diffusion of the blue stained areas at the microneedle insertion sites was greater for liquid loaded PMDs (Figures 4.6 A, B and 4.7 A) than for dry coated NPMDs (Figures 4.3 A, 4.4 A, B), thus suggesting an increased diffusion of β-gal when delivered in a liquid state. This aspect will be discussed further in Section 4.4.3.2.

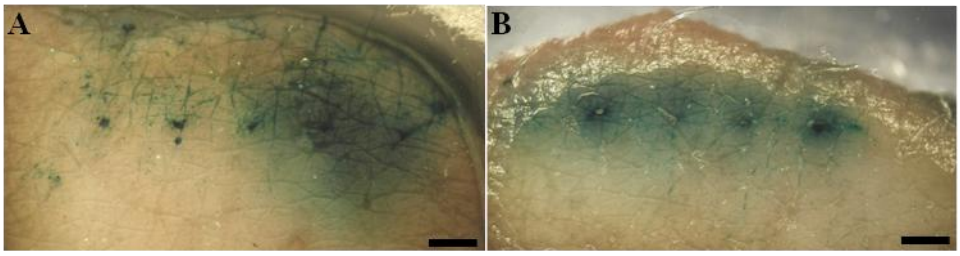

Figure 4.6 (A, B): Delivery of the BTX A model (β-gal) to human skin from liquid loaded PMDs. E*n face* images of human skin treated with liquid loaded PMDs. PMDs were manually immersed into a β-gal formulation (1.3 µg/µl) before being inserted into the skin for 5 seconds. Delivery of β-gal is indicated by the appearance of blue pigmented areas at the microneedle insertion sites. Scale bar = 1 mm.

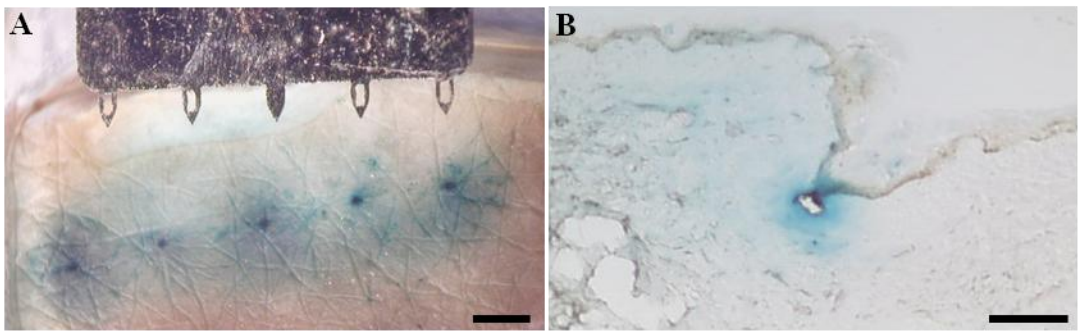

Figure 4.7: En face image (A) and histological section (B) of human skin treated with liquid loaded PMDs. PMDs were loaded following one immersion into a β-gal formulation (1.3 µg/µl) before being inserted and left for 1 min in the skin (B). (A) scale bar = 1 mm, (B) scale bar = 100 µm.

4.4.3.2 Application of a mechanical vibration to enhance the cutaneous delivery capabilities of liquid loaded PMDs

Further experiments were performed with the aim to compare β-gal delivery efficiency from liquid loaded PMDs with and without the application of a mechanical vibration. Although (as highlighted by the Section above) the application of the vibration was not considered essential for a complete release of the loaded solution from the pockets, it was hypothesized that it might facilitate distribution of a formulation within the skin. A study published by Wang *et al.* (2006) reported insertion of hollow microneedles into *ex vivo* hairless rat skin by using a vibration. According to this study application of the vibration significantly enhanced delivery of a tissue-marking dye from the microneedles, however the distribution of the dye was assessed only by *en face* analysis and no histological sectioning was conducted. Therefore, deposition of the dye within the different layers of the skin was not investigated. Our results indicated successful delivery of the BTX A model for all the skin samples treated by PMDs/NPMDs both with and without mechanical vibration (Figures 4.8 A-D and 4.9 A-H). Histological analysis suggested a greater diffusion of the BTX A model in samples treated with microneedle vibration (Figure 4.8 B and 4.9 B) compared to samples treated without vibration (Figure 4.8 D and 4.9 D). This was more pronounced for samples treated by PMDs than by NPMDs. It is possible that the mechanical vibration may have facilitated release of the formulation from the pockets. It may also be that mechanical vibration increased diffusion of the formulation by reducing the skin dynamic stiffness and/or assisting the disruption created by the microneedles within the skin. Although this suggests the feasibility of a vibrational approach as a means to increase dermal delivery and diffusion, the results cannot be considered conclusive as additional studies are needed in order to better evaluate this method.

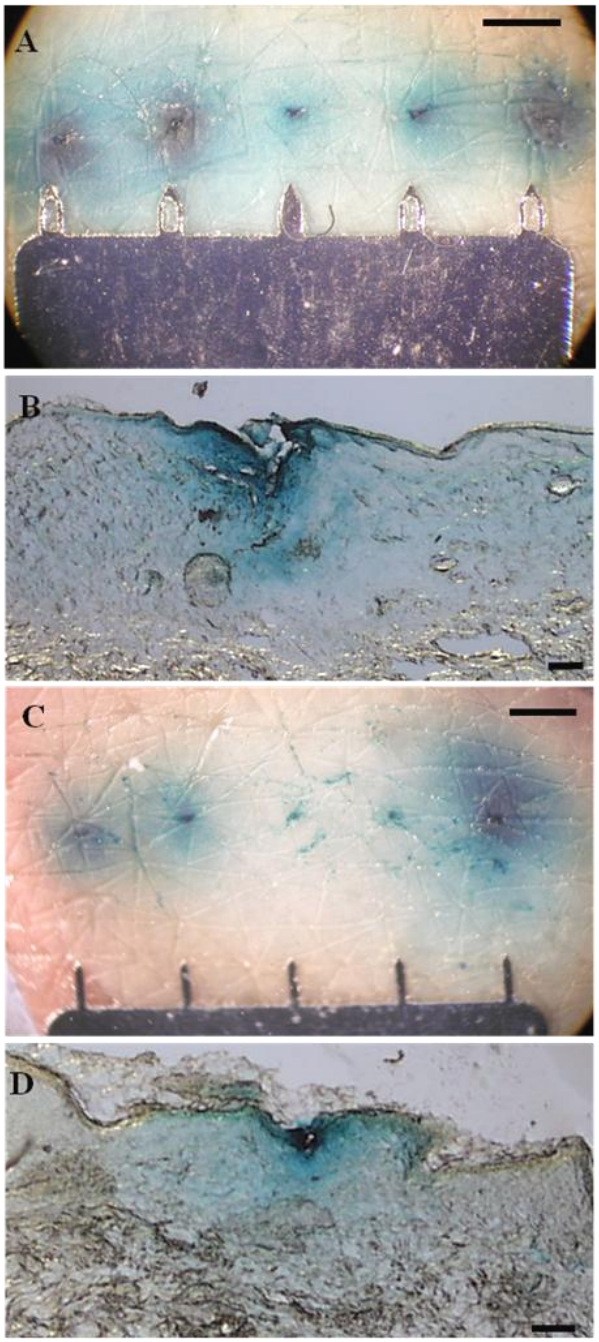

Figure 4.8 (A-D): *En face* (A, C) images and histological cryosections (B, D) of human skin treated with PMDS (A, B) and NPMDs (C, D) loaded with the BTX A model. PMDs and NPMDs were loaded by one immersion into a β-gal formulation (β-gal 0.65 µg/µl) and subsequently inserted into the skin for 5 seconds. PMDs were applied in the skin with mechanical vibration, whereas NPMDs were applied without vibration. (A, C): scale bar 1mm; (B, D): 100 µm

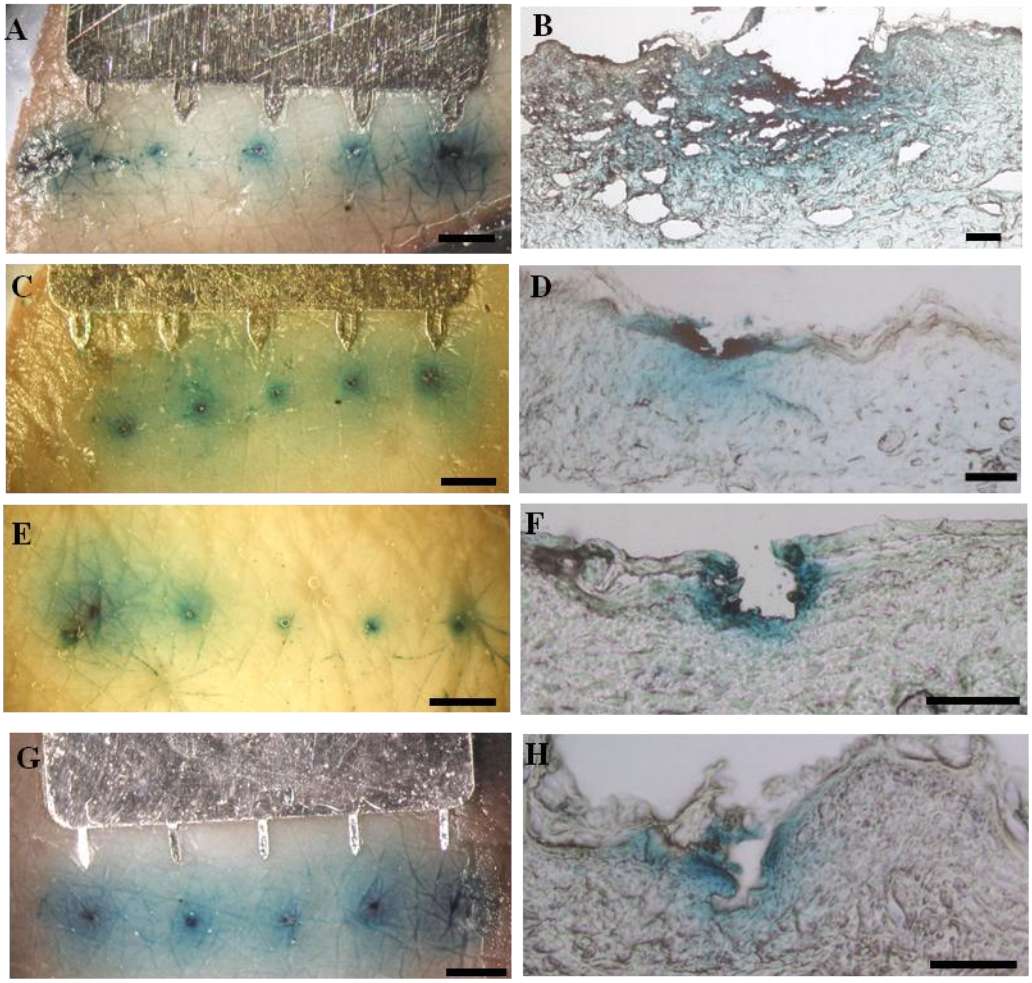

Figure 4.9 (A-H): Comparison of cutaneous delivery capabilities of liquid loaded PMDs/NPMDs with and without mechanical vibration. *En face* images (A, C, E and G) and cryosections (B, D, F, H) of human skin treated with β-gal loaded PMDS (A-D) and NPMDs (E-H) either attached (A, B, E, F) or not (C, D, G, H) to an electric toothbrush. PMDs and NPMDs were loaded following one immersion into a β-gal formulation and subsequently inserted the skin for 5 seconds. Scale bars (A, C, E, G) = 1 mm; (B, D, F, H) = 100 µm.

When comparing *en face* images of skin samples treated with dry coated NPMDs (Figures 4.3 A and 4.4 A, B) and liquid loaded PMDs (Figure 4.9 C), more diffuse staining at the microneedle insertion sites could be detected when β-gal was delivered as a liquid. For the purpose of this comparison skin samples treated with liquid loaded PMDs with vibration (Figure 4.8 A and 4.9 A) are not taken into account as the increased diffusion observed in these samples may have been a feature of the vibration (which conversely was not applied for dry coated NPMDs). An

increased diffusion of the protein β-gal in a liquid form was also suggested by histological analysis (Figure 4.9 D). However diffusion areas surrounding the microneedles insertion sites may have not been determined only by diffusion of β-gal out from the microneedles within the skin, but also by diffusion of the formulation released on skin surface upon contact of the microneedles and the base of the array with the tissue. As this formulation was not removed after each PMD application, it might have diffused laterally from the microchannels and/or internally within the microchannels thus generating the stained areas detected on the surface of the skin (as depicted by *en face* images) and within the skin (as depicted by the cryosection images). It is reasonable to assume that if the formulation had been removed from the skin surface, i.e., by cleansing the surface of the tissue following PMD removal, diffusion may have been reduced. Therefore, although the use of liquid loaded PMDs may facilitate greater diffusion of medicaments such as BTX A, in comparison to dry coated NPMDs, the degree of diffusion highlighted by our experiments may be overestimated.

For the treatment of a skin disorder such as PFHH, BTX A has to be delivered to a specific depth of the dermis to ensure optimal interaction with its therapeutic targets (the sweat glands). As previously mentioned (Section 1.2.3), cholinergic fibres surround the secretory portion of the sweat glands that are located in the deep dermis. It is therefore to this site that BTX A has to migrate to block the cholinergic message and thus inhibit sweating. As the thickness of the dermis ranges between 1 and 3 mm (Jensen and Proksch 2009), if BTX A was to be delivered by PMDs, it would have to diffuse to at least 1 mm from the skin surface to reach its therapeutic target. In our experiments, PMDs were able to penetrate the epidermis and reach the superficial layer of the dermis to a depth ranging between 100 and 300 µm. Extensive diffusion of β-gal was observed within the dermis especially when vibration was applied as the protein migrated to a depth of approximately 600 µm (Figure 4.8 B and 4.9 B) although, as mentioned above, diffusion of BTX A from liquid loaded PMDs may be slightly overestimated. In all cases, not one treated sample showed a degree of diffusion of β-gal to a sufficient depth in the dermis, which would guarantee optimal contact with its therapeutic target. However, as reported in the Material and Method Section (4.3.3.1), following application of the PMDs, skin samples were only incubated for 1 ½ hours in organ culture before being fixed in glutaraldehyde. As the fixation stopped the diffusion of β-gal, it would be reasonable to assume that the

protein may have diffused further if it had been incubated for an increased period of time and therefore the PMD delivery technique may be feasible for BTX A.

In addition, evaluation of the diffusion of β-gal on treated samples relied on the visible detection of the blue insoluble pigment generated by the reaction between the enzyme and its substrate X-gal. By Fick's first law (Amorosa 1998a; Wonglertnirant et al. 2011), molecules diffuse according to their concentration gradient. Therefore, β-gal would diffuse from the point of maximal concentration (the microneedle insertion site) to the more internal layers of the skin. As the concentration of β-gal at those sites would be considerably lower than that on the surface of the skin, such concentrated protein may have resulted in undetectable signal. This implies that the protein may have reached deeper layers in the dermis but the signal generated may have been below the limit of detection of the methodology employed in our experiments.

BTX A is a highly hydrophilic molecule whose capability to diffuse to anatomical sites adjacent to the site of injection has been assessed in both humans and animals (Borodic et al. 1994; Carli et al. 2009; Stone et al. 2011; Trindade de Almeida et al. 2007). Hexsel et al. (2008) assessed the halo of anhidrosis (i.e., the area surrounding the injection site where reduction or absence of sweating is observed) following injections of the BTX A commercial preparation Botox® (BTX A=5ng) into the frontal muscle of 18 volunteers. In this study Botox® was reconstituted in 1 ml of 0.9% saline and injected in one site (per patient) of the forehand at a volume of 20 µl (0.1 ng of BTX A per application site). Injections were performed by using 0.3 ml syringes with a 29-gauge needle (0.7 cm in length) whose caps were cut to enable control of the needle insertion depth which was performed at ~2-3 mm from the skin surface. Patients were evaluated 28 days after the treatment by measuring the diameter of the anhydrotic halos with Minor's test. The mean diameter calculated was equivalent to 1.73 cm (+/- 0.37) and thus, given the spherical shape of the halos, we could assume a diffusion area of 2.34 cm^2. PMDs employed in our study possess 5 in-plane microneedles placed at a distance of ~1.5 mm to each other. Therefore, PMDs containing an increased number of microneedles, i.e., 10 x 10 out-of-plane microneedles, would permit delivery of BTX A to a surface of the skin equal to 2.25 cm^2, which is almost identical to the one highlighted by the experiment mentioned above. This therefore suggests that PMDs may represent a realistic alternative to the standard intradermal injections.

Alternatively designed MDs with an increased loading capacity may also be considered for BTX A administration. For example, hollow microneedles have been shown to deliver drug formulations with volumes ranging between a few microlitres (Hafeli et al. 2009; McAllister et al. 2003; Nordquist et al. 2007; Wang et al. 2006) up to millilitres (Burton et al. 2011; Gupta et al. 2009), whereas our experiments have suggested that ~100 nl can be loaded on the PMD (Sections 3.4.2.1 and 3.4.2.3). Similarly designed hollow microneedles would ensure greater diffusion of the toxin throughout the dermis as a result of the increased volume injected by the microneedles and the pressure applied to eject the formulation (Wonglertnirant et al. 2011). However, diffusion of BTX A would have to be carefully controlled as excessive diffusion of the toxin, resulting from large injected volumes (i.e. higher than 100 µl), have a greater potential to cause side effects (i.e. muscle paralysis) due to unwanted migration of the toxin to the subcutaneous muscles (Glaser et al. 2007).

The use of larger microneedles (i.e. with increased length) would also have to be considered especially for the treatment of the hyperhydrotic sites characterised by high skin thickness. For example, if palmar or plantar hyperhidrosis were to be treated, microneedles with a length of 700 µm (such as the ones constituting the PMDs employed in our study) would not be able to deliver the drug to the dermis. The thickness of the epidermis at these anatomic sites is the highest in the body, being ~0.8-1 mm (Barry 1983b) with a stratum corneum measuring ~200-500 µm (Alekseev and Ziskin 2007; Egawa et al. 2007). Previous studies assessed the penetration efficiency of NPMDs in human volunteers at the palmar site (Coulman et al. 2011). NPMDs were applied on the palm and the microneedle insertion was imaged *in situ* by a sophisticated optical imaging method called Optical Coherence Tomography. These studies indicated that NPMDs penetrated to a depth in the skin, which was primarily limited to the stratum corneum (i.e. ~300 µm). A similar behaviour is expected for PMDs as they contain microneedles with the same length (700 µm). This strongly suggests that longer microneedles, i.e., 1000 µm in length or more, would be needed to facilitate delivery of BTX A to the superficial layer of the dermis at the palmar and plantar sites. Delivery of the BTX A exclusively in the epidermis would presumably prevent diffusion of the medicament to the underlying dermis due to the presence of the dermo-epidermal junction (Section 1.2) and so it is important to breach this barrier. Wang *et al.* (2006) published a study assessing the use of hollow microneedles as a means to deliver fluorescently tagged insulin *in vitro*

to the dermis of rat skin. The authors indicated that although the injection was performed at a specific depth in the dermis (i.e. 500-800 µm), the large volume of fluid injected (i.e. ~5 µl) distributed throughout the dermis and an intense signal was detected from this region of the skin.

Conversely, only small fluorescence was detected from within the epidermis, thus suggesting that the peptide had difficulty in crossing the dermal-epidermal junction. In contrast, microneedle injections of the small molecule calcein (~900 Da) resulted in comparable distribution of the compound between dermis and epidermis. This suggests that for high molecular weight medicaments such as BTX A, a microneedle capable of perforating the dermo-epidermal junction would have to be employed. This would allow direct loading of the medicament to the upper dermis. However, the need for longer microneedles may potentially increase the invasiveness of the microneedle-aided treatment. As previously discussed (Sections 1.2.1 and 1.2.2), the epidermis is devoid of vasculature, whereas the dermis contains a capillary bed which is located just below the dermo-epidermal junction (Sorrell and Caplan 2004). Therefore, microneedles penetrating deeper than the epidermis could breach these capillaries and cause bleeding. Despite this expectation, bleeding has not been reported for the majority of the microneedles studies conducted in animals and humans (Prausnitz et al. 2009). In humans subjects, bleeding is uncommon when using solid microneedles with a length ranging between 500-1000 µm (Gill et al. 2008) whereas application of 1.5 mm solid or hollow microneedles has lead to the occurrence of small droplets of blood at the microneedle insertion sites (Gill et al. 2008; Laurent et al. 2007b). However, within these studies microneedles were applied to anatomical sites (i.e. the forearm) whose epidermis thickness is considerably smaller compared to palms and soles (i.e. ~100 µm versus 800 µm). As a consequence, it may be expected that insertion of up to 1.5 mm long microneedles in thickened anatomical sites such as palms and soles would not cause significant damage or bleeding. Moreover, the pain and discomfort associated with insertion of relatively long microneedles would be expected to be minimal in these areas of the body, especially in comparison to standard hypodermic needles.

In conclusion, the results indicate that liquid loaded PMDs are suitable tools to administer macromolecules such as BTX A to the upper dermis of human skin. The macromolecule β-gal diffused to deeper sites of the dermis from the microneedle insertion site and this seemed to be more prominent when mechanical vibration was

applied. Longer microneedles would be required to administer BTX A to the dermis of thickened skin sites such as the palm of the hands and the soles of the feet.

4.4.4 Diffusion of the BTX A model β-gal into the dermis of human skin

In an attempt to predict the diffusion of high molecular weight molecules, such as BTX A, in human skin, the BTX A model (β-gal) was topically applied to the dermis of excised human skin tissue. The presence of β-gal was confirmed by the emergence of a coloured (blue) area after X-gal staining (Figure 4.10 A and B). Table 4.5 outlines the diffusion area (cm^2) of the enzyme after application of 10 µl of either β-gal 0.65 µg/µl or 0.065 µg/µl to the dermis on three different skin samples (1-3). The data indicated that thirty minutes after application of 10 µl of β-gal 0.65 µg/µl on skin samples, the area measured approximately 0.4 cm^2 and after 240 minutes lateral diffusion of the protein extended to approximately 0.7 cm^2. The results show increased diffusion of the formulation with time, as expected according to Fick's law (Amorosa 1998a). Higher diffusion values were registered for another skin donor tissue as an area of 0.73 (+/-0.21) cm^2 and 1.39 (+/-0.59) cm^2 was reported after 30 and 240 minutes respectively of incubation in organ culture. Such variability can be expected when comparing samples excised from different donors as the properties of the skin (e.g. hydration and skin thickness) vary between different individuals (Laurent et al. 2007a).

Topical application of a less concentrated formulation (i.e., β-gal 0.065 µg/µl) did not seem to affect diffusion of the protein within the first 30 minutes as a diffusion area similar to that obtained for skin samples treated with a more concentrated formulation (i.e., β-gal 0.65 µg/µl) was registered (Table 4.5). However, a slightly reduced area was reported when the skin samples were incubated for prolonged time (i.e., a diffusion area of 0.54 (+/- 0.03) cm^2 was recorded after 4 hours of incubation). This suggests that dermal diffusion of less concentrated protein formulations may be reduced, as expected by Fick's law (Amorosa 1998a). Within the experiments reported in this Section a mass of either 6.5 or 0.65 µg of β-gal was topically applied to the surface of the skin (i.e., 10 µl of either β-gal 0.65 µg/µl or 0.065 µg/µl). As previously mentioned (Section 3.4.2.3) doses of BTX A ranging between 0.1-0.25 ng are generally delivered intradermally at each application site by a standard needle

and a syringe. The dose of protein used in our experiments was therefore 6,500 to 65,000 times higher than the actual dose of BTX A delivered in the clinical setting. Doses of β-gal comparable to therapeutic doses of BTX A could not be assessed in our experiments as they would have not been detectable by the staining methodology employed. Therefore, if BTX A was to be delivered to the epidermis/dermis by PMDs, less rapid diffusion, compared to the one estimated in our experiments for the model β-gal, may be expected. However, due to the high potency of BTX A and the elevated density of sweat glands in hyperhydrotic sites such as the palm of the hand and the sole of the foot (600-700 glands/cm^2) (Sato et al. 1989), BTX A may nevertheless reach its therapeutic targets and induce a therapeutic response.

Skin samples incubated for extended times in organ culture (480 and 1200 minutes) did not display any increase in the diffusional area of the enzymatic protein. This suggested that diffusion of β-gal occurs readily, reaching the maximum extent within the first hour.

The diffusive capability of proteins within the dermis has been previously reported. Widera *et al.* (2006) assessed the distribution profile of ovalbumin (~44 kDa) within the epidermal/dermal layer of skin samples excised from euthanised rats treated with ovalbumin coated MDs containing different microneedle lengths (details of this study has been described in Section 4.1.3).

Quantitative analysis of the dose of ovalbumin delivered within the different layers of the skin indicated that, independent of the microneedle length employed, almost 20% of the protein was delivered to the epidermis whereas the remaining 80% was found in the dermis at a depth that was located beyond the maximal penetration depth of the microneedles.

According to the authors, this was due to the rapid diffusion of the hydrophilic protein within the dermal environment. Similar ovalbumin distribution profiles were found in skin samples excised immediately and 1 hour after ovalbumin delivery, thus indicating that the protein diffused readily within the skin. These findings are in agreement with the data highlighted by our experiments, despite the considerably larger size of the studied protein β-gal (~465 kDa) in comparison to ovalbumin (~ 44 kDa).

In a more recent study the diffusion of the hydrophilic macromolecules fluorescein isothiocyanate dextrans (average m.w. = 4.3 kDa) was assessed *in vitro* into hairless rat skin (Wonglertnirant et al. 2011). The study compared the diffusivity of these

compounds in full thickness skin and skin samples devoid of the stratum corneum. Diffusivity of the compounds was found to be significantly lower in the stratum corneum compared to the underlying viable epidermis/dermis. The authors concluded that hydrophilic molecules directly delivered to the epidermis/dermis of the skin by using MDs, would be expected to readily diffuse through the deeper layers of the skin, as these layers contain more water compared to the stratum corneum.

In conclusion, the results indicated that high molecular weight proteins can readily diffuse within the dermal layer of human skin. Therefore if MDs facilitate dermal delivery of BTX A, diffusion should ensure that the therapeutic distributes within the dermal tissue and interacts with the therapeutic target (the eccrine sweat glands).

Table 4.5: Diffusion area (cm^2) of a β-gal solution topically applied to the dermis of human skin. β-gal diffusion area is shown as a function of incubation time of the skin tissues in organ culture and the enzymatic concentration used (β-gal 0.65 and 0.065 µg/µl). Enzymatic diffusion within the dermis of three skin tissues obtained from three different skin donors were compared (skin tissues 1-3 aged respectively 43, 86 and 52 years old). The incubation times of the skin samples are indicated as time 1 (30 minutes), time 2 (240 minutes), time 3 (480 minutes) and time 4 (1200 minutes). Data are presented as mean+/-SD, n = 2. n.a. = not applicable

Skin sample	Concentration of β-gal (µg/µl)	Dose (µg) of β-gal topically applied to the dermis	Diffusion area (cm^2) at time 1	Diffusion area (cm^2) at time 2	Diffusion area (cm^2) at time 3	Diffusion area (cm^2) at time 4
1	0.65	6.5	0.44 (+/- 0.09)	0.77 (+/- 0.01)	n.a.	n.a.
2	0.65	6.5	0.39 (+/- 0.03)	0.67 (+/- 0.06)	n.a.	n.a.
	0.065	0.65	0.33 (+/- 0.08)	0.54 (+/- 0.03)	n.a.	n.a.
3	0.65	6.5	0.73 (+/-0.21)	1.39 (+/-0.59)	0.52 (+/- 0.05)	1.1(+/- 0.04)

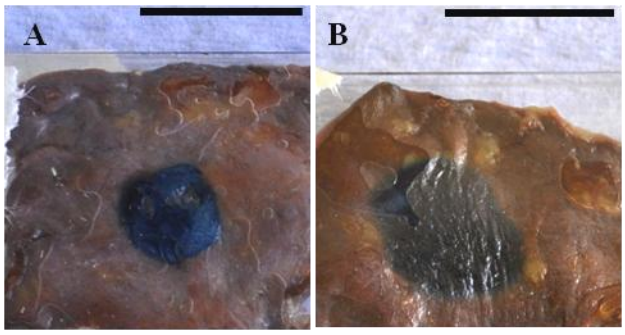

Figure 4.10 (A, B): Diffusion of the BTX A model β-gal within the dermis of human skin as a function of time. *En face* images of human skin samples (dermis side up) following topical application of 10 µl of β-gal (0.65 µg/µl) and incubation in organ culture for 30 (A) and 240 (B) minutes. The presence of β-gal was confirmed by the emergence of a coloured (blue) area after X-gal staining. The skin samples were obtained from an 86 year old donor (skin tissue 2). Scale bar = 1cm.

4.5 Conclusion

The MDs can rapidly (within seconds) facilitate delivery of high molecular weight molecules into the dermal layer of human skin. The results suggest that although BTX A could be successfully delivered to the dermal layer of human skin by established dry coated NPMDs, lateral diffusion in the dermis is enhanced following liquid loading via PMDs. Although the application of a mechanical vibration may facilitate diffusion of a protein formulation within the cutaneous tissue, the results highlighted by the experiments reported in this Chapter cannot be considered conclusive.

The capability of the ~465 kDA macromolecule β-gal to readily diffuse through the dermis when topically applied has also been demonstrated. This indicates that BTX A should diffuse to the therapeutic targets (the eccrine sweat glands) located in the deep dermis, once delivered to the epidermis/dermis by PMDs. Therefore, the results suggest that a liquid loaded PMD may provide a suitable tool to deliver BTX A to the dermis of human skin for the treatment of skin disorders such as PFHH.

Administration of BTX A to thick hyperhydrotic areas such as palms and soles would require optimization of PMD design, i.e., longer microneedles and possibly sharper tips due to the increased thickness of the stratum corneum at these anatomic sites.

Chapter 5

Delivery and detection of BTX A therapeutic formulation Vistabel® and botulinum toxoid A (BT A) within human skin following application of liquid loaded pocketed microneedle devices (PMDs)

5.1 Introduction

The aim of this Chapter was to demonstrate intradermal delivery of BTX A by liquid loaded PMDs. The commercial BTX A preparation Vistabel® and the formaldehyde inactivated BTX A, i.e. botulinum toxoid A (BT A) was employed for this purpose. The use of BTX A in its detoxified form was enforced by safety reasons, due to the extremely high toxicity of the active protein (BTX A). Two main methodologies were employed for protein detection within the skin: immunohistochemical techniques and fluorescence imaging following conjugation of BT A to a tandem fluorophore constituted by phycoerythrin and a cyanine (PE/Cy7®).

5.1.1 Botulinum toxins (BTXs) detection

BTXs represent the most toxic substances known, with systemic lethal doses in humans estimated at ~1 ng/kg of body weight (Gill 1982). Due to the high risk associated with these toxins, extremely sensitive and accurate BTXs detection has to be ensured. Due to the tremendously high potency of the toxins, BTXs detection has been analytically challenging, especially when toxins are contained in complex samples such as food or clinical specimens (i.e. blood and faeces). To date, the only accepted method for the detection of BTXs in foodstuff, clinical samples and pharmaceutical formulations is the mouse *in vivo* bioassay. In this method, toxin samples are injected intraperitoneally into the mouse. Signs of botulism are subsequently observed in the animal over a period of 2-4 days. This method can detect BTX to < 10 pg/ml (Grate 2010; Scarlatos et al. 2005). The quantity which determines death in a mouse, so termed mouse lethal dose (MLD) is ~ 10 pg. As samples are usually injected in 0.5 ml volumes, the limit of detection (LOD) for this assay is 2 MLD/ml (Cai et al. 2007; Grate 2010). Although sensitive, this assay is time consuming, potentially dangerous to personnel during injection, requires a large number of animals and it is associated with inherent variability between assays (due to a different response to the toxins between different animals) and laboratories.

Over the last three decades, numerous investigations have been carried out with the aim of developing sensitive and rapid *in vitro* assays that could replace the mouse bioassay. A large variety of sophisticated assays have been developed in the form of immune-PCR assays (Chao et al. 2004), enzyme-amplified protein microarray

(Varnum et al. 2006), mass spectrophotometric assays (Kalb et al. 2006), real time PCR based assays (Mason et al. 2006), assays based upon the peptidase activity of the toxins (i.e. the capability to cleave proteins of the SNARE complex) (Rasooly and Do 2008) and enzyme-linked immunosorbent assays (ELISA) (Ekong et al. 1995; Frevert 2010; Grate et al. 2009; Shone et al. 1985). Assays detecting the activity of BTXs in tissue samples (e.g. mouse muscles with attached nerves) (Foster K. 2006) or neuronal cells (e.g. cells obtained from rat spinal cord) (Pellett et al. 2007) have also been reported. Advances in BTXs assays have extensively been reviewed by Grate *et al.* (2010). Particular attention will be given in this introduction to the ELISA methodology as it is considered more closely aligned to the immunodetection methods adopted in the experiments reported within this Chapter.

5.1.2 ELISA principle

ELISA assays for BTX A rely on the binding of a specific portion of the toxin (epitope) to an antibody labelled with an enzyme that can provide amplification of the signal detected. The majority of the ELISA methods employ antibodies directed against specific features contained in either the entire 150 kDa (i.e., the holotoxin), the toxin complex (~500 or ~900 kDa) or defined portions of the holotoxin. As the binding affinity of antibody for its specific antigen site is the most important factor determining the sensitivity of an immunoassay, many research groups have produced their own antibody preparations. These are usually obtained by the sera of animals of different species (such as mouse, guinea pig, chicken and others) previously immunised with botulinum antigens in the form of either formaldheyde inactivated toxin (i.e. botulinum toxoid) or chemically synthesized peptides corresponding to a specific portion of the toxin (e.g. a specific region of the 100 kDa heavy chain). Monoclonal (reacting with a single antigenic epitope in the toxin) or polyclonal antibodies (reacting with multiple epitopes) have been produced either as fragments or whole antibodies. ELISAs have been generally used in the form of a sandwich ELISA in which a primary capture antibody previously coated to the microwell surface of a microtiter plate binds to the botulinum toxin antigen. After antigen capture, a primary detection antibody binds to the antigen in a different epitope, thus creating the ‘sandwich’ structure. Subsequently, a secondary detection antibody conjugated with an enzyme (usually horseradish peroxidase (HRP) or alkaline

phosphatase (AP)) binds to the primary detection antibody. The enzyme catalyzes the reaction of a specific enzymatic substrate (usually a precipitating chromogen) to a coloured product which allows for antigen detection. Between each step, the microtiter plate is usually washed in appropriate buffer solution to avoid unspecific binding of proteins to antibodies. The optical density of the solution generated in each well of the microtiter plate can therefore be measured at the appropriate wavelengths (depending on the specific substrate employed) and the quantity of antigen determined by calibrated spectroscopy. ELISA assays are usually faster than the mouse bioassay as they can generally be performed within 5-6 hours. Although a variety of substrates and antibodies have been described for BTXs detection, all the ELISA methodologies share the same fundamental immunodetection principle.

5.1.3 Use of amplified ELISA for high sensitivity quantification of BTXs

Many of the ELISA assays developed have reached LODs equal or close to the mouse bioassay, i.e. ranging between ~10-60 pg/ml. This has been achieved by using high sensitive amplified ELISAs, which allow increases in sensitivity of 100-1,000 fold, compared to non amplified ELISAs. Use of non amplified ELISAs with LODs approaching the mouse bioassay have also been reported (Ekong et al. 1995) (this study will be discussed in greater detail in Section 5.1.4).

Shone *et al*. (1985) reported an amplified ELISA assay for rapid and sensitive detection of BTXs in food and botulinum strain culture. In this study microtiter plates were coated with a monoclonal antibody as a capture antibody directed against botulinum toxin A. Following addition of the sample solution, an alkaline phosphatase conjugated secondary antibody was added as a primary detection antibody. A solution of the enzymatic substrate NADP+ was added to the plate and converted into to product NAD+ by the enzyme. Amplification was achieved by using an amplifier solution containing enzymes catalysing a cycle reaction, which allowed the formation of several hundred coloured molecules for each NAD+. By using such amplified ELISA the authors achieved a LOD of 66 pg/ml in about 5 hours and demonstrated the suitability of this assay as a means to detect BTX A in both botulinum culture and foodstuff. As a comparison standard (not amplified)

ELISA assay for botulinum toxin detections (described within the same study) resulted in a LOD 100 fold lower than the amplified method. Doellgast *et al*. (1993) reported the use of a primary detection antibody labelled with an enzyme obtained from the venom of Russel's viper. This initiated a complex cascade reaction, which lead to the formation of thrombin. Subsequent addition of alkaline phosphatase-fibrinogen determined the formation of alkaline phosphatase-fibrin. The latter, following incubation with the appropriate substrate for alkaline phosphatase, gave rise to the production of the coloured compound. Previous studies published by the same research group reporting the use of such amplified ELISA for the detection of other protein antigens revealed that this method allowed increases in sensitivity of 100-1,000 fold compared to non amplified ELISAs (Doellgast 1987). The high sensitivity of the method was confirmed for botulinum toxin antigens as it lead to a LOD of < 10pg/ml during a period of > 16 hours. Given the complexity of the method reported above, further efforts have been made to develop simpler tests. In a more recent report published by Sharma *et al.* (2006), a sensitive amplified ELISA was developed by using a primary detection antibody labelled with the steroid digoxigenin. Production of secondary antibodies with a high affinity to this molecule resulted in a LOD for the 500-kDa BTX A complex of 60 pg/ml within a period of 4 hours.

While sensitive and relatively rapid, not one of the *in vitro* assays reported in literature have currently been used to replace the mouse bioassay. The reason for that resides in different factors comprising the complexity of the method (e.g., the need to perform multiple amplification steps to increase the sensitivity of the assay), expense of the reagents, unwanted interactions of reagents of the assay with some components of the samples to be tested (e.g. antibodies produced in chicken cannot be used to detect BTXs in foodstuff such as chicken meat and yolk egg) and lack of validation for screening a large variety samples. In addition these tests do not assess the proteolytic activity of the toxin (capability of the toxins to cleave the proteins of the SNARE complex in the neuronal cells) but only the capability of the antibody to recognise the toxins. Although some assays determining the proteolytic activity have been published (i.e., endopeptidase assays as previously mentioned) their use for food testing has generally been limited due to interference by peptidases present in food specimens (Rasooly and Do 2008).

5.1.4 Quantification of BTX A contained in therapeutic preparations

While the majority of published works report detection of BTXs from foodstuff and botulinum strain cultures, only two studies have described detection of BTXs in therapeutic preparations (Ekong et al. 1995; Frevert 2010). Both studies selected ELISA as a suitable methodology. In particular Frevert (2010) determined the quantity of BTX A contained in the commercial preparations Botox®, Dysport® and Xeomin®. In this study primary detection antibodies were specifically raised against the 150 kDa BTX A (purified from *Clostridium botulinum* A culture) detoxified by treatment with formaldehyde, i.e. botulinum toxoid. Detection of BTX A contained within the three commercial preparations was performed by using a HRP-conjugated secondary antibody with a LOD of 0.2 ng/ml. Similarly, Ekong *et al* (1995) reported detection of BTX A in therapeutic preparations by using a primary monoclonal antibody specific for BTX A and a high titre HRP-conjugated antibody. The authors indicate a sensitivity of the test comparable to the mouse bioassay (LOD ~ 8-25 pg/ml)

5.1.5 Immunohistochemical techniques for the detection of BTX A

5.1.5.1 IHC principle

IHC is an immunoassay relying on the specific interaction between an antigen of interest and an antibody and subsequent determination of the distribution of the antigen in a particular tissue. IHC has been largely used for diagnostic purpose as a means to detect tumoral antigens specifically expressed or up-regulated in certain cancers (Jordan et al. 2002). It has also been used to evaluate the efficacy of new therapeutic molecules during drug development by assessing their capability to regulate the expression of disease targets (Dobson et al. 2010). During IHC analysis tissue samples are cut into sections, which are subsequently incubated with a specific antibody. Biopsies can be processed either as unfixed frozen or formalin fixed paraffin embedded tissue sections. While frozen sections guarantee the best antigen conservation, paraffin embedded sections are usually associated with a better

morphological preservation of the tissue (Beckstead 1994). However, the effect of fixation can be detrimental to the antigen-antibody interaction as the protein of interest can be masked due to the capability of the fixative to create cross-linkages between specific portions of the antigen (i.e. epitopes) and other proteins present in the sample. Epitopes on formalin fixed paraffin embedded sections are usually unmasked by heating in an appropriate buffer, a procedure known as antigen retrieval (Shi et al. 2011).

As for other immunoassays (such as the aforementioned ELISA) antigen-antibody interactions in IHC are identified by an appropriate detection system, which usually relies on the formation of an insoluble coloured product. Different detection systems are currently available with the two most commonly employed being represented by avidin–biotin and polymer-based systems. Avidin-biotin systems rely on the strong affinity of the protein avidin for the low molecular weight vitamin biotin. The bond between those two molecules is considered irreversible as the affinity between those two molecules is over million times stronger than that of most antigen antibody interactions (http://www.vectorlabs.com 2011). These systems consist of a three-step procedure in which the antigen of interest is recognised by a primary antibody (1^{st} step) to which a biotinylated secondary antibody is attached (2^{nd} step). An avidin-HRP (or AP) complex will bind the secondary antibody via avidin-biotin bonds to produce a coloured reaction (3^{rd} step). The signal can be amplified as avidin possesses four binding sites for biotin, thus several biotin-peroxidase complexes can be attached to each antigen molecule.

While sensitive these systems are usually associated with unspecific staining due to the presence of endogenous biotin in certain tissues specimens. The more recently developed polymer-based systems consist of a two-step procedure and are based on dextran technology (EnVision; Dako Corporation). In the first step the antigen of interest is recognised by a primary antibody. In the second step the primary antibody is attached by a dextran, which is conjugated to numerous secondary antibodies and enzyme molecules. These systems have the advantage of allowing an increased sensitivity in comparison to the biotin-avidin assays and are less time consuming. For this reason they will be employed in the experiments reported within this Chapter.

In a study conducted by Pacini *et al*. (2007), delivery of BTX A from the therapeutic BTX A preparation Vistabel® (commercialised as a Vistabex® in Italy, the country where the study was performed) was demonstrated *in vitro* by IHC. In this study

Vistabel® was delivered by iontophoresis in living rats. Skin specimens excised from the treated animals were assessed for BTX A presence by using a commercially available monoclonal antibody (against BTX A) and a biotin/avidin system detection kit. To the best of our knowledge this represents the only published study showing transdermal delivery of BTX A in a tissue and its detection by IHC. Triggered by these findings we selected IHC methodology to detect BT A within skin tissue.

5.1.6 Dot blot for the detection of BTX A

Dot blotting is a simple technique used to identify a protein from solutions without the need for protein separation by SDS PAGE. It is an immunoassay in which the protein of interest is immobilised on a protein binding membrane usually consisting of nitrocellulose or polyvinylidene fluoride. Once the protein is bound to the membrane, it can be probed by a primary antibody. As for the aforementioned immunoassays, detection of the antigen is obtained by addition of a secondary antibody labelled with a specific enzyme (i.e., HRP or AP). Substrates can be used to produce either colour (chromogenic detection method) that can be visualised on the membrane (to the naked eye) or light (chemiluminescent detection method) that is detected with radiography film. Dot blot will be employed in this Chapter as a preliminary detection method to assess the capability of the antibodies used in IHC techniques to detect BTX A onto a membrane.

5.1.7 Cutaneous delivery of fluorescent conjugated BT A by liquid loaded PMDs

Fluorescence imaging of BT A following its conjugation to a fluorophore, PE/Cy7®, will be performed in this Chapter in order to support detection of the toxoid in the skin by immunohistochemistry techniques. PE/Cy7® is a tandem conjugate with PE (the energy donor) having an excitation wavelength of 565 nm and Cy5 (the energy acceptor) having an emission wavelength of 778 nm. The compound will be employed in the experiments reported in this Chapter as part of a commercial kit conceived to label primary antibodies for further applications such as ELISA, Western Blot or IHC. However, as specified by the manufacture

(http://www.abcam.com 2011), the kit is suitable to tag any protein in solution as the the fluorophore binds free amine groups present in lysines and N-terminus of a protein. The presence of lysines in BTX A was confirmed by a study evaluating the amino acid composition of the neurotoxin (Sathyamoorthy and DasGupta 1985).

5.1.8 Specific aims and objectives of the Chapter

In this Chapter we aim to demonstrate successful delivery of BTX A (Vistabel®) and BT A to the dermal layer of human skin using liquid loaded PMDs.

The experimental objectives are to:

- Develop an IHC methodology to detect therapeutic BTX A (Vistabel®) delivered within the skin from intradermal (ID) injections and PMDs.
- Detect BTX A (Vistabel®) and BT A by dot blot immunoassay.
- Develop an IHC methodology to detect BT A delivered within the skin from ID injections and liquid loaded PMDs.
- Use fluorescence microscopy to assess delivery and distribution of PE/Cy7®-BT A into the skin by using liquid loaded PMDs.

5.2 Materials

5.2.1 Reagents

All reagents were used as received and were purchased from Sigma Aldrich Ltd (Poole UK), unless otherwise stated.

Deionised water was obtained from an Elga reservoir (High Wycombe, UK). OCT embedding media was purchased from RA Lamb Limited (Eastbourne, UK). Tris buffer (Tris (hydroxyethyl) methylamine), sodium chloride, Tris base (Tris (hydroxymethyl) aminomethane), Triton X-100, Tris HCl (Tris (hydoxymethyl) aminomethane hydrochloride), Whatman Protran® nitrocellulose transfer membrane, methylene blue, stabilized goat anti-mouse IgG, (H+L), peroxidase conjugated antibody (32430), Super Signal® West Pico Kit and formaldeyde solution 37% was purchased from Fisher Scientific (Loughborough, UK). Dako EnVision+ System-HRP (DAB) kit was purchased from Dako Ltd. (Cambridgeshire, UK). Mouse monoclonal anti *Clostridium botulinum* A toxoid primary antibody (ab40786) and antibody dilution buffer were purchased from AbCam (Cambridge, UK). Vistabel® was purchased from University of Wales Hospital (Cardiff, UK). Neurotoxin type A *Clostridium botulinum* toxoid (133A) and chicken anti *Clostridium botulinum* neurotoxin/toxoid type A IgY polyclonal primary antibody (730A) was purchased from List Biological Laboratories, Inc. (Campbell, California).

5.3 Methods

5.3.1 Cutaneous delivery of a BTX A commercial formulation (Vistabel®)

A vial of Vistabel® (BTX A, 2.5 ng) was dissolved in 0.9% saline solution to a concentration of 2.5 pg/µl. A skin tissue excised from a 34 year old donor on the day of the experiment (‘fresh’ skin sample) was prepared as previously described (Section 4.3.2). Subsequently, the tissue sample was processed as described for the following treatments:-

Treatment 1: four ID injections of Vistabel®, each one of 50 µl (125 pg/ID injection), were performed in the skin sample.

Treatment 2: 20 µl of the Vistabel® formulation was topically applied to three distinct sites (50 pg/site) on the skin surface. A PMD (n=3) was repeatedly inserted (10-20 times) onto each site where the solution was applied.

Treatment 3 (negative control): 50 µl of 0.9% saline solution was intradermally injected into the skin sample (negative control 1). In addition, a PMD was loaded with 0.9% saline solution (PMD loading was performed as described in Section 2.3.4) and inserted into the skin sample (negative control 2).

Treated regions of the skin were excised and the samples obtained were cultured for 1½ hours, as previously described (Section 4.3.3.1). Following incubation in organ culture, each tissue sample was washed in PBS for 15 minutes and subsequently frozen in OCT before being stored at -80°C (Section 4.3.3.3). Samples were subsequently cryosectioned using a cryomicrotome (CM3050S cryostat, Leica Microsystems, Milton Keynes, UK). Sections (10-12 µm) were collected on microscope slides (Superfrost Plus®) and analysed under light microscopy (Olympus BX50 light/fluorescent microscope, Watford, UK) to detect areas of microneedle/ID injection induced distruption.

Selected slides were fixed in acetone at – 20°C for 5 minutes and then rinsed thrice in PBS, once at 4°C for 5 minutes and then twice, 5 minutes each time, at room temperature, in order to allow the tissues to gradually equilibrate to the environmental temperature. Subsequently, the tissue sections were processed by IHC according to the methodology outlined below.

5.3.1.1 IHC methodology

IHC was performed by incubating selected tissue sections with a primary monoclonal antibody directed against botulinum toxoid A. Reagents, including the secondary antibodies which were purchased as parts of a commercial kit (Dako EnVision+ System-HRP kit), were used according to the supplier's recommended protocol and by washing the tissue samples between each step with the wash buffer (PBS or PBS Tween 0.025% v/v). The tissue samples to be stained were first incubated with Dual Endogenous Peroxidase Block (0.03% hydrogen peroxide containing sodium azide) for 5 minutes +/- 1 minute to quench endogenous peroxidases. Subsequently, they were incubated with anti botulinum toxoid A primary monoclonal antibody, diluted either 1/50 or 1/200 (stock concentration not determined by the manufacture) with a

commercial antibody dilution buffer. This latter consisted of 1% BSA in PBS pH 7.4 and 0.005% sodium azide as preservative. Incubation was performed for 60 minutes (+/- 1 minute) at room temperature in a humidified chamber in order to prevent drying of the tissues. Specimens were subsequently incubated with labelled polymer-HRP anti mouse reagent consisting of a HRP labelled polymer conjugated to goat anti-mouse secondary antibodies in Tris-HCl buffer (containing stabilising proteins and antimicrobic agents). Incubation with secondary antibody was performed for 30 minutes (+/- 1 minute) at room temperature in a humidified chamber. Staining was completed by incubation for 5-10 minutes with 3,3'-diaminobenzidine (DAB)+ substrate-chromogen. The skin specimens were washed with distilled water in order to stop the chromogenic reaction and they were subsequently allowed to dry.

After IHC staining, processed sections were visualised under light microscopy (Olympus BX50 light/fluorescent microscope) with representative images captured with a digital camera (Olympus DP 10). Selected representative slides were counterstained by quick immersion (approximately ten seconds) in Harris' Haematoxylin. All tissue sections were analysed by light microscopy at various magnifications. A microscope graticule was employed to determine the image scale.

5.3.2 Dot blot assay

5.3.2.1 Detection of α-tubulin by dot blot

Initial dot blot experiments were performed using the protein α-tubulin as a positive control. These experiments had the aim to assess the suitability of the dot blot methodology adopted to detect proteins. Dot blot was performed according to the protocol outlined by Qiagen (http://www.qiagen.com 2011).

Preparation of the samples solutions

A solution containing the protein α-tubulin was obtained by cell solubilisation techniques. A total protein concentration of 3 µg/µl was previously determined for this solution using the bicinchoninic acid (BCA) assay method (Walker 2002). Starting from this solution, two more diluted solutions were prepared in PBS, having a total protein concentration of 1.5 and 1 µg/µl. An aliquot (10 µl) of each solution was added to (5 µl) of denaturation buffer (8 M urea, 100 mM NaH_2PO_4, 100 mM

Tris-HCl, pH 8.0) to obtain a final α-tubulin concentration of respectively 2.4, 1.2 and 0.8 µg/µl. Denaturation buffer is usually employed in dot blot to increase epitope exposure of an antigen to the antibody and thus assist antigen-antibody interaction. In this experiment the protein of interest was tested under both native (N) and denaturing (D) conditions as the capability of the antibody to detect the antigen in either native or denaturing conditions had not been previously tested. Two solutions, constituted by only PBS and the denaturation buffer (10 µl of PBS plus 5 µl of denaturation buffer), were used as negative controls.

Dot blot procedure

One µl samples of each prepared solution were spotted in duplicate onto a nitrocellulose membrane. A pencil was used to indicate the application site of each sample solution on the membrane. The membrane was allowed to dry approximately 40 minutes and then stored overnight at 4 °C. The following day, dot blot was performed according to the protocol outlined by Qiagen. Briefly, the membrane was washed twice, ten minutes each time, in TBS buffer (i.e., Tris-buffered saline buffer consisting of 10 mM Tris-HCl and 150 mM NaCl, pH 7.5) before being incubated in freshly prepared blocking buffer (BSA 3% w/v in TBS buffer) for 1 hour to block unspecific binding by the antibodies. Subsequently, the membrane was washed twice, 10 minutes each time, in TBS-Tween/Triton buffer ((20 mM Tris-HCl, 500 mM NaCl, 0.05% (v/v) Tween 20, 0.2% (v/v) Triton X-100, pH 7.5)) before being incubated with a 1:1000 dilution of mouse monoclonal anti α-tubulin antibody (Sigma Aldrich, T9026, antibody stock concentration not determined by the supplier). The antibody was diluted using the same diluent used for IHC (containing 1% BSA in PBS pH 7.4 and 0.005% sodium azide). Incubation was performed for 1 hour. Subsequently, the membrane was washed twice in TBS-Tween/Triton buffer and then once in TBS buffer, 10 minutes each time, before being incubated for 1 hour with the same secondary antibody reagent ((supplied as one of the reagents of Dako EnVision+ System-HRP (DAB) kit)) used for IHC. The membrane was subsequently washed four times, 10 minutes each time, in TBS-Tween/Triton buffer. Staining was completed by incubation with DAB+ chromogen solution (as for IHC) for approximately 10-15 minutes.

All the steps described were performed at room temperature with the membrane placed onto an orbital shaker to ensure uniform coverage during incubation. When

incubation was performed for a longer period (i.e. 1 hour) the vessel (containing the membrane) was sealed with plastic film to prevent the membrane from drying out.
The chromogenic reaction was stopped by washing the membrane with deionised water. The membrane was subsequently allowed to dry before being imaged by a digital camera (Canon Digital Ixus 82 IS, Canon, Surrey, UK or ChemiDoc XRS + System, Bio-Rad Laboratories, Hemel Hempstead, UK) and then stored at 4 °C.
The same experiment was repeated. In this case α-tubulin standard solutions having a protein concentration ranging between 3 µg/µl and 1 pg/µl were employed with the aim to evaluate the limit of detection of the dot blot methodology for this protein. Eight α-tubulin standard solutions were prepared from a stock solution containing 3 µg/µl of total protein content. Starting from this solution, a more diluted solution (1 µg/µl) was prepared in PBS buffer. Six serial dilutions were then prepared (in PBS buffer), each solution having a concentration 10 times smaller than the previous. Denaturation buffer was not employed for this experiment.

5.3.2.2 Dot blot for BTX A (Vistabel®) detection

Preparation of BTX A samples

A vial of Vistabel® was dissolved in 200 µl of 0.9% saline solution to a BTX A concentration of 12.5 pg/µl. An aliquot (10 µl) of Vistabel® solution was mixed to denaturation buffer (5 µl) to a final BTX A concentration of ~8.3 pg/µl. One µl samples of Vistabel® formulation and Vistabel® in denaturating condition (i.e. Vistabel® added to denaturation buffer) were spotted in duplicate directly onto each of four nitrocellulose membranes. As a negative control, one µl samples constituted of 0.9% saline solution and denaturation buffer (10 µl of 0.9% saline solution + 5 µl of denaturation buffer) were spotted in duplicate, onto each of the four membranes. The membranes were allowed to dry for 40 minutes at room temperature. Once dried, each membrane was transferred into a plastic vessel and dot blot was performed as previously described. In particular the membranes were probed with the same primary antibody (directed against botulinum toxoid A) as for IHC with each membrane being incubated for 1 hour at room temperature with a different antibody titration (i.e. 1/50, 1/200, 1/1000, 1/2000).
The dot blot experiment for Vistabel® formulation was repeated using higher sample volumes (3 µl) of Vistabel® formulation (12.5 pg/µl) that were spotted onto the

membrane together with 1 µl samples. This was performed in order to increase the dose of BTX A loaded on the membrane. All the samples were spotted in duplicate under both denaturing and native conditions. Dot blot was performed as previously described except for the following modifications: i) the membrane was probed with the same primary antibody as above diluted 1/100; ii) a different secondary antibody (goat anti mouse HRP-conjugated antibody purchased from Fisher Scientific, stock concentration 10 µg/µl)) was used at a dilution of 1/100 in freshly prepared blocking buffer (BSA 3% (w/v) in TBS buffer).

5.3.2.3 Dot blot for detection of formaldehyde inactivated botulinum toxoid A (BT A)

A vial of formaldehyde inactivated botulinum toxoid A (BT A) containing 10 µg of BT A was reconstituted in 100 µl of nuclease free water, as recommended by the manufacturer. An aliquot of the solution obtained was used to prepare 5 more diluted standard solutions in nuclease-free water with a BT A concentration ranging from 100 ng/µl to 1 pg/µl. Each solution had a concentration ten times smaller than the previous one. An aliquot (9 µl) of BT A stock solution (100 ng/µl) was mixed to freshly prepared denaturation buffer (4 µl) to a final BT A concentration of ~ 64.3 ng/µl. From this solution five diluted standard solutions were prepared in nuclease free water to a final concentration of BT A equal to 6.43 pg/µl. Each solution was ten fold less concentrated than the previous one. One µl samples of each of the standard solutions prepared were applied in duplicate onto each one of two nitrocellulose membranes. In addition, one µl samples of PBS and PBS plus denaturation buffer were spotted in duplicate onto each membrane as negative controls as described previously.

The membranes were then allowed to dry for 40 minutes and stored at 4°C overnight. The following day, immunoassay was performed on the membranes as previously described with the following modifications: i) all the membranes were incubated with the same monoclonal antibody as for IHC, diluted 1/1000; ii) one membrane was incubated with the same secondary antibody used for IHC while the other membrane was incubated with stabilized goat anti mouse peroxidase conjugated secondary antibody (Fisher Scientific) at a dilution of 1/500.

Prolonged incubation time of BT A with a primary antibody

The experiment was repeated in order to assess the effect of a prolonged incubation time of BT A with the primary antibody. For this experiment two sample solutions one constituted by BT A 100 ng/µl in nuclease free water and one by BT A ~ 66.67 ng/µl in freshly prepared denaturation buffer were used. One µl samples of each solution were spotted in duplicate onto a membrane. Negative controls (consisting of nuclease free water and nuclease free water in denaturation buffer) were also applied in duplicate. Dot blot was performed as described above with the following modifications: i) incubation with the primary antibody was carried out overnight at 4°C; ii) goat anti mouse peroxidase conjugated secondary antibody (Fisher Scientific) was used as secondary antibody at a dilution of 1/500.

Using a different primary antibody against BT A

Dot blot experiments were furthermore repeated in order to evaluate the capability of a different primary antibody to react with BT A. Three µl samples of BT A solution (100 ng/µl) were applied onto each one of two membranes in duplicate. One µl samples of the same solution were singularly spotted onto each membrane. The membranes were allowed to dry for 40 minutes before dot blot was performed as described above with the following modifications: i) membranes were incubated overnight at 4°C with a chicken anti *Clostridium botulinum* neurotoxin/toxoid A polyclonal antibody (stock concentration: 1 mg/ml) at a dilution 1/1000 in freshly prepared blocking buffer (1% (w/v) milk powder/TBS buffer); ii) the membranes were subsequently incubated for 1 hour at room temperature with a rabbit anti chicken peroxidase antibody (purchased from Sigma Aldrich (A 9046), stock concentration: 5.9 mg/ml) at a dilution of 1/500.

5.3.3 Using IHC to detect BT A delivered into human skin by ID injections

Initial experiments were carried out by delivering the toxoid using an ID injection. Due to the higher loading capability of standard syringes compared to microneedles, delivery of the toxoid by ID injection was used as a positive control.

The experiment was performed on a freshly excised skin sample (aged 64 years old), which was prepared for the experiment as previously described (Section 4.3.2). The skin sample was treated as follows:-

Treatment 1: ten µl of BT A (100 ng/µl) was delivered into the skin by an ID injection.

Treatment 2: four ID injections of nuclease free water, each one of a volume of 10 µl, were performed in the same skin tissue (negative control).

Each treated skin area was excised from the samples and fixed by immersion into 10% neutral buffered formalin for 48 h. (+/-1 hour) at room temperature. Afterwards, each skin sample was rinsed twice in PBS for five minutes each time, before being dehydrated using an increasing gradient of ethanol. The dehydrating agents used and the different incubation times are outlined by Table 5.1.

Table 5.1: Composition of dehydrating agents, incubation times and temperatures employed to dehydrate skin samples.

		Volume %		
Step	**Dehydrating agent**	**Deionised H_20**	**Ethanol**	**Time (hour) and incubation temperature**
1	20% aqueous ethanol	80	20	1hour, room temperature
2	30% aqueous ethanol	70	30	1hour, room temperature
3	50% aqueous ethanol	50	50	1hour, room temperature
4	70% aqueous ethanol	30	70	1hour, room temperature
5	70% aqueous ethanol	30	70	Overnight, 4 °C
6	80% aqueous ethanol	20	80	2 changes x 2 hours (each one), room temperature
7	90% aqueous ethanol	10	90	2 changes x 2 hours (each one), room temperature
8	100% aqueous ethanol	-	100	Overnight, 4°C

The dehydrated samples were subsequently cleared by two immersions in chloroform-ethanol (50%-50% v/v) (for 1 hour each change). The samples were subsequently immersed in pure chloroform for 1 hour at room temperature. Dehydrated samples were incubated in two changes of molten paraffin (56°C) (2 hours each change) to allow infiltration of paraffin into the tissue. The tissues were then transferred into histological cassettes at -20°C to allow solidification of the paraffin. Histological sections of approximately 7 µm generated by using the Leica RM2125 RT microtome (Leica Microsystems, Milton Keynes, UK) were floated in water at 40°C and collected onto Superfrost® Plus microscope slides (Ng 2010).

Paraffin was removed from the sections by incubating thrice in fresh xylene (3 rinses in xylene, 3 minutes each one). The sections were subsequently rehydrated in an (v/v) ethanol gradient (i.e., 100%, 90%, 70%, 50%, 30%, 10% aqueous ethanol, 2 changes of 2 minutes each one, in the order listed) and kept hydrated in deionised water. Selected slides were processed by IHC. IHC protocol was carried out as described previously (Section 5.3.1.1). Skin sections were incubated with the same antibodies at the same dilutions and incubation times as for dot blot (Section 5.3.2.3). After IHC staining, sections were analysed by light microscopy as previously described (Section 5.3.1.1).

5.3.3.1 Reagent (antibody) controls

The following experiment was performed to confirm the specificity of the reagent involved in IHC assay and to assess the degree of non-specific background staining when the primary antibody was omitted.

Selected slides, containing tissue sections generated by treatment 1 and 2 were incubated with the only chromogenic substrate DAB+. In addition, slides were incubated with peroxidase block, primary antibody dilution buffer (blocking buffer), secondary antibody and DAB+ substrate. ICH protocol was performed as outlined above (Section 5.3.3).

5.3.3.2 Investigation of the effect of different primary antibody dilutions and primary antibody incubation conditions on the degree of nonspecific background staining

Two different incubation conditions (one hour at room temperature versus overnight at 4°C) and dilutions of primary antibody (1/1000 versus 1/5000) were compared in order to assess the degree of the effect of those two factors on the IHC background staining.

Selected slides, containing sections generated by treatment 1 and 2, were stained by IHC using the same protocol earlier described (Sections 5.3.1.1 and 5.3.3). Slides were incubated with anti *Clostridium botulinum* neurotoxin/toxoid A IgY polyclonal primary antibody diluted 1/1000 with commercial antibody dilution buffer either 1 hour at room temperature or 24 hours at 4°C in a humidified chamber. In addition, slides were incubated with the same primary antibody diluted 1/5000 (in the same dilution buffer) for 24 hours at 4°C in a humidified chamber. Once processed by IHC, the slides were analysed as previously described (Section 5.3.3).

5.3.3.3 Assessing the effect of different blocking buffers on the degree of nonspecific background staining

Different buffers used to dilute the primary antibody were compared in order to assess their effect on the presence of non specific background staining. The buffers were constituted by: i) milk powder 1% w/v in TBS; ii) commercial (AbCam) antibody dilution buffer (containing BSA 1%); iii) TBS buffer.

Selected slides were processed by the IHC methodology previously outlined (Section 5.3.3) with few modifications: for each experiment, slides containing skin sections generated by treatment 1 and 2 were incubated with the primary antibody overnight at 4°C in a humidified chamber. The antibody was diluted 1/000 respectively with each one of the three dilution buffer mentioned above. Once processed by IHC, the slides were analysed as previously described (Section 5.3.3).

5.3.4 Cutaneous delivery of BT A by PMDs

A PMD was liquid loaded, as previously described (Section 2.3.4), with a formaldehyde inactivated BT A solution (100 ng/µl). As a negative control, a PMD was likewise loaded with PBS. PMDs were inserted into a skin sample, excised from a 41 year old patient, defrosted on the day of the experiment and treated as previously described (Section 4.3.2). PMDs were held *in situ* for approximately 5 seconds and subsequently withdrawn. The PMD treated areas were then excised, mounted in OCT and stored at -80°C prior to cryosection, as indicated previously (Section 4.3.3.3). Transverse sections were analysed to detect areas of microneedle induced tissue disruption and were subsequently processed by IHC, in order to detect BTX A. IHC was performed as previously described (Section 5.3.1.1) except for the following modifications: i) sections were incubated for 1 hour at room temperature with the same primary polyclonal antibody anti BT A used for dot blot (Section 5.3.2.3) (anti botulinum toxin/toxoid type A chicken IgY). The primary antibody was diluted with freshly prepared blocking buffer containing BSA 1% w/v in PBS/Tween 20 0.05% v/v; ii) sections were subsequently incubated for 1 hour with the same secondary antibody used for dot blot (anti chicken IgY (IgG)-Peroxidase antibody). The secondary antibody was used at a dilution of 1/500 in freshly prepared blocking buffer containing BSA 3% w/v in PBS/Tween 20 0.05% v/v. After IHC, representative slides were counter stained with Harris' Haematoxylin and imaged with a digital camera (Olympus DP 10) as described previously (5.3.1.1).

5.3.4.1 Using a dye to facilitate visualisation of BT A delivered into the skin by PMDs

The experiment was performed with the aim to load a PMD with a BT A formulation containing a dye in order to facilitate visualization of BT A delivered into the skin. The experiment was performed on a skin sample freshly excised ('fresh' skin, Section 4.3.2) from a 65 year old donor. A PMD was loaded with a formulation consisting of BT A 50 ng/µl in methylene blue 1% w/v in PBS. The formulation (~ 2 µl) was withdrawn by a Gilson pipette before being loaded directly onto the needles. The PMD was inserted into a skin sample and manually held in position for approximately 5 seconds. After withdrawal of the PMD, the treated area was

removed and treated as described previously (Section 5.3.4). Transverse sections collected on microscope slides were analysed under light microscopy (Olympus, BX50) to detect sites of microneedles insertions indicated by the appearance of blue coloured areas in the skin. Selected slides were processed by IHC and analysed by light microscopy as previously described (Section 5.3.4).

5.3.4.2 Assessing the presence of false positive staining generated in the skin by PMD disruption

The experiment was performed in order to assess whether the disruption induced into the skin following PMD application caused retention of IHC reagents (i.e., antibodies and substrate) and thus false positive staining. The experiment was performed on 'frozen' skin tissue, defrosted on the day of the experiment (Section 4.3.2). The sample was excised from a 54 year old patient.

A PMD was loaded with a formulation consisting of methylene blue 1% w/v in PBS (negative control). Loading was performed as previously described (Section 2.3.4). The PMD was applied into the skin and the sample obtained was processed for IHC as outlined in Section 5.3.4.

5.3.5 Cutaneous delivery of fluorescent conjugated BT A by liquid loaded PMDs

BT A was fluorescently labelled with the compound PE/Cy7 by using the commercial conjugation kit EasyLink PE/Cy7® (3 x 10 µg PE/Cy7®). The kit consisted of the following reagents: i) EL-PE/Cy5 mix 100 µg; ii) EL-Modifier reagent; iii) EL-Quencher FD reagent.

The conjugation process was performed according to the protocol outlined by the manufacture (http://www.abcam.com 2011). Briefly, 1 µl of EL-Modifier reagent was mixed gently to 10 µl of BT A (100 ng/µl). Next, the screw cap was removed from the vial of EL-PE/Cy5 mix and the BT A solution (BT A 100 ng/µl with added EL-Modifier) was pipetted directly onto the lyophilised material. The compound was re-suspended gently by withdrawing and re-dispensing the liquid twice using a pipette. The cap was placed back on the vial and the solution was incubated

overnight at 4°C. After incubation, 1 µl of EL-Quencher FD reagent was added to the BT A solution and incubated for 30 minutes at room temperature prior to use. Subsequently, approximately 2 µl of the prepared solution were withdrawn by a pipette and dropped into the pockets of a PMD as described previously (Section 5.3.4.1).

The needles of a PMD were observed under light/fluorescent microscope (DM IRB, Leica Microsystems, Milton Keynes, UK) immediately and approximately 15 minutes after loading and imaged by a digital camera attached to the microscope (Retiga, Exi digital camera, QImaging, Surrey, Canada). Afterwards, the PMD was inserted into excised 'frozen' human skin (Section 4.3.2) (age 63 years old) and manually held in situ for 1 minute before being withdrawn. After being removed from the skin, the PMD was furthermore observed by fluorescent/light microscope in order to assess the release of the fluorescent coating from the pockets. An additional PMD was loaded with the same formulation and inserted immediately into the skin where it was manually held for approximately 5 seconds before being withdrawn. As a negative control, a PMD was loaded with PBS and inserted into the skin as described above. The PMDs treated areas were then excised, mounted in OCT and stored at -80°C prior to cryosection (Section 4.3.3.3). Transverse sections were analysed by light/fluorescence microscope to detect delivery of the fluorescent compound at the sites of microneedle induced disruptions. Representative images were captured by a digital camera.

5.4. Results and Discussion

5.4.1 Cutaneous delivery of BTX A (Vistabel®)

The Vistabel® formulation was delivered into excised human skin by intradermal injections and microneedle applications. Selected cryosections obtained from the skin samples were analysed by IHC to detect the protein BTX A. Figure 5.1 (A-G) depicts representative cryosections processed by IHC for the detection of BTX A. In particular, Figure 5.1 (A) depicts a skin disruption area, which was likely generated by microneedle insertion. No positive brown staining could be detected around this site, thus suggesting either unsuccessful BTX A detection or a failure to deliver the toxin.

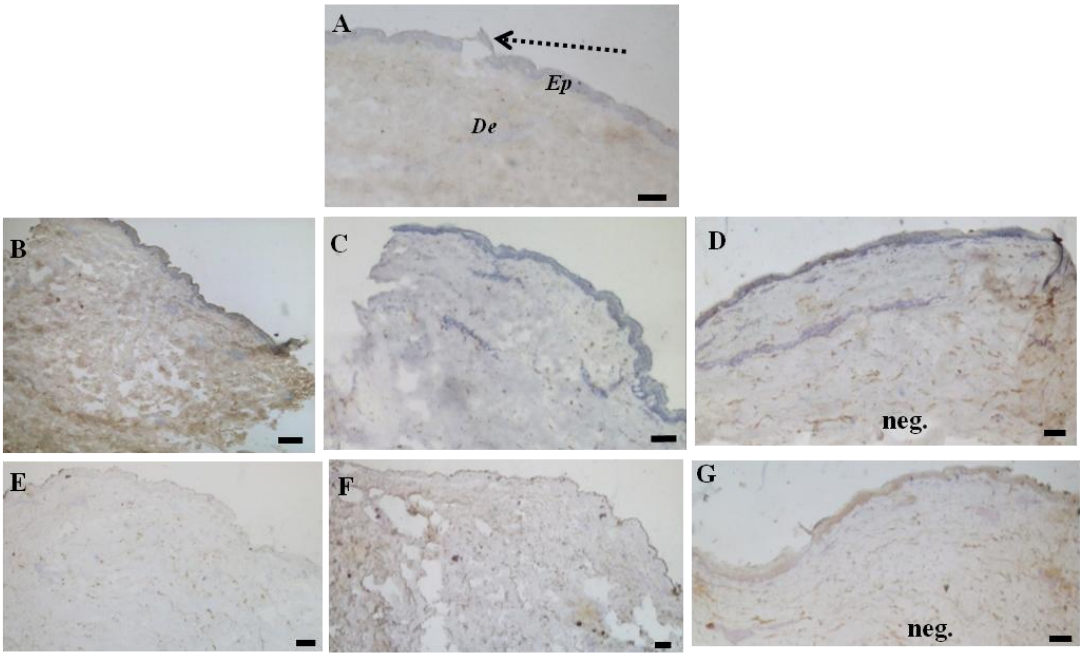

Figure 5.1 (A-G): Immunohistochemical analysis of the therapeutic BTX A formulation (Vistabel®) delivered into human skin by PMDs and ID injections. Representative haematoxylin counterstained histological cryosections of human skin treated with Vistabel® formulation (2.5 pg/µl) (A, B, C, E, F) or 0.9% saline solution (negative control) (D, G) and processed by IHC for BTX A detection. Vistabel® (50 µl) was injected intradermally (B, C, E, F) or applied topically (20 µl) on the top of the epidermis following multiple PMDs insertions (A). The pictures (B, C, E, F) depict images of various degree of staining which could be detected at different times showing lack of reproducibility. The arrow in (A) points to disruption sites in the skin generated by a PMD insertion. The absence of a brown area surrounding this site indicates lack of detection of BTX A (Vistabel®). Sections (A-D) were incubated with primary antibody titration: 1/50, Sections (E-G) with primary antibody titration 1/200. Scale bar = 100 µm. *Ep* = epidermis, *De* = dermis, neg.= negative control.

As described in the Material and Methods Section (5.3.1), PMDs were used in this experiment were repeatedly inserted into the skin surface within an area where a small volume (20 µl) of the Vistabel® formulation had been topically applied. This implies that even though microneedle application had facilitated transdermal delivery of BTX A, the volume of formulation and thus the dose of toxin delivered would have been extremely small. Increased volumes of Vistabel® were therefore injected by using a conventional needle and syringe in order to increase the mass of BTX A delivered into the skin and thus ease detection of the toxin by IHC. When skin samples in which Vistabel® was injected intradermally were analysed under the light

microscope, signs of penetration of the hypodermic needle could not be detected in the skin tissue. However, when the solution was injected into the tissue, a typical raised bleb was observed, indicating successful intradermal delivery of the injected fluid.

This therefore suggests that although the needle track could not be detected, the formulation was certainly delivered within the tissue. However, IHC stained cryosections did not provide conclusive results due to the inconsistency of staining between equally treated sections generated by the area of the tissue injected with the toxin (Figure 5.1 B, C, E and F). In particular, Figure 5.1 (B) showed lack of positive staining on the epidermis and a certain brown discoloration of the dermis. Although this discolouration might have been determined by a successful detection of BTX A in the dermis (BTX A was intradermally injected and thus most of the toxin would be expected to be delivered to the dermal region), this was considered unlikely, as the stain was not detected into other sections generated from the same skin sample and processed by the same IHC methodology (Figure 5.1 C). As a consequence, the brown discolouration observed (Figure 5.1 B) was considered to be most likely generated by unspecific background staining. This might have been determined by the poor quality of the cryosection, for example the presence of loose dermis, which may have resulted in excessive antibody/substrate retention or by an excessive antibody concentration (Ramos-Vara et al. 2008). A more diluted primary antibody (1/200 instead of 1/50) was thus tested. This resulted in a less intense stain (Figures 5.1 E and 5.1 F), thus suggesting that the staining depicted by Figure 5.1 B was likely due to an inappropriate primary antibody concentration. Primary antibody was initially used at a concentration of 1/50 as this was the titration indicated by the antibody's provider (AbCam) for immunofluorescence. As the antibody had never been used for IHC, this dilution was chosen as starting concentration for our initial experiments. The data strongly suggested that BTX A formulation Vistabel® could not successfully be detected into the skin tissues by ICH.

As previously mentioned (Section 5.1.4), only two studies regarding detection of BTX A in therapeutic formulations have been published (Ekong et al. 1995; Frevert 2010). These studies reported the use of highly sensitive ELISA methods and 'in house' produced antibodies to reach LODs in the lower nanograms or picograms range. Additionally, only one study reporting detection of a commercial BTX A preparation (Vistabel®) in human skin by IHC has been published (Pacini et al.

2007). In this study 40 U/ml of Vistabel® (corresponding to 2 ng/ml) was applied on living rat skin, which was subsequently treated by iontophoresis.

The authors indicated delivery of BTX A within the deep dermis. Detection of the toxin was achieved by using commercially available antibodies. In particular, the authors reported the use of a monoclonal antibody directed against BTX A, purchased from US Biological (Swampscott, Massachusetts) and a biotin/avidin system detection kit (Vectastain® ABC) purchased from Vector Laboratories (Burlingame, California). In our experiments, the same primary antibody used in the cited study could not be employed, as this was not available. In addition, a polymer-based system (EnVision; Dako Corporation) was used as this has been reported to be more sensitive than a biotin/avidin system.

Failure to detect BTX A in this series of investigations may have been caused by a number of different factors. The quantity of protein delivered into the skin may have been under the LOD for the IHC methodology employed (i.e. 125 picograms of BTX A was delivered for each ID injection). Another possible cause is that the antibody could not recognise the antigenic epitope on BTX A. The antibody used in our experiments was directed against a synthetic peptide analogue of a specific epitope contained in the carboxy-terminal region of BT A. As BTX A (Vistabel®) was delivered in the skin as a macromolecular complex (i.e., the 150 kDa holotoxin complexed with additional non toxic proteins with a resulting molecular weight of ~ 900 kDa), it may be that the antigenic epitope was masked by the presence of these additional proteins and thus not recognised by the antibody.

In addition, as described in the Material and Methods Section (5.3.1), the skin samples were incubated in organ culture for 1½ hours, after being treated with BTX A (Vistabel®). This was performed in order to assess the distribution of the toxin within the skin as it was previously described for the model protein β-gal (Section 4.3.3.1). When incubated, the protein would have diffused within the skin. This could have resulted in a reduced concentration of the toxin at the application site. In addition skin samples were not fixed in formalin (the fixative usually employed in IHC) due to the known masking effect of the fixation on the antigenic epitopes (Section 5.1.5.1). As a consequence, as IHC involved several washing steps, the protein could have been diluted in the unfixed tissue or even removed completely.

5.4.2 Dot blot immunoassay

5.4.2.1 Dot blot for α-tubulin immunodetection

Initial dot blot experiments were performed with an aim to assess the suitability of the dot blot methodology for protein detection. Lysate cell samples with an estimated total protein concentration ranging between 1 to 3 µg/µl were used for this purpose. Figure 5.2 shows the appearance of a nitrocellulose membrane loaded with 1 µl samples of the solubilised cell solutions and subsequently incubated with an anti α-tubulin antibody and a HRP-polymer conjugated secondary antibody. Positive immunodetection was indicated by the appearance of brown-coloured spots at the sites where the solutions were applied (indicated by a point and a circle in Figure 5.2). This was observed for samples tested under both native and denaturing conditions, thus indicating that the antigenic epitope in the protein α-tubulin was exposed to the antibody even when native conditions were employed. The absence of brown areas at the sites where the negative control solutions were applied confirmed the specificity of the assay.

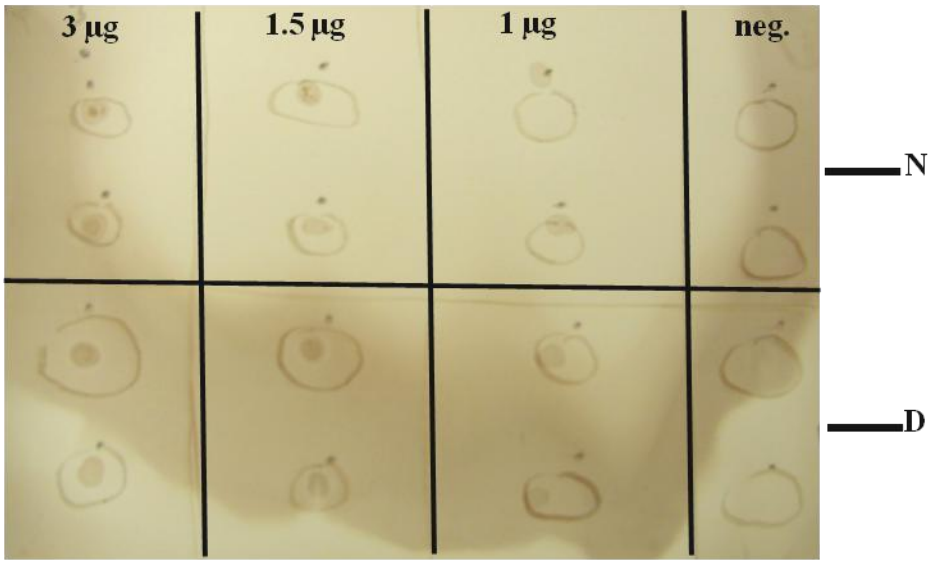

Figure 5.2: Micrograph of a nitrocellulose membrane loaded with α-tubulin and processed by dot blot for α-tubulin immunodetection. One µl samples of three standard solutions with a total protein concentration of 3, 1.5 and 1 µg/µl were loaded in duplicate onto the membrane. The presence of brown-coloured areas on the sites of the membrane where the solutions were applied (indicated by the circles and the points), reveals successful detection of α-tubulin. The intensity of the signal detected is proportional to the total protein concentrations. N=protein under native conditions, D=protein under denaturing conditions. neg.= negative control.

Dot blot experiments were repeated on α-tubulin standard solutions with a total protein concentration ranging between 3 µg/µl and 1 pg/µl (Figure 5.3). This was performed with the aim to investigate the limit of detection of this methodology. The results indicated that the lowest quantity of protein detectable was 10 ng.

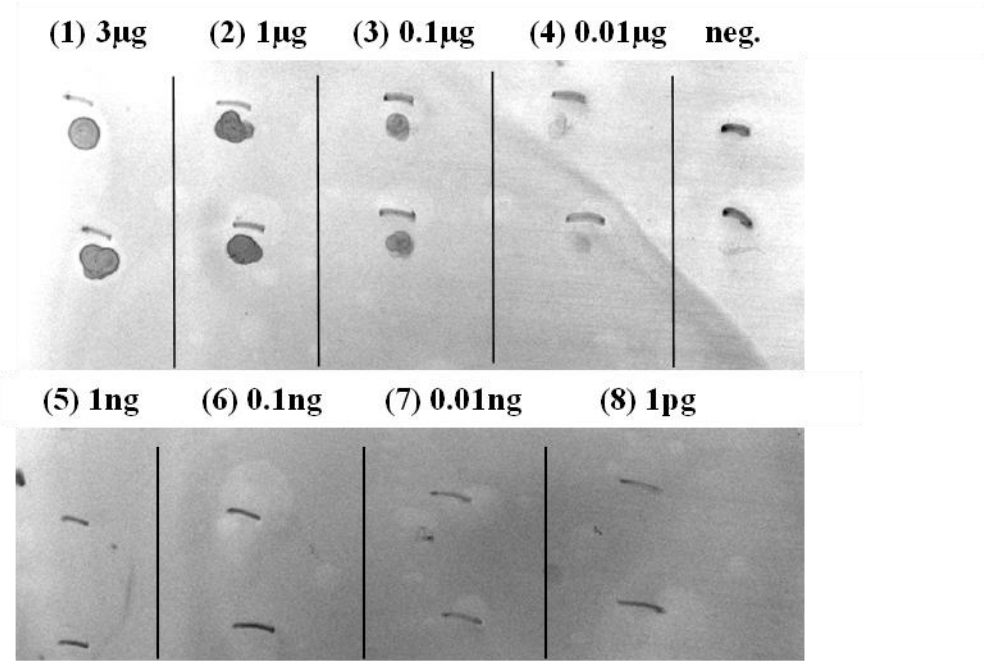

Figure 5.3: Dot blot for α-tubulin detection. Evaluation of the limit of detection. The images depict the appearance of a nitrocellulose membrane loaded with α-tubulin standard solutions and processed by dot blot. One µl samples of eight standard a-tubulin solutions with a total protein concentration ranging between 3 µg/µl (1) and 1 pg/µl (8) were applied in duplicate on the membrane. Marker lines indicate the areas where the solutions were spotted. Successful detection, revealed by the appearance of spots on the membrane, was observed for the first four standard solutions. Intensity of the signal detected appeared to be proportional to protein standard solutions, neg.= negative control.

However, as previously mentioned (Section 5.3.2.1), the concentration of the sample solutions tested was determined by using a spectrophotometric assay (the BCA assay) which measured the total protein content of the sample and not specifically the α-tubulin contained in it. This therefore implies that the actual mass of α-tubulin detected will have been less than 10 ng. However, the typical limit of detection of the dot blot methodology resides in the lower nanograms range when using chromogenic detection methods (as the one employed in our experiments) and therefore the method was considered appropriate. The sensitivity of the dot blot can also be dramatically increased by employing HRP-chemiluminescent substrates. By using these substrates LODs approaching the picograms or even the femtograms range can be achieved. However, as the aim of the experiments reported in this Chapter was the

detection of BTX A within the skin, such substrates were not employed as we did not possess suitable facilities to detect chemiluminescent signal within the skin tissue.

5.4.2.2 Dot blot for BTX A commercial formulation (Vistabel®) immonodetection

Figure 5.4 (A) depicts the appearance of a representative nitrocellulose membrane loaded by 1 µl samples of Vistabel® (12.5 pg/µl) and incubated with primary antibody against BT A (AbCam) used at a dilution of 1/2000. The experiment was also performed by simultaneously incubating three additional membranes with three more dilute concentrations of primary antibody (i.e. 1/50, 1/100 and 1/1000). None of the four dilutions used resulted in positive BTX A detection. The experiment was furthermore repeated using a different HRP conjugated secondary antibody (Figure 5.4 B) in order to investigate whether the failure in BTX A detection was due to the secondary antibody employed in the first experiment. In addition, increased volumes of Vistabel® solution (3 µl together with 1 µl samples) were loaded onto the membrane (Figure 5.4 B) in order to increase the amount of BTX A loaded (respectively 12.5 and 37.5 pg). No successful detection of the protein was observed.

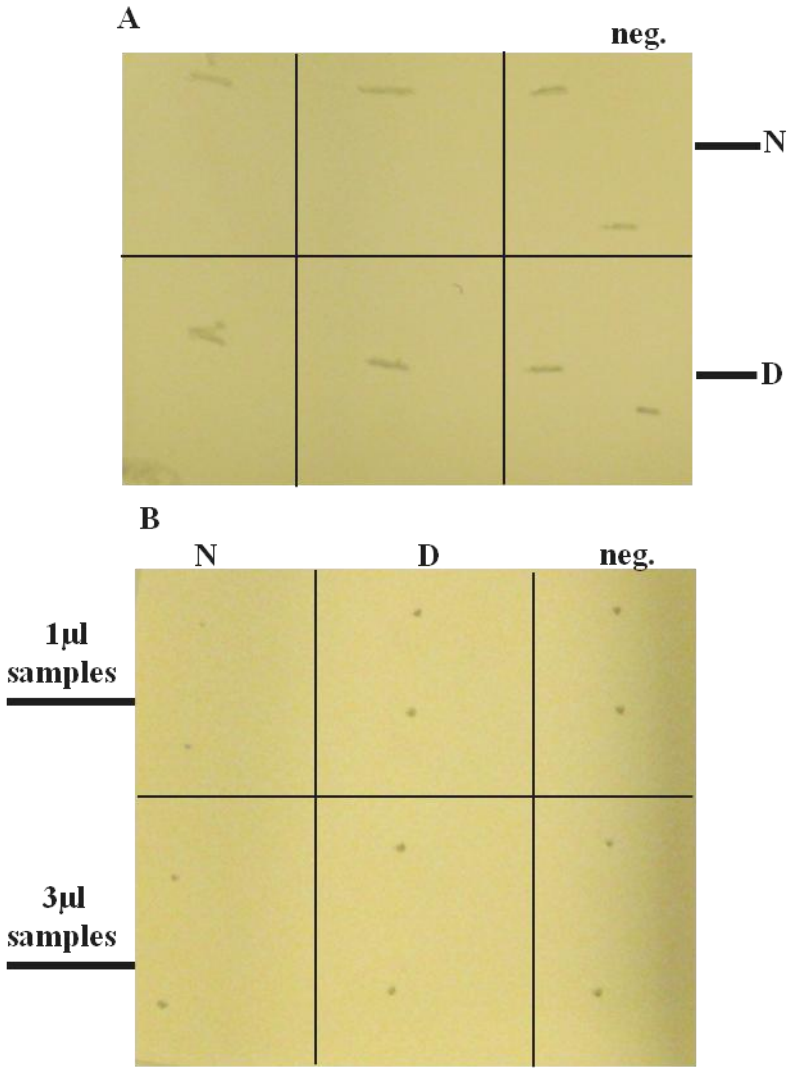

Figure 5.4 (A, B): Dot blot for BTX A (Vistabel®) detection. The images depict the appearance of two nitrocellulose membranes loaded with 1 (A) or 1 and 3 µl (B) samples of BTX A (Vistabel®, 12.5 pg/µl). Absence of brown areas at the sites where the solutions were applied (indicated by either a line or a point) shows lack of detection of BTX A. The same primary antibody (AbCam), directed against BT A, was used for (A) and (B). Two HRP-conjugated secondary antibodies purchased from two different suppliers (details in the text) were employed. N= protein under native conditions, D= protein under denaturing conditions, neg.= negative control.

The results confirmed that immunodetection of BTX A contained in the commercial preparation Vistabel® is not possible using the primary antibody employed in our experiments. This is most likely due to the constrained dose of BTX A protein loaded onto the membrane due to the low dose of BTX A in Vistabel® and explains the lack

of detection of BTX A (Vistabel®) in the skin during the previous IHC experiment (Section 5.4.1).

5.4.2.3 Dot blot for immunodetection of botulinum toxoid A (BT A)

Due to the extremely small dose of BTX A contained in the commercial formulation Vistabel® (BTX A 2.5 ng), subsequent experiments were performed using an inactivated form of the toxin (i.e. formaldehyde inactivated botulinum toxoid A (BT A)), which could be obtained commercially and used at increased doses without posing safety concerns.

Initial dot blot experiments were performed by employing a dose of BT A ranging between 100 ng and 1 pg and incubating the membrane with the same primary antibody used for the previous experiments. The results (Figure 5.5 A) indicated failure in BT A detection as no positive signal could be reported on the membrane where the sample solutions were spotted. The same was observed when the membrane was incubated for a longer period of time with the primary antibody (i.e., overnight at 4°C compared to 1 hour at room temperature) (Figure 5.5 B).

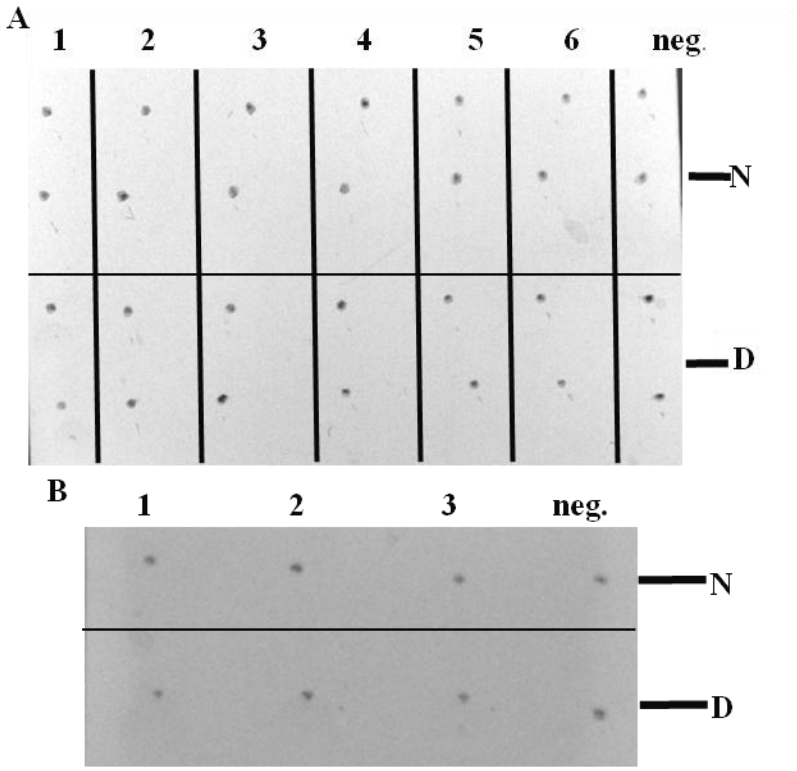

Figure 5.5 (A, B): Dot blot for botulinum toxoid A (BT A) detection: use of a primary antibody purchased from AbCam. The images depict the appearance of two nitrocellulose membranes loaded with 1 µl samples of differently concentrated BT A solutions and processed by dot blot for BT A immunodetection. BT A standard solutions ranging between 100 ng/µl (1) to 1 pg/µl (6) were used for the first membrane (A). BT A stock solution (100 ng/µl) was loaded in triplicate on the second membrane (B). Both membranes were incubated with a primary antibody (AbCam) diluted 1/1000 respectively 1 hour at room temperature (A) and overnight at 4°C (B). The absence of stained areas located where the samples solutions were applied (indicated by the points) revealed failure in protein detection. N = protein under native conditions, D = protein under denaturing conditions, neg.= negative control.

As doses equal to 100 ng were tested in these experiments, absence of detection was not expected to be caused by a lack of sensitivity of the assay, but most likely by absence of interaction between the protein and the antibody. The primary antibody used in our experiments was purchased by AbCam. As specified by the manufacturer, this antibody was raised against a synthetic peptide analogue of the carboxy-terminal region (heavy chain) of BT A. As BT A used in our experiments was produced by a different supplier (List Biological Laboratories), the lack of

interaction may be explained by the conditions adopted during the detoxification process of the toxin. The immunogenicity of the toxin is usually retained after the deactivation process. However, some studies have reported a certain variation of antigenic structure and thus the immunogenicity of commercially available toxoids can differ depending on the severity of formaldehyde reaction conditions (i.e. formaldehyde concentration/time of exposure) (Grate 2010; Keller 2008). As a consequence, the epitope, which should have specifically been recognised by the primary antibody, may have been chemically altered during the detoxification process, causing the absence of antigen-antibody interaction. Driven by this consideration, dot blot experiments were subsequently performed by using a primary antibody produced by List Biological Laboratories. This antibody was specifically raised against the binding domain (heavy chain) of BT A used in our experiments. By using this antibody a positive BT A detection was achieved (Figure 5.6).

Detection was observed for membranes loaded with 1 and 3 µl samples of BT A 100 ng/µl (thus corresponding to a dose of BT A equal to 100 and 300 ng). However, for the 3 µl samples, a weaker signal was detected, probably due to greater diffusion of the solution applied. This would have resulted in subsequent dilution of BTA concentration and thus reduction of the staining intensity. Immunoassay of solutions not containing any BT A (negative control) resulted in a complete absence of signal confirming the specificity of the assay.

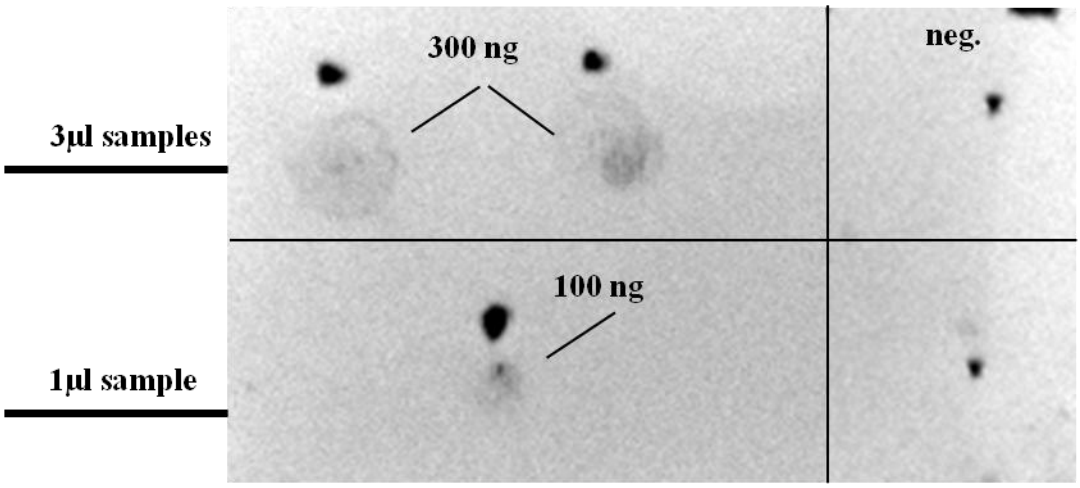

Figure 5.6: Dot blot for botulinum toxoid A (BT A) detection: use of a primary antibody purchased from List Biological Laboratories. The images depict the appearance of a nitrocellulose membrane loaded with 1 and 3 µl samples of BT A solution (100 ng/µl) and processed by dot blot for BT A immunodetection. The presence of stained areas located where the samples solutions were applied revealed successful detection of the protein.

5.4.3 Cutaneous delivery of botulinum toxoid A (BT A) by intradermal (ID) injections

Driven by the successful immunodetection of BT A previously achieved, IHC was used to detect BT A delivered into the skin by ID injections. As previously reported for Vistabel® delivery (Section 5.4.1), the toxoid was injected by using a conventional needle and syringe in order to increase the dose of BT A delivered. Figure 5.7 (A-H) show representative formalin fixed paraffin embedded sections of a human skin sample intradermally injected with BT A (A, B, E and F). The images depict brown staining localised in the epidermis. No trace of brown staining could be detected at a dermal level. However, it was expected to be stained as BT A formulation was injected intradermally. Although the intensity of the staining seemed to be higher for skin intradermally injected by BT A (A, B, E, F), a certain background level of brown discoloration was also detected for the negative control sections (C, D, G, H). The possible causes of the unspecific background staining include i) the concentration of primary antibody, ii) the incubation time with the primary antibody, iii) the poor specificity of IHC assay reagents and, iv) blocking

buffers used. Each of these factors was therefore investigated during the experiments described by the following Sections.

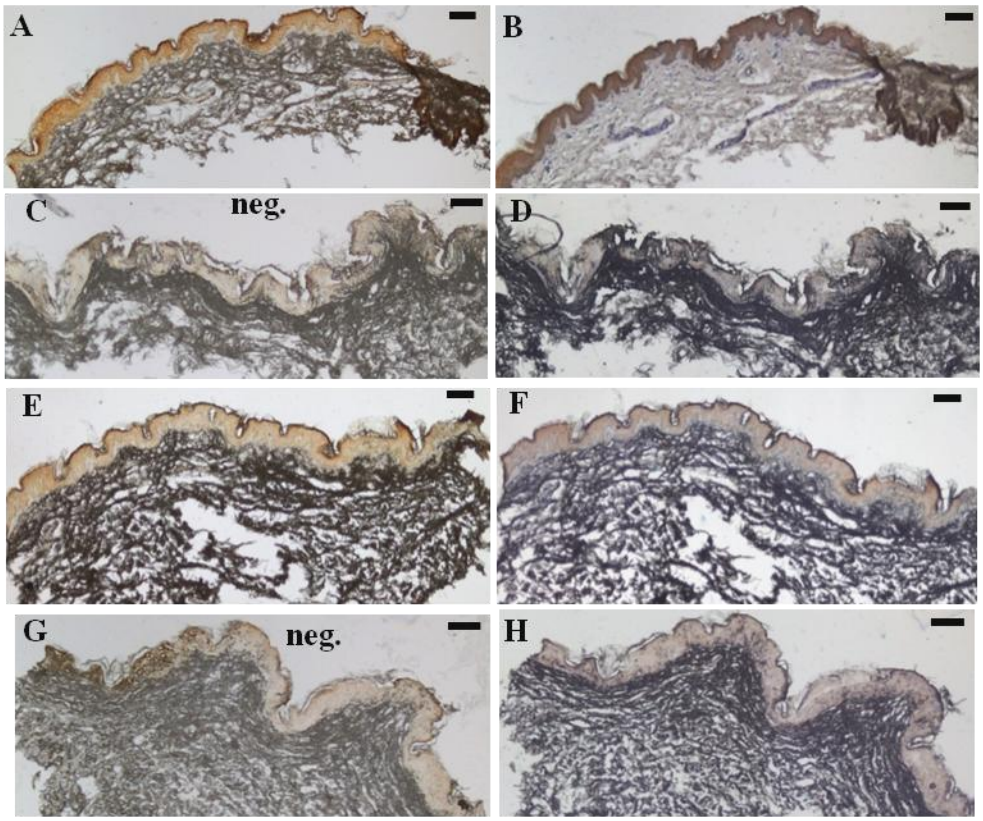

Figure 5.7 (A-H): **Immunohistochemical analysis of botulinum toxoid A (BT A) delivered into human skin by ID injections** Representative formalin fixed paraffin embedded sections of human skin intradermally injected with 10 µl of BT A solution (100 ng/µl) (A, B, E, F) and nuclease free water (negative control) (C, D, G, H) and processed by IHC for BT A detection. The sections were imaged before (A, C, E, G) and after (B, D, F, H) counterstaining with haematoxylin. Scale bar: 100 µm, neg.= negative control.

5.4.3.1 Investigating the effect of reagents (non-primary antibody) on the degree of nonspecific background staining

The experiment was performed in order to assess the specificity of the reagents of the IHC methodology and the presence of non-specific background staining when omitting primary antibody. IHC analysis was performed by incubating selected slides with either the substrate only, DAB+ (Figure 5.8 A, B, E, F), or with peroxidise block, primary antibody dilution buffer, secondary antibody and DAB+ (Figure 5.8

C, D). The absence of any significant background staining confirmed the specificity of the assay. In addition, the lack of staining reported for samples for which peroxidise blocking was not performed (A, B, E, F) indicated that the activity of any endogenous peroxidases in the skin tissue was negligible.

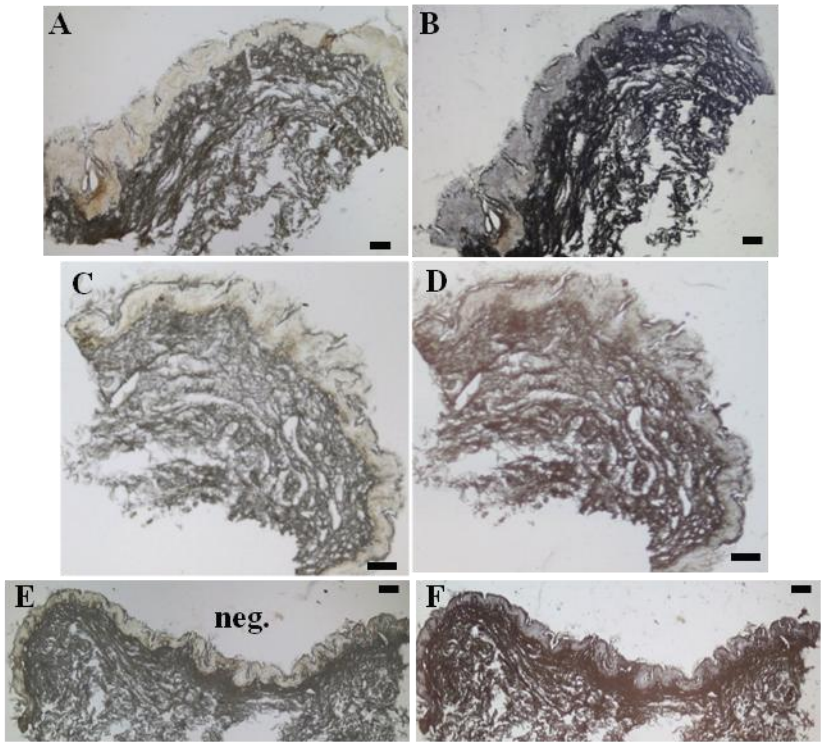

Figure 5.8 (A-F): Immunohistochemical analysis of botulinum toxoid A (BT A) delivered into human skin: reagent (primary antibody) control. Representative formalin fixed paraffin embedded sections of human skin intradermally injected with 10 µl of BT A solution (100 ng/µl) (A-D) and nuclease free water (negative control) (E, F) and processed for reagent (antibody) control. Sections were incubated with either the only chromogenic substrate (DAB+) (A, B, E, F) or with peroxidise block, primary antibody dilution buffer, secondary antibody and DAB+ (C, D). The sections were imaged before (A, C, E) and after (B, D, F) counterstaining with haematoxylin. Scale bar: 100 µm. neg.= negative control.

5.4.3.2 Investigating the effect of primary antibody dilutions and primary antibody incubation conditions on the degree of nonspecific background staining

IHC was performed on selected slides by comparing two different primary antibody incubation times (1 hour at room temperature versus overnight at 4°C) and two different primary antibody dilutions (1/1000 versus 1/5000). Figure 5.9 (A-F) depicts haematoxylin counterstained sections generated from a skin sample intradermally injected by BT A (Figure 5.9 A, C and E) or nuclease free water (negative control) (Figure 5.9 B, D and F). Sections were incubated for 1 hour (Figure 5.9 A, B) or

overnight (Figure 5.9 C, D) with primary antibody diluted 1/1000 with a commercial antibody dilution buffer. A slightly more intense staining was detected for longer incubation times of the primary antibody (Figure 5.9 C, D) as would be expected. In particular, skin specimens generated from the negative control (Figure 5.9 D) appeared more intensely stained than samples injected by BT A solution (Figure 5.9 C). Figure 5.9 (E, F) depicts the appearance of cryosections incubated overnight with a more diluted primary antibody (1/5000). No excessive background staining was detected for these sections (Figure 5.9 E, F) probably due to the higher dilution of the primary antibody used. The results obtained by this experiment showed that different antibody concentrations and incubation times did not result in significant variation in background staining. However, they indicated that the data previously reported related to the delivery of BT A by ID injections (Section 5.4.3) were not reproducible as no positive BT A detection was obtained for any of the processed sections.

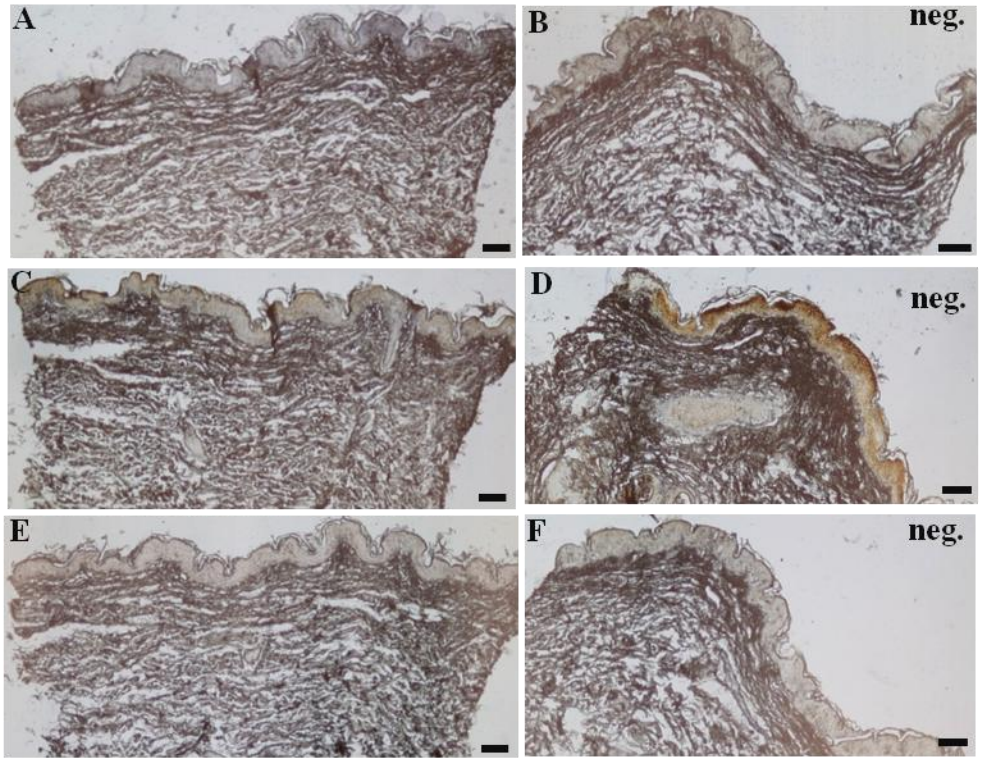

Figure 5.9 (A-F): Immunohistochemical analysis of botulinum toxoid A (BT A) delivered into human skin: evaluation of different primary antibody dilutions and incubation times. Representative formalin fixed paraffin embedded sections generated from human skin intradermally injected with 10 µl of BT A solution (100 ng/µl) (A, C, E) and nuclease free water (negative control) (B, D, F) and processed by IHC for BT A detection. Sections were counterstained with haematoxylin. Primary antibody was diluted 1/1000 (A-D) and 1/5000 (E, F). Sections were incubated 1 hour at room temperature (A, B) or overnight at 4°C (C-F). Scale bar: 100 µm, neg.= negative control.

5.4.3.3 Assessing the effect of different blocking buffers on the degree of nonspecific background staining

The presence of background staining in IHC can often be caused by non-specific interaction between the antibodies and sites on non-specific proteins (‘active sites’) that are similar to the epitopes on the target antigens. For these reasons, samples are incubated with specific blocking buffers. By definition, blocking buffers, so called as they block unspecific sites to which antibodies could otherwise bind, are used to improve the sensitivity of the assay by reducing background interference (http://www.piercenet.com). Blocking buffers commonly used are normal serum,

non-fat dry milk and BSA. The efficiency of a specific blocking buffer cannot be predicted for all IHC experiments. Experimental testing is essential to achieve the best results for specific antigen and antibodies. For this reason IHC analysis was repeated in order to compare the effectiveness of two different blocking buffers (the commercial antibody dilution buffer (AbCam) and non fat dry milk 1% w/v/TBS buffer) with a non-blocking buffer (TBS). The results show (Figure 5.10 A-N) that reduced background staining, indicated by complete absence of brown discolouration on the negative control sections, was obtained when dry milk 1% w/v/TBS was used (A-D). This blocking buffer was used in the previous IHC assays, and therefore the presence of certain background interference in the negative control sections (Section 5.4.3) remained unexplained.

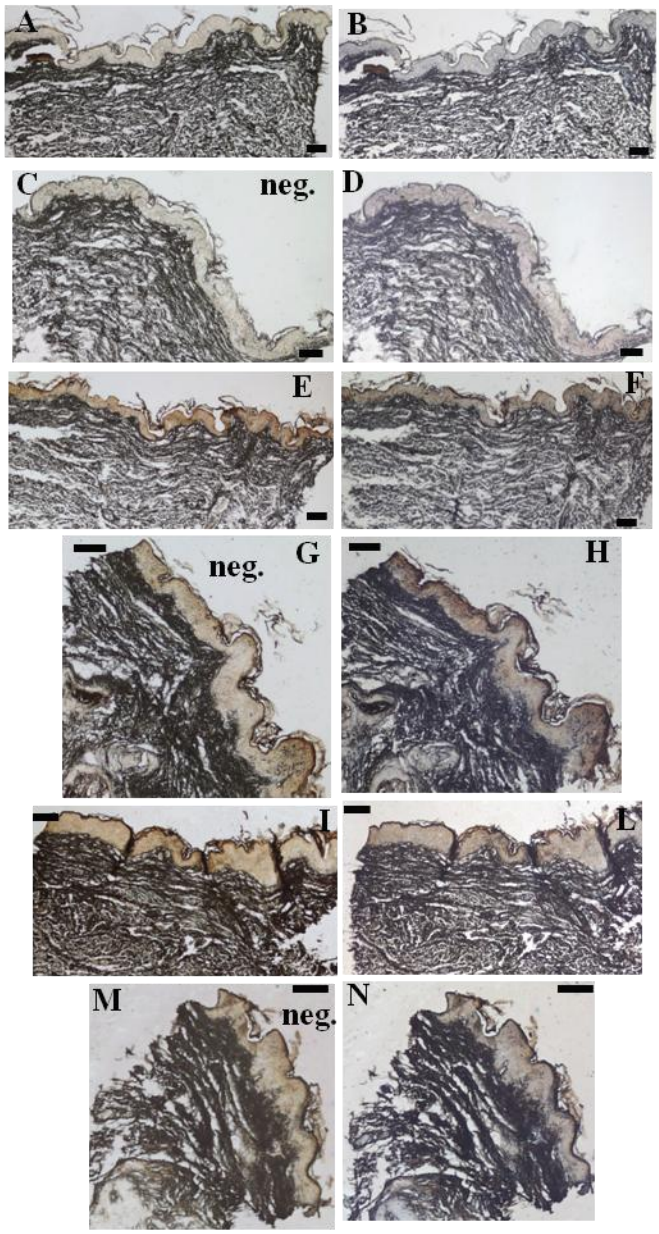

Figure 5.10 (A-N): Immunohistochemical analysis of botulinum toxid A (BT A) delivered into human skin: evaluation of different antibodies dilution buffers. Representative formalin fixed paraffin embedded sections of human skin intradermally injected with 10 µl of BT A solution (100 ng/µl) (A, B, E, F, I, L) and nuclease free water (negative control) (C, D, G, H, M, N) and processed by IHC for BT A detection. Sections were imaged before (A, C, E, G, I, M) and after haematoxylin counterstaining (B, D, F, H, L, N). The following buffers were used to dilute 1/1000 the primary antibody: i) non fat milk 1% (w/v) /TBS (A-D), ii) a commercial buffer (AbCam) containing BSA 1% (w/v) in TBS (E-H), iii) TBS (I-N).

5.4.4 Cutaneous delivery of botulinum toxoid A (BT A) by liquid loaded PMDs

IHC analysis of skin samples treated with BT A loaded PMDs suggested successful delivery of the protein by the microneedle. This was indicated by the appearance of brown staining areas specifically located at the penetration sites (Figure 5.11 A, B). No background staining was reported in non BT A treated skin (negative control) (Figure 5.11 C). This suggested that IHC methodology used was suited to selectively detect the target antigen. As previously mentioned, initial experiments were conducted by delivering BT A by conventional ID injection (Section 5.4.3). Conventional needle and syringe enable delivery of higher volumes compared to PMDs. Therefore, it was hypothesised that delivery of BT A by ID injections would have resulted in a larger area of staining and a means to ensure intradermal delivery of a dose. However, this was not indicated by the experiments previously reported. Conversely, a more intense and localised staining was reported here for PMD-mediated delivery. It may be hypothesised that due to the greater volume injected by ID injections, a more diluted BT A formulation was delivered in the tissue thus resulting in a weaker staining. In addition due to the pressure applied during ID injections, BT A would have diffused extensively within the tissue, this contributing to the reduced intensity of the staining. Moreover, as described in the Material and Methods Section (5.3.4), the skin tissue processed by IHC in this experiment was snap frozen immediately after application of the BT A loaded-PMD and subsequently cryosectioned. Conversely, for the experiment reported in Section 5.4.3, the tissue was fixed in formalin and then processed in paraffin-embedded sections (Section 5.3.3). This process involves a large number of washing steps and exposure of the skin sample to different solvents (i.e., ethanol and chloroform) and relatively high temperatures (i.e., equal or higher than 60°C). As a consequence, it may be that the brown staining observed in the epidermis of the skin sections was caused by alteration of the skin structure, which resulted in retention of one or more IHC reagents during the incubation steps.

As mentioned above, in the experiment reported within the present Section the skin samples was not fixed in formalin, while the ones reported in the previous Section (5.4.3) were. Due to the known masking effect of this fixative on the antigens, it may be hypothesised that the lack of fixation of the tissue facilitated detection of BT A.

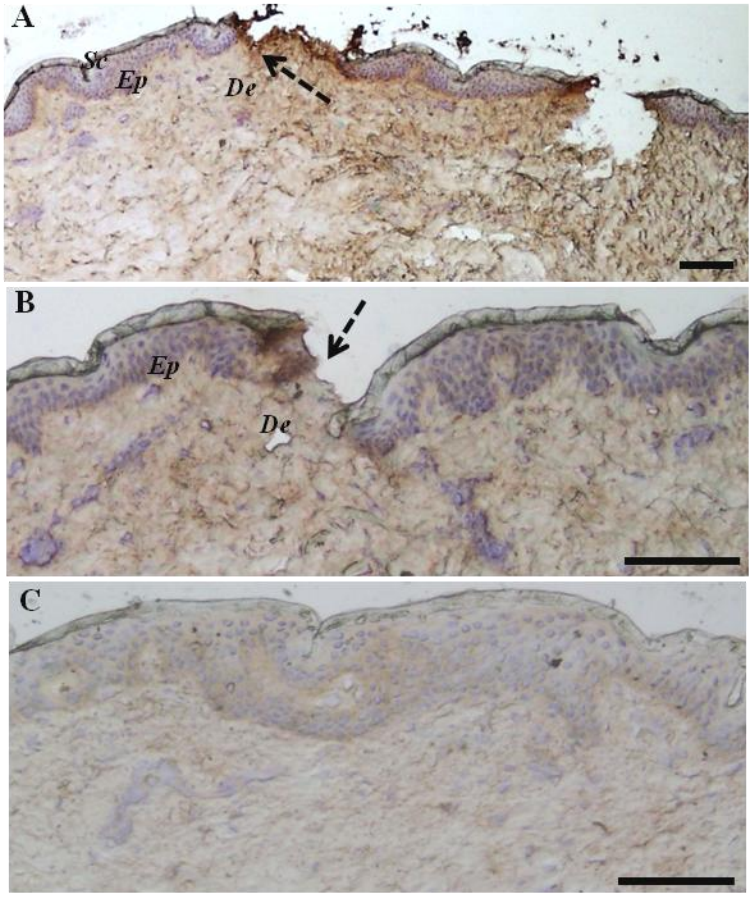

Figure 5.11 (A-C): Delivery of BT A within human skin by liquid loaded PMDs. Haematoxylin counterstained histological cryosections of human skin inserted with BT A (A, B) and PBS (C) (negative control) liquid loaded PMDs and processed by IHC for BT A detection. The arrows point to disruption sites in the skin. The presence of a brown area surrounding those sites suggests a successful delivery of BT A into the epidermal and dermal layers of the skin. Scale bar = 100 µm. *Sc* = stratum corneum, *Ep* = epidermis, *De* = dermis

5.4.4.1 Using a dye to facilitate visualisation of botulinum toxoid A (BT A) delivered into the skin by PMDs

In order to support detection of BT A in the skin by IHC, PMDs were loaded with a BT A formulation containing a dye (methylene blue) to enable visualisation of microneedle penetration within the tissue. PMD delivery of the formulation into skin was confirmed by the presence of blue stained areas at the microneedle disruption sites (Figure 5.12 A, C). IHC analysis failed to detect BT A (Figure 5.12 B), as brown stained areas could not be observed, as expected, at those specific sites. The

blue areas detected disappeared after IHC staining, thus indicating that the dye was washed away when the tissue sections were processed. The results highlighted by this experiment did not confirm what previously indicated (Section 5.4.4) (i.e., successful detection of BT A, delivered by a PMD, by IHC).

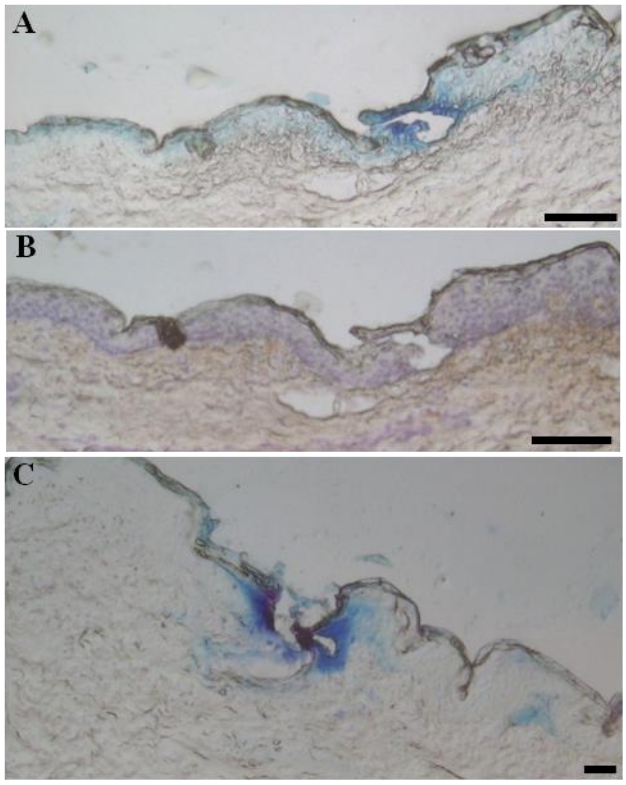

Figure 5.12 (A-C): Using a dye to facilitate visualisation of BT A delivered into the skin by PMDs. Representative hystological cryosections of human skin inserted with BT A/methylene blue liquid loaded PMDs. The sections were imaged before (A, C) and after (B) being processed by IHC for BT A detection. The appearance of diffused blue stained areas at the microneedles insertion points indicates successfully delivery of the BT A solution. The absence of brown stained areas after IHC (B) indicates lack of detection of BT A. Scale bar: 100 μm.

However, in this experiment, a 50% less concentrated BT A loading formulation was used for PMD loading, as BT A formulation was mixed at a 50-50% v/v ratio with methylene blue solution. As a consequence, the dose of BT A loaded on the PMD and thus delivered into the skin may have been too small to be detected. Moreover, the presence of the dye may have affected the immunogenic detection of BT A by the

primary antibody. Chemical or electrostatic interactions between the protein and the dye could be hypothesised due to the hydrophilic nature of both compounds.

5.4.4.2 Assessing the presence of false positive staining generated in the skin by PMD disruption

In order to confirm that skin disruption generated by PMDs insertion did not result in excessive antibody/substrate retention and thus false positive staining, sections generated by skin samples treated with methylene blue liquid loaded PMDs (negative control) were processed by IHC methodology. Figure 5.13 (A, B) depicts the appearance of a microneedle channel before (A) and after IHC staining (B). The absence of brown colouration around the microneedles insertion site, confirmed that disruption of the skin did not result in reagents retaining and thus false positive brown staining. This suggests that the presence of darkened area surrounding the microchannels depicted previously (Section 5.4.4) was generated by the delivery of BT A more that an artefact of the IHC staining.

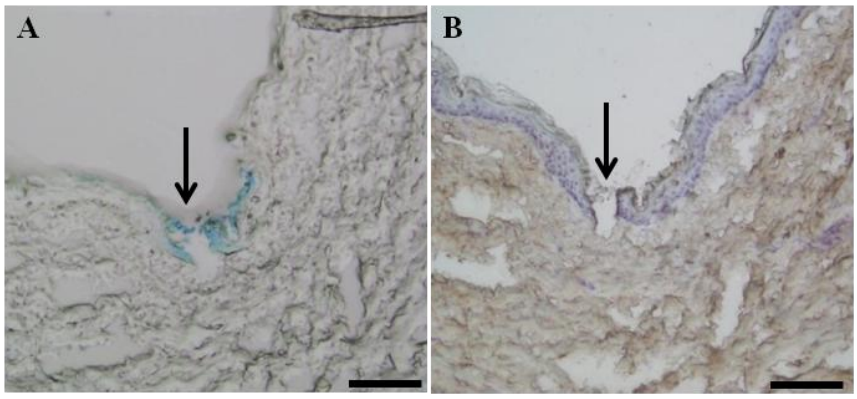

Figure 5.13 (A, B): **Assessing the presence of false positive staining generated in the skin by PMD disruption.** Representative hystological cryosections of human skin inserted with PMDs liquid loaded with methylene blue (negative control). Sections were imaged before (A) and after (B) IHC staining for BT A detection. The sections were subsequently counterstained with haematoxylin. Distinct microneedles channels could be detected (as indicated by the arrow). The absence of brown staining (B) at the microneedles insertion site indicates that skin disruption does not result in reagents retention and false positive staining. Scale bar: 100 μm.

5.4.5 Cutaneous delivery of fluorescent tagged botulinum toxoid A (BT A) by liquid loaded PMDs

BT A detection in the skin by IHC techniques was not as robust as hoped and therefore it was supported by fluorescence imaging of BT A following its conjugation to a fluorophore, PE/Cy7®.

Figure 5.14 (A-I) depicts brightfield (A, C) and fluorescent (B, D) micrographs of a single pocketed microneedle loaded with fluorescent BT A before (A, B) and after (C, D) being inserted into human skin. The absence of any fluorescence in the pocket after application of the PMD into the skin, suggests successful BT A release from the PMD. The fluorescent loading depicted by the micrographs (B) was likely to be a dried film as the image was captured approximately 10 minutes after PMD loading. When the PMD was observed straight away after being immersed into the formulation, the fluorescence signal detected was considerably less intense than the depicted image. In particular the pocket appeared devoid of formulation. Following approximately 10 minutes, a pink film visible to the naked eye, could be detected on the pockets of the microneedles. When analysed under the fluorescence microscope the entire microneedles (pocket plus shaft) appeared completely fluorescent (B). This indicates that the aqueous component of the formulation may have evaporated, thus concentrating the fluorescent toxoid and generating a stronger signal. Cutaneous delivery of BT A was confirmed by histological analysis. Figure 5.14 (E-G) depicts successful deposition of fluorescent BT A into the skin surrounding microneedle disruption sites at both epidermal and dermal level. The images illustrated were generated from a skin sample that was treated by a PMD loaded just before being inserted into the tissue and BT A was therefore assumed to be delivered into this sample as a liquid. Figure 5.14 (H, I) depicts the appearance of cryosections generated by a skin sample treated with the (presumably) dry coted PMD. The intensity of the signal detected appeared weaker compared to the other sections, thus suggesting that a higher dose of BT A was delivered in a liquid form. This may have been a result of incomplete release of the dry coating from the microneedles during their insertion into the skin. As depicted by Figure 5.14 (D), the microneedle pocket appeared devoid of fluorescent coating following application into the skin. However, fluorescence was detected on the microneedle shaft. This suggests that some BT A may be retained at this level and thus not delivered to the skin. However, direct

comparisons cannot be made as the liquid loaded PMD was not imaged after application into the skin. This would have provided an indication of the efficiency of delivery of the liquid formulation from the PMDs.

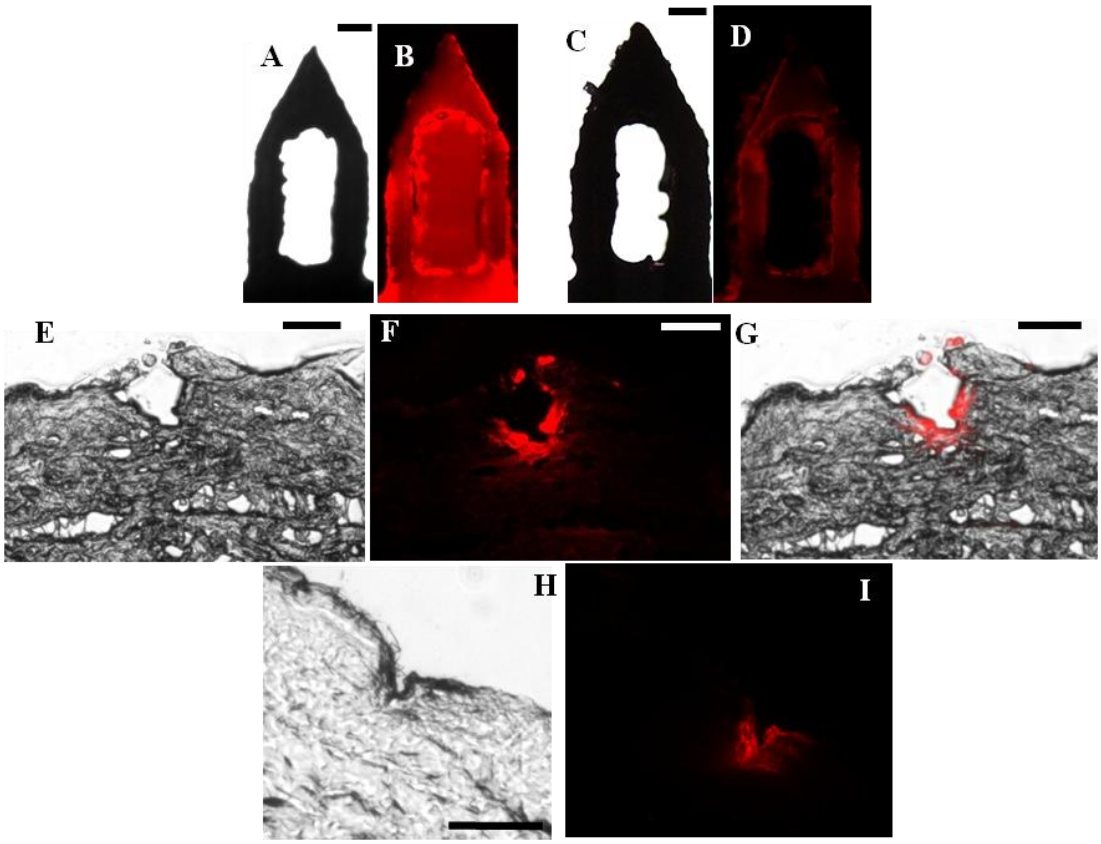

Figure 5.14 (A-I): Delivery of PE/Cy7® conjugated BT A within human skin by liquid loaded PMDs. Fluorescent and brightfield micrographs of a single pocketed microneedle (A-D) loaded with PE/Cy7® conjugated BT A before (A, B) and after insertion (C, D) into human skin. Representative histological cryosections of human skin inserted with a PE/Cy7® conjugated BT A liquid loaded (E-G) and (possibly) dry coated PMD (H, I) observed under light and fluorescence microscopy. (G) was obtained by overlying figures (E) and (F). The fluorescent area detected at the microneedles disruption sites indicates a successful delivery of BT A to the epidermal and dermal layer of the skin**.** Scale bar= 100µm.

Differences in the degree of diffusion of the BT A within the two skin samples were not observed. This was presumably because both tissues were snap frozen immediately after being treated. Therefore, diffusion of the protein within the skin tissue was prevented. The data indicated that PMDs can successfully load and subsequently deliver BT A into the dermal layer of human skin as a liquid formulation. Experiments previously performed using the model protein β-gal (Section 4.4.3.2) highlighted the capability of high molecular weight molecules to diffuse readily within the skin. Similar behaviour may be expected for BTX A. Further studies are therefore now required to characterise delivery and distribution of

the BTX A and establish the clinical efficacy of the toxin delivered by liquid loaded PMDs.

5.5 Conclusion

BTX A contained in the commercial preparation Vistabel® cannot be detected by standard IHC techniques. IHC analysis of human skin treated with PMDs liquid loaded with BT A tentatively suggests successful delivery of the toxoid into the epidermal and dermal layer of the tissue. IHC data were supported by fluorescence microscopy analysis of skin samples treated with BT A following its conjugation to an appropriate fluorophore. The results have demonstrated that BTX-A loaded microneedle devices are a feasible minimally invasive intradermal delivery system for this macromolecular therapeutic.

Chapter 6

General Discussion

6.1 Significance, limitations and future work

The aim of this Thesis was to investigate the suitability of liquid loaded PMDs to deliver BTX A to the dermis of human skin for the treatment of PFHH. Pocketed microneedles, metallic 700 μm-long needles containing a cavity within the needle shaft, were selected as an appropriate delivery device for the task. Initial experiments were performed with the aim of investigating the suitability of a PMD to uniformly accommodate a liquid formulation within the microneedle pockets (Chapter 2). Microneedle pockets were loaded following a single immersion into a formulation that mimicked the composition of the commercial Botox® formulation, with the exception of BTX A, which was replaced by the model protein β-galactosidase (β-gal, ~465 kDa) and a water-soluble dye, which was included to enable visualization. The inherent viscosity of the formulation enabled retention of the solution in the pockets for a sufficient time that would enable application of the device into the skin and delivery of the drug as a liquid formulation. This suggests that Botox® could be loaded onto a PMD and retained as a liquid without requirement to reformulate. Avoiding reformulation would significantly reduce regulatory hurdles and would simplify clinical use of the PMD as a means to deliver BTX A. Moreover, addition of a dye to the formulation has enabled visualisation of the loaded solution in the pockets. This may prove particularly useful in the clinical context, as it would allow the clinician and/or patient to ensure that the formulation has been successfully loaded on the microneedle device and the drug released into the skin following microneedle application.

Loading uniformity of a microneedle device will be important in order to ensure dose reproducibility. This is critical for therapeutic drug delivery and is particularly important for potent and potentially toxic therapeutics such as BTX A. Determination of microneedle loading capacity and reproducibility of dose loading was assessed in Chapter 3 by using an established spectrophotometric assay for the model β-gal. The data indicated that the loading capacity of microneedle devices is appropriate for therapeutic BTX A formulations, as nanograms doses of protein can be accommodated on individual microneedles (for comparison the entire vial of Botox® contain only 5 ng of BTX A). However, dose reproducibility cannot be guaranteed using the loading methodology employed in our experiments. Spatial control of the deposition of the formulation on the microneedle array is challenging

when the loading process is performed manually. This would certainly not be acceptable from a clinical prospective, as it would result in delivery of variable doses and thus unpredictable therapeutic effects. In the future, automation of the process and/or optimization of the microneedle design would help to reduce such variability.

Although the Botox® manufacturing company (Allergan Pharmaceuticals, Irvine, CA, USA) recommends to reconstitute the drug in 4 ml of saline solution (http://www.allergan.com/index.htm 2011), dilution volumes ranging between 1.5 and 5 ml are most commonly employed in the practice setting, dictated mainly by the clinician's preference. Due to the constrained dimensions of the pocket within the microneedle, loading a PMD with effective doses of BTX A would require further concentration of the Botox® preparation (i.e. reconstitution of the entire vial by using volumes as small as 50 µl) and use of a larger PMD containing a higher number of microneedles (i.e., at least 25 pocketed microneedles would be needed instead of the current 5 microneedles contained on a PMD). The use of MDs containing 50 microneedles with a similar design as the ones used in our study has already been reported and thus this is not expected to represent a technical issue (Gill and Prausnitz 2007a). Conversely, the need to reconstitute the entire vial of medicament with extremely low volumes (i.e., 50 µl) may represent a practical challenge in the clinical setting. If the entire vial of Botox® was to be reconstituted in a volume of diluent as low as 50 µl, the solution obtained would be difficult to withdraw from the vial. As a consequence, this would result in waste of a costly medicament.

Using larger volumes, comparable to those currently used in the clinical setting would certainly ease handling of the formulation and would eliminate concerns related to complete dissolution of the therapeutic preparation. However, this would require PMDs with a considerable greater number of microneedles (i.e., microneedle arrays containing more than 1000 pocketed needles would be required to load effective doses of medicament). Alternative microneedle devices with increased loading capacity, such as hollow microneedles, may therefore be more suitable for BTX A delivery as they would not require concentration of the Botox® formulation. Studies indicate that hollow microneedles can load volumes spanning from a few microliters up to 1.5 ml (Burton et al. 2011; McAllister et al. 2003). In particular Micronjet® received FDA approval in February 2010 (http://www.nanopass.com). This device consists of four 450 µm-long hollow microneedles attached to a plastic

device that can be mounted on any conventional syringe. As such, this device could theoretically deliver any volume that has been previously loaded in the syringe.

The Micronjet® has been used for intradermal delivery of commercially available drug formulations including influenza vaccines, lidocaine and insulin, to human subjects and its application has been reported as effective, accurate and almost painless (http://www.nanopass.com ; Van Damme et al. 2009). Therefore, the use of a similarly designed microneedle device would enable administration of the existing formulation Botox® using the same dilutions and injection volumes that are currently used in the clinical setting. By using such devices, loading of Botox® could be performed by using a conventional syringe. This would avoid the need for the manual load process used for the MD, as discussed in this Thesis, and thus would reduce the variability associated with the loading process.

Liquid loaded PMDs facilitated rapid delivery (within seconds) of high molecular weight molecules to the epidermal/dermal layer of human skin. Experiments reported in Chapter 4 indicated that the high molecular weight molecule β-gal, used as a model for BTX A, diffused readily through the more internal layers of the dermis following incubation of the skin samples in organ culture. This therefore suggests that BTX A should diffuse to the therapeutic target (the eccrine sweat glands), once delivered intradermally by PMDs.

However, the results did not indicate diffusion of the model protein to a skin depth, which would enable successful interaction of BTX A with the eccrine sweat glands. While those glands are located in the deep dermis, diffusion of the model protein following PMD application appeared to be restricted within the central portion of the dermis. Skin samples were incubated for a defined period (1 and ½ hours) in organ culture before being fixed in glutaraldehyde. The fixative prevents further migration of the protein within the tissue and therefore it is reasonable to assume that greater diffusion could have been observed if the samples had been incubated for longer periods (i.e., 12 hours or even days). Unfortunately, due to time constraints, it has not been possible to investigate the effect of the time on β-gal diffusion following delivery by PMDs. In the future, additional experiments are warranted in order to further investigate this parameter.

In addition, evaluation of the diffusion of β-gal on treated samples relied on the visible detection of a blue insoluble product, i.e., the product of the reaction between the enzyme and its substrate, X-gal. As a consequence, the intensity of the staining

detected in the skin decreased from the microneedle application site (where the concentration of β-gal was maximal) to the more internal layer of the skin (where the enzymatic concentration was reduced). Protein may have reached deeper layers in the dermis, but the staining generated in these areas may not have been detectable. In the future, experiments could be performed by using more sensitive detection systems (e.g., fluorescently tagged proteins) in order to detect lower levels of protein and therefore greater diffusion.

Moreover, studies assessing distribution of the eccrine sweat glands in the skin would also be useful. They would provide information of whether a protein, delivered to the skin by a PMD, would diffuse to a depth of the tissue that would allow interaction with the eccrine sweat glands. Several studies in the literature report the use of histological and immunohistological methodologies to visualize the sweat glands in cutaneous tissues (Saga 2001; Saga and Morimoto 1995). Such techniques rely on the detection of specific markers (usually enzymes or other proteins), which are abundantly expressed in the eccrine sweat glands. In the future, similar techniques could be employed in order to assess distribution of proteins delivered by PMDs in relation to the eccrine sweat glands in the skin.

The design of the MDs employed would have to be tailored to the anatomical characteristics of the specific hyperhidrotic body site. Treatment of palmar/plantar PFHH would require the use of longer microneedles compared to facial or axillary PFHH, due to the increased thickness of the stratum corneum. Optical imaging methods such as optical coherence tomography (OCT) have been recently employed to characterise microneedle penetration *in vivo* in human subjects (Coulman et al. 2011; Donnelly et al. 2011). *In vivo* data produced by the OCT system revealed real time imagining of morphological changes induced in the skin following microneedle insertion and provided a more accurate evaluation of microneedle penetration in comparison to conventional histological methods. In addition, it provided real time information of structural features of the skin, such as thickness of stratum corneum, epidermis and dermis and enabled visualisation of skin appendages such as sweat glands and pilosebaceous units. Therefore, this technique could be employed in the future to design MDs to target delivery of BTX A to specific regions of the skin at different anatomical sites, where skin thickness differs.

In particular, optimal delivery of BTX A may have to be targeted within the central portion of the dermis, i.e., the region underlying the papillary dermis (located at the

interface between epidermis and dermis) to reduce systemic absorption of the medicament from the capillary network of the papillary layer and thus reduce depletion of the medicament in the underlying dermis. Moreover, it would prevent microneedles reaching larger blood vessels and nerve fibres located in the reticular layer (at the bottom of the dermis), thus reducing the invasiveness of the treatment, while enabling delivery of BTX A to a region of the skin which would be relatively close to the deep dermis where the sweat glands are located. On the contrary, if the toxin was to be delivered to the upper layer of the dermis it would have to migrate further from the application site in order to reach its therapeutic target and this may result in a delayed therapeutic effect or even reduced or absent effect (e.g., if the toxin failed to reach the glands or if the concentration of the toxin in proximity of the glands was too low to be effective).

The two most common side effects associated with the administration of BTX A are pain and temporary weakness of the muscles adjacent to the injection site. While the former is caused by the penetration of the hypodermic needle into the skin, as well as by the extrusion of the liquid formulation by the needle, the latter is mainly determined by difficulty in selective delivery of the drug to the dermis using the traditional Mantoux technique. Due to the reduced dimensions of the microneedles, insertion of a MD into the skin should result in minimum pain and discomfort. This may possibly eliminate the need for local anaesthesia upon administration of BTX A, especially in highly innervated anatomic sites such as the palms of the hands and soles of the feet. BTX A administration by microneedles may also reduce the occurrence of muscle weakness. The Mantoux technique is technically challenging to perform, as the hypodermic needle has to be oriented almost parallel to the skin surface due to its relative high length. Conversely microneedles can be applied perpendicularly into the skin. This would likely reduce the risk for accidental delivery of the toxin to non-targeted sites (i.e. the muscles) as it would ease placing and maintaining the microneedles within the dermis. However, a certain variability of the delivery depth could be expected due to the difference in skin thickness between different areas of the body in the same individual (intra-variability) as well as the difference in skin thickness existing between different individuals (inter-variability). In addition the diffusion pattern of the delivered toxin would be difficult to predict and therefore muscle weakness may still be an adverse effect with microneedles. However, the capability of microneedles to facilitate targeted

intradermal delivery of vaccines has extensively been reported and thus similar results may be expected for BTX A administration (Koutsonanos DG 2009; Van Damme et al. 2009; Widera et al. 2006).

With the aim of confirming the findings highlighted for the model protein β-gal, experiments reported in Chapter 5 were conducted using the protein BTX A. Working with BTX A was associated with number of technical issues. First of all, BTX A is one of the most toxic substances known (Gill 1982). As such, laboratory use of the toxin in high doses requires specific containment facilities and poses risk to the researcher. Experiments could be performed using therapeutic doses of BTX A (in the form of the commercial preparation Vistabel®-BTX A 2.5 ng), without safety concerns. However, in studies detailed in this Thesis, BTX A could not be detected using standard laboratory methodologies due to the extremely low dose of medicament contained in the commercial preparation. Further studies were performed using higher (non-therapeutic) doses of the detoxified form of BTX A (formaldehyde inactivated BTX A, i.e botulinum toxoid A (BT A)). BT A loaded PMDs were applied into the skin and the deposition pattern of the protein was investigated by IHC. Although the data suggested the presence of BT A in the treated skin, BT A detection by IHC was not particularly robust. Therefore, delivery and deposition of BT A via PMDs were further investigated following conjugation of the protein to an appropriate fluorophore. PMDs were shown to uniformly accommodate the fluorescent formulation and to successfully deliver BT A to the dermis of human skin.

Despite this, eccrine sweat glands were not localised within the tissue in our experiments. As a consequence it was not possible to establish with certainty whether the protein delivered by a PMD migrated to its therapeutic target and, most importantly, whether this would have resulted in a therapeutic effect. Delivery of the toxin in proximity of its therapeutic target may not necessarily represent an indication of its efficacy. Induction of a therapeutic effect would be the result of a complex series of events including: migration of the toxin to the secretory portion of the glands (located at the bottom of the dermis), internalization of the toxin within the cholinergic fibres, cleavage of specific SNARE complex proteins within the cytosol of the nerve cells and finally inhibition of the release of Ach into the synaptic space.

Evaluation of the occurrence of all these events can only be determined by performing *in vivo* studies. Due to the lack of animal models for PFHH, efficacy of BTX A is usually assessed *in vivo* in human subjects by measuring the level of anhidrosis by qualitative (i.e. quality of life questionnaires assessing how the treatment has been perceived by the patient and whether or not it has improved his/her quality of life) and quantitative methods (including the gravimetry and the Minor starch-iodine tests) (Trindade de Almeida et al. 2007).

Given these considerations, clinical studies would certainly be required in the future in order to evaluate the effectiveness of a microneedle-mediated BTX A administration for the treatment of PFHH. Clinical trials could be carried out as a means to compare efficacy of Botox® when administered by standard hypodermic needles and MDs. If patients with palmar PFHH were to be treated, microneedles could be applied to one palm and standard injections to the other. Efficacy of the treatment could be assessed by evaluating the difference in sweat production before and after the treatment on each palm. As sweating reduction is usually observed 1-2 weeks following Botox® administration, evaluation of the therapeutic effect could be assessed 7 and 14 days after the treatment and then every month for a follow up period of at least 4 months, which is usually the time at which the therapeutic effect starts to decrease. Microneedles could be applied by using the injection grid currently used for ID injections in such a way as to mimic Botox® administration by conventional hypodermic needles. As the PMDs used within this research project would not guarantee loading of effective and reproducible doses of BTX A, it may be more appropriate, at this stage, to use hollow microneedles. The use of hollow microneedles may not require reformulation of the botulinum product and would enable delivery of the same volumes as standard ID injections (i.e., 100 µl per injection site). In this way Botox® could be administered at both sites (i.e., one vial per each palm) at the same dilution (i.e., by using a volume of 4 ml of saline solution to reconstitute each Botox® vial) and this would allow accurate comparison of the two delivery methods. Clinical studies would also provide crucial information regarding invasiveness and safety of the microneedle application in comparison to conventional hypodermic needles and would enable a more comprehensive understanding of the advantages of the delivery tool.

Beside clinical trials, *in vitro* studies could be used in the future to assess the activity of BTX A in the skin once delivered by MDs and could possibly be used in

conjunction with *in vivo* studies. As reported in Chapter 5, numerous efforts have been made to develop sensitive *in vitro* assays for the detection of BTX A, as a means to replace the gold standard mouse bioassay. In particular, Pellett *et al.* (2007) described the use of a neuronal-cell based immunoassay which is able to detect doses of BTX A as small as 1.5 pg (for comparison, the mouse bioassay can detect ~10 pg of BTX A). Within this assay, neuronal cells obtained through homogenization of rat spinal cords were incubated with different dilutions of BTX A. Detection of the toxin was subsequently achieved by assessing the presence of cleaved SNAP 25 proteins in the cell lysate by Western blot analysis. SNAP 25 is the substrate of BTX A in the cholinergic fibres and therefore detection of cleaved proteins provided a clear indication of the functionality of the toxin. As a consequence, one may assume that a similar assay could be employed to assess the activity of BTX A once delivered to the skin from a MD. Moreover, as the presence of cleaved proteins is directly proportional to the dose of BTX A present in a given sample, this method might provide information of the quantity of toxin delivered in the skin (i.e., by comparing the intensity of the signal of the protein bands against standard concentration of the toxin).

However, future application of this methodology would require the use of active toxin. As mentioned above, the use of BTX A in doses higher than the therapeutic ones is associated with a series of safety concerns. For this reason, this method could only be performed if therapeutic preparations of BTX A, i.e. containing only 5 ng of medicament, were to be used.

As this assay is able to detect BTX A doses of 1.5 pg, one would have to ensure that microneedles would load and thus deliver doses of toxin which would be above this LOD. As previously mentioned, therapeutic doses of BTX A range between 0.1-0.25 ng per each administration site. Therefore, if microneedles able to deliver effective doses of BTX A were to be used (i.e. PMDs containing an increased number of pocketed microneedles or hollow microneedles), this methodology could be employed to detect the presence of active BTX A within the skin. Although potentially useful in the future, this methodology may be technically challenging as it would rely on detection of extremely low doses of proteins (generated by the proteolytic activity of BTX A) released form nervous cells in such complex matrix as the human skin.

Alternatively, Ellies *et al.* (2000) investigated the activity of Botox® in *ex vivo* excised parotid glands by assessing variation in production of the enzyme acetylcholinesterase (AchE). The role of this enzyme resides in the depletion of excess of Ach from the synaptic space. As a consequence, application of BTX A results in reduction of the synthesis and activity of this enzyme through inhibition of the release of Ach from the cholinergic nerves. Within this study the parotid glands of living rats were locally injected with BTX A (Botox®) and subsequently excised (at specific time intervals) and processed into sections. Detection of the AchE enzyme was performed by IHC and the intensity of staining was assessed against untreated samples in order to determine the effect of BTX A on the glands. It may be assumed that a similar methodology could be used in the future to investigate the activity of BTX A therapeutic formulations in the eccrine sweat glands in human skin. This method would provide indication of the functionality of the toxin but it may be practically easier to perform as it would not require cell extraction from the skin tissue.

As a final note it is worth considering the effect that microneedle-mediated administration would have of the cost of BTX A treatment. Patients who have not responded to over the counter antiperspirants (the first-line therapy for PFHH) are usually referred by their general practitioners (GP) to a dermatologist for BTX A treatment in hospitals or clinics within secondary care (http://www.nhs.uk 2011b). However, due to the high cost of the procedure, the availability of BTX A on the NHS is extremely variable and it generally depends on the policy of the local primary care trust. As a consequence, many patients are forced to approach private clinics to access the treatment. Cost for private treatment varies considerably depending on the area of the body to be treated. Larger sites require more injections and are therefore associated with higher costs (e.g., treating the forehand usually costs around £150 while injecting both axillae costs between £350-600 (http://www.healthcentre.org.uk)). In addition, due to the large number of injections required to treat each hyperhidrotic area and the need to administer local anaesthesia to certain anatomic sites, BTX A administration is also time consuming for consultants, with a consequent additional effect on the total cost of the procedure. Cost of the treatment is furthermore increased by the need to repeat the procedure several times a year due to the temporary effect of BTX A on the sweat glands.

BTX A administration by microneedles is expected to be technically easier compared to the Mantoux technique, due to the reduced length of the needles. Furthermore, microneedle application may also be safer as it is less likely to be associated with unwanted delivery of the toxin to non-targeted sites (i.e. the muscles) and will hopefully be blood free. As a consequence, a microneedle-mediated BTX A administration might be delivered by less trained personnel such general practitioners or nurses within primary care. This would reduce secondary care cost for BTX A treatment and would also be advantageous for the patients due to the improved accessibility to primary care. However, in order for microneedles to replace current intradermal injections, we would have to ensure that microneedle mediated BTX A administration would be at least as safe and effective as standard hypodermic needles. Those two aspects can only be determined in clinical studies.

6.2 Concluding remarks

PMDs can be loaded after one single immersion into a Botox® like formulation. This suggested that PMDs could be suitable as a means to successfully load existing Botox® formulations without the need to add excipients and reformulate.

PMDs containing a large numbers of microneedles (i.e., at least 25 pocketed microneedles) would have the capacity to accommodate therapeutic doses of the Botox® preparation when re-constituted with volumes in the microlitre range. However, due to the inherent level of variability associated with the loading process, reproducible and efficient dose loading is not guaranteed. Robustly engineered loading methodologies and/or specifically tailored PMD designs would have to be employed in future to reduce this variability. Different microneedle designs, i.e. hollow microneedles, could also be employed in the future to increase microneedle loading capacity and potentially reduce the variability associated with the loading process.

Liquid loaded PMDs enabled rapid delivery of high molecular weight molecules to the dermis of human skin. The capability of proteins to readily diffuse within the dermis was also demonstrated. This suggests that following delivery of BTX A from a liquid loaded PMD, the medicament should migrate through the tissue to its therapeutic target (the sweat glands) located in the deep dermis.

Therapeutic doses of BTX A could not be detected by standard laboratory techniques. IHC analysis of human skin treated with PMDs liquid loaded with botulinum toxoid A (BT A) suggested successfully delivery of the toxoid into the epidermal and dermal layer of the tissue. IHC data were supported by fluorescence microscopy analysis of skin samples treated with BT A following its conjugation with an appropriate fluorophore.

This study has demonstrated that PMDs are able to accommodate and deliver liquid formulations into human skin and that BTX A (Botox®)-loaded microneedle devices are a feasible minimally invasive delivery system for this macromolecular therapeutic. Future studies are now required in order to optimise a microneedle device that is most suited to clinical practice.

Publications, abstracts and conference proceedings

Torrisi B.M., Anstey A., Zarnitsyn V., Prausnitz, M., Birchall, J.C., Coulman S.A.
Pocketed microneedles for rapid delivery of a liquid state botulinum toxin A formulation into human skin (submitted to The Journal of Controlled Release).

Torrisi B.M., Anstey A., Pearton M., Zarnitsyn V., Prausnitz, M. Birchall, J.C, Coulman S.A.
Determining the feasibility of a microneedle delivery system for intradermal botulinum toxin administration (2012), 2nd International Microneedle Conference, Cork, Ireland (UK) (5 minute oral and poster presentation).

Torrisi B.M., Anstey A., Pearton M., Zarnitsyn V., Prausnitz, M. Birchall, J.C, Coulman S.A.
Evaluating the capability of a pocketed microneedle device to facilitate delivery of potent therapeutic proteins into human skin (2011), Welsh School of Pharmacy Post-Graduate Research Day, University of Cardiff, UK (oral presentation).

Torrisi B.M., Anstey A., Pearton M., Zarnitsyn V., Prausnitz, M. Birchall, J.C, Coulman S.A.
Evaluating the capability of a pocketed microneedle device to facilitate delivery of potent therapeutic proteins into human skin (2010), Cardiff Institute of Tissue Engineering and Repair (CITER) 9th Annual Meeting and Arthritis Research UK Biomechanic and Bioengineering Centre 1st Annual Meeting, Eastwood Park, Falfield, Gloucestershire, UK (oral presentation).

Torrisi B.M., Anstey A., Pearton M., Zarnitsyn V., Prausnitz, M. Birchall, J.C, Coulman S.A.
Solid and pocketed microneedle devices for the delivery of therapeutic proteins into human skin (2010), United Kingdom and Ireland Controlled Release Society (UKICRS) Symposium, University of Hertfordshire, UK (poster presentation).

Bibliography

Abell, E. and Morgan, K. 1974. Treatement of idiophatic hyperhidrosis by glycopyrronium bromide and tap water iontophoresis. *British Journal of Dermatology* 91(1), pp. 87-91.

Alam, M. et al. 2002. Pain associated with injection of botulinum A exotoxin reconstituted using isotonic sodium chloride with and without preservative: a double-blind, randomized controlled trial. *Archives of Dermatology* 138(4), pp. 510-514.

Alarcon, J. B. et al. 2007. Preclinical evaluation of microneedle technology for intradermal delivery of influenza vaccines. *Clinical and Vaccine Immunology* 14(4), pp. 375-381.

Alekseev, S. I. and Ziskin, M. C. 2007. Human skin permittivity determined by millimeter wave reflection measurements. *Bioelectromagnetics* 28(5), pp. 331-339.

Ameri, M. et al. 2009. Demonstrated solid-state stability of parathyroid hormone PTH(1-34) coated on a novel transdermal microprojection delivery system. *Pharmaceutical Research* 26(11), pp. 2454-2463.

Ameri, M. et al. 2010. Parathyroid hormone PTH(1-34) formulation that enables uniform coating on a novel transdermal microprojection delivery system. *Pharmaceutical Research* 27(2), pp. 303-313.

Amorij, J. P. et al. 2008. Development of stable influenza vaccine powder formulations: challenges and possibilities. *Pharmaceutical Research* 25(6), pp. 1256-1273.

Amorij, J. P. et al. 2007. Rational design of an influenza subunit vaccine powder with sugar glass technology: preventing conformational changes of haemagglutinin during freezing and freeze-drying. *Vaccine* 25(35), pp. 6447-6457.

Amorosa, M. 1998a. Forme farmaceutiche a rilascio modificato. In: Amorosa, M. ed. *Principi di tecnica farmaceutica*. Bologna: Librearia Universitaria L. Tinarelli. pp. 510-538.

Amorosa, M. 1998b. Preparati per uso dermatologico In: Amorosa M. ed. *Principi di tecnica farmaceutica*. Bologna: Libreria Universitaria L. Tinarelli. pp. 367-402.

Andrade, P. C. et al. 2011. Use of iontophoresis or phonophoresis for delivering onabotulinumtoxinA in the treatment of palmar hyperidrosis: a report on four cases. *Anais Brasileiros De Dermatologia* 86(6), pp. 1243-1246.

Andrianov, A. K. et al. 2009. Poly[di(carboxylatophenoxy)phosphazene] is a potent adjuvant for intradermal immunization. *Proceedings of the National Academy of Sciences of the United States of America* 106(45), pp. 18936-18941.

Aoki, K. R. et al. 2006. Using translational medicine to understand clinical differences between botulinum toxin formulations. *European Journal of Neurology* 13 Suppl 4, pp. 10-19.

Arnon, S. S. et al. 2001. Botulinum toxin as a biological weapon: medical and public health management. *The Journal of the American Medical Association* 285(8), pp. 1059-1070.

Arora, A. et al. 2008. Micro-scale devices for transdermal drug delivery. *International Journal of Pharmaceutics* 364(2), pp. 227-236.

Atkins, J. L. and Butler, P. E. M. 2002. Hyperhidrosis: A review of current management. *Plastic and Reconstructive Surgery* 110(1), pp. 222-228.

Atkinson, J. L. D. et al. 2011. Endoscopic transthoracic limited sympathotomy for palmar-plantar hyperhidrosis: outcomes and complications during a 10-year period. Mayo Clinic Proceedings 86(8), pp. 721-729.

Bains, B. K. 2010. Novel pDNA particles for pulmonary administration. Ph.D. Thesis, Cardiff University.

Bajaj, V. and Langtry, J. A. A. 2007. Use of oral glycopyrronium bromide in hyperhidrosis. *British Journal of Dermatology* 157(1), pp. 118-121.

Baroni, A. et al. 2012. Structure and function of the epidermis related to barrier properties. *Clinics in Dermatology* 30(3), pp. 257-262.

Barry, B. W. 1983a. Skin trasport. In: Barry, B. W. ed. *Dermatological formulations. Percutaneous absorption.* New York: Marcel Dekker, Inc., pp. 95-126.

Barry, B. W. 1983b. Structure, function, diseases, and topical treatment of human skin. In: Barry, B. W. ed. *Dermatological formulations. Percutaneous absorption*. New York: Marcel Dekker. Inc., pp. 1-48.

Beckstead, J. H. 1994. A Simple technique for preservation of fixation-sensitive antigens in paraffine-embedded tissues. *Journal of Histochemistry & Cytochemistry* 42(8), pp. 1127-1134.

Benecke, R. et al. 2011. Botulinum type A toxin complex for the relief of upper back myofascial pain syndrome: how do fixed-location injections compare with trigger point-focused injections? *Pain Medicine* 12(11), pp. 1607-1614.

Benohanian, A. 2007. Needle-free anaesthesia prior to botulinum toxin type A injection treatment of palmar and plantar hyperhidrosis. *British Journal of Dermatology* 156(3), pp. 593-596.

Benson, H. A. E. and Namjoshi, S. 2008. Poteins and peptides: strategies for delivery to and across the skin. *Journal of Pharmaceutical Sciences* 97(9), pp. 3591-3610.

Beran, J. et al. 2009. Intradermal influenza vaccination of healthy adults using a new microinjection system: a 3-year randomised controlled safety and immunogenicity trial. *Biomed Central Medicine* 7(13), pp. 1-15.

Birchall, J. C. et al. 2005. Cutaneous DNA delivery and gene expression in ex vivo human skin explants via wet-etch micro-fabricated micro-needles. *Journal of Drug Targeting* 13(7), pp. 415-421.

Birchall, J. C. 2006. Microneedle array technology: the time is right but is the science ready? *Expert Review of Medical Devices* 3(1), pp. 1-4.

Blake, T. D. and Rushak, K. J. 1997. Wetting: static and dynamic contact lines. In: Kistler, S.F., Schweizer, P. M. eds. *Liquid film coating. Scientific principles and their technological implications*. London: Chapman and Hall, pp. 63-66.

Borodic, G. E. et al. 1994. Histologic assessment of dose-related diffusion and muscle fiber response after therapeutic botulinum A toxin injections. *Movement disorders*: official journal of the *Movement Disorder Society* 9(1), pp. 31-39.

Bovell, D. L. et al. 2001. Ultrastructure of the hyperhidrotic eccrine sweat gland. *British Journal of Dermatology* 145(2), pp. 298-301.

Brandt, F. 2011. Efficacy and safety evaluation of a novel botulinum toxin topical gel for the treatment of moderate to severe lateral canthal lines. *Dermatologic Surgery* 37(7), pp. 2111-2118.

Burton, S. A. et al. 2011. Rapid intradermal delivery of liquid formulations using a hollow microstructured array. *Pharmaceutical Research* 28(1), pp. 31-40.

Byl, N. N. 1995. The use of ultrasound as an enhancer for transcutaneous drug-delivery – phonophoresis. *Physical Therapy* 75(6), pp. 539-553.

Cai, S. et al. 2007. Botulism diagnostics: from clinical symptoms to in vitro assays. *Critical Reviews in Microbiology* 33(2), pp. 109-125.

Campanati, A. et al. 2004. Local neural block at the wrist for treatment of palmar hyperhidrosis with botulinum toxin: technical improvements. *Journal of the American Academy of Dermatology* 51(3), pp. 345-348.

Campanati, A. et al. 2003. Quality-of-life assessment in patients with hyperhidrosis before and after treatment with botulinum toxin: results of an open-label study. *Clinical Therapeutics* 25(1), pp. 298-308.

Carli, L. et al. 2009. Assay of diffusion of different botulinum neurotoxin type a formulations injected in the mouse leg. *Muscle & Nerve* 40(3), pp. 374-380.

Carpenter, C. L. et al. 1965. Dermojet histopathological artifacts, *Archives of Dermatology* 92(3), pp. 304.

Carruthers, A. and Carruthers, J. 2008. Botulinum toxin products overview. *Skin therapy letter* 13(6), pp. 1-4.

Chao, H.-Y. et al. 2004. A highly sensitive immuno-polymerase chain reaction assay for Clostridium botulinum neurotoxin type A. *Toxicon* 43(1), pp. 27-34.

Chen, B. T. 1983. Investigation of the solvent-evaporation effect on spin coating of thin films. *Polymer Engineering & Science* (23), pp. 399-403.

Chen, X. et al. 2012.Rapid kinetics to peak serum antibodies is achieved following influenza vaccination by dry-coated densely packed microprojections to skin. *Journal of Controlled Release* 158(1), pp 78-84.

Chen, X. et al. 2011. Improving the reach of vaccines to low-resource regions, with a needle-free vaccine delivery device and long-term thermostabilization. *Journal of Controlled Release* 152(3), pp. 349-355.

Chen, X. et al. 2009. Dry-coated microprojection array patches for targeted delivery of immunotherapeutics to the skin. *Journal of Controlled Release* 139(3), pp. 212-220.

Chen, X. F. et al. 2010. Improved DNA vaccination by skin-targeted delivery using dry-coated densely-packed microprojection arrays. *Journal of Controlled Release* 148(3), pp. 327-333.

Chow, A. and Wilder-Smith, E. P. 2009. Effect of transdermal botulinum toxin on sweat secretion in subjects with idiopathic palmar hyperhidrosis. *British Journal of Dermatology* (160)3, pp 721-722.

Collins, A. and Nasir, A. 2010. Topical botulinum toxin. *The Journal of Clinical and Aesthetic Dermatology* 3(3), pp. 35-39.

Corbett, H. J. et al. 2010. Skin vaccination against cervical cancer associated human papillomavirus with a novel micro-projection array in a mouse Model. *PloS One* 5(10), pp 1-9.

Cormier, M. et al. 2004. Transdermal delivery of desmopressin using a coated microneedle array patch system. *Journal of Controlled Release* 97(3), pp. 503-511.

Coulman, S. A. 2006. Gene delivery to human skin using microneedle arrays. Ph.D. Thesis, Cardiff University.

Coulman, S. A. et al. 2009. Microneedle mediated delivery of nanoparticles into human skin. *International Journal of Pharmacy Practice* 366(1-2), pp. 190-200.

Coulman, S. A. et al. 2011. In vivo, in situ imaging of microneedle insertion into the skin of human volunteers using optical coherence tomography. *Pharmaceutical Research* 28(1), pp. 66-81.

Crichton, M. L. et al. 2010. The effect of strain rate on the precision of penetration of short densely-packed microprojection array patches coated with vaccine. *Biomaterials* 31(16), pp. 4562-4572.

Crommelin, D. J. et al. 2003. Shifting paradigms: biopharmaceuticals versus low molecular weight drugs. *International Journal of Pharmaceutics* 266(1-2), pp. 3-16.

Daddona, P. et al. 2011. Parathyroid Hormone (1-34) coated microneedle patch system: clinical pharmacokinetics and pharmacodynamics for treatment of osteoporosis. *Pharmaceutical Research* 28(1), pp. 159-165.

Dahl, J. C. and Glent-Madsen, L. 1989. Treatment of hyperhidrosis manuum by tap water iontophoresis. *Acta Dermato-Venereologica* 69(4), pp. 346-348.

Das, C. P. et.al. 2009. Treatment of focal hand dystonia. In: Truong, D. D., et al. eds. *Manual of botulinum toxin therapy*. New York: Cambridge University Press, pp. 61-75.

Davarian, S. et al. 2008. Effect and persistency of botulinum toxin iontophoresis in the treatment of palmar hyperhidrosis. *Australasian Journal of Dermatology* 49(2), pp. 75-79.

Davis, S. P. et al. 2004. Insertion of microneedles into skin: measurement and prediction of insertion force and needle fracture force. *Journal of Biomechanics* 37(8), pp. 1155-1163.

De Almeida, A. R. T. et al. 2001. Improving botulinum toxin therapy for palmar hyperhidrosis: wrist block and technical considerations. *Dermatologic Surgery* 27(1), pp. 34-36.

De Almeida, A. R. T. et al. 2011. Handling Botulinum toxins: an updated literature review. *Dermatologic Surgery* 37(11), pp. 1553-1565.

De Bree, R. et al. 2009. Repeated Botulinum toxin type A injections to treat patients with Frey Syndrome. *Archives of Otolaryngology-Head & Neck Surgery* 135(3), pp. 287-290.

De Paiva, A. et al. 1999. Functional repair of motor endplates after botulinum neurotoxin type A poisoning: biphasic switch of synaptic activity between nerve sprouts and their parent terminals. *Proceedings of the National Academy of Sciences of the United States of America* 96(6), pp. 3200-3205.

Dean, C. H. et al. 2005. Cutaneous delivery of a live, attenuated chimeric flavivirus vaccine against Japanese encephalitis (ChimeriVax)-JE) in non-human primates. *Human Vaccines* 1(3), pp. 106-111.

Denys, P. et al. 2012. Efficacy and safety of low doses of onabotulinumtoxinA for the treatment of refractory idiopathic overactive bladder: a multicentre, double-blind, randomised, placebo-controlled dose-ranging study. *European Urology* 61(3), pp. 520-529.

Dobson, L. et al. 2010. Image analysis as an adjunct to manual HER-2 immunohistochemical review: a diagnostic tool to standardize interpretation. *Histopathology* 57(1), pp. 27-38.

Doellgast, G. J. 1987. Enzyme-linked coagulation assay. IV. Sensitive sandwich enzyme-linked immunosorbent assays using Russell's viper venom factor X activator-antibody conjugates. *Analytical Biochemistry* 167(1), pp. 97-105.

Doellgast, G. J. et al. 1993. Sensitive enzyme-linked immunosorbent assay for detection of Clostridium botulinum neurotoxins A, B, and E using signal amplification via enzyme-linked coagulation assay. *Journal of Clinical Microbiology* 31(9), pp. 2402-2409.

Doft, M. A. et al. 2012. Treatment of hyperhidrosis with Botulinum toxin. *Aesthetic Surgery Journal* 32(2), pp. 238-244.

Dolianitis, C. et al. 2004. Iontophoresis with glycopyrrolate for the treatment of palmoplantar hyperhidrosis. *The Australasian Journal of Dermatology* 45(4), pp. 208-212.

Dolly, J. O. and Aoki, K. R. 2006. The structure and mode of action of different botulinum toxins. *European Journal of Neurology* 13(4), pp. 1-9.

Donnelly, R. F. et al. 2011. Design, optimization and characterisation of polymeric microneedle arrays prepared by a novel laser-based micromoulding technique. *Pharmaceutical Research* 28(1), pp. 41-57.

Dressler, D. 2009a. Routine use of Xeomin in patients previously treated with Botox: long term results. *European Journal of Neurology* 16(2), pp. 2-5.

Dressler, D. 2012. Five-year experience with incobotulinumtoxinA (Xeomin (R)): the first botulinum toxin drug free of complexing proteins. *European Journal of Neurology* 19(3), pp. 385-389.

Dressler, D. et al. 2002. Botulinum toxin type B for treatment of axillar hyperhidrosis. *Journal of Neurology* 249(12), pp. 1729-1732.

Dressler, D. and Bigalke, H. 2009. Pharmacology of botulinum toxin drugs. In: Truong, D. D., et al. eds. *Manual of Botulinum toxin therapy*. New York Cambridge University Press, pp. 13-22.

Dressler, D. et al. 2008. Equivalent potency of Xeomin® and BOTOX®. *Toxicon* 51, pp. 10-10.

Dunn, M. 2002. Detection of proteins in polyacrylamide gels by silver staining. In: Walker, J., M. ed. *The protein protocols handbook.* New Jersey: Human Press. pp. 265-271.

Egawa, M. et al. 2007. In vivo estimation of stratum corneum thickness from water concentration profiles obtained with raman spectroscopy. *Acta Dermato-Venereologica* 87(1), pp. 4-8.

Eisele, K. H. et al. 2011. Studies on the dissociation of botulinum neurotoxin type A complexes. *Toxicon* 57(4), pp. 555-565.

Eisele, K. H. and Taylor, H. V. 2008. Dissociation of the 900 kDa neurotoxin complex from C. botulinum under physiological conditions. *Toxicon* 51(1), pp. 10-10.

Ekong, T. A. et al. 1995. Immunological detection of Clostridium botulinum toxin type A in therapeutic preparations. *Journal of Immunological Methods* 180(2), pp. 181-191.

Elias, P. M. 2005. Stratum corneum defensive functions: An integrated view. *Journal of Investigative Dermatology* 125(2), pp. 183-200.

Ellies, M. et al. 2000. The effect of local injection of botulinum toxin A on the parotid gland of the rat: An immunohistochemical and morphometric study. *Journal of Oral and Maxillofacial Surgery* 58(11), pp. 1251-1256.

Ellis, R. A. 1965. Fine structure of the myoepithelium of the eccrine sweat glands of man. *The Journal of Cell Biology* 27(3), pp. 551-563.

Erbguth, F. J. 2009. The pretherapeutic history of botulinum toxin. In: Truong D. D. et al. eds. *Manual of Botulium toxin therapy*. Cambridge: Cambridge University Press, pp 1-7.

Farrugia, M. K. and Nicholls, E. A. 2005. Intradermal botulinum A toxin injection for axillary hyperhydrosis. *Journal of Pediatric Surgery* 40(10), pp. 1668-1669.

Feily, A. et al. 2011. A succinct review of botulinum toxin in dermatology; update of cosmetic and noncosmetic use. *Journal of Cosmetic Dermatology* 10(1), pp. 58-67.

Fernando, G. J. et al. 2010. Potent immunity to low doses of influenza vaccine by probabilistic guided micro-targeted skin delivery in a mouse model. *PloS One* 5(4), pp 1-11.

Forch R., S. H. and Jenkins A. T. A. 2009. Appendix C. Contact angle goniometry. In: Forch R., S. H. and Jenkins A. T. A. eds. *Surface design: applications in bioscience and nanotechnology*. Weinheim: Wiley-VCH, pp. 471-475.

Foster K., B. H., Aoki R. 2006. Botulinum neurotoxin - From laboratory to bed side. *Neurotoxicity Research* 9(2, 3), pp. 133-140.

Fowler, A. V. and Zabin, I. 1977. Amino Acid Sequence of β-Galactosidase of Escherichia Coli. *Proceedings of the National Academy of Science of the United States of America* 74(4), pp. 1507-1510.

Frevert, J. 2010. Content of botulinum neurotoxin in Botox®/Vistabel®, Dysport®/Azzalure® and Xeomin®/Bocouture®. *Drugs in R&D* 10(2), pp. 67-73.

Fuchs, E. 1990. Epidermal differentiation – the bare essentials. *Journal of Cell Biology* 111(6), pp. 2807-2814.

Fukushima, K. et al. 2011. Two-layered dissolving microneedles for percutaneous delivery of peptide/protein drugs in rats. *Pharmaceutical Research* 28(1), pp. 7-21.

Garland, M. J. et al. 2012. Dissolving polymeric microneedle arrays for electrically assisted transdermal drug delivery. *Journal of Controlled Release* 159(1), pp. 52-59.

Geddoa, E. et al. 2008. The successful use of botulinum toxin for the treatment of nasal hyperhidrosis. *International Journal of Dermatology* 47(10), pp. 1079-1080.

German, W. J., Stanfield, C. L. 2005. The immune system. In: German, W. J., Stanfield, C. L. eds Principles of human physiology. 1st ed. San Francisco: Benjamin Cummings, pp. 726-736.

Gerstel, M., S. and Place, V., A. 1976. United States Patent 3964482: Drug delivery device. Available at: http://www.freepatentsonline.com/3964482.html [Accessed: 2nd June 2010]

Ghalamkarpour, F. et al. 2010. Supraciliary wrinkles and botulinum toxin A. *Clinical and Experimental Dermatology* 35(4), pp. 388-391.

Gill, D. M. 1982. Bacterial toxins: a table of lethal amounts. *Microbiological Reviews* 46(1), pp. 86-94.

Gill, H. S. et al. 2008. Effect of microneedle design on pain in human volunteers. *The Clinical Journal of Pain* 24(7), pp. 585-594.

Gill, H. S. and Prausnitz, M. R. 2007a. Coated microneedles for transdermal delivery. *Journal of Controlled Release* 117(2), pp. 227-237.

Gill, H. S. and Prausnitz, M. R. 2007b. Coating formulations for microneedles. *Pharmaceutical Research* 24(7), pp. 1369-1380.

Gill, H. S. and Prausnitz, M. R. 2008. Pocketed microneedles for drug delivery to the skin. *The Journal of Physics and Chemistry of Solids* 69(5-6), pp. 1537-1541.

Gill, H. S. et al. 2010. Cutaneous vaccination using microneedles coated with hepatitis C DNA vaccine. *Gene Therapy* 17(6), pp. 811-814.

Glaser, D. A. et al. 2007a. Facial hyperhidrosis: best practice recommendations and special considerations. *Cutis* 79(5), pp. 29-32.

Glaser, D. A. et al. 2007b. Palmar and plantar hyperhidrosis: best practice recommendations and special considerations. *Cutis* 79(5), pp. 18-28.

Glaser, D. A. et al. 2007c. Primary focal hyperhidrosis: scope of the problem. *Cutis* 79(5), pp. 5-17.

Glogau, R. G. 2007. Topically applied botulinum toxin type A for the treatment of primary axillary hyperhidrosis: results of a randomized, blinded, vehicle-controlled study. *Dermatologic Surgery* 33(1), pp. 76-80.

Grate, J. W. et al. 2009. Renewable surface fluorescence sandwich immunoassay biosensor for rapid sensitive botulinum toxin detection in an automated fluidic format. *The Analyst* 134(5), pp. 987-996.

Grate, J. W. e. a. 2010. Advances in assays and analytical approaches for botulinum-toxin detection. *Trends in Analytical Chemistry* 29(10), pp. 1137-1156.

Gregoriou, S. et al. 2010. Effects of Botulinum toxin-A therapy for palmar hyperhidrosis in plantar sweat production. *Dermatologic Surgery* 36(4), pp. 496-498.

Griffith, K. L. and Wolf, R. E., Jr. 2002. Measuring beta-galactosidase activity in bacteria: cell growth, permeabilization, and enzyme assays in 96-well arrays. *Biochemical and Biophysical Research Communications* 290(1), pp. 397-402.

Grunfeld, A. et al. 2009. Botulinum toxin for hyperhidrosis a review. *American Journal of Clinical Dermatology* 10(2), pp. 87-102.

Gulec, A. T. 2012. Dilution of botulinum toxin A in lidocaine vs. in normal saline for the treatment of primary axillary hyperhidrosis: a double-blind, randomized, comparative preliminary study. *Journal of the European Academy of Dermatology and Venereology* 26(3), pp. 314-318.

Gupta, J. et al. 2012. Rapid local anesthesia in humans using minimally invasive microneedles. *The Clinical Journal of Pain* 28(2), pp. 129-135.

Gupta, J. et al. 2009. Minimally invasive insulin delivery in subjects with type 1 diabetes using hollow microneedles. *Diabetes Technology & Therapeutics* 11(6), pp. 329-337.

Gupta, J. et al. 2011a. Rapid pharmacokinetics of intradermal insulin administered using microneedles in type 1 diabetes subjects. *Diabetes Technology & Therapeutics* 13(4), pp. 451-456.

Gupta, J. et al. 2011b. Infusion pressure and pain during microneedle injection into skin of human subjects. *Biomaterials* 32(28), pp. 6823-6831.

Haake, A. et al. 2001. Structure and function of the skin: overview of the epidermis and the dermis. In: Freinkel, R.K. and Woodley, D. T. eds. *The biology of the skin*. New York: The Parthenon Publishing Group. pp. 19-45.

Hafeli, U. O. et al. 2009. In vivo evaluation of a microneedle-based miniature syringe for intradermal drug delivery. *Biomedical Microdevices* (11)5, pp. 943-950.

Hamm, H. et al. 2006. Primary focal hyperhidrosis: disease characteristics and functional impairment. *Dermatology* 212(4), pp. 343-353.

Hamm, H. and Naumann, M. K. 2009. Hyperhidrosis. In: Truong D. D., et al. eds. *Manual of botulinum toxin therapy*. New York: Cambridge University Press., pp. 123-131.

Hansen, K. et al. 2009. Trasdermal delivery. A hollow microstrucured trasdermal system (hMTS) for needle-free delivery of biopharmaceuticals. [online]. Available at: http://www.drugdeliverytechonline.com/drugdelivery/200909?pg=39&search_term=hMTS&doc_id=-1&search_term=hMTS#pg39 [Accessed 28th December 2011].

Haq, M. I. et al. 2009. Clinical administration of microneedles: skin puncture, pain and sensation. *Biomed Microdevices* 11(1), pp. 35-47.

Harvey, A. J. et al. 2011. Microneedle-based intradermal delivery enables rapid lymphatic uptake and distribution of protein drugs. *Pharmaceutical Research* 28(1), pp. 107-116.

Hayton, M. J. et al. 2003. A review of peripheral nerve blockade as local anaesthesia in the treatment of palmar hyperhidrosis. *British Journal of Dermatology* 149(3), pp. 447-451.

Henry, S. et al. 1998. Microfabricated microneedles: a novel approach to transdermal drug delivery. *Journal of Pharmaceutical Sciences* 87(8), pp. 922-925.

Hexsel, D. et al. 2008. A randomized pilot study comparing the action halos of two commercial preparations of botulinum toxin type A. *Dermatologic Surgery* 34(1), pp. 52-59.

Hexsel, D. M. et al. 2009. Increasing the field effects of similar doses of clostridium botulinum type A toxin-hemagglutinin complex in the treatment of compensatory hyperhidrosis. *Archives of Dermatology* 145(7), pp. 837-840.

Holland, D. et al. 2008. Intradermal influenza vaccine administered using a new microinjection system produces superior immunogenicity in elderly adults: A randomized controlled trial. *Journal of Infectious Diseases* 198(5), pp. 650-658.

Holmes, S. and Mann, C. 1998. Botulinum toxin in the treatment of palmar hyperhidrosis. *Journal of the American Academy of Dermatology* 39(6), pp. 1040-1041.

Holzle, E. 2002. Pathophysiology of sweating. *Current Problems in Dermatology* 30, pp. 10-22.

Hoorens, I. and Ongenae, K. 2012. Primary focal hyperhidrosis: current treatment options and a step-by-step approach. *Journal of the European Academy of Dermatology and Venereology* 26(1), pp. 1-8.

Hotchkiss S. A. M. 1998. Dermal Metabolism. In: Roberts, M.S. and Walters, K. A. eds. *Dermal absorption and toxicity assessment*. New York: Marcel Dekker, p 58

http://2011.igem.org/Team:NTNU_Trondheim/rrnB. 2011. Available at: http://2011.igem.org/wiki/images/6/6e/ONPG.png [Accessed: 23th June 2012].

http://en.sanofi.com. 2009. FDA licences new influenza vaccine designed specifically for people 65 years of age and older. Available at: http://en.sanofi.com/Images/14032_20091223_FLU_HIGH_DOSE_en.pdf [Accessed: 3rd June 2012].

http://www.abcam.com. 2011. EasyLink PE/Cy7® Conjugation Kit (3 x 10µg PE/Cy7®) (ab102904). Available at: http://www.abcam.com/EasyLink-PECy7-Conjugation-Kit-3-x-10g-PECy7-ab102904.pdf [Accessed: 10th August 2011].

http://www.allergan.com/index.htm. 2011. Botox (botulinum toxin type A) purified neurotoxin complex prescribing information. Available at: http://www.allergan.com/assets/pdf/botox_pi.pdf [Accessed: 15th June 2012].

http://www.bd.com. 2012. BD Soluvia™ Prefillable Microinjection System. Available at: URL: http://www.bd.com/pharmaceuticals/products/microinjection.asp [Accessed: 3rd June 2012].

http://cai.md.chula.ac.th. Available at: http://cai.md.chula.ac.th/lesson/lesson4410/data/image_s17.jpg [Accessed: 7th June 2012].

http://www.dermaroller.com. 2011. Available at: http://dermaroller.com/index.php?option=com_content&view=frontpage&Itemid=1&lang=en [Accessed: 3rd June 2012].

http://www.dkimages.com. Human skin, cross section. Available at: http://www.dkimages.com/discover/home/Health-and-Beauty/Human-Body/Skin-Hair-and-Nails/Skin-Hair-and-Nails-43.html [Accessed: 7th June 2012]

http://www.fda.gov. 2003. Draft guidance for industry on powder blends and finished dosage units-stratified in process dosage unit sampling and assesment. Available at: http://www.fda.gov/OHRMS/DOCKETS/98fr/03d-0493-gdl0001.pdf [Accessed: 7th March 2012].

http://www.fda.gov. 2011. Guidance for industry residual drug in transdermal and related drug delivery systems. Available at: http://www.fda.gov/downloads/Drugs/GuidanceComplianceRegulatoryInformation/Guidances/UCM220796.pdf [Accessed 7th March 2012].

http://www.healthcentre.org.uk. Cost of Botox for Hyperhidrosis. Available at: http://www.healthcentre.org.uk/cosmetic-treatments/botox-hyperhidrosis-cost.html [Accessed: 21st June 2012].

http://www.ismp-canada.org. 2005. Overdose a risk of transdermal patch in diverse settings. Problems occur even with discarded patch. Available at: http://www.ismp-canada.org/download/CPJ2005SepOct.pdf [Accessed: 8th March 2012].

http://www.microscopy-uk.org.uk/mag/indexmag.html?http://www.microscopy-uk.org.uk/mag/artaug02/gohisto.html. Human histology for amateur microscopists. Available at http://www.microscopy-uk.org.uk/mag/imgaug02/HistPaper01_Fig2.jpg [Accessed: 18th July 2012].

http://www.nanomed-skincare.com. 2010. LitClear. Available at: http://www.nanomed-skincare.com/ [Accessed: 3rd June 2012].

http://www.nanopass.com. Microneedle technology at your fingertips. Available at: http://www.nanopass.com/content-d.asp?tcid=19&cid=24 [Accessed: 15th June 2012].

http://www.nanopass.com. Microneedle technology at your fingertips (Available at: http://www.nanopass.com/content-c.asp?cid=22) [Accessed: 15th June 2012].

http://www.nhs.uk. 2011a. Hyperhidrosis. Available at: http://www.nhs.uk/conditions/Hyperhidrosis/Pages/Introduction.aspx [Accessed: 15th June 2012].

http://www.nhs.uk. 2011b. Hyperhidrosis. Treatment Available at: http://www.nhs.uk/Conditions/Hyperhidrosis/Pages/Treatment.aspx [Accessed: 15th June 2012].

http://www.pharmacopoeia.co.uk. 2012. Sodium Chloride. Available at: http://www.pharmacopoeia.co.uk/bp2012/ixbin/bp.cgi?a=display&r=OCy_ifw7GFI&n=85&id=6729&tab=search [Accessed: 2nd July 2012].

http://www.piercenet.com. Overview of immunohistochemistry. Available at: http://www.piercenet.com/browse.cfm?fldID=F95B91A9-3DC1-4B56-8E8D-59CA044A8BA7#blocking [Accessed: 21st February 2011].

http://www.promega.com. 2006. β-Galactosidase Enzyme Assay System with Reporter Lysis Buffer. Technical bullettin. Available at: http://www.promega.com/tbs/tb097/tb097.html [Accessed: 5th June 2009].

http://www.qiagen.com. 2011. Protein. Available at: http://www.qiagen.com/literature/benchguide/pdf/1017778_benchguide_chap_4.pdf. [Accessed: 3th March 2011].

http://www.robbinsinstruments.com/equipment/dermojet/modelg.html. The Original Dermo-jet "Model G". Available at: http://www.robbinsinstruments.com/downloads/dj_instructions.pdf [Accessed: 9th June 2012]

http://www.sciencedaily.com/releases/2012/03/120306073011.htm. 2012. Microneedle vaccine patch boosts flu protection through robust skin cell immune

response. Available at: http://images.sciencedaily.com/2012/03/120306073011.jpg. [Accessed: 9th June 2012].

http://www.sigmaaldrich.com. 1994. Enzymatic assay of beta galactosidase. Available at: http://www.sigmaaldrich.com/etc/medialib/docs/Sigma/Enzyme_Assay/bgalactosidaseonp.Par.0001.File.tmp/bgalactosidaseonp.pdf [Accessed: 7th July 2009].

http://www.sigmaaldrich.com. 1996. Albumin Human. Product information. Available at: http://www.sigmaaldrich.com/etc/medialib/docs/Sigma/Product_Information_Sheet/a4327pis.Par.0001.File.tmp/a4327pis.pdf [Accessed: 22nd June 2012].

http://www.sigmaaldrich.com. 1999. Enzymatic assay of beta galactosidase. Available at: http://www.sigmaaldrich.com/etc/medialib/docs/Sigma/Enzyme_Assay/g5635enz.Par.0001.File.tmp/g5635enz.pdf [Accessed: 5th July 2009].

Hurley, H. J. 2001. The eccrine sweat glands: structure and function. In: Freinkel, R.K. and Woodley, D. T. eds. *The biology of the skin*. New York: Parthenon Publishing. pp. 47-76.

Ishida-Yamamoto, A. et al. 2011. Order and disorder in corneocyte adhesion. *The Journal of Dermatology* 38(7), pp. 645-654.

Ito, Y. et al. 2008. Evaluation of self-dissolving needles containing low molecular weight heparin (LMWH) in rats. *International Journal of Pharmaceutics* 349(1-2), pp. 124-129.

Jay, J. M., Loessner, M. J, Golden, D. A. 2005. Food poisoning caused by Gram-positive sporeforming bacteria In: Jay, J.M. et al eds *Modern food microbiology*. New York: Springer Science p. 582.

Jensen, J. M. and Proksch, E. 2009. The skin's barrier. *Giornale Italiano di Dermatologia e Venereologia* 144(6), pp. 689-700.

Jordan, R. C. K. et al. 2002. Advanced diagnostic methods in oral and maxillofacial pathology. Part II: Immunohistochemical and immunofluorescent methods. *Oral Surgery Oral Medicine Oral Pathology Oral Radiology and Endodontics* 93(1), pp. 56-74.

Kadler, K. E. et al. 1996. Collagen fibril formation. *Biochemical Journal* 316, pp. 1-11.

Kalb, S. R. et al. 2006. The use of Endopep-MS for the detection of botulinum toxins A, B, E, and F in serum and stool samples. *Analytical Biochemistry* 351(1), pp. 84-92.

Kanitakis, J. 2002. Anatomy, histology and immunohistochemistry of normal human skin. *European Journal of Dermatology* 12(4), pp. 390-400.

Karakoc, Y. et al. 2002. Safe control of palmoplantar hyperhidrosis with direct electrical current. *International Journal of Dermatology* 41(9), pp. 602-605.

Kaushik, S. et al. 2001. Lack of pain associated with microfabricated microneedles. *Anesthesia and Analgesia* 92(2), pp. 502-504.

Kavanagh, G. M. 2006. Botulinum toxin type A by iontophoresis for primary palmar hyperhidrosis. *Journal of the American Academy of Dermatology* 55(5), pp. S115-S117.

Keller, J. E. 2008. Characterization of new formalin-detoxified botulinum neurotoxin toxoids. *Clinical and Vaccine Immunology* 15(9), pp. 1374-1379.

Kendall, M. 2006. Engineering of needle-free physical methods to target epidermal cells for DNA vaccination. *Vaccine* 24(21), pp. 4651-4656.

Kenney, R. T. et al. 2004. Dose sparing with intradermal injection of influenza vaccine. *The New England Journal of Medicine* 351(22), pp. 2295-2301.

Keshtgar, A. S. et al. 2009. Transcutaneous needle-free injection of botulinum toxin: a novel treatment of childhood constipation and anal fissure. *Journal of Pediatric Surgery* 44(9), pp. 1791-1798.

Kielty, C. M. and Shuttleworth, C. A. 1997. Microfibrillar elements of the dermal matrix. *Microscopy Research and Technique* 38(4), pp. 413-427.

Kim, W. O. et al. 2009a. Botulinum Toxin: A Treatment for Compensatory Hyperhidrosis in the Trunk. Dermatologic Surgery 35(5), pp. 833-838.

Kim, W.O. et al. 2008. Topical glycopyrrolate for patients with facial hyperhidrosis. *British Journal of Dermatology* 158(5), pp. 1094-1097.

Kim, Y. C., Park, J.H., Prausnitz, M. P. 2012. Microneedles for drug and vaccine delivery. *Advanced Drug Delivery Reviews*, in press.

Kim, Y. C. et al. 2010. Formulation and coating of microneedles with inactivated influenza virus to improve vaccine stability and immunogenicity. *Journal of Controlled Release* 142(2), pp. 187-195.

Kim, Y. C. et al. 2011. Stability kinetics of influenza vaccine coated onto microneedles during drying and storage. *Pharmaceutical Research* 28(1), pp. 135-144.

Kim, Y. C. et al. 2009b. Improved influenza vaccination in the skin using vaccine coated microneedles. *Vaccine* 27(49), pp. 6932-6938.

Kinkelin, I. et al. 2000. Effective treatment of frontal hyperhidrosis with botulinum toxin A. *British Journal of Dermatology* 143(4), pp. 824-827.

Komericki, P. and Ardjomand, N. 2012. Hyperhidrosis of face and scalp: repeated successful treatment with botulinum toxin type A. *Indian Journal of Dermatology Venereology & Leprology* 78(2), pp. 201-U177.

Koutsonanos D. G. et al. 2009. Transdermal influenza immunization with vaccine-coated microneedle arrays. *PloS One* 4(3), pp. 1-10.

Koutsonanos, D. G. et al. 2011. Serological Memory and Long-term Protection to Novel H1N1 Influenza Virus After Skin Vaccination. *Journal of Infectious Diseases* 204(4), pp. 582-591.

Kurzen, H. et al. 2004. Phenotypical and molecular profiling of the extraneuronal cholinergic system of the skin. *The Journal of Investigative Dermatology* 123(5), pp. 937-949.

Laurent, A. et al. 2007a. Echographic measurement of skin thickness in adults by high frequency ultrasound to assess the appropriate microneedle length for intradermal delivery of vaccines. *Vaccine* 25(34), pp. 6423-6430.

Laurent, P. E. et al. 2007b. Evaluation of the clinical performance of a new intradermal vaccine administration technique and associated delivery system. *Vaccine* 25(52), pp. 8833-8842.

Lee, J. W. et al. 2011. Dissolving microneedle patch for transdermal delivery of human growth hormone. *Small* 7(4), pp. 531-539.

Lee, J. W. et al. 2008. Dissolving microneedles for transdermal drug delivery. *Biomaterials* 29(13), pp. 2113-2124.

Li, G. et al. 2009. In vitro transdermal delivery of therapeutic antibodies using maltose microneedles. *International Journal of Pharmaceutics* 368(1-2), pp. 109-115.

Lin, T. S. et al. 2001a. Pitfalls and complication avoidance associated with transthoracic endoscopic sympathectomy for primary hyperhidrosis (analysis of 2200 cases). *International Journal of Surgical Investigation* 2(5), pp. 377-385.

Lin, W. et al. 2001b. Transdermal delivery of antisense oligonucleotides with microprojection patch (Macroflux) technology. *Pharmaceutical Research* 18(12), pp. 1789-1793.

Lowe, N. J. et al. 2002. Efficacy and safety of botulinum toxin type A in the treatment of palmar hyperhidrosis: a double-blind, randomized, placebo-controlled study. *Dermatologic Surgery* 28(9), pp. 822-827.

Maa, Y. F. et al. 2004. Influenza vaccine powder formulation development: spray-freeze-drying and stability evaluation. *Journal of Pharmaceutical Sciences* 93(7), pp. 1912-1923.

Martanto, W. et al. 2004. Transdermal delivery of insulin using microneedles in vivo. *Pharmaceutical Research* 21(6), pp. 947-952.

Martin, C. J. et al. 2012. Low temperature fabrication of biodegradable sugar glass microneedles for transdermal drug delivery applications. *Journal of Controlled Release* 158(1), pp. 93-101.

Mason, J. T. et al. 2006. Liposome polymerase chain reaction assay for the sub-attomolar detection of cholera toxin and botulinum neurotoxin type A. *Nature Protocols* 1(4), pp. 2003-2011.

Matriano, J. A. et al. 2002. Macroflux microprojection array patch technology: a new and efficient approach for intracutaneous immunization. *Pharmaceutical Research* 19(1), pp. 63-70.

McAllister, D. V. et al. 2003. Microfabricated needles for transdermal delivery of macromolecules and nanoparticles: fabrication methods and transport studies. *Proceedings of the National Academy of Sciences of the United States of America* 100(24), pp. 13755-13760.

Merad, M. et al. 2002. Langerhans cells renew in the skin throughout life under steady-state conditions. *Nature Immunology* 3(12), pp. 1135-1141.

Mikszta, J. A. et al. 2002. Improved genetic immunization via micromechanical disruption of skin-barrier function and targeted epidermal delivery. *Nature Medicine* 8(4), pp. 415-419.

Mikszta, J. A. et al. 2006. Microneedle-based intradermal delivery of the anthrax recombinant protective antigen vaccine. *Infection and Immunity* 74(12), pp. 6806-6810.

Montagna, W., Parakkal, P. F. 1974. The dermis. In: Montagna, W. and Parakkal, P. F. eds. *The structure and function of the skin*. New York: Academic Press pp. 96-141.

Moreau, M. S. et al 2003. A double-blind, randomized, comparative study of Dysport vs. Botox in primary palmar hyperhidrosis. *British Journal of Dermatology* 149(5), pp. 1041-1045.

Naumann, M. et al. 1998a. Botulinum toxin for focal hyperhidrosis: technical considerations and improvements in application. *British Journal of Dermatology* 139(6), pp. 1123-1124.

Naumann, M. and Hamm, H. 2002. Treatment of axillary hyperhidrosis. *British Journal of Surgery* 89(3), pp. 259-261.

Naumann, M. et al. 1998b. Focal hyperhidrosis: effective treatment with intracutaneous botulinum toxin. *Archives of Dermatology* 134(3), pp. 301-304.

Naumann, M. et al. 2001. Botulinum toxin type A in, treatment of bilateral primary axillary hyperhidrosis: randomised, parallel group, double blind, placebo controlled trial. *British Medical Journal* 323(7313), pp. 596-599.

Naver, H. et al. 1999. Treatment of focal hyperhidrosis with botulinum toxin type A. Brief overview of methodology and 2 years' experience. *European Journal of Neurology* 6, pp. S117-S120.

Naver, H. et al. 2000. Palmar and axillary hyperhidrosis treated with botulinum toxin: one-year clinical follow-up. *European Journal of Neurology* 7(1), pp. 55-62.

Ng, K. W. 2010. Microneedles for intraepidermal hepatitis B vaccination. Ph.D. Thesis, Cardiff University.

Ng, K. W. et al. 2009. Development of an ex vivo human skin model for intradermal vaccination: tissue viability and Langerhans cell behaviour. *Vaccine* 27(43), pp. 5948-5955.

Nordquist, L. et al. 2007. Novel microneedle patches for active insulin delivery are efficient in maintaining glycaemic control: an initial comparison with subcutaneous administration. *Pharmaceutical Research* 24(7), pp. 1381-1388.

Oh, J. H. et al. 2011. Changes in glycosaminoglycans and related proteoglycans in intrinsically aged human skin in vivo. *Experimental Dermatology* 20(5), pp. 454-456.

Pacini, S. et al. 2007. Transdermal delivery of Clostridium botulinum toxin type A by pulsed current iontophoresis. *Journal of the American Academy of Dermatology* 57(6), pp. 1097-1099.

Panicker, J. N. and Muthane, U. B. 2003. Botulinum toxins: pharmacology and its current therapeutic evidence for use. *Neurology India* 51(4), pp. 455-460.

Park, J. H. et al. 2005. Biodegradable polymer microneedles: fabrication, mechanics and transdermal drug delivery. *Journal of Controlled Release* 104(1), pp. 51-66.

Park, J. H. et al. 2006. Polymer microneedles for controlled-release drug delivery. *Pharmaceutical Research* 23(5), pp. 1008-1019.

Pearton, M. et al. 2010. Influenza virus-like particles coated onto microneedles can elicit stimulatory effects on Langerhans cells in human skin. *Vaccine* 28(37), pp. 6104-6113.

Pellett, S. et al. 2007. A neuronal cell-based botulinum neurotoxin assay for highly sensitive and specific detection of neutralizing serum antibodies. *FEBS Letters* 581(25), pp. 4803-4808.

Pinder, R. M. 2007. Botulinum toxin - From WMD to therapeutic agent and cosmetic aid. *Neuropsychiatric Disease and Treatment* 3(6), pp. 703-704.

Praharaj, S. K. and Arora, M. 2006. Paroxetine useful for palmar-plantar hyperhidrosis. *Annals of Pharmacotherapy* 40(10), pp. 1884-1886.

Prausnitz, M. R. 2004. Microneedles for transdermal drug delivery. *Advanced Drug Delivery Reviews* 56(5), pp. 581-587.

Prausnitz, M. R. et al. 2009. Microneedle-based vaccines. *Current Topics in Microbiology and Immunology* 333, pp. 369-393.

Price J. et.al 2008a. Botulinum toxin: its form, formulation and pharmacology. *Hospital Pharmacist* 15, pp. 319-321.

Price J. et al. 2008b. Botulinum toxin, its place in therapy. *Hospital Pharmacist* 15, pp. 323-328.

Quan, F. S. et al. 2010. Intradermal vaccination with influenza virus-like particles by Using microneedles induces protection superior to that with intramuscular immunization. *Journal of Virology* 84(15), pp. 7760-7769.

Ramos-Vara, J. A. et al. 2008. Suggested guidelines for immunohistochemical techniques in veterinary diagnostic laboratories. *Journal of Veterinary Diagnostic Investigation* 20(4), pp. 393-413.

Ranoux, D. et al. 2002. Respective potencies of Botox and Dysport: a double blind, randomised, crossover study in cervical dystonia. *Journal of Neurology Neurosurgery and Psychiatry* 72(4), pp. 459-462.

Rasooly, R. and Do, P. M. 2008. Development of an in vitro activity assay as an alternative to the mouse bioassay for Clostridium botulinum neurotoxin type A. *Applied and Environmental Microbiology* 74(14), pp. 4309-4313.

Reinauer, S. et al. 1993. Iontophoresis with alternating current and direct current offset (AC/DC iontophoresis): a new approach for the treatment of hyperhidrosis. *British Journal of Dermatology* 129(2), pp. 166-169.

Rizwan, M. et al. 2009. Enhanced transdermal drug delivery techniques: an extensive review of patents. *Recent Patents on Drug Delivery & Formulation* 3(2), pp. 105-124.

Ro, K. M. et al. 2002. Palmar hyperhidrosis: Evidence of genetic transmission. *Journal of Vascular Surgery* 35(2), pp. 382-386.

Roberge, R. J. et al. 2000. Transdermal drug delivery system exposure outcomes. *The Journal of Emergency Medicine* 18(2), pp. 147-151.

Roberts, M. S. et al. 1978. The percutaneous absorption of phenolic compounds: the mechanism of diffusion across the stratum corneum. *Journal of Pharmacy and Pharmacology* 30(1), pp. 486-490.

Roberts, M. S., Walters, K. A. 1998. The relationship between structure and barrier function of the skin. In: Roberts, M.S. and Walters, K. A. eds. *Dermal absorption and toxicity assessment.* New York: Marcel Dekker, pp. 1-42.

Saadia, D. et al. 2001. Botulinum toxin type A in primary palmar hyperhidrosis: randomized, single-blind, two-dose study. Neurology 57(11), pp. 2095-2099.

Saga, K. 2001. Histochemical and immunohistochemical markers for human eccrine and apocrine sweat glands: an aid for histopathologic differentiation of sweat gland tumors. *The Journal of Investigative Dermatology* 6(1), pp. 49-53.

Saga, K. 2002. Structure and function of human sweat glands studied with histochemistry and cytochemistry. *Progress in Histochemistry and Cytochemistry* 37(4), pp. 323-386.

Saga, K. and Morimoto, Y. 1995. Ultrastructural localization of alkaline phosphatase activity in human eccrine and apocrine sweat glands. *The Journal of Histochemistry and Cytochemistry* 43(9), pp. 927-932.

Sakai, L. Y. et al. 1986. Fibrillin, a new 350-KD glycoprotein, is a component of extracellular microfibrils. *Journal of Cell Biology* 103(6), pp. 2499-2509.

Sanchez, A. I. G. et al. 2010. Effectiveness and safety of glycopyrrolate for hyperhidrosis. *European Journal of Hospital Pharmacy Practice* 16(1), pp. 38-41

Sanli, H. et al. 2004. Idiopathic localized crossed (left side of the upper part of the body, right side of the lower part of the body) hyperhidrosis: successful treatment of facial area with botulinum a toxin injection. *Dermatologic Surgery* 30(4), pp. 552-554.

Saray, Y. and Gulec, A. T. 2005. Treatment of keloids and hypertrophic scars with dermojet injections of bleomycin: a preliminary study. *International Journal of Dermatology* 44(9), pp. 777-784.

Sathyamoorthy, V. and DasGupta, B. R. 1985. Separation, purification, partial characterization and comparison of the heavy and light chains of botulinum neurotoxin types A, B, and E. *The Journal of Biological Chemistry* 260(19), pp. 10461-10466.

Sato, K. et al. 1989. Biology of sweat glands and their disorders. I. Normal sweat gland function. *Journal of the American Academy of Dermatology* 20(4), pp. 537-563.

Saurer, E. M. et al. 2010. Layer-by-Layer Assembly of DNA- and Protein-Containing Films on Microneedles for Drug Delivery to the Skin. *Biomacromolecules* 11(11), pp. 3136-3146.

Scarlatos, A. et al. 2005. Methods for detecting botulinum toxin with applicability to screening foods against biological terrorist attacks. *Journal of Food Science* 70(8), pp. 121-130.

Sevim, S. et al. 2002. Botulinum toxin-A therapy for palmar and plantar hyperhidrosis. *Acta Neurologica Belgica* 102(4), pp. 167-170.

Sharma, S. K. et al. 2006. Detection of type A, B, E, and F Clostridium botulinum neurotoxins in foods by using an amplified enzyme-linked immunosorbent assay with digoxigenin-labeled antibodies. *Applied and Environmental Microbiology* 72(2), pp. 1231-1238.

Shelley, W. B. et al. 1998. Botulinum toxin therapy for palmar hyperhidrosis. *Journal of the American Academy of Dermatology* 38(2), pp. 227-229.

Shi, S. R. et al. 2011. Antigen retrieval immunohistochemistry: review and future prospects in research and diagnosis over two decades. *Journal of Histochemistry & Cytochemistry* 59(1), pp. 13-32.

Shone, C. et al. 1985. Monoclonal antibody-based immunoassay for type A Clostridium botulinum toxin is comparable to the mouse bioassay. *Applied and Environmental Microbiology* 50(1), pp. 63-67.

Shrivastava, S. N. and Singh, G. 1977. Tap water iontophoresis in palmoplantar hyperhidrosis. *British Journal of Dermatology* 96(2), pp. 189-195.

Silberstein, S. D. 2009. The use of botulinum toxin in the management of headache disorders. In: Truong, D. D., et al. eds. *Manual of Botulinum toxin therapy*. New York: Cambridge University Press pp. 175-183.

Simpson, C. L. et al. 2011. Deconstructing the skin: cytoarchitectural determinants of epidermal morphogenesis. *Nature Reviews Molecular Cell Biology* 12(9), pp. 565-580.

Simpson, L. L. 2004. Identification of the major steps in botulinum toxin action. *Annual Review of Pharmacology and Toxicology* 44, pp. 167-193.

Smidfelt, K. and Drott, C. 2011. Late results of endoscopic thoracic sympathectomy for hyperhidrosis and facial blushing. *British Journal of Surgery* 98(12), pp. 1719-1723.

Sondell, B. et al. 1995. Evidence that stratum-corneum chymotryptic enzyme is transported to the stratum-corneum extracellular-space via lamellar bodies. *Journal of Investigative Dermatology* 104(5), pp. 819-823.

Sorrell, J. M. and Caplan, A. I. 2004. Fibroblast heterogeneity: more than skin deep. *Journal of Cell Science* 117(5), pp. 667-675.

Sposito, M. M. M. 2002. New indications for botulinum toxin type A in cosmetics: Mouth and neck. *Plastic and Reconstructive Surgery* 110(2), pp. 601-611.

Steinsträsser, I. and Merkle, H. P. 1995. Dermal metabolism of topically applied drugs: pathways and models reconsidered. *Pharmaceutica Acta Helvetiae* 70(1), pp. 3-24.

Stone, H. F. et al. 2011. Characterization of diffusion and duration of action of a new botulinum toxin type A formulation. *Toxicon* 58(2), pp. 159-167.

Sueki, H. et al. 2000. Hairless guinea pig skin: anatomical basis for studies of cutaneous biology. *European Journal of Dermatology* 10(5), pp. 357-364.

Swartling, C. et al. 2001a. Side-effects of intradermal injections of botulinum A toxin in the treatment of palmar hyperhidrosis: a neurophysiological study. *European Journal of Neurology* 8(5), pp. 451-456.

Swartling, C. et al. 2001b. Botulinum A toxin improves life quality in severe primary focal hyperhidrosis. *European Journal of Neurology* 8(3), pp. 247-252.

Talarico-Filho, S. et al. 2007. A double-blind, randomized, comparative study of two type A botulinum toxins in the treatment of primary axillary hyperhidrosis. *Dermatologic surgery* 33(1 Spec No.), pp. S44-50.

Tan, S. R. and Solish, N. 2002a. Long-term efficacy and quality of life in the treatment of focal hyperhidrosis with botulinum toxin A. *Dermatologic Surgery* 28(6), pp. 495-499.

Trautman, J. C. et al. 2008. United States Patent 7435299: Method and apparatus for coating skin piercing microneedles. Available at: http://www.freepatentsonline.com/7435299.html [Accessed 17th February 2012].

Trindade de Almeida, A. R. et al. 2007. Pilot study comparing the diffusion of two formulations of botulinum toxin type A in patients with forehead hyperhidrosis. *Dermatologic Surgery* 33(1), pp. 37-43.

Truong, D. D. 2012. Botulinum toxins in the treatment of primary focal dystonias. *Journal of the Neurological Sciences* 316(1-2), pp. 9-14.

Truong, D. D. and Jost, W. H. 2006. Botulinum toxin: clinical use. *Parkinsonism & Related Disorders* 12(6), pp. 331-355.

Vadoud-Seyedi, J. 2004. Treatment of plantar hyperhidrosis with botulinum toxin type A. *International Journal of Dermatology* 43(12), pp. 969-971.

Vadoud-Seyedi, J. et al. 2000. Treatment of plantar hyperhidrosis with dermojet injections of botulinum toxin. *Dermatology* 201(2), pp. 179-179.

Van Damme, P. et al. 2009. Safety and efficacy of a novel microneedle device for dose sparing intradermal influenza vaccination in healthy adults. *Vaccine* 27(3), pp. 454-459.

Van Ermengem, E. P. 1897. U¨ ber einen neuen anaeroben Bacillus und seine Beziehung zum Botulismus. *Z Hyg Infektionskrankh* 26(1) 56 (English version: Van Ermengem, E. P. 1979. A new anaerobic bacillus and its relation to botulism. *Reviews of Infectious Diseases* 1(4), pp. 701-719.

Varnum, S. M. et al. 2006. Enzyme-amplified protein microarray and a fluidic renewable surface fluorescence immunoassay for botulinum neurotoxin detection using high-affinity recombinant antibodies. *Analytica Chimica Acta* 570(2), pp. 137-143.

Verbaan, F. J. et al. 2008. Improved piercing of microneedle arrays in dermatomed human skin by an impact insertion method. *Journal of Controlled Release* 128(1), pp. 80-88.

Walker, J. M. 2002. The bicinchoninic acid (BCA) assay for protein quantitation In: Walker, J. M. *The protein protocols handbook* 2nd ed. New Jersey: Human Press. pp. 11-14.

Wang, P. M. et al. 2006. Precise microinjection into skin using hollow microneedles. *Journal of Investigative Dermatology* 126(5), pp. 1080-1087.

Weber, A. et al. 2005. Psychosocial aspects of patients with focal hyperhidrosis. Marked reduction of social phobia, anxiety and depression and increased quality of life after treatment with botulinum toxin A. *British Journal of Dermatology* 152(2), pp. 342-345.

Weldon, W. C. et al. 2011. Microneedle vaccination with stabilized recombinant influenza virus hemagglutinin induces improved protective immunity. *Clinical and Vaccine Immunology* : CVI 18(4), pp. 647-654.

Wendorf, J. R. et al. 2011. Transdermal delivery of macromolecules using solid-state biodegradable microstructures. *Pharmaceutical Research* 28(1), pp. 22-30.

Wermeling, D. P. et al. 2008. Microneedles permit transdermal delivery of a skin-impermeant medication to humans. *Proceedings of the National Academy of Sciences of the United States of America* 105(6), pp. 2058-2063.

Widera, G. et al. 2006. Effect of delivery parameters on immunization to ovalbumin following intracutaneous administration by a coated microneedle array patch system. *Vaccine* 24(10), pp. 1653-1664.

Wilke, K. et al. 2007. A short history of sweat gland biology. *International Journal of Cosmetic Science* 29(3), pp. 169-179.

Wonglertnirant, N. et al. 2011. A Hollow Microneedle Carrier for Enhancing Skin Penetration of Large Molecular Compounds. *Biological and Pharmaceutical Bullettin* 33(12), pp. 1988-1993.

Wu, Y. et al. 2010. Sustained release of insulin through skin by intradermal microdelivery system. *Biomedical Microdevices* 12(4), pp. 665-671.

Xie, Y. et al. 2005. Controlled transdermal delivery of model drug compounds by MEMS microneedle array. *Nanomedicine: Nanotechnology, Biology, and Medicine* 1(2), pp. 184-190.

Yagima Odo, M. E. et al. 2011. Botulinum toxin for the treatment of menopausal hot flushes: a pilot study. *Dermatologic Surgery* 37(11), pp. 1579-1583.

Yamashita, N. et al. 2008. Local injection of botulinum toxin A for palmar hyperhidrosis: usefulness and efficacy in relation to severity. *Journal of Dermatology* 35(6), pp. 325-329.

Yamauchi, P. S. and Lowe, N. J. 2004. Botulinum toxin types A and B: Comparison of efficacy, duration, and dose-ranging studies for the treatment of facial rhytides and hyperhidrosis. *Clinics in Dermatology* 22(1), pp. 34-39.

Zaiac, M. et al. 2000. Botulinum toxin therapy for palmar hyperhidrosis with ADG needle. *Dermatologic Surgery* 26(3), pp. 230-230.

Zhang, Y. et al. 2011. Development of lidocaine-coated microneedle product for rapid, safe, and prolonged local analgesic action. *Pharmaceutical Research*, pp. 1-8.

Zhu, Q. et al. 2009. Immunization by vaccine-coated microneedle arrays protects against lethal influenza virus challenge. *Proceedings of the National Academy of Sciences of the United States of America* 106(19), pp. 7968-7973.